

# Climatic and anthropogenic impacts on the variability of water resources

## *Impacts climatiques et anthropiques sur la variabilité des ressources en eau*

22-24 November / novembre 2005  
Maison des Sciences de l'Eau de Montpellier  
Montpellier, France

Programme / Programme  
Papers / Communications  
List of Participants / Liste des participants



International Hydrological Programme

IHP

IHP-VI | Technical Documents in Hydrology | No. 80  
IHP-VI | Documents Techniques en hydrologie | No. 80







United Nations  
Educational, Scientific and  
Cultural Organization

Organisation  
des Nations Unies  
pour l'éducation,  
la science et la culture



International Hydrological  
Programme (IHP)

*Programme hydrologique  
international (PHI)*

# **Climatic and anthropogenic impacts on the variability of water resources**

## ***Impacts climatiques et anthropiques sur la variabilité des ressources en eau***

**International seminar / *Séminaire international***

22-24 November / *novembre* 2005  
Maison des Sciences de l'Eau de Montpellier  
Montpellier, France

Programme / *Programme*  
Papers / *Communications*  
List of Participants / *Liste des participants*

**Published in 2007 by the International Hydrological Programme (IHP) of the United Nations Educational, Scientific and Cultural Organization (UNESCO)**  
1 rue Miollis, 75732 Paris Cedex 15, France

**Publié en 2007 par le Programme hydrologique international (PHI) de l'Organisation des Nations Unies pour l'éducation, la science et la culture (UNESCO)**  
1 rue Miollis, 75732 Paris Cedex 15, France

**IHP-VI Technical Document in Hydrology N°80**  
**IHP-VI Document technique en hydrologie N°80**

**UNESCO Working Series SC-2007/WS/8**

© UNESCO/IHP 2007

The authors are responsible for the choice and presentation of the viewpoints and information contained in their articles, which in no way commit UNESCO. The designations employed and the presentation of data throughout this publication do not imply the expression of any opinion whatsoever on the part of UNESCO concerning the legal status of any country, territory, city or area or of its authorities, or concerning the delimitation of its frontiers or boundaries.

*Les auteurs sont responsables du choix et de la présentation des points de vue et informations figurant dans leurs articles, lesquels n'engagent en aucune façon l'UNESCO. Les désignations employées dans cette publication et la présentation des données qui y figurent n'impliquent de la part de l'UNESCO aucune prise de position quant au statut juridique des pays, territoires, villes ou zones, ou de leurs autorités, ni quant à leurs frontières ou limites.*

**Edition prepared by the group of authors and finalized by  
Gil Mahé, Scientific Editor**  
***Edition préparée par l'ensemble des auteurs et finalisée par  
Gil Mahé, Editeur scientifique***

Publications in the series 'IHP Technical Documents in Hydrology' are available from /  
*Les publications dans la série 'Documents techniques en hydrologie du PHI' sont disponibles auprès de:*

IHP Secretariat | UNESCO | Division of Water Sciences  
1 rue Miollis, 75732 Paris Cedex 15, France  
Tel: +33 (0)1 45 68 40 01 | Fax: +33 (0)1 45 68 58 11  
E-mail: [ihp@unesco.org](mailto:ihp@unesco.org)  
<http://www.unesco.org/water/ihp>

## PREFACE

### SEMINAIRE INTERNATIONAL

#### IMPACTS CLIMATIQUES ET ANTHROPIQUES SUR LA VARIABILITE DES RESSOURCES EN EAU

Eric Servat, Président du FIGCC, Coordonnateur Général du Programme FRIEND-AMHY

Gil Mahé, Co-coordonnateur du thème de recherche « Changement climatique et relations pluie-débit » de FRIEND-AOC

Le séminaire « **Impacts Climatiques et Anthropiques sur la Variabilité des Ressources en Eau** » s'est déroulé au Laboratoire HydroSciences Montpellier, Maison des Sciences de l'Eau, du 22 au 24 novembre 2005.

Le programme FRIEND (Flow Regimes from International and Experimental Network Data), dans le cadre du programme hydrologique international de l'UNESCO, a pour but de mettre en place des réseaux de chercheurs hydrologues à une échelle sous-continentale, développant une animation scientifique et un partage de données transfrontalières. Il y a 8 grands programmes FRIEND dans le monde : Afrique de l'Ouest et Centrale, Afrique Australe, Nil, Asie-Pacifique, Indukush-Himalaya, Caraïbes-Amérique Latine, Alpes et Méditerranée, Europe du Nord-Ouest.

L'objectif était de réunir au moins deux scientifiques par grande région FRIEND afin de confronter, par des débats au sein de la communauté des chercheurs du réseau FRIEND, les multiples approches autour des deux questions clés du Séminaire : « *Quelles ressources en eau pour le XXIème siècle ?* », et « *Relations homme-climat-environnement et ressources en eau* ».

L'organisation a été assurée par **Mike Bonell** de l'UNESCO Paris, **Emmanuel Naah** de l'UNESCO Afrique à Nairobi et par **Gil Mahé** d'HSM.

Cet appel à communication a été lancé au sein de chaque réseau régional FRIEND sous le couvert des **Coordinateurs Régionaux FRIEND**, qui ont sélectionné 4 communications. Ces dernières ont été envoyées au **Comité Scientifique** composé de **Serge Janicot** (LOCEAN-Paris), **Eric Servat** (Directeur d'HSM), **Denis Hughes** (Univ. Grahamstown-Afrique du Sud), **Declan Conway** (UEA-Norwich) et **Eduardo Planos Gutiérrez** (Instituto de Meteorologia-La Habana), complété par les services de **Jean-Marie Fritsch** (Représentant IRD-Afrique du Sud), **Marcel Kuper** (CIRAD-Rabat), **Arona Diedhiou** (IRD-Niamey), **Pierre Hubert** (Ecole des Mines-Paris), et **Gil Mahé**, qui ont établi un classement. Les deux premiers de chaque région ont reçu une subvention de l'organisation du Séminaire pour venir à Montpellier. Selon les régions, certains chercheurs ont obtenu des financements locaux, ce qui a permis de faire venir 1 voire 2 participants supplémentaires. Plusieurs scientifiques ont été invités à présenter des communications introductives sur les thèmes proposés. Enfin, dans la limite des places disponibles, plusieurs chercheurs, européens pour la plupart, ont souhaité participer à ce Séminaire.

Il faut noter que nous avons reçu un grand nombre de demandes de participation pour ce Séminaire, qui a été annoncé dans la lettre d'information de l'AISH, qui a également apporté son soutien scientifique par l'intermédiaire de sa Commission Internationale des Eaux de Surface.

Si, pour des raisons d'organisation, nous avons choisi de limiter le nombre de participants à une soixantaine, il est évident que ce thème aurait été susceptible d'en rassembler beaucoup plus.

Ce Séminaire se situait également à un an de la grande conférence quadriennale FRIEND qui aura lieu à Cuba, et était une bonne occasion de mobiliser le réseau pour bien préparer cet événement.

Le Séminaire a rassemblé 57 chercheurs venant de 25 pays. Trois chercheurs n'ont pu venir mais se sont fait représenter et ont envoyé une présentation.

Chaque région FRIEND a été représentée par 2 à 5 chercheurs, la région Europe du Nord-Ouest fournissant la contribution la plus importante, et en particulier la France, pour raison de proximité. La région Afrique de l'Ouest et Centrale a rassemblé un grand nombre de participants du

fait de l'organisation par HydroSciences Montpellier de l'Atelier Scientifique et du Comité de Pilotage annuel de ce groupe le lendemain du Séminaire, toujours à la Maison des Sciences de l'Eau, sous financement conjoint de l'IRD et de l'UNESCO (Bureau de Nairobi).

Durant la journée qui a précédé le Séminaire nous avons également organisé une formation au modèle ACCRU, réalisée par le Professeur Roland Schulze et Mark Horan, de l'Université Pietermaritzburg en Afrique du Sud, qui a rassemblé 8 chercheurs.

La contiguïté de ces deux évènements a permis à un grand nombre de chercheurs de la région AOC de participer au Séminaire International et de rencontrer des partenaires FRIEND des autres régions.

La journée de présentations a rassemblé 23 communications, dont 8 invitées et 15 sélectionnées dans le réseau FRIEND, autour de 3 thèmes :

- **1 Knowledge of climatic regimes and drainages and their spatio-temporal variability** (8 présentations) ;
- **2 Relationships between human activities, climate, water resources and environment** (8 présentations) ;
- **3 Climatic scenarios for XXI<sup>st</sup> century and forecasted water resources** (7 présentations).

Plusieurs posters ont également été affichés durant les Journées.

Deux ateliers d'une demi-journée ont été organisés sur les thèmes 2 et 3 et ont donné lieu à des synthèses, publiées à la fin de ce livre.

L'après-midi de session plénière a permis d'ouvrir la discussion sur le thème des ressources en eau à travers les groupes régionaux, sur l'avenir du programme FRIEND, et a donné lieu à la rédaction de recommandations générales rédigées par le Professeur Trevor Daniell (Coordinateur régional FRIEND-Asie-Pacifique) et Luc Sigha (Coordinateur régional FRIEND AOC).

Beaucoup des participants ont pu nouer des liens avec des équipes travaillant au Laboratoire HSM et à la MSE durant leur séjour, ouvrant des perspectives de collaborations futures inter-universitaires.

Nous terminerons en remerciant les sponsors qui se sont joints à HydroSciences pour rendre possible cette rencontre scientifique : l'**UNESCO (Paris et Nairobi)**, l'**IRD**, la **Maison des Sciences de l'Eau de Montpellier**, le **Conseil Général du Département de l'Hérault (CG34)**, la **Région Languedoc-Roussillon**, l'**Université Montpellier 1**, l'**Université Montpellier 2**, le **CNRS (SDU)**, le **Ministère des Affaires Etrangères** et **EGIDE**, le **Ministère de l'Ecologie et du Développement Durable**, l'**AISH**, l'**Ambassade de France en Afrique du Sud**, le **British Council**.

Tous les éléments du Séminaire sont disponibles sur le site web de HSM : <http://www.hydrosciences.fr>. La plupart des communications qui ont été présentées sont reprises dans ce document, toutefois quelques-unes n'y figurent pas, soit parce qu'elles ont déjà été publiées dans d'autres revues, soit parce que les auteurs n'ont pas souhaité les finaliser. Une sélection de papiers sera envoyée à la revue Hydrological Processes pour un numéro spécial.

Nous remercions vivement les participants, les sponsors et le personnel d'HydroSciences Montpellier qui a participé à l'organisation, avec une mention spéciale à Noémie Cauquil, qui a assuré le secrétariat de la conférence.

# **SOMMAIRE**

## **COMMUNICATIONS**

### **CLIMAT ET RELATIONS AVEC OCEAN ET ATMOSPHERE**

<b>Janicot S.</b>	<b>3</b>
<b>PREDICTABILITY OF THE SHORT RAINS IN NORTHEAST TANZANIA</b>	
<b>Valimba P., Mkhandi S.H.</b>	<b>11</b>
<b>ASSESSING LARGE-SCALE HYDROCLIMATIC LINKAGES IN NORTHWEST EUROPE</b>	
<b>Kingston D. G., McGregor G. R., Lawler D. M., Hannah D. M.</b>	<b>19</b>
<b>A SUITABLE SELECTION OF RAINFALL-RUNOFF FORECASTING MODELS FOR THE NILE RIVER BASIN</b>	
<b>Sonbol M.A., El-Bihery M.A., Abdel-Motaleb M.</b>	<b>27</b>
<b>CHANGING FLOW REGIMES IN SOUTHERN AFRICA AND ITS RELATIONSHIP TO RAINFALL VARIATIONS</b>	
<b>Valimba P., Mkhandi S.H., Servat E., Hughes D.</b>	<b>43</b>
<b>MASS BALANCE AND SNOUT RECESSON MEASUREMENTS (1991-2000) OF DOKRIANI PLACIER, GARHWAL HIMALAYA, INDIA</b>	
<b>Dobhal D.P., Gergan J.T., Thayyen R.J.</b>	<b>53</b>
<b>CLIMATE CHANGE SIGNALS DETECTED THROUGH MASS BALANCE MEASUREMENTS ON BENCHMARK PLACIER, HIMACHAL PRADESH, INDIA</b>	
<b>Kumar R., Hasnain S.I., Wagnon P., Arnaud Y., Chevallier P., Linda A., Sharma P.</b>	<b>65</b>
<b>DROUGHT ANALYSIS AND THE EFFECT OF CLIMATE CHANGE IN THE WEST BANK/PALESTINE</b>	
<b>Carmi N., Bachir B., Rabi A.</b>	<b>75</b>
<b>INFLUENCES DES VARIATIONS CLIMATIQUES SUR LE REGIME HYDROLOGIQUE DU BASSIN VERSANT DU QSOB (ESSAOUIRA MAROC)</b>	
<b>Laftouhi N., Persoons E.</b>	<b>85</b>
<b>LOW FLOW AND DROUGHT STUDIES WITHIN THE NE-FRIEND GROUP</b>	
<b>Tallaksen L., Demuth S., van Lanen H.</b>	<b>99</b>
<b>COMPARATIVE HYDROLOGICAL DROUGHT-FLOOD RISK MODELLING IN NORTHERN MEXICO AND WEST AFRICAN SAHEL REGIONS</b>	
<b>Gutiérrez-Lopez A., Onibon H.</b>	<b>107</b>
<b>BUSHFIRES AND THEIR IMPLICATIONS FOR MANAGEMENT OF FUTURE WATER SUPPLIES IN THE AUSTRALIAN CAPITAL TERRITORY</b>	
<b>Daniell T., White I.</b>	<b>117</b>
<b>CLIMATIC AND HUMAN INFLUENCES ON WATER RESOURCES IN LOW ATOLLS</b>	
<b>White I., Falkland T., Metutera T., Metai E., Perez P., Dray A., Overmars M.</b>	<b>129</b>
<b>VARIABILITY AND CHANGES IN THE HYDROLOGICAL VARIABLES AND</b>	

<b>PERSPECTIVES HYDROLOGICAL SCENARIOS IN THE CARIBBEAN REGION</b>	
<b>Planos Gutiérrez E., Limia Martínez M.</b>	<b>143</b>
<b>PREVISION DES RESSOURCES EN EAU EN AFRIQUE AU 21<sup>EME</sup> SIECLE</b>	
<b>Ardoin-Bardin S., Boyer J.F., Dezetter A., Dieulin C., Mahé G., Paturel J.E., Servat E.</b>	<b>155</b>
<b>CLIMATE CHANGE SCENARIOS AND IMPACTS ON THE SURFACE WATER</b>	
<b>RESOURCES OF THE VOLTA RIVER BASIN</b>	
<b>Opoku-Ankomah Y., Minia Z.</b>	<b>165</b>
<b>IMPACTS DES FLUCTUATIONS CLIMATIQUES SUR LE REGIME DES ECOULEMENTS</b>	
<b>DU FLEUVE SANAGA AU CAMEROUN, PROSPECTIVES POUR LE XXI<sup>EME</sup> SIECLE</b>	
<b>Sighomnou D., Sigha L., Liéno G., Dezetter A., Mahé G., Servat E., Paturel J.E.,     Olivry J.C., Tchoua F., Ekodeck G.E.</b>	<b>173</b>
<b>COMPARISON OF DIFFERENT SOURCES OF UNCERTAINTY IN CLIMATE</b>	
<b>CHANGE IMPACT STUDIES ON A LOW FLOW INDICATOR IN GREAT BRITAIN</b>	
<b>Prudhomme C., Davies H.</b>	<b>183</b>
<b>RESUME DES ATELIERS</b>	<b>191</b>
<b>PROGRAMME</b>	<b>195</b>
<b>LISTE DES PARTICIPANTS</b>	<b>197</b>

# CLIMATE RELATIONSHIPS WITH OCEAN AND ATMOSPHERE - THE EXAMPLE OF THE WEST AFRICAN MONSOON

**Serge JANICOT**

IRD, IPSL/LOCEAN, 4 Place Jussieu, 75252 Paris cedex 05, France.

*serge.janicot@lodyc.jussieu.fr*

## ABSTRACT

This paper presents a short review of the most recent papers dealing with the connections and interactions between the ocean and the West African monsoon. We focus first on the annual cycle of the monsoon, then on intra-seasonal variability of the African convection, and at last on the interannual to multi-decadal variability of the monsoon including the global change of climate.

**Keywords:** African monsoon, atmosphere, climate, ocean, precipitation

## INTRODUCTION

Ocean is a fundamental part of the climate dynamics of the Earth, in particular in the Tropics. The most well-known phenomena illustrating this issue is the El Niño event in the Pacific which modifies drastically the atmospheric circulation not only in the Tropics through the coupled ocean-atmosphere ENSO (El Niño / Southern Oscillation) system, but also in mid-latitudes by perturbing atmospheric teleconnection systems like the PNA (Pacific / North America) Oscillation. To illustrate this question, the example of the West African monsoon and its links with the global climate is reviewed here taking into account the most recent results published in international literature.

## THE ANNUAL CYCLE OF RAINFALL OVER WEST AFRICA

The mean seasonal cycle of rainfall over West Africa is presented on Fig. 1 through a latitude cross-section. It corresponds to a south-north-south displacement of the Inter-Tropical Convergence Zone (ITCZ), which is not a smooth one but is characterized by a succession of active phases and pauses in the convective activity. These different steps have been identified statistically by Louvet *et al.* (2003). Two of them are located at the time of the first rainy season along the Guinean Coast in April and May, the third one is what is called the “monsoon onset” at the end of June, and a weaker one occurs during the monsoon season in August. The monsoon onset is the strongest one and corresponds to a weakening of the convective activity associated with an abrupt shift to the north of the ITCZ, from 5°N to 10°N (Le Barbé *et al.*, 2002, Sultan and Janicot 2003, Gu and Adler 2004). Over the period 1968-2004, its average date is June 24<sup>th</sup>, with a standard deviation of 7 days.

The mechanism associated to this abrupt ITCZ shift is still unclear and it is one of the scientific objectives of the AMMA (African Monsoon Multidisciplinary Analysis<sup>1</sup>) project (2005-2007). One hypothesis highlights the role of the Saharan thermal low, which increases at the time of the onset, leading to higher moisture advection inland, and which could be due to some interactions with the North Africa orography (Drobinski *et al.*, 2005) combined with the spatial distribution of albedo and net shortwave radiative budget at the surface (Ramel 2004).

Outside of any forcing from the atmospheric circulation over the land, the coupled air-sea character of the African monsoon is well-known and could regulate the different steps of the ITCZ annual cycle. The annual cycle of the sea surface temperature (SST) in the Gulf of Guinea is asymmetrical with a rapid cooling from the highest SST in April to the lowest SST in August. The fact that SST begins to cool in April, that is at the onset of the first rainy season along the Guinean Coast, is probably not a coincidence. This evolution results from positive feedbacks between the enhancement of the monsoon winds above the Guinea Gulf associated with the convection enhancement in the ITCZ, the set-up of the equatorial upwelling, the extension of the cooling in the southern tropical Atlantic associated with the strengthening

---

<sup>1</sup> <http://amma.mediasfrance.org/>

of the Santa Helena anticyclone and the enhancement of the southern Hadley circulation, and the occurrence of low-level stratus clouds over these cold waters (Okumura and Xie 2004).

This scenario has been examined recently both through new observational datasets and modelling experiments. Gu and Adler (2004) confirmed it by using recent satellite observation of the 1998-2003 high-quality Tropical Rainfall Measuring Mission (TRMM), water vapour and cloud liquid water, TMI SST, and QuikSCAT surface wind products. Okumura and Xie (2004) tested the impact of the SST in the Guinea Gulf on the West African monsoon. They compared in modelling experiments the evolution of the monsoon forced in an atmosphere model by the annual cycle of the SST with this evolution where the annual cycle of the SST is held constant in time from mid-April onward. They showed that the equatorial cooling exerts a significant influence on the African monsoon by intensifying the southerly winds in the Guinea Gulf and pushing the continental rainband inland. This evolution feeds back positively: first, it contributes to trigger this oceanic cooling in the east; second, easterly winds accelerate in the equatorial Atlantic during northern summer, inducing local upwelling and raising the thermocline in the east, and contributes to the propagation of the cool equatorial SST westward. In a set of experiments, Biasutti *et al.* (2003, 2004, 2005) investigated the mechanisms controlling the annual cycle of the ITCZ over West Africa and the tropical Atlantic by comparing the relative importance of insolation over land and of the SST. As for Okumura and Xie (2004), they compared the evolution of the ITCZ in an atmospheric model between a realistic annual cycle and an annual cycle where SST and/or insolation is held constant in time from March onward. They concluded that West African rainfall is significantly influenced by SST through the advection of marine boundary layer temperature anomalies over Africa which causes the development of sea level pressure and surface wind convergence anomalies. They showed also that the seasonal changes in insolation control the seasonal changes in the net budget of energy input in the atmospheric column, which is balanced by horizontal energy export in the thermally direct circulation associated to convection in the ITCZ. This modulates the moisture flow advection inland and controls the rainfall production over West Africa.

### **Intra-seasonal variability of rainfall during the northern summer over West Africa**

It is shown on Fig. 1 that the annual cycle of the ITCZ is not regular and is characterized by fluctuations at shorter time scales and especially at intra-seasonal time scales, e.g. between 10 and 90 days (Sultan *et al.*, 2003). Grodsky and Carton (2001) investigated the origin of quasi-byweekly disturbances in the surface winds observed over the tropical Atlantic with the QuikSCAT measurements. This oscillation in the wind field is due to the modulation of its zonal component and it is associated with a zonal dipole of rainfall intensity in the ITCZ between the Guinea Gulf and the western Atlantic. They suggested that this quasi-stationary oscillation is controlled by coupled land-atmosphere interactions in the West African monsoon, including a feedback cycle between the monsoon winds and clouds development in the ITCZ, soil moisture and land surface temperature, and the zonal pressure gradient between the land and the ocean. The larger scale context of this oscillation has been described by Mounier and Janicot (2004) through a Principal Component Analysis of outgoing longwave radiation (OLR) satellite measurements signing the activity of the ITCZ. They identified two independent modes of variability of the convection in the area at a time scale of about 15 days. The first one, linked to Grodsky and Carton results, is characterized by a stationary dipole of convection between West/Central Africa and the western equatorial Atlantic, modulating the low-level zonal wind component over the equatorial Atlantic. The second one depicts a meridional dipole of convection over West Africa linked to the modulation of the ITCZ latitude and associated with a westward propagative signal over the Sahel initiated over Central Africa. This second mode is similar to the signal previously identified over the Sahel by Sultan *et al.* (2003).

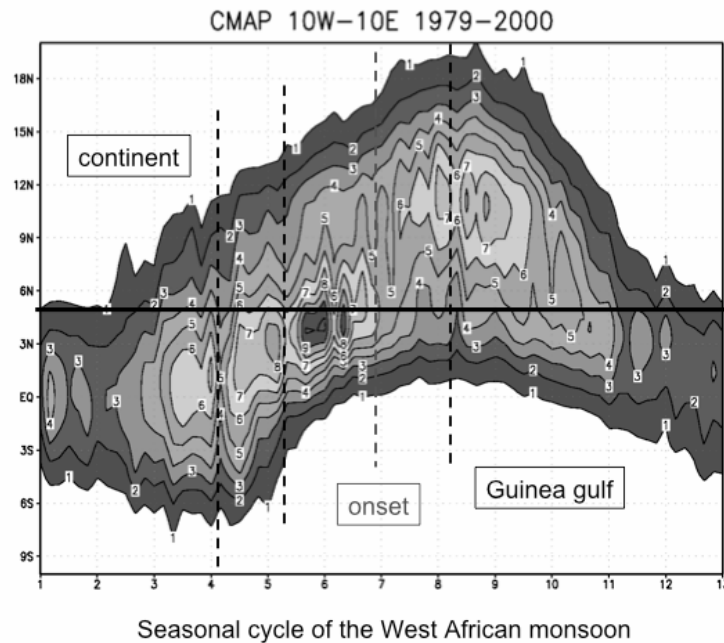


Fig. 1: The mean seasonal cycle of rainfall over West Africa through a latitude cross-section. Precipitation values ( $\text{mm}\cdot\text{day}^{-1}$ ) from CMAP dataset are averaged over  $10^{\circ}\text{W}$ - $10^{\circ}\text{E}$  and over the period 1979-2000. The black horizontal line represents the Guinean coast. Vertical lines represent the different steps of the annual cycle, detected through Varimax Principal Component Analysis (Louvet *et al.*, 2003). The red vertical line corresponds to the summer monsoon onset.

At longer time scales, Matthews (2004) highlighted the role of the Madden-Julian Oscillation (MJO) on the convective activity in the African monsoon. About twenty days prior to a maximum of convection over West Africa detected by the first main mode of convective activity at 30-70-day variability, convection is reduced over the equatorial warm pool. An equatorial Kelvin wave response to this change in warm pool convection propagates eastward and an equatorial Rossby wave response propagates westward. These two waves complete a circuit of the equator and meet up 20 days later over Africa, inducing convection enhancement through an increase of the boundary layer monsoon flow and moisture supply.

### **Interannual variability of rainfall during the northern summer over West Africa**

While the annual cycle is the main signal of the African monsoon, interannual and decadal time scales variability of precipitation over West Africa and especially the Sahel is very high and modulates significantly the annual cycle of the monsoon. Fig. 2 shows the well-known time series of rainfall anomalies over the Sahel, updated over the period 1898-20004. While the first part of the XX<sup>th</sup> century has been characterized by a succession of short wet and dry periods, the second part of the century has known a very unusual evolution of rainfall with a 20-year wet period followed by another 20-year dry period. Since the 1990's, no more persistence is evident and we see an unorganized occurrence of wet and dry years. This long-term negative trend of rainfall has an amplitude that has not been observed anywhere in the world during this century (see Fig. 3).

A lot of papers have been published since the 1970's to investigate the causes of such a trend. Two main factors have been involved, the evolution of SST at the global scale and the desertification and deforestation at the regional scale of West Africa due to the anthropogenic pressure. In this paper, we describe the most recent results involving the role of the ocean only.

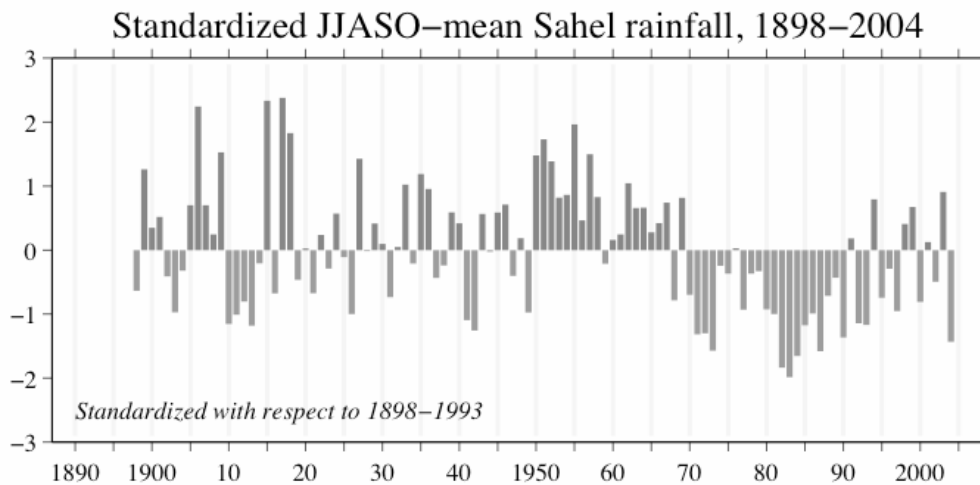


Fig. 2: Standardized mean Sahel rainfall index June-October from 1898 to 2004. From Todd Mitchell; [http://tao.atmos.washington.edu/data\\_sets/sahel/](http://tao.atmos.washington.edu/data_sets/sahel/); Joint Institute for the Study of the Atmosphere and Ocean.

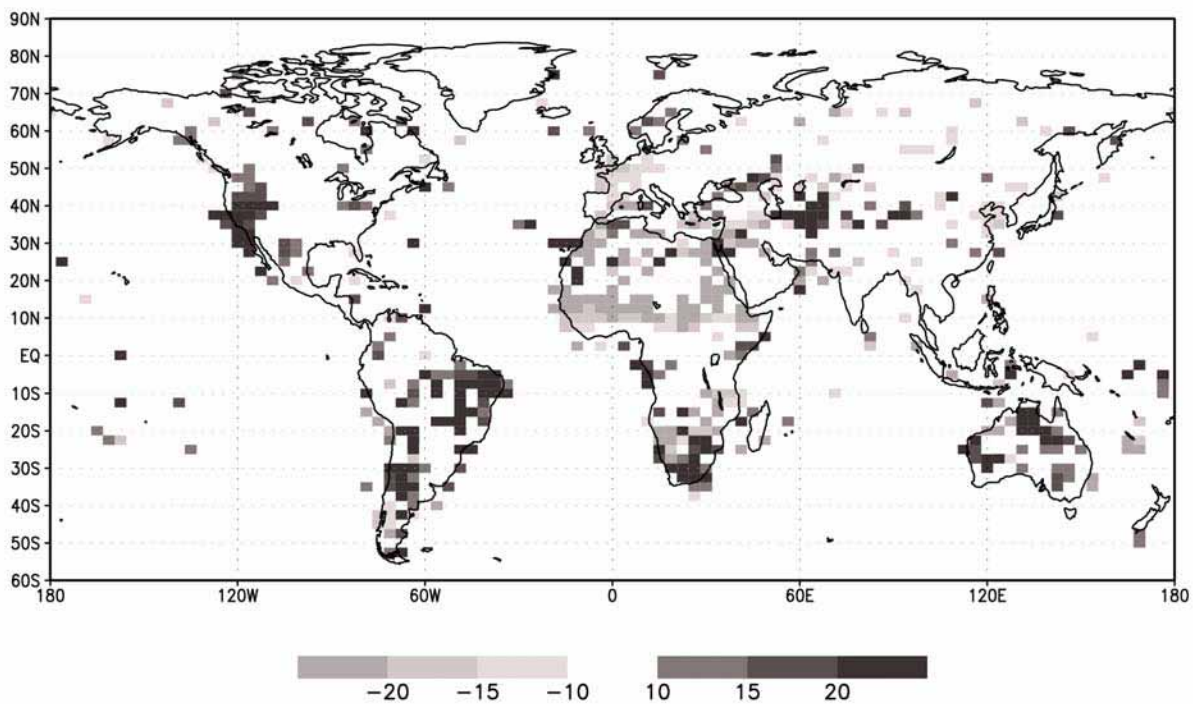


Fig. 3: Mean rainfall differences between the period 1970-1990 and the period 1950-1970 expressed in percentage of the mean over the period 1950-1990. Anomalies lower than 10% in absolute value are not represented.

Fig. 4 shows the four main modes of interannual and decadal time scales variability of SST at the global scale, computed from a Varimax Principal Component Analysis on de-seasonalised SST anomalies over the period 1945-1994. The first mode (“Global Tropical”) depicts the El Niño - La Niña occurrences at interannual time scale with the highest weights located in the Pacific and the Indian oceanic basins. We see also on this pattern the effect of El Niño events in weakening the northern Atlantic trade winds and enhancing SST in the western tropical Atlantic. The second mode (“Global Extratropical”) has a decadal time scale evolution with a reversal of sign between the period 1945-1973 and the period 1974-1994. The weight pattern is dominated by the Indian oceanic basin and depicts a contrast between the SST anomalies in the Southern oceans and the Northern basins. If these two first modes have a global scale extension, the third (“North Atlantic”) and fourth (“South Atlantic”) modes are regional ones. They cover

respectively the northern and the southern parts of the Atlantic Ocean and show a quasi-decadal time scale variability.

All of these modes show more or less high connection with Sahel rainfall variability. One of the recent key published papers is the work of Giannini *et al.* (2003) examining the oceanic forcing of Sahel rainfall on interannual and interdecadal time scales. Through diagnostic analysis and an ensemble of integrations of an atmospheric model forced only by observed SST over the period 1930–2000, they show that variability of rainfall in the Sahel results from the response of the African monsoon to oceanic forcing, amplified by land-atmosphere interaction. In particular the decadal scale drying trend in the Sahel is attributed to warmer-than-average low-latitude water around Africa, and especially in the Indian oceanic basin. This impact of this global SST mode including the Indian Ocean on decadal-scale Sahelian rainfall was also found by Janicot *et al.* (2001), and Bader and Latif (2003), and Chelliah and Bell (2004) showed its impact on the global atmospheric circulation in the Tropics.

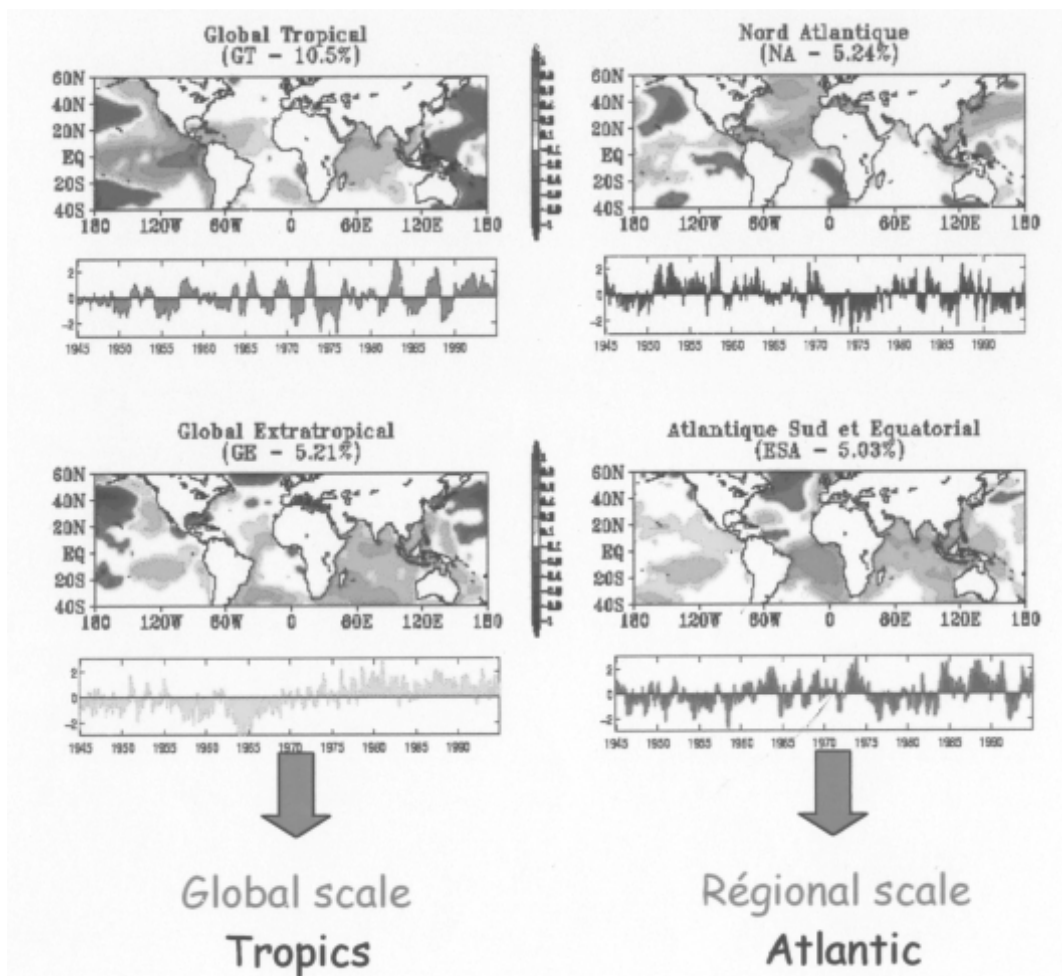


Fig. 4: Varimax Principal Component Analysis of the sea surface temperatures anomalies from 1945 to 1994 (provided by Centre de Recherches de Climatologie, Univ. Dijon). The four main modes are presented through their spatial pattern and time series. See details in the text.

At the interannual time scale, the impact of El Niño events of Sahel drought has been described in several papers including for the most recent ones Rowell (2001), Janicot *et al.* (2001), Giannini *et al.* (2003). Rowell (2001) examined in details the mechanisms of this atmospheric teleconnection between the Pacific Ocean and Africa. He demonstrated, as for the mechanism linking MJO and African convection variability (Matthews 2004), the role of the development of equatorial eastward propagating Kelvin wave from east Pacific convective heating anomalies, and westward propagating Rossby waves from the Indian Ocean in response to the anomalous west Pacific–Indian Ocean SST gradients via convective heating

anomalies over the Indian Ocean. These interact over Africa to enhance large-scale subsidence over the Sahel and reduce seasonal rainfall totals. Janicot *et al.* (2001) showed that this Sahel–El Niño teleconnection has not been strong during the whole second part of the last century but has been significantly modulated by the decadal time scale SST anomaly pattern during this period. The long-term warming of the global SST mode, not only favours the long-term drying over the Sahel, but helps also to enhance the atmospheric teleconnection pattern linking El Niño events to Sahel rainfall deficits after 1980, through a fill-in of the monsoon trough and a moisture advection deficit over West Africa.

West African monsoon and ocean are also linked at the regional scale. It is well-known that warming events in the Guinea Gulf are associated with a southward location of the ITCZ and higher (lower) seasonal rainfall amounts over the Guinea Coast (Sahel) during the summer monsoon season. This is due in part to the reduced meridional gradient of temperature between the Guinea Gulf and West Africa. Vizy and Cook (2001) showed also that such an event enhances evaporation, and that the southerly flow across the Guinean Coast carries more moisture inland. This leads to increased precipitation south from the usual latitude of the ITCZ. This was confirmed by Bader and Latif (2003), among others. This scenario associates frequently a meridional anomaly of the ITCZ latitude to a rainfall dipole over West Africa between the Guinea Coast and the Sahel, and to the occurrence of what is called the “tropical Atlantic dipole” combining SST anomalies of one sign in the northern tropical Atlantic with SST anomalies of opposite sign in the equatorial and southern tropical Atlantic. It occurred very often before 1970, but after that, the rainfall dipole over West Africa has been less frequent and the Pacific-Indian ocean forcing has become more and more dominant (Janicot *et al.*, 2001).

Another ocean–African monsoon relationship at the regional scale concerns the role of the SST anomalies in the Mediterranean Sea. Rowell (2003) explored this teleconnection by forcing an atmospheric model in northern summer with idealized SST anomalies in this basin (positive (negative) anomalies up (down) to 2°C) with climatological SST elsewhere. This experiment shows that positive Mediterranean SST anomalies leads to a wetter Sahel : local evaporation enhances over this basin, increasing the moisture content in the lower troposphere; this additional moisture is advected southward across the eastern Sahara by the mean flow, leading to enhanced low-level moisture convergence over the Sahel which feeds enhanced rainfall. Then positive feedbacks between convection and the local atmospheric circulation help to extend this anomaly. Raicich *et al.* (2003) showed that Sahel rainfall is sensitive to sea level pressure anomalies over the Mediterranean Sea and especially to a zonal pressure dipole at these latitudes which is modulated in part by the activity of the Indian monsoon.

### **Scenarios of the climate change impact on the West African monsoon**

Simulations of the climate change impact on the West African monsoon must be considered with great caution. Such scenarios are based on integrations of ensembles of coupled ocean-atmosphere climate models combined with projections of various socio-economical developments. At the global scale, uncertainties come for an equal part from weaknesses of the models and incomplete knowledge of the future economical orientation. At the regional scale, uncertainties are larger, due in particular to the non-capability of the models to simulate accurately the small-scale processes. Another problem, specific to the simulation of the West African monsoon, is the existence of a warm bias in the SST of the eastern oceanic basins in the coupled models. This is true for the eastern part of the southern tropical and equatorial Atlantic, which induces a weaker than normal African monsoon as we have seen above. It is however possible to analyse such scenarios after having eliminated this permanent bias.

The scenarios which have been produced for the Third Report of the Intergovernmental Panel on Climate Change (IPCC) in 2001 do not provide a coherent response for West Africa and the Sahel region, even if they go in average towards a slight increase of rainfall and of the water cycle of the African monsoon. Available new simulations seem to confirm this scenario with a northward shift of the Sahara in a number of models (Liu *et al.*, 2002). For instance, Maynard *et al.* (2002) showed with a transient climate simulation of 150 years increased monsoon rainfall over West Africa at the end of the XXI<sup>st</sup> century with an enhancement of the atmospheric water cycle. The main factors explaining this evolution are the relative increase of the moisture content and atmospheric moisture transport, greater than the rainfall and evaporation relative increases, which means a weaker atmospheric water recycling. Work is presently going on towards the next publication of the fourth report of IPCC.

## **Conclusion**

This paper has presented a short review of the most recent papers dealing with the connections and interactions between the ocean and the West African monsoon. More work is necessary to better understand the teleconnection mechanisms and the degree of coupling between the ocean and the atmosphere. Available ocean-atmosphere coupled models show significant interactions between the African monsoon system, the air-sea fluxes and the oceanic circulation (see for instance Zhao *et al.*, 2005). However these models must to be improved to eliminate their biases, particularly important in the equatorial and southern tropical Atlantic, and which limits the confidence that we can have on their results.

Ocean is not the only factor explaining the African monsoon variability from intra-seasonal to multi-decadal time scales. Another crucial factor is the interactions with the land surface processes and the role played by the soil moisture and the vegetation (see for instance Douville 2002, Philippon and Fontaine 2002). However in-situ data are very few to quantify these processes and evaluate the results produced by the climate models. This is one of the objectives of the AMMA project which is implementing in West Africa over two and three seasonal cycles a network of flux stations measuring the radiative budget at the surface, sensible and latent heat fluxes, and soil moisture profiles.

Statistical schemes of seasonal forecast of summer Sahel rainfall totals work well when they integrate both oceanic and derived land surface information (Fontaine *et al.*, 1999), as well as statistico-dynamical models predicting atmospheric indexes closely linked to the monsoon intensity rather than rainfall (Garric *et al.*, 2002). However forecasts from climate models do not work as well over West Africa, and to monitor and forecast monsoon variability in the changing climate where we live now, a high quality of these tools will be absolutely necessary.

## **ACKNOWLEDGEMENTS**

The author thanks all the members of the Work Package *West African Monsoon and the Global Climate* of the international project AMMA (African Monsoon Multidisciplinary Analyses) for helping to review the most recent published results of this topic and for fruitful discussions.

## **REFERENCES**

- Bader, J. and M. Latif (2003) The impact of decadal-scale Indian ocean SST anomalies on Sahelian rainfall and the North Atlantic Oscillation. *Geophys. Res. Lett.*, 30, 2169, doi:10.1029/2003GL018426.
- Biasutti, M, Battisti, D.S. and Sarachik, E.S. (2003) The Annual Cycle over the Tropical Atlantic, South America, and Africa. *J. Climate*, 16, 2491-2508.
- Biasutti, M, Battisti, D.S. and Sarachik, E.S. (2004) Mechanisms controlling the annual cycle of precipitation in the Tropical Atlantic sector in an AGCM. *J. Climate*, 17, 4708-4723.
- Biasutti, M, Battisti, D.S. and Sarachik, E.S. (2005) Terrestrial influence on the annual cycle of the Atlantic ITCZ in an AGCM coupled to a slab ocean model. *J. Climate*, 18, 211-228.
- Chelliah, M and Bell, G.D. (2004) Tropical multidecadal and interannual climate variability in the NCEP-NCAR reanalysis. *J. Climate*, 17, 1777-1803.
- Douville, H (2002) Influence of soil moisture on the Asian and African monsoons. Part II: Interannual variability. *J. Climate*, 15, 701-720.
- Drobinski, P., Sultan, B. and Janicot, S. (2005) Role of the Hoggar mountain in West African monsoon onset. *Geophys. Res. Lett.*, 32, L01705, doi :10.1029/2004GL020710.
- Garric, G., Douville, H. and Deque, M. (2002) Prospects for improved seasonal predictions of monsoon precipitation over Sahel. *Int. J. Climatol.*, 22, 331-345.
- Giannini, A., Saravanan and Chang, (2003) Ocean forcing of Sahel rainfall on Interannual to Interdecadal time-scales. *Science*, 302, 1027-1030.
- Grodsky, S.A. and Carton, J.A. (2001) Coupled land/atmosphere interactions in the West African monsoon. *Geophys. Res. Lett.*, 28, 1503-1506.
- Gu, G. and Adler, R.F. (2004) Seasonal evolution and variability associated with the West African monsoon system. *J. Climate*, 17, 3364-3377.

- Janicot, S., Trzaska, S. and Pocard, I. (2001) Summer Sahel-ENSO teleconnection and decadal time scale SST variations. *Clim. Dyn.*, 18, 303-320.
- Le Barbe, L., Lebel, T. and Tapsoba, D. (2002) Rainfall variability in West Africa during the years 1950–90. *J. Climate*, 15, 187–202.
- Liu, P., Meehl, G.A. and Wu, G.X. (2002) Multi-model trends in the Sahara induced by increasing CO<sub>2</sub>. *Geophys. Res. Lett.*, 29, 1881.
- Louvet, S., Fontaine, B. and Roucou, P. (2003) Active phases and pauses during the installation of the West African monsoon through 5-day CMAP rainfall data (1979-2001). *Geophys. Res. Lett.*, 30, 10.1029/2003GL018058.
- Maynard, K., Royer, J.F. and Chauvin, F. (2002) Impact of greenhouse warming on the West African summer monsoon. *Clim. Dyn.*, 19, 499–514.
- Matthews, A.J. (2004) Intraseasonal Variability over Tropical Africa during Northern Summer. *J. Climate*, 17, 2427-2439.
- Mounier, F. and Janicot, S. (2004) Evidence of two independent modes of convection at intraseasonal timescale in the West African summer monsoon. *Geophys. Res. Lett.*, 31, L16116, doi :10.1029/2004GL020665.
- Okumura and Xie (2004) Interaction of the Atlantic Equatorial Cold Tongue and the African Monsoon. *J. Climate*, 17, 3589-3602.
- Philippon, N. and Fontaine, B. (2002) The relationship between the Sahelian and previous second Guinean rainy seasons: a monsoon regulation by soil wetness? *Ann. Geoph.*, 20, 575-582.
- Raichich, Pinardi and Navarra (2003) Teleconnections between Indian monsoon and Sahel rainfall and the Mediterranean. *Int. J. Climatol.*, 23, 173-186.
- Ramel, R. (2004) *Impacts des processus de surface sur le climat en Afrique de l'Ouest*. Thèse LTHE, Grenoble.
- Rowell, D.P. (2001) Teleconnections between the tropical Pacific and the Sahel. *Q.J.R. Met. Soc.*, 127, 1683-1706.
- Rowell (2003) The impact of Mediterranean SSTs on the Sahelian rainfall season. *J. Climate*, 16, 849–862.
- Sultan, B., Janicot, S. and Diedhiou, A. (2003) The West African Monsoon Dynamics. Part I: Documentation of Intraseasonal Variability. *J. Climate*, 16, 3389–3406.
- Sultan, B. and Janicot, S. (2003) The West African monsoon dynamics. Part II: The pre-onset and the onset of the summer monsoon. *J. Climate*, 16, 3407-3427.
- Vizy, E.K. and Cook, K.H. (2001) Mechanisms by Which Gulf of Guinea and Eastern North Atlantic Sea Surface Temperature Anomalies Can Influence African Rainfall. *J. Climate*, 14, 795-821.
- Zhao, Y., Braconnot, P., Marti, O., Harrison, S.P., Hewitt, C., Kitoh, A., Liu, Z., Mikolajewicz, U., Otto-Bliesner, B. and Weber, S.L. (2005) A multi-model analysis of the role of the ocean on the African and Indian monsoon during the mid-Holocene. *Clim. Dyn.*, revised version.

# PREDICTABILITY OF THE SHORT RAINS IN NORTHEAST TANZANIA

**Patrick VALIMBA, Simon H. MKHANDI**

Department of Water Resources Engineering, Faculty of Civil Engineering and the Built Environment, University of Dar Es Salaam, P.O. Box 35131, Dar Es Salaam, Tanzania.

*pvalimba@hotmail.com*

## ABSTRACT

Multiple linear regression (MLR) models were developed between regional rainfall amounts in each class of daily rainfall (predictands) for each of the two coherent regions in Northeast Tanzania and Southern Oscillation Index (SOI) and Sea Surface Temperatures (SSTs) (predictors) in the selected influencing basins in the Atlantic and Indian Oceans. To reduce the influences of changes in the relationships between rainfall and climatic variables in the 1960s and mid-1980s, the models were developed separately for the pre- and post-1970 periods. Those developed for the period 1970-1984 were checked using the 1970-1998 period and then used to produce rainfall hindcasts/forecasts.

Results indicated i) high model efficiencies, ii) high prediction skills during strong El Niño-Southern Oscillation (ENSO) events and low skills during moderate/weak ENSO and non-ENSO events and iii) the importance of SSTs in the Somali and South Madagascar (Agulhas) basins for the occurrence of intense rainfall amounts during ENSO events. The models further indicated that SSTs in the Somali (which are influenced by ENSO phenomenon) contributed respectively about 37% and 68% of the anomaly sign of the OND overall intense rainfall amounts during the strong 1982 and 1997 El Niños. The Agulhas SSTs contributed 28% and 11% during the 1982 and 1997 El Niños respectively suggesting a reduced influence of the Agulhas SSTs with an increase of the strength of the El Niño event. The influence of Agulhas SSTs remained positive contrasting those of Somali SSTs and SOI during La Niña years. The models results therefore highlighted the importance of the communication of an ENSO signal into local water on the occurrence of intense rainfall events. Moreover, the 1-2 months lead of climatic variations provide a valuable moderate forecast period for the defence against the impacts of flood producing intense rainfalls.

**Keywords:** rainfall intensities, ENSO, SST, multiple linear regression models, coherent regions

## INTRODUCTION

There have been significant global scale changes in oceanic and atmospheric conditions in the 1960s through 1970s. They include warming of the tropical Pacific and Indian Oceans in the late 1970s (Trenberth, 1990, Kerr, 1992, Wang, 1995, Trenberth and Hoar, 1996), of the southwest Indian Ocean in the 1970s (Trzaska *et al.*, 1996) and of surface air temperatures after 1960 (IPCC, 2001). According to Flohn and Kapala (1989), the warming of the tropical troposphere in the 1960s could have contributed to the delayed oceanic warming in low latitudes in the 1970s. Some of the consequences are an increase in the frequency and amplitude of warm ENSO events since the mid-1960s (Gu and Philander, 1995, Kestin *et al.*, 1998, Torrence and Compo, 1998), changes of ENSO/SST-southern Africa rainfall relationships (Richard *et al.*, 2000; Valimba, 2004; Valimba *et al.*, 2004b) and changes of rainfall and streamflow characteristics in eastern and southern Africa in the 1960s through 1970s (Valimba, 2004; Valimba *et al.*, 2004a, Valimba *et al.*, 2005). The changes generally led to a declining occurrence of light rainfalls across much of southern Africa and increasing the occurrence of intense rainfalls in certain areas in the region particularly the eastern part of the sub-continent. Moreover, flow changes were related to general flow decreases in some parts of the region like Namibia while in some other areas, such as the eastern Lake Victoria region, amplification of flow extremes with relatively no change of mean flows has been observed (Valimba *et al.*, 2005).

For appropriate management of water resources and provision of adequate defense against devastating floods and droughts, while improving the availability of water to southern African communities, it is important to properly predict the timing and behaviour of hydrological (rainfall and flow) extremes at relatively long lead times. This will allow for appropriate measures to be taken to safeguard people and property against floods and droughts. Forecasting models for these hydrological extremes are therefore necessary. Unfortunately, this area of prediction of hydrological extremes has received less attention despite its known negative impacts on socio-economic development. Most of the past studies (Mutai *et*

*al.*, 1998; Phillipon *et al.*, 2002) provide suitable models for “overall” unclassified seasonal rainfall amounts during the October-December (OND) short rains, which are not very relevant for hydrological extremes unless verified.

This study therefore attempts to incorporate the new advances that use the rainfall classification and dynamic ENSO/SST-rainfall relationships in forecasting models for the short rains in northeast Tanzania.

## DATA

Time series of regional rainfall, SST and SOI were adopted from the study of Valimba *et al.* (2004b) which investigated the relationships between interannual variations of rainfall amounts in different classes of daily rainfall amounts and SST and SOI. In summary, classes of daily rainfall amounts adopted from Valimba *et al.* (2004a) were based mainly on the impacts of these daily rainfall amounts upon water resources and socio-economic activities. They are the class 2 (1-9.9 mm) defining the light daily rainfall events, the moderate (10-19.9 mm, class 3) and moderate heavy (20-29.9 mm, class 4) daily events and the heavy class 5 (30-39.9 mm) and extreme heavy (or intense) class 6 ( $\geq 40$  mm) daily events. The latter classes, as well as the persistent class 5 rainfalls, are considered to be the major causes of flooding. Time series of cumulative seasonal rainfall amounts were established for each class at each station and their standardised series used to construct regional standardised series for each class. The two inland and coastal sub-regions in northeast Tanzania (Fig. 1) as distinguished by Principal Component Analysis (PCA) (Valimba *et al.*, 2004b) were used. Areal average series of SSTs in the selected four basins of Somali (SOM) and Agulhas (AGUL) in the Indian Ocean and Benguela (BENG) and South Atlantic Surface Ocean Current Recirculation Gyre (SACG) in the South Atlantic Ocean (Valimba *et al.*, 2004b) were computed from gridded data set from UKMET Office.

### Model development

Multiple Linear Regression (MLR) models were developed for the period 1950-1984. To suitably cater for operational forecasting purposes, the MLR models were developed mainly for the recent post-1970 period when most of the changes in the rainfall-climatic variables relationships were identified. The 1970-1984 period was then considered for the development of forecasting models whereas the records ended in 1984 to avoid an inclusion of inconsistent relationships identified in the mid-1980s (Valimba *et al.*, 2004b). To assess the impacts of changing relationships between rainfall and climatic variables, MLR models were also developed for the pre-change 1950-1969 and for the whole 1950-1984 period. Moreover, the suitability of the models established using records in the 1970-1984 period for forecasting use in the post-1984 period was assessed through a comparison of model estimates and computed rainfall anomalies in the 1985-1998 period.

The general MLR model for dependent variable Y on quasi-independent variables  $X_i$ s has the form

$$Y = a_0 + a_1X_1 + a_2X_2 + \dots + a_nX_n \quad (1)$$

where  $n$  is the number of predictors and  $a_i$  are the regression coefficients which represent the *independent* contributions of each independent variable to the prediction of the dependent variable.

Model performance was evaluated by the Nash-Sutcliffe (1970) coefficient of efficiency (CE) given by

$$CE = 1 - \frac{\sum (y_{obs} - y_{pred})^2}{\sum (y_{obs} - \bar{y}_{obs})^2} \quad (2)$$

where  $y_{obs}$  and  $y_{pred}$  are observed and predicted elements,  $\bar{y}_{obs}$  is the average of the observed elements and  $n$  is the record length.

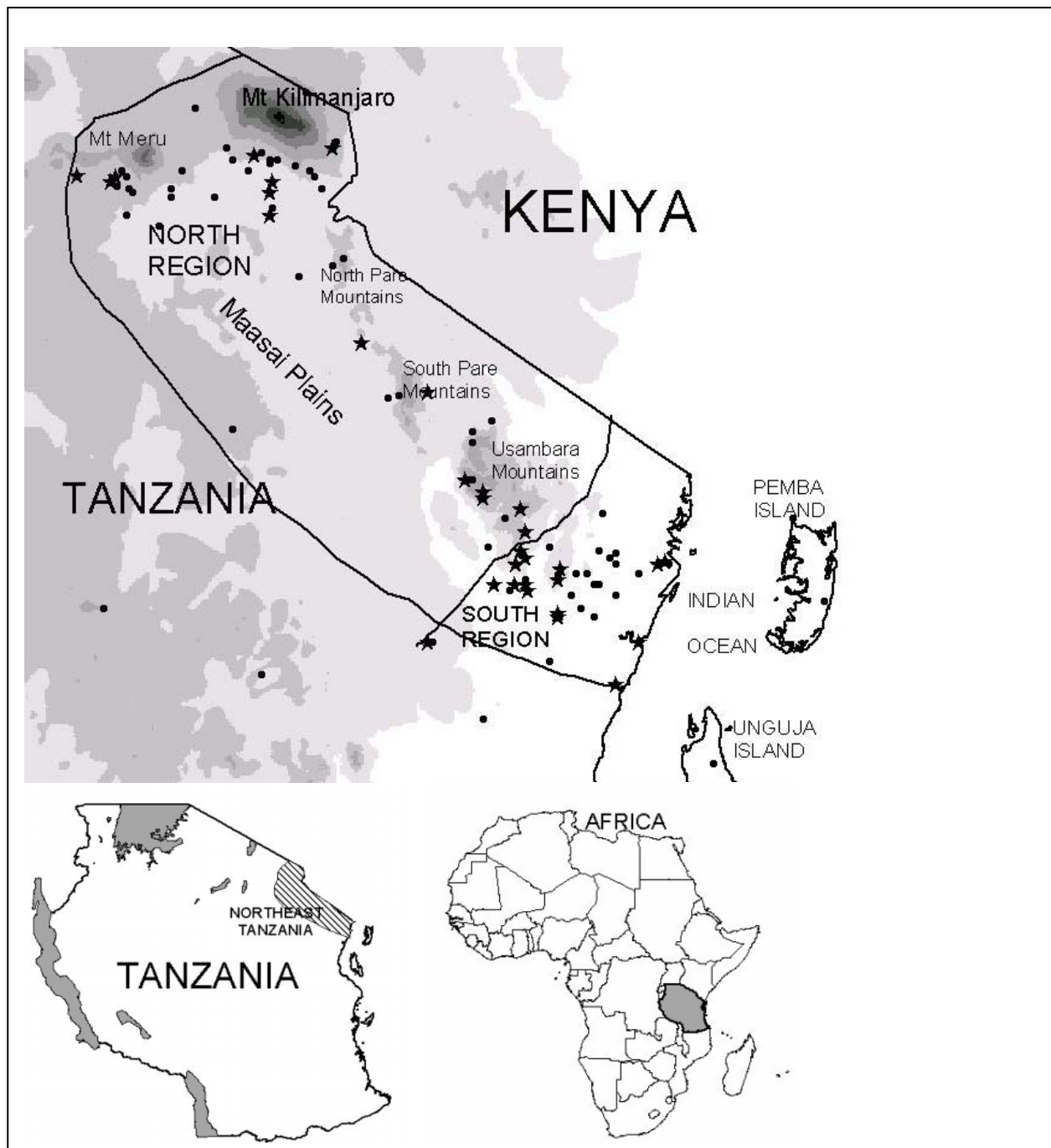


Fig. 1: Location of northeast Tanzania, the spatial distribution of rainfall stations and the general coherent rainfall regions. Stars represent stations which were used in this study while topography is shown on the background.

The results of correlation analysis between classified seasonal rainfall amounts and climatic indices (SOI and SSTs) indicated the influences of August, September and October SOI and SSTs on rainfalls during the short rains (Valimba *et al.*, 2004b). Moreover, the correlations usually peak at a lag of 0-2 month and therefore a one-month lead of climatic variables against rainfall was considered appropriate for forecasting purposes. Predictors for rainfall during the short rains were therefore September values of SOI, Somali and Benguela SSTs and August values of SACG and Agulhas SSTs. Despite the known high correlations between ENSO and SSTs in some of the selected ocean basins, the predictors were left for the MLR models to filter out the correlated variables. This was considered from the knowledge that local SSTs have significant influences on heavy/intense rainfall amounts particularly when warmer than normal (Valimba, 2004). The winds then advect the resulting high moisture over the warmer ocean basins into adjacent landmasses leading to the occurrence of intense rainfall events over the land.

# RESULTS

## Model parameters

The results of model fitting between rainfall anomalies in northeast Tanzania and SOI and SSTs in the selected ocean basins for the 1970-1984 period generated moderately high efficiencies. The parameters and anomalies of the retained predictors (Tab. 1 and 2) indicated the dominant influence of ENSO on all types of rainfall in northeast Tanzania. The efficiencies for the inland sub-region (Tab. 1) were consistently high for all classes of rainfall amounts while those in the coastal sub-region were moderately high for light and moderate (Class 2 and 3) and heavy (Class 5) rainfall amounts (Tab. 2). However, model efficiencies for moderate heavy (Class 4) and intense (Class 6) rainfall amounts in the coastal sub-region were below 50%. The models established for the post-change 1980-1998 and whole 1970-1998 periods gave similar low efficiencies (Tab. 1 and 2) reflecting the possible impacts of inconsistent relationships in the mid-1980s. It should be noted that despite the dominance of ENSO, the models consistently retained Agulhas SSTs in all periods, while Somali SSTs were retained in the post-change period. The Agulhas SSTs have the highest contributions on intense rainfalls in the inland sub-region (Tab. 1) while Somali SSTs have in the coastal sub-region (Tab. 2).

Similarly, models developed for the pre-change 1950-1969 period (not shown) showed moderately high efficiencies which were significantly reduced when the whole 1950-1984 period was used. A comparison of predictors retained in the 1950-1969 and 1970-1984 periods indicated the changing influences of ENSO and SSTs. While ENSO is dominant in the post-1970 period, SSTs in the SACG and Somali basins were contributing largely in the pre-1970 period. Consequently, the parameters of the established models using the whole 1950-1984 period represent an average state and could not be useful for operational forecasting of rainfall anomalies in northeast Tanzania.

Tab. 1: Model parameters for various classes of rainfall for the 1970-1984, 1980-1998 and 1970-1998 periods (Inland).

Class	Period	a	Predictor parameters					CE
			Sep SOI	Sep SOMALI	Aug AGUL	Aug SACG	Sep BENG	
2	1970 - 1984	-0.265	-0.3276	-0.0346	0.0826	0.0603	0.0286	56.7
	1980 - 1998	-0.319	-0.7446	-0.1004	0.1491		0.0736	33.1
	1970 - 1998	-0.201	-0.4812	-0.0358	0.0982	0.0120	0.0446	29.5
3	1970 - 1984	-0.015	-0.3866	0.0165	0.0813	0.0338	0.0431	71.8
	1980 - 1998	-0.184	-0.8914	-0.0402	0.0908		0.0937	42.6
	1970 - 1998	-0.028	-0.6101		0.0773		0.0524	39.9
4	1970 - 1984	-0.105	-0.2930	0.0193	0.0934	0.0589	0.0396	72.4
	1980 - 1998	-0.205	-0.4530		0.0631		0.0412	48.7
	1970 - 1998	-0.225	-0.3471	0.0095	0.0689	0.0326	0.0321	51.2
5	1970 - 1984	0.043	-0.4135	0.0022	0.0882	-0.0132	0.0304	67.9
	1980 - 1998	-0.291	-0.4605	0.0133	0.0987	-0.0239	0.0739	46.9
	1970 - 1998	-0.190	-0.3606	0.0118	0.0979	-0.0170	0.0404	45.5
6	1970 - 1984	0.020	-0.4612	0.0681	0.1352	-0.0215	0.0150	79.6
	1980 - 1998	-0.380	-0.4875	-0.0315	0.1334	0.0280	0.0585	48.2
	1970 - 1998	-0.309	-0.3834		0.1213	0.0238	0.0293	52.9

## Predictive skills

The plots of observed against hindcasted rainfall anomalies for the 1970-1984 training period indicated that models have moderately higher predictive skills for positive anomalies than for negative anomalies. This is exemplified in the plots for heavy (class 6) rainfall amounts (Fig. 2) which indicate wide scatters in the negative-negative domain (Fig. 2b). This low prediction skill of negative anomalies (e.g. Fig. 2a) contributed to low model efficiencies for classes 4 and 6 rainfalls in the coastal areas. A comparison of hindcasted and observed rainfall anomalies during the training period further indicates that the models failed to reproduce the anomaly signs mostly during non-ENSO years (Tab. 3). Moreover, the models for the inland sub-region forecast more accurately the rainfall anomaly signs during El Niño than during La Niña events in the 1985-1998 forecast period although the opposite is observed in the 1970-1984 training

period (Tab. 3). Out of the four El Niños in the 1985-1998 period, the models forecasted correctly the signs of rainfall anomalies in the inland sub-region in three events including the strong 1997 El Niño event.

Tab. 2: Model parameters for various classes of rainfall for the 1970-1984, 1980-1998 and 1970-1998 periods (Coastal).

Class	Period	a	Predictor parameters					CE
			Sep SOI	Sep SOMALI	Aug AGUL	Aug SACG	Sep BENG	
2	1970 – 1984	-0.683	-0.2268		0.0684	0.0736		61.1
	1980 – 1998	-0.835	-0.7016	-0.1541	0.1664			44.2
	1970 – 1998	-0.625	-0.3439	-0.0489	0.0768	0.0240	0.0303	26.2
3	1970 – 1984	-0.227	-0.4444		0.0559	0.0367	0.0472	70.6
	1980 – 1998	-0.168	-0.7116	-0.0745	0.1296		0.0816	50.1
	1970 – 1998	-0.046	-0.5135	-0.0033	0.0803	-0.0113	0.0719	53.1
4	1970 – 1984	-0.175	-0.3014		0.0964	0.0247	0.0445	49.9
	1980 – 1998	-0.123	-0.5034	-0.0395	0.0818	0.0144	0.0483	36.2
	1970 – 1998	-0.142	-0.4088		0.0803	0.0079	0.0307	39.6
5	1970 – 1984	-0.145	-0.4645	-0.0564	0.1315	0.0412	0.0471	65.2
	1980 – 1998	-0.323	-0.4506	0.0448	0.0836	0.0129	0.1012	35.2
	1970 – 1998	-0.290	-0.4053	0.0075	0.1280	0.0147	0.0512	38.4
6	1970 – 1984	-0.225	-0.3885			0.0983		49.7
	1980 – 1998	0.176	-0.4635	0.1334	0.0116	-0.0481	0.0283	22.8
	1970 – 1998	0.082	-0.5081	0.1159	0.0484	-0.0194	0.0143	32.9

Although the models were successful in predicting the anomaly signs during ENSO events, they frequently underestimated the magnitude of the anomalies during both training and forecasting periods. The models correctly predicted the signs of anomalies in all classes during the strongest 1982 and 1997 El Niños but significantly underestimated the magnitude of the anomalies (Tab. 4). The underestimation was higher during strong El Niño events than during weak events. The very wet (anomalies exceeding 1.5) OND 1997 season, for example, is predicted as wet or just above normal with the highest class 6 anomaly in the coastal sub-region being substantially underestimated. However, a comparison of model outputs during the 1977, 1982 and 1997 El Niños (Tab. 4) indicates more accurate hindcasts during the 1977 and 1982 El Niño than forecasts during the 1997 event. This was not an artifact of the model training period since models established for the 1980-1997 period produced good forecasts of the 1977 anomalies.

Tab. 3: Number of model failures to predict the correct sign of the anomalies. C stands for class e.g. C2 refers to class 2.

Period	Number of failures	Inland					Coastal					El Niño/La Niña Years*
		C2	C3	C4	C5	C6	C2	C3	C4	C5	C6	
1970-1984 (Training)	Total	2	4	4	4	1	2	3	1	4	5	1970,1971,1972,1973, 1974,1975,1976,1977, 1982,1984
	During El Niño	0	1	0	1	0	1	1	0	1	1	
	During La Niña	0	0	0	0	1	1	0	0	0	1	
1985-1998 (Forecasting)	Total	8	6	5	9	7	6	4	6	10	3	1986, 1988, 1993, 1994, 1995, 1997, 1998
	During El Niño	1	1	1	2	1	2	0	2	2	1	
	During La Niña	3	2	2	3	2	2	1	2	3	0	

\* From Trenberth, K. E., 1997: Definition of El Niño.

It was then tempting to reveal the underlying causes of such substantial underestimation of intense rainfall amounts in the coastal sub-region during the 1997 El Niño. An investigation of the spatial variation of daily rainfall amounts for the wettest periods during the wettest short rains (1961, 1968, 1982 and 1997, e.g. Fig. 3) indicated the occurrence of very heavy rainfall events in the Usambara Mountains and along the Indian Ocean coast. It was therefore presumed that local SSTs (in the Somali and Agulhas ocean basins), which are lacking in the 1970-1984 model for class 6 rainfalls in the coastal areas, could be the cause.

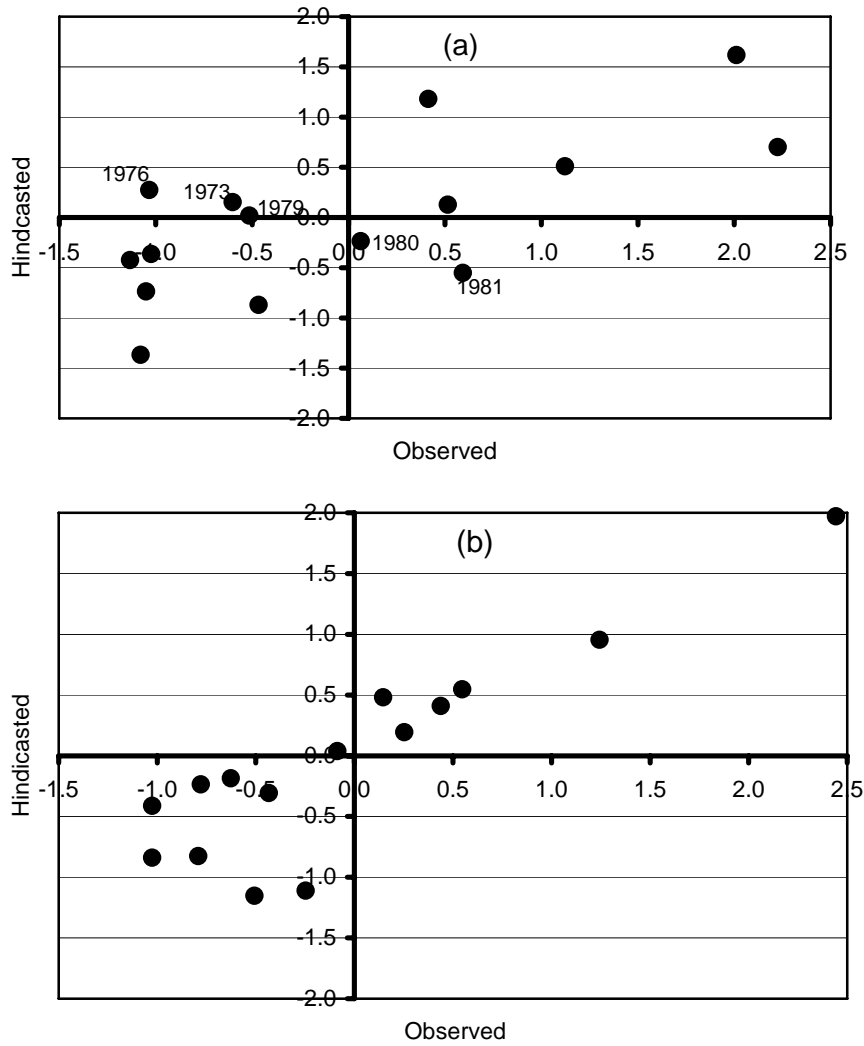


Fig. 2: Plots of observed against predicted OND class 6 rainfall amounts in the a) coastal and b) inland sub-regions in northeast Tanzania for the 1970–1984 training period.

Tab. 4: Forecasted (Pred) and computed (Obs) OND rainfall anomalies in northeast Tanzania during El Niño (red) and La Niña (blue).

Year	Inland Sub-region										Coastal Sub-region									
	CLASS 2		CLASS 3		CLASS 4		CLASS 5		CLASS 6		CLASS 2		CLASS 3		CLASS 4		CLASS 5		CLASS 6	
	Obs	Pred	Obs	Pred	Obs	Pred	Obs	Pred	Obs	Pred	Obs	Pred	Obs	Pred	Obs	Pred	Obs	Pred	Obs	Pred
1975	-1.11	-1.22	-0.93	-1.14	-0.98	-1.07	-0.81	-0.89	-1.03	-0.84	-0.62	-1.30	-1.12	-1.55	-0.51	-1.07	-0.99	-1.38	-1.08	-1.37
1988	0.35	-0.45	-0.54	-0.16	-0.83	-0.05	-0.25	0.00	-0.81	0.37	0.41	-0.79	0.90	-0.72	0.16	-0.04	0.43	-0.17	-0.29	-1.25
1977	0.16	0.43	1.11	0.60	0.82	0.57	0.40	0.42	0.15	0.48	-0.07	0.01	0.70	0.42	1.39	0.31	1.23	0.60	2.23	0.70
1982	1.39	1.09	1.81	1.55	1.63	1.49	1.72	1.36	2.44	1.97	1.08	0.63	1.73	1.25	1.21	1.16	2.05	1.56	0.41	1.18
1997	3.42	0.75	4.71	1.51	1.60	1.41	2.63	1.31	2.02	2.02	0.10	0.25	2.77	1.15	2.03	1.14	3.80	1.22	6.10	0.67

Tab. 5: Revised model parameters for intense (Class 6) rainfall amounts in the coastal sub-region.

Class	Period	a	Predictor parameters					CE(%)	C6 estimate	
			Oct SOI	Oct SOMALI	Aug AGUL	Aug SACG	Sep BENG		All	Som SST
6	1970 – 1984	-0.146	-0.4134	0.1169	-0.0194	0.0402	-0.0402	72.8	1.61	1.14
	1980 – 1998	-0.418	-0.4044	0.2992	0.0896	-0.0720	0.0283	54.5	4.02	2.91
	1970 – 1998	-0.016	-0.2358	0.2552	0.0704	-0.0534		57.4	3.09	2.48

Tab. 6: Variable contributions of Somali and Agulhas SSTs to intense rainfall anomalies in the coastal sub-region for selected El Niños and La Niñas.

Year	Total	Somali SST		Agulhas SST	
		Contr	% Contr	Contr	% Contr
1975	-1.71	-0.87	50.8	-0.03	1.8
1977	2.02	1.38	68.2	0.09	4.4
1982	1.82	0.67	36.9	0.51	28.1
1997	4.23	2.91	68.8	0.47	11.1

The models were then established for the 1980-1998 period, most of which retained Somali and Agulhas SSTs (Tab. 2). The one for class 6 rainfalls was used to provide the hindcast of class 6 rainfall anomalies in the coastal sub-region. This model produced an anomaly of 2.05 against the former 0.67 (Tab. 4). However, when only SOI and Somali SSTs were used, the model still produced an anomaly of magnitude 1.97, slightly less than 2.05 suggesting that Somali SSTs are more influential in the occurrence of intense rainfalls in northeast Tanzania during the short rains than Agulhas SSTs.

Further attempts aiming at investigating the effects of the peaking influence of SOI and Somali SSTs (in October) used October values of SOI and Somali SST to fit the MLR models for the 1970-1984 and 1980-1998 periods. The models retained SOI and SSTs in all four ocean basins as predictors (Tab. 5). The results indicated significantly improved model efficiencies and an enhanced influence of Somali SSTs (Tab. 5) compared to the use of September values (Tab. 2). The enhanced influence of Somali SSTs is indicated by increased parameter values which correspond to increased magnitude of the forecasted/hindcasted anomaly. For the 1970-1984 period, the parameter of the model related to Somali SSTs is 0.1169 (Tab. 5) and the computed class 6 anomaly is 1.61. The parameter and anomaly magnitude almost tripled for the 1980-1998 established model (Tab. 5). When parameters for SOI and SSTs in the other basins were kept to zero, SSTs in the Somali still predict high anomalies (Tab. 5 last column) suggesting that they have important influences on the occurrence of intense rainfall events along the coast of northeast Tanzania. This is confirmed by the high contribution of Somali SSTs on the total class 6 anomaly magnitude (Tab. 6). During the strong 1997 El Niño event, for example, the high Somali SST anomaly contributed more than two thirds of the predicted positive anomaly and negative anomaly during the strong 1975 La Niña event. These results further suggest that much of the influence of the Somali SSTs is experienced in October and could be missed in models which use long lead times.

This point is particularly important for intense rainfall amounts suggesting that their occurrence can best be predicted along the coastal areas at relatively shorter lead times. Correlation analysis between daily rainfall amounts at individual stations and daily Somali SSTs for selected wettest periods during the short rains (e.g. the 4<sup>th</sup>–9<sup>th</sup> November 1961, 17<sup>th</sup>–24<sup>th</sup> October 1997, etc) indicated correlation peaks at lags of 3-6 days and 10-21 days with warmer Somali SSTs leading the occurrence of intense rainfall amounts in coastal northeast Tanzania.

## CONCLUSIONS

This modelling study attempted to provide preliminary forecasting tools for different types of rainfall amounts during the short rains in northeast Tanzania to aid in the management of water resources in general and hydrological extremes (floods and droughts) in particular. The use of advances of rainfall classification and dynamic relationships between rainfall and climatic factors were beneficial to deriving appropriate operational forecasting models. The models developed confirmed the dominant influence of ENSO and changing contributions of SSTs in the Atlantic and Indian Oceans on different types of rainfall in northeast Tanzania. However, an investigative modelling procedure that aims at highlighting the cause of significant underestimation of the intense rainfall amounts along the coast during the 1997 El Niño event indicated that SSTs in the Somali were an important predictor of intense rainfall amounts. The model parameters and forecasts further indicated the importance of the coupling effect of ENSO conditions and warmer Somali and Agulhas SSTs on the occurrence of intense rainfall amounts in northeast Tanzania. This coupling could be a result of the communication of an ENSO signal into the Indian Ocean water. The results further suggested that models using long lead times may miss the peaking influences of SSTs in the Somali basin around October and consequently may underestimate significantly the magnitude of rainfall extremes in northeast Tanzania.

The study was the first modelling attempt to quantify the influence of various atmospheric and oceanic climatic factors on the occurrence of different types of rainfall amounts in northeast Tanzania. The approach used empirical multiple linear regression models and was restricted to a few important climatic factors (SOI and SSTs in Atlantic and Indian Oceans). It is therefore recommended to incorporate other climatic variables such as atmospheric winds, moisture flux, etc in these empirical models. To further our understanding of the extreme rainfalls-climatic variations, it is also considered important to use regional general circulation models forced with specific climatic conditions in the key regions to simulate the extreme rainfalls.

## REFERENCES

- Flohn, H. and Kapala, A. (1989) Changes of tropical sea-air interaction processes over 30-year period, *Nature*, 338, 244–246.
- Gu, D. and Philander, S.G.H. (1995) Secular changes of annual and interannual variability in the tropics during the past century. *J. Climate*, 8, 864–876.
- IPCC (2001) *Climate change: The scientific basis*, Cambridge University Press, 881 p.
- Kerr, R.A. (1992) Unmasking a shifty climate system. *Science*, 255, 1508–1510.
- Kestin, T.S., Karoly, D.J., Yano, J.I. and Rayner, N.A. (1998) Time-frequency variability of ENSO and stochastic simulation. *J. Climate*, 11, 2258–2272.
- Mutai, C.C., Ward, N.M. and Colman, A.W. (1998) Towards the prediction of the east Africa short rains based on sea-surface temperature-atmosphere coupling. *Int. J. Climatol.*, 18, 975–997.
- Nash, J.E. and Sutcliffe, J.V. (1970) River flow forecasting through conceptual models: Part 1. A discussion of principles. *J. Hydrol.*, 10, 282–290.
- Phillipon, N., Camberlin, P., Fauchereau, N. (2002) Empirical predictability study of October-December East African rainfall. *Q.J.R. Met. Soc.*, 128, 2239–2256.
- Richard, Y., Trzaska, S., Roucou, P. and Rouault, M. (2000) Modification of the southern Africa rainfall variability/ENSO relationship since the late 1960s. *Clim. Dyn.*, 16, 883–895.
- Torrence, C. and Compo, G.P. (1998) A practical guide to wavelet analysis. *Bull. Amer. Meteor. Soc.*, 79, 61–78.
- Trenberth, K.E. (1990) Recent observed interdecadal climate changes in the northern Hemisphere. *Bull. Amer. Meteorol. Soc.*, 71, 988–993.
- Trenberth, K.E. and Hoar, T.J. (1996) The 1990-1995 El Niño-Southern Oscillation event: longest on record. *Geophys. Res. Lett.*, 23, 57–60.
- Trzaska, S., Moron, V. and Fontaine, B. (1996) Global atmospheric response to specific linear combination of the main SST modes. Part I: Numerical experiments and preliminary results. *Ann. Geophys.*, 14, 1066–1077.
- Valimba, P. (2004) *Rainfall variability in southern Africa, its influences on streamflow variations and its relationships with climatic variations*. PhD Thesis, Rhodes University.
- Valimba, P., Servat, E, Mkhandi, S.H. and Hughes, D. (2004a) Interannual variability of rainfall intensities in northeast Tanzania. *Submitted to Int. J. Climatol.*
- Valimba, P., Mkhandi, S.H., Servat, E. (2004b) Interannual variability of rainfall amounts in northeast Tanzania and its relation to ENSO and SST variations, *Submitted to Int. J. Climatol.*
- Valimba, P., Kimaro, T. and Mtalo, F.W. (2005) Streamflow changes in the Mara River Basin: An implication of the effects of landuse changes. *Proc of the International Conference on Monitoring, Prediction and Mitigation of Water-Related Disasters*, Kyoto (Japan), 12<sup>th</sup> –15<sup>th</sup> January 2005, 457-462.
- Wang, B. (1995) Interdecadal changes in El Niño onset in the last four decades. *J. Climate*, 8, 267–285.

# ASSESSING LARGE-SCALE HYDROCLIMATOLOGICAL VARIABILITY AND LINKAGES ACROSS NORTHWEST EUROPE

Daniel G. KINGSTON, David M. HANNAH, Glenn R. McGREGOR, Damian M. LAWLER

School of Geography, Earth and Environmental Science, University of Birmingham, Birmingham, B15 2TT, UK.  
*dgk366@bham.ac.uk*

## ABSTRACT

To assess the nature and extent of hydrological response to climatic change a clear understanding of process-linkages in the atmosphere-surface-runoff cascade is necessary. Such hydroclimatological linkages are poorly defined for northwest Europe. This research gap is addressed through a composite analysis of large-scale climatic controls on monthly high and low streamflow across this region for 1968-1997. Analyses are conducted for hydrological regions defined by hierarchical cluster analysis. Presentation and discussion of results focus on one region (northern and central-southern Norway) as a demonstration of the utility of this methodology. High streamflow is generally characterized by a more intense and easterly positioned Icelandic Low and Azores High, and an enhanced pressure gradient between these centres (compared to low streamflow situations). Atmospheric thickness is greater under high flow, as are 1000 hPa windspeeds. The results show limited evidence of a North Atlantic Oscillation signature in streamflow variation, although this requires further research.

**Keywords:** atmosphere-surface-runoff process cascade; composite analysis; hydroclimatology; North Atlantic Oscillation; northwest Europe; streamflow regionalization

## INTRODUCTION

Improving understanding of climatic causes of hydrological variability is an important research goal because such knowledge is vital to identifying water stress and developing strategies for management of water resources, particularly given IPCC predictions of climate change (Houghton *et al.*, 2001). Central to achieving this objective is better quantification of links in the atmosphere-surface-runoff cascade (referred to here as the hydroclimatological system). Indices of atmospheric circulation patterns are potentially useful in the development of explanatory models of the hydroclimatological system as they summarise large-scale climate in a single variable. Indices of the North Atlantic Oscillation (NAO), for example, are positively correlated with temperature, precipitation, windspeed and moisture transport into northwest Europe, with the reverse relationships present in southern Europe (Hurrell 1995). Although the mechanisms are more complex, the NAO also influences North American climate, with positive (negative) associations with temperature in northeast USA (eastern Canada) (Hurrell 1995). Northwest European river flow appears to respond to NAO-related climate variations, showing positive correlation with NAO indices in winter (Shorthouse and Arnell 1999; Phillips *et al.*, 2003). Studies of river flow behaviour in Denmark and southwest Norway (Roald *et al.*, 1997), southern and central Finland (Hyvarinen 2003) and western Scotland (Black 1996, Mansell 1997) offer further (qualitative) support for NAO-driven variation, as does the conceptual model of winter NAO-river flow linkages proposed by Kingston *et al.* (2005).

Despite these apparent NAO-river flow relationships, much scope remains for research in this field (Kingston *et al.*, 2005). There is a need to investigate the range of processes linking the atmosphere with streamflow (Lawler *et al.*, 2003), rather than correlation of individual elements in this process chain. Research is also required over the full hydrological year and with a spatial domain large enough to permit quantitative examination and modelling of continental-scale variation in these linkages. Accordingly, this paper aims to demonstrate a methodology for multivariate assessment of relationships between large-scale climate and monthly river flow. This is carried out for northwest Europe over the period 1968-1997, with a particular emphasis given to examining the presence of NAO-river flow links. This aim is achieved through a composite analysis of the climatic situation under high and low regional streamflow conditions

in Scotland, Norway, Finland and Denmark. Composite analysis has previously been shown to be extremely effective in providing information on climatic forcing of streamflow (e.g. Barros *et al.*, 2004; Yarnal and Frakes 1997) due to the simplicity and flexibility of this technique. The size of the study area and streamflow data set make analysis of climatic controls on individual rivers impractical and inefficient. Composite analysis is therefore carried out on objectively defined streamflow regions. Identification of streamflow regions is accomplished through Principal Components Analysis (PCA) and hierarchical cluster analysis (CA), following Yarnal (1993). Given that these analyses seek to demonstrate the utility of regionalization and composite analysis methodologies rather than provide a definitive evaluation of spatial variation in the circulation-climate-streamflow process cascade, only results for selected regions and months are presented here.

## DATA AND METHODOLOGY

The climate data employed herein are the European Centre for Medium Range Weather Forecasting (ECMWF) ERA-40 reanalysis products, which provide gridded data at 2.5° resolution (Simmons and Gibson 2000). The streamflow data consists of 55 monthly discharge time series (covering Norway, Finland, Denmark and Scotland—Fig. 1) from three sources: the Flow Regimes from International Experimental and Network Data European Water Archive (FRIEND-EWA), the Global Runoff Data Centre and the UK National River Flow Archive. Only gauging stations with catchment areas between 50-1000 km<sup>2</sup> were used, to assure a comparable magnitude of response to climatic forcing of discharge between the basins studied.

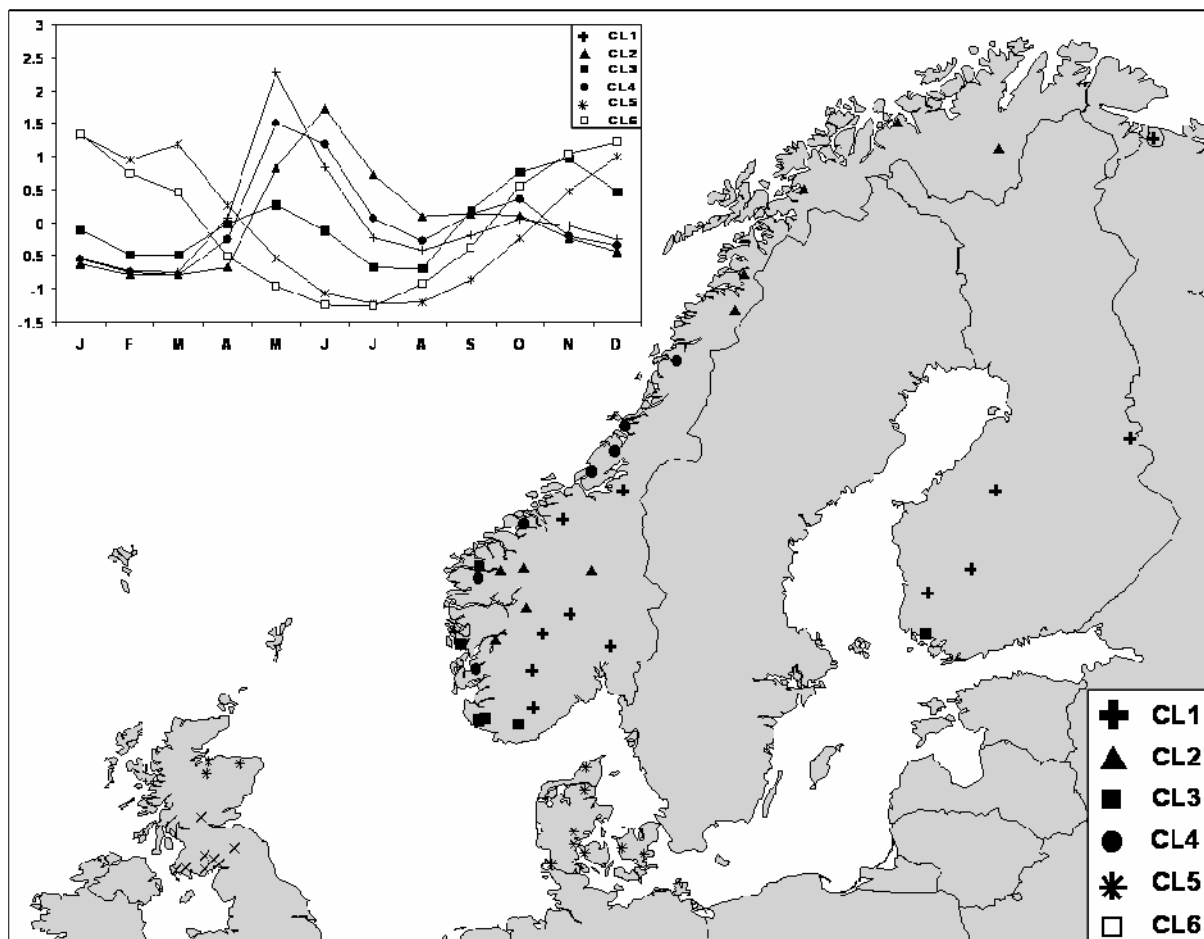


Fig. 1: Locations of streamflow gauges and regions defined by cluster analysis. Inset: mean annual hydrographs for each cluster (units are z-scores).

Regionalization was performed on standardized (z-scored) monthly discharge values using varimax rotation (Richman 1986) of an S-mode PCA followed by CA. Only principal components with

eigenvalues  $> 1$  were retained. Following Yarnal (1993), the loadings on the rotated components were entered into a CA to identify streamflow groupings. The Ward's clustering algorithm was found to offer the most physically interpretable solutions, in accordance with Bower *et al.* (2004). The number of clusters to retain was determined from inspection of the dendrogram and natural breaks in the cluster agglomeration schedule (Bower *et al.*, 2004).

Streamflow was averaged across all stations within each cluster to produce regional streamflow series. This was done for January, May, August and October over the period 1968-97. Composites of 1000 hPa geopotential height, atmospheric thickness and 1000 hPa wind vector across the North Atlantic region were produced based on high and low flow episodes for each monthly regional streamflow series. Atmospheric thickness was calculated as the difference between the 500 and 1000 hPa geopotential heights, thus indicating the warmth of the atmosphere. January, May, August and October were selected to represent the main seasons of the annual hydrograph across all regions (Fig. 1). January represents mid-winter low flow conditions, May the spring snow-melt in the Scandinavian countries, August represents the mid-summer low flow minimum, and October the autumnal rise in discharge. The composites were formed from the approximate upper and lower quartiles of streamflow from each monthly river flow series (equating to eight high and eight low years). The upper and lower quartiles were chosen to define high and low streamflow as this was felt to be the best compromise between sampling only genuinely high or low flow months while also maintaining an acceptable sample size. A fixed number of months have been used for each composite due to the difficulty of consistently defining a high and low discharge level between different regions and different months. T-tests were conducted on a grid cell basis to determine the statistical significance of differences between climatic fields associated with high and low streamflow in each month.

## RESULTS

### Regionalization

Results of the regionalization are presented in Fig. 1, which identified six clusters. Cluster 1 includes gauging stations in inland southern and southeastern Norway, northeast Norway and southern and central Finland. Cluster 2 covers northwest Norway and central-southern Norway, while cluster 3 stations are located in southwest Norway and southwest Finland. Cluster 4 covers coastal mid-Norway and southwest Norway, cluster 5 is Denmark and northeast Scotland, with cluster 6 containing stations from southern and central Scotland. The mean annual hydrograph of each cluster is also displayed in Fig. 1. Clusters 1, 2 and 4 are characterized by strong melt-driven discharge peaks in May and June, whereas clusters 5 and 6 peak in January and cluster 3 peaks in November. All clusters have a low flow period in July or August, but the lowest annual streamflow for clusters 1, 2 and 4 occurs in March.

### Composite analysis

The following section describes results of the composite analysis, focusing on cluster 2. This cluster is concentrated on as although it is a 'typical' cluster in some ways, with a moderate number of gauging stations (10) and a clear annual cycle, it also covers a wide spatial domain, with stations in both inland southern Norway and coastal northern Norway. It is therefore felt to provide a good test of the potential of the regionalisation and composite analysis techniques to provide information on climatic controls of regional streamflow. Cluster 2 results are summarized in Tab. 1, with further details given below. Statistical significance refers to  $p = 0.05$ .

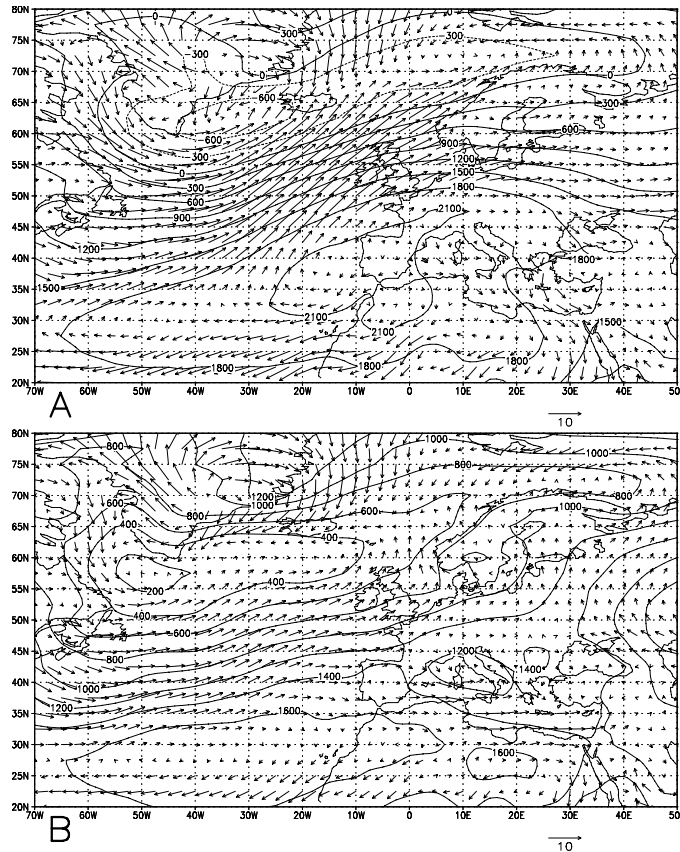


Fig. 2: Composite 1000hPa geopotential height and wind vector for January high (A) and low (B) cluster 2 streamflow (length of arrow indicates wind strength in  $\text{m s}^{-2}$ : see scale).

Tab. 1: Summary of differences in climate between high and low cluster 2 streamflow.

	<b>Geopotential height</b>	<b>Atmospheric thickness</b>	<b>Wind vector</b>
<b>January</b>	High flow: IL deeper, larger and extended to northeast; AH stronger and further east.	Greater when high flow.	High flow: strong, south-westerly wind. Low flow: weaker and more variable.
<b>May</b>	High flow: IL in E. Atlantic and deeper. Low flow: weaker and in W. Atlantic.	As January, but weaker differences.	Low flow: variable; high flow: southerly. Little difference in speed.
<b>August</b>	IL and AH stronger when high flow. AH ridges northeast-ward towards UK when high flow.	Pattern similar to January/May, but weaker, shifted south so no significant difference over most of region.	High flow: strong south-westerlies. Low flow: northerly and much weaker.
<b>October</b>	High flow: IL deeper and extended to northeast, AH strength same as low flow, but more zonally extensive.	As January and May, similar magnitude of differences to May.	South-westerly in high and low flow composites, stronger when high flow.

AH: Azores High; IL: Icelandic Low

**January** The northeast-ward extension and movement of the Icelandic Low (IL) and Azores High (AH) in the high flow composite (Fig. 2A, Tab. 1) and greater intensity of these features results in an enhanced pressure gradient between these centres, together with a more southwest-northeast orientation of this axis (Fig. 2B). These differences are associated with stronger winds from a more southwesterly direction under high flow conditions (Fig. 2). The increased atmospheric thickness over cluster 2 catchments associated with high flow (Tab. 1) is complemented by another area of increased thickness over the eastern USA, and reduced thickness over southern Europe/north Africa and eastern Canada (Fig. 3).

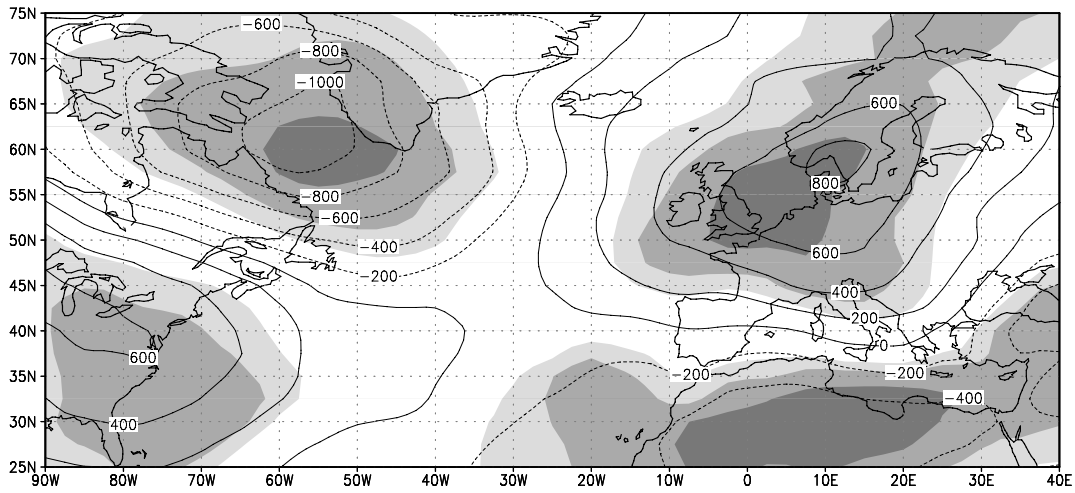


Fig. 3: Difference in January atmospheric thickness (500-1000hPa geopotential height) between cluster 2 high and low streamflow composites (high minus low). (Shading indicates significant difference with  $p = 0.05, 0.01$  and  $0.001$  from light to dark.).

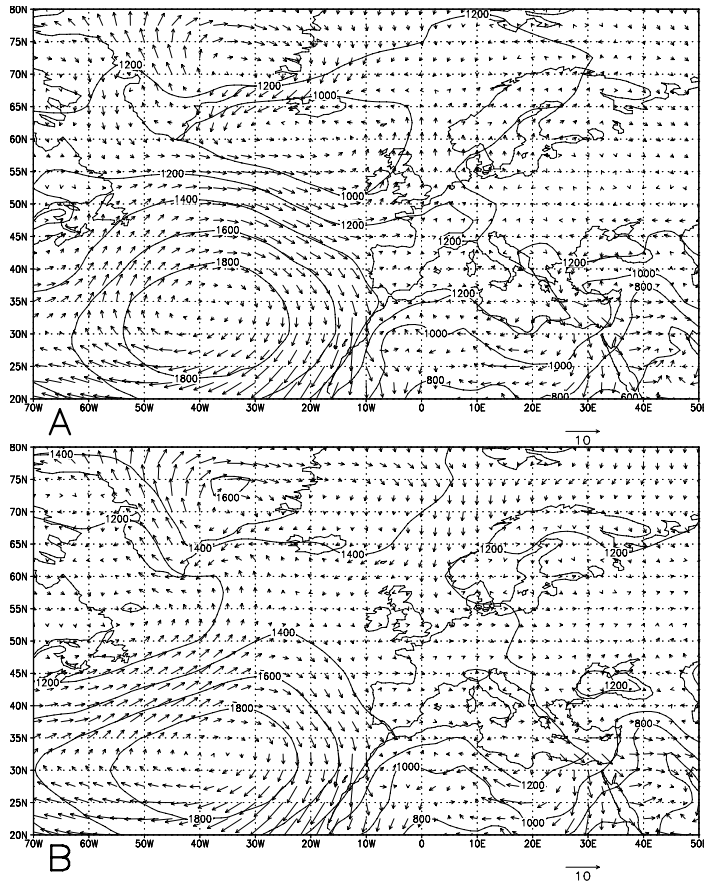


Fig. 4: Composite 1000hPa geopotential height and wind vector for May high (A) and low (B) cluster 2 streamflow (length of arrow indicates wind strength in  $\text{m s}^{-2}$ : see scale).

**May** The movement and variation in the IL described in Tab. 1 and Fig. 4 have a large influence on wind direction, although differences in windspeed between high and low flow are weaker than in January. High flow conditions are associated with southerly (cyclonic) winds, with more variable and light winds in low flow situations. Thickness differences over cluster 2 basins and across the North Atlantic basin are similar to January, but are much weaker in southern Europe.

**August** The enhanced ridge of the AH and slightly stronger IL characteristic of high flow conditions (Fig. 5) result in similar pressure gradient and wind direction differences to January. Differences in windspeed and direction between flow levels are greater compared to May, but are weaker than January. Although the pattern of thickness differences between flow states present across the North Atlantic is similar to

January, shifts in the positions of the pattern centres mean that there are no significant thickness differences over the cluster 2 region in this month.

**October** Differences in geopotential height and wind vector between high and low streamflow are similar to January, although not as strong or statistically significant. Changes in thickness between high and low streamflow over cluster 2 basins and across the North Atlantic are comparable to May, but with no significant differences over the eastern USA.

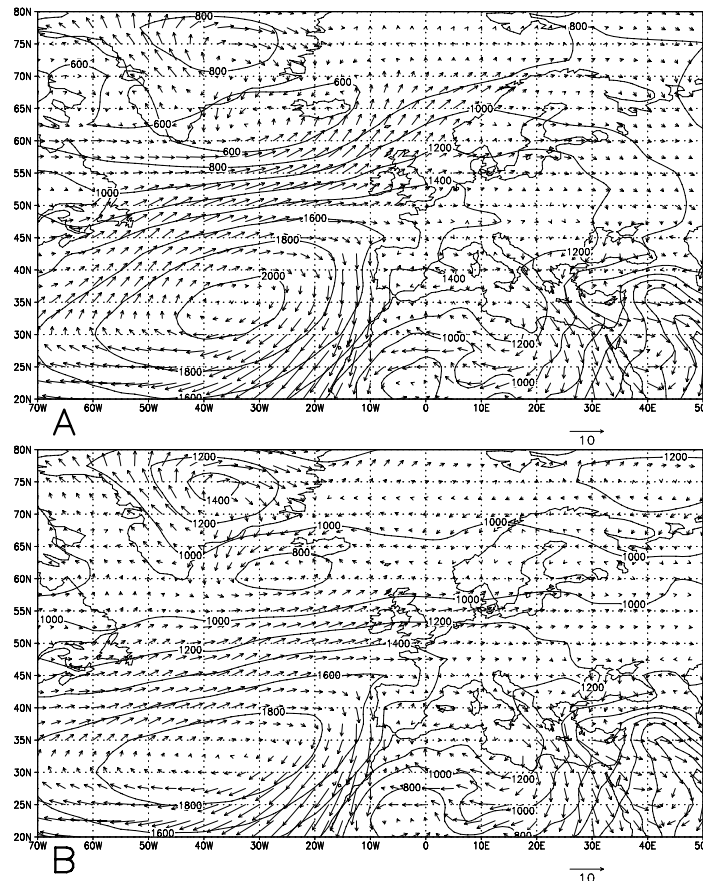


Fig. 5: Composite 1000hPa geopotential height and wind vector for August high (A) and low (B) cluster 2 streamflow (length of arrow indicates wind strength in  $\text{m s}^{-2}$ : see scale).

## DISCUSSION

The following section offers interpretations of the differences in climate between high and low streamflow events as a basis for inferring large-scale atmospheric streamflow forcing mechanisms, focusing on cluster 2 (northern and central southern Norway). These hydroclimatological associations are discussed with particular reference to hypothesized NAO impacts.

January, May and October differences in atmospheric thickness between high and low streamflow indicate a strong thermal control of streamflow. This reflects the importance of temperature in determining the snow: rain ratio, which affects whether precipitation influences streamflow concurrently or accumulates as snow or ice to be released with a lagged melt response (Hartley and Dingman 1993). Temperature also affects the onset and rate of meltwater generation, which is likely to be an important hydroclimatological process in cluster 2 catchments given their regime and inland/far northern location (Fig. 1).

Wind vector and geopotential height associations with streamflow suggest a mechanism for the observed temperature differences between high and low streamflow. The more active Atlantic centres of action, enhanced pressure gradients between these centres and consequent stronger southwesterly winds associated with high flow are likely to result in increased advection of mild maritime air over cluster 2 basins (Hanssen-Bauer and Førland 2000). Wind vector and geopotential height differences are also consistent with an increased frequency of storm tracks into the region under high flow conditions (Rogers 1997), which would lead to increased frontal and orographic rainfall. This is likely to be the primary

large-scale control on streamflow during August, given the reduced differences in atmospheric thickness between high and low flow states during this month.

The climatic differences between high and low streamflow and hypothesized chain of causality linking these to streamflow can be summarized in a conceptual model (Tab. 2). In addition to revealing a number of intra-annual differences in atmosphere-surface-runoff linkages, many of the differences and processes highlighted in this model appear similar to theoretical NAO-climate-streamflow links, such as the movement and variations in strength of the IL, together with associated wind and thickness behaviour (Kingston *et al.*, 2005). This is exemplified by thickness associations with streamflow (Fig. 3), which appear very close to the typical NAO temperature signature (Hurrell 1995). Despite this apparent NAO signal, geopotential height results (Fig. 2, 4 and 5) reveal the large-scale atmospheric field associated with high and low streamflow to be too complex and subtle to simply be categorized by either high or low NAO index values. For example, whereas the NAO is characterized by the inverse correlation of the AH and IL, it is shown here that changes in the strength of the IL do not always occur with similar variation in the AH (e.g. October), and movement of these centres can also occur with only relatively minor pressure changes (e.g. May). Although indices of the NAO may allow moderately powerful statistical relationships between the NAO and climate/streamflow to be constructed, these results demonstrate that such statistical models would reveal relatively little about the processes involved in such climate-flow interactions (such as the relative importance and nature of variations in the IL or AH). This is likely to be of particular importance when seeking to extend explanatory models of atmosphere-surface-runoff relationships over large spatial scales and develop predictive relationships, and highlights the value of the multivariate process-based approach outlined in this paper.

Tab. 2: Conceptual model of atmosphere-surface-runoff linkages for high cluster 2 streamflow.

<b>Jan</b>	IL deeper and extended northeastward	AH higher and further east	Stronger Atlantic pressure gradient and change from E-W to SW-NE orientation	Stronger and more southwesterly winds over region	Greater maritime influence: increased temperature and precipitation	Reduced frozen water stores; more precipitation as rain	Increased streamflow
<b>May</b>	IL deeper and further east	Reduced influence of northerly arctic wind	Greater influence of temperate southerly winds	Increased temperature	Reduced frozen water stores; more precipitation as rain		Increased streamflow
<b>Aug</b>	IL slightly stronger	AH stronger and extended northeastward	Stronger and more northeasterly position of Atlantic pressure gradient	Stronger and more southwesterly winds over region	Increased maritime influence on climate	Increased precipitation over region	Increased streamflow
<b>Oct</b>	IL deeper and extended northeastward	AH extended east and west into Europe and N. America	Stronger Atlantic pressure gradient and change from E-W to slightly more SW-NE orientation	Stronger and more southwesterly winds over region	Greater maritime influence: increased temperature and precipitation	Reduced frozen water stores; more precipitation as rain	Increased streamflow

## CONCLUSION

A range of differences in large-scale atmospheric fields are evident between high and low streamflow states for an objectively defined hydrological region of northwest Europe. Thermal controls are the foremost influence on streamflow during January and May, and are also important in October. The influence of wind direction on precipitation delivery appears important throughout the year, particularly in August. These differences appear physically consistent, implying that both the definition of high and low streamflow composites and streamflow regions are not methodological artefacts. That wind and thickness differences can largely be explained by variation in the position and strength of the climatological Azores High and Icelandic Low would suggest NAO control of streamflow, but large-scale atmospheric fields associated with high and low streamflow appear too complex to be simply defined in terms of high or low NAO phases, emphasising the importance of a process multivariate approach to the investigation of climate-streamflow relationships. Further research is planned to clarify this situation, and

to provide a more in-depth evaluation of the spatial and temporal variability of the atmosphere-surface-runoff process cascade across the northern North Atlantic.

## ACKNOWLEDGEMENTS

Daniel Kingston is funded by a PhD scholarship from the University of Birmingham School of Geography, Earth and Environmental Science. The authors gratefully acknowledge Gwyn Rees and David Pitson for permitting and providing access to the FRIEND-EWA, and also to Lars Roald for supplying updates and metadata for this database. Thanks also to Tom Lüllwitz at the Global Runoff Data Centre in Koblenz, Germany, for supplying streamflow data. The Grid Analysis and Display System (GrADS) was used to produce Fig. 2, 3, 4 and 5. The authors would like to thank an anonymous reviewer for their comments on this paper.

## REFERENCES

- Barros, V., Chamorro, L., Coronel, G. and Baez, J. (2004) The major discharge events in the Paraguay River: magnitudes, source regions, and climate forcings. *J. Hydrometeorol.*, 5, 1161-1170.
- Black, A.R. (1996) Major flooding and increased flood frequency in Scotland since 1988. *Phys. Chem. Earth.*, 20, 463-468.
- Bower, D., Hannah, D. M. and McGregor, G. R. (2004) Techniques for assessing the climatic sensitivity of river flow regimes. *Hydrol. Processes*, 18, 2515-2543.
- Hanssen-Bauer, I. and Førland, E. (2000) Temperature and precipitation variations in Norway 1900-1994 and their links to atmospheric circulation. *Int. J. Climatol.*, 20, 14, 1693-1708.
- Hartley, S. and Dingman, S. L. (1993) Effects of Climatic Variability on Winter-Spring Runoff in New-England River Basins. *Phys. Geogr.*, 14, 4, 379-393.
- Houghton, J. T., Ding, Y., Griggs, D. J., Noguer, M., van der Linden, P. J., Dai, X., Maskell, K. and Johnson, C. A. (2001) *Climate Change 2001: The Scientific Basis*. IPCC Third Assessment Report, Cambridge University Press, Cambridge.
- Hurrell, J.W. (1995) Decadal Trends in the North-Atlantic Oscillation - Regional Temperatures and Precipitation. *Science*, 269, 5224, 676-679.
- Hyvarinen, V. (2003) Trends and characteristics of hydrological time series in Finland. *Nordic Hydrol.*, 34, 1-2, 71-90.
- Kingston, D. G., Lawler, D. M. and McGregor, G. R. (2005) Atmospheric circulation-climate-streamflow linkages in the northern North Atlantic: research prospects. *Prog. Phys. Geog.*, in press.
- Lawler, D.M., McGregor, G.R. and Phillips, I.D. (2003) Influence of atmospheric circulation changes and regional climate variability on river flow and suspended sediment fluxes in southern Iceland. *Hydrol. Processes.*, 17, 16, 3195-3223.
- Mansell, M.G. (1997) The effect of climate change on rainfall trends and flooding risk in the West of Scotland. *Nordic Hydrol.*, 28, 1, 37-50.
- Phillips, I.D., McGregor, G.R., Wilson, C.J., Bower, D. and Hannah, D.M. (2003) Regional climate and atmospheric circulation controls on the discharge of two British rivers, 1974-97. *Theor. Appl. Climatol.*, 76, 3-4, 141-164.
- Richman, M. B. (1986) Rotation of principal components. *J. Climatol.*, 6, 293-335.
- Roald, L.A., Hisdal, H., Hiltunen, T., Hyvarinen, V., Jutman, T., Gudmundsson, K., Jonsson, P. and Oveson, N. B. (1997) Historical runoff variation in the Nordic countries. *IAHS Pub.* 246, 87-96.
- Rogers, J.C. (1997) North Atlantic storm track variability and its association to the north Atlantic oscillation and climate variability of northern Europe. *J Climate*, 10, 7, 1635-1647.
- Simmons, A. J. and Gibson, J. K. (2000) The ERA-40 project plan. *ERA-40 project report series No. 1*.
- Shorthouse, C. and Arnell, N. (1999) The effects of climatic variability on spatial characteristics of European river flows. *Phys. Chem. Earth. Pt. B.*, 24, 1-2, 7-13.
- Yarnal, B. (1993) *Synoptic climatology in environmental analysis*. Belhaven Press, London.
- Yarnal, B. and Frakes, B. (1997) Using synoptic climatology to define representative discharge events. *Int. J. Climatol.*, 17, 323-341.

# A SUITABLE SELECTION OF RAINFALL-RUNOFF FORECASTING MODEL(S) FOR THE RIVER NILE BASIN

**Mohamed A. SONBOL, Medhat A. EL-BIHERY, Mohamed ABDEL-MOTALEB**

Water Resources Research Institute, NWRC–Egypt  
*wrri@wrri.org.eg*

**Francis M. MUTUA**

Department of Meteorology, University of Nairobi–Kenya

**K. BASHAR**

UNESCO Chair of Sudan, Sudan

## ABSTRACT

Flow forecasting is an important step in river basin management in particular and water resources management in general. River flow models are used as components in actual flow forecasting schemes. They are also used in providing for efficient operation of storage reservoirs. Usually, flow forecasts are obtained in real time by transforming the input into a discharge using models. These forecasts may subsequently be modified or updated in accordance with the errors observed in the previous forecasts up to the time of making the new forecast.

This paper presents an appraisal study to select a suitable model(s) that can be used in forecasting flows in the rivers of the Nile basin. In this appraisal study, systems and conceptual modeling techniques are applied to the Blue Nile catchment up to Eddeim, Upper Awash catchments in Ethiopia, and Eastern Lake Victoria catchments to Nzoia and Sondu rivers. The models were applied in non-parametric and parametric forms. Parameter optimization is carried out by ordinary least squares, Rosenbrok, Simplex and generic algorithm.

It is shown that the simple assumption of linearity is not adequate in modelling the rainfall runoff transformation. However, in catchments which exhibit marked seasonal behaviour good results can be obtained with Linear Perturbation Model (LPM) which involves the assumption of linearity between the departures from seasonal expectations in input and output series. Within the range of the tested models, the application of the GFFS (collection of systems and conceptual models) software proved to be possible with variable efficiencies in the Nile River basin LPM was found to be the best candidate model that can forecast the flows under a wide range of conditions ranging from marked seasonality to marked storage effects.

**Keywords:** rainfall-runoff model, forecasting, Nile

## INTRODUCTION

The development and the application of rainfall-runoff models have been a corner-stone of hydrological research for many decades. In general, the purpose of the development of these models is a two-fold. The first is to advance our understanding and state of knowledge about the hydrological processes involved in the rainfall-runoff transformation. The second is to provide practical solutions to many of the related environmental and water resources management problems. Rainfall-runoff models are normally used as components in river flow forecasting systems. The efficient forecasting of river flows is beneficial in many aspects for the prosperity of those societies living in river basins. These forecasts are necessary to provide warnings against floods in order to prevent loss of life and to minimize damages to both properties and livestock. Floods are the cause of 40% of all deaths due to natural disasters.

Extensive hydrological studies regarding the runoff generation process in the Nile river basin were carried out. Large number of data sets corresponding to the daily observed data series for rainfall, evaporation, discharge, and other meteorological parameters (such as temperature, humidity, etc.), as available for different sites from some selected catchments were analyzed. Pre-processing of many data series was required either to fill the missing values or to extrapolate in time, for the purpose of checking the consistency of the data sets, to correlate the data from different sites, and to use these for calibration and verification of different model forms. Hydrological models used in the study to simulate the process of runoff generation are two system theoretic black box models namely, the Parametric Simple Linear Model (PSLM) and the Parametric Seasonally based Linear Perturbation Model (PLPM), and a physically inspired conceptual model namely, the Soil Moisture Accounting and Routing (SMAR) Model. These

models were developed at the Department of Engineering Hydrology, National University of Ireland, and Galway, the details of which is not included in this write-up. Interested reader may refer to the relevant papers and technical notes, presented as reference materials.

## DESCRIPTION OF THE SELECTED MODELS

The basic concepts and a description of the structures of the models included in the GFFS are provided below.

### The Simple Linear Model (SLM)

Nash and Foley (1982) introduced the Simple Linear Model (SLM) not as a substantive rainfall-runoff model in its own right but rather as a naïve black-box model to be used mainly for the purpose of model efficiency comparisons. The intrinsic hypothesis of the SLM is the assumption of a linear time-invariant relationship between the total rainfall  $R_i$  and the total discharge  $Q_i$ . In its discrete non-parametric form, the SLM, including the forecast error term  $e_i$ , is expressed by the convolution summation relation (Kachroo and Liang, 1992),

$$Q_i = \sum_{j=1}^m R_{i-j+1} h'_j + e_i = G \sum_{j=1}^m R_{i-j+1} B_j \quad \text{where} \quad \sum_{j=1}^m B_j = 1 \quad (1)$$

where  $Q_i$  and  $R_i$  are the discharge and rainfall respectively at the  $i$ -th time-step,  $h'_j$  is the  $j$ -th discrete pulse response ordinate or weight,  $m$  is the memory length of the system and  $G$  is the gain factor. This can be viewed as a multiple linear regression model of the observed discharge on the previous observed rainfall values and hence estimates of the unit pulse response ordinates can therefore be obtained directly by the method of ordinary least squares (OLS) (See Nash and Foley (1982); Kachroo and Liang (1992)). In the SLM, when the rainfall and discharge are expressed in the same units of measurements (e.g. mm/day over the catchment area, for daily data), then the arithmetic sum of the discrete pulse response ordinates  $B_j$  defines the 'gain factor'  $G$  of the model, which may also be considered as the long term 'coefficient of runoff' approximately reflecting the ratio of the total volume of the observed discharge hydrograph to that of the observed rainfall input (Kachroo and Liang, 1992). The SLM is included in the GFFS for use as a naïve model in model performance intercomparison studies with the option; in the context of discharge forecast combination, of its inclusion as a very primitive rainfall-runoff model. Any model that does not perform better than the SLM can hardly be considered as a serious rainfall-runoff model.

### The Linear Perturbation Model (LPM)

This model exploits the seasonal information inherent in the observed rainfall and discharge series. It was originally introduced in the context of rainfall-runoff modelling by Nash and Barsi (1983). Initially referred to as the *hybrid* model, in a series of subsequent publications it is referred to as the **Linear Perturbation Model (LPM)** (e.g. Kachroo *et al.*, 1988; Liang and Nash, 1988; Kachroo, 1992a; Kachroo *et al.*, 1992; Liang *et al.*, 1992; Liang and Guo, 1994; Abdo *et al.*, 1996; Elmahi and O'Connor, 1996; Shamseldin *et al.*, 1997).

In the LPM, it is assumed that, during a year in which the rainfall is identical to its seasonal expectation, the corresponding discharge hydrograph is also identical to its seasonal expectation. However, in all other years, when the rainfall and the discharge values depart from their respective seasonal expectations, these departures series are assumed to be related by a linear time invariant system. Hence, the LPM structure reduces reliance on the linearity assumption of the SLM and gives substantial weight to the observed seasonal behavior of the catchment).

### The Linearly Varying Gain Factor Model (LVGFM)

The overall operation of the LVGFM has the mathematical form:

$$G_i = a + bz_i \quad (\text{a and b being constants}) \quad (2)$$

$$\begin{aligned} Q_i &= a \sum_{j=1}^m R_{i-j+1} B_j + b z_i \sum_{j=1}^m R_{i-j+1} B_j + e_i = \sum_{j=1}^m R_{i-j+1} (aB_j) + \sum_{j=1}^m (z_i R_{i-j+1}) (bB_j) + e_i \\ &= \sum_{j=1}^m R_{i-j+1} B'_j + \sum_{j=1}^m R'_{i-j+1} B''_j + e_i \end{aligned} \quad (3)$$

Where:  $B'_j = a B_j$ ,  $R'_{i-j+1} = z_i R_{i-j+1}$ ,  $B''_j = b B_j$ , and  $\sum B_j = 1.0$ .

Although the antecedent precipitation index (API) provides a crude index of the current soil moisture state  $z_i$ , Ahsan and O'Connor (1994) suggested that  $z_i$  be conveniently obtained from the outputs of the naïve SLM, operating as an auxiliary model (Fig. 1), according to the relation:

$$z_i = \frac{\hat{G}}{\bar{Q}} \sum_{j=1}^m R_{i-j+1} \hat{h}_j \quad (4)$$

where  $\hat{G}$  and  $\hat{h}$  are estimates of the gain factor and the pulse response ordinates respectively of the SLM and  $\bar{Q}$  is the mean discharge in the calibration period. Although, in the systems sense, the overall LVGFM is non-linear, in terms of the model weighting sequences  $B'_j$  and  $B''_j$ , Eq. (3) can be viewed as a multiple linear regression model (Shamseldin *et al.*, 1997). Hence, the weighting sequences  $B'_j$  and  $B''_j$  can be estimated directly by the method of ordinary least squares (OLS).

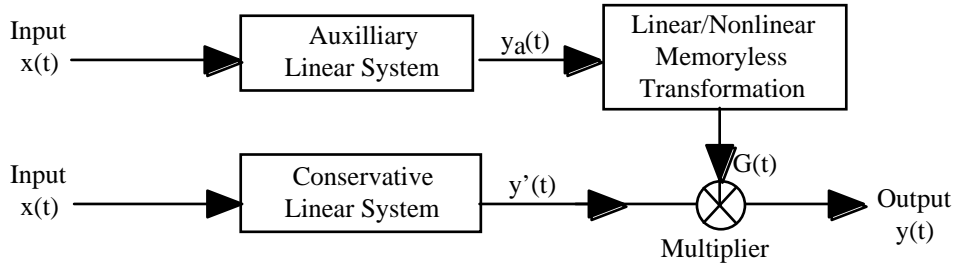
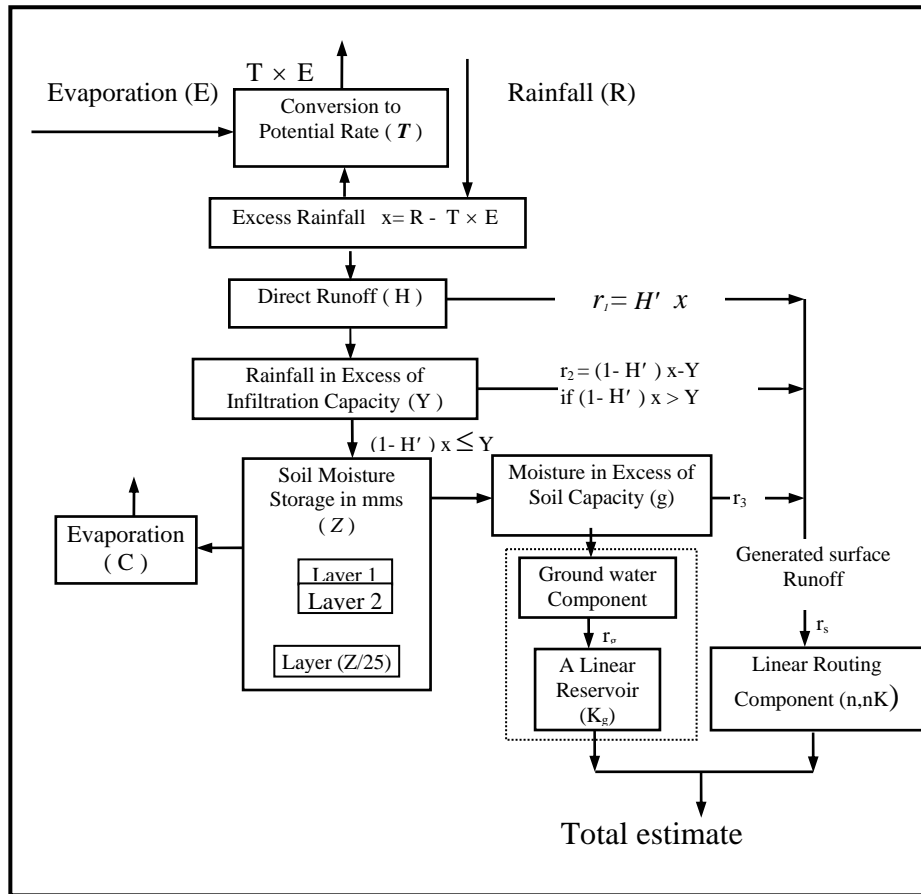


Fig. 1: Schematic diagram of the Linearly-Varying Gain Factor Model (Ahsan and O'Connor, 1994)

### The SMAR Conceptual Model

The Soil Moisture Accounting and Routing (SMAR) Model is a development of the 'Layers' conceptual rainfall-runoff model introduced by O'Connell *et al.* (1970), its water-balance component being based on the 'Layers Water Balance Model' proposed in 1969 by Nash and Sutcliffe (Clarke, p. 307, 1994). Typical of its class, the SMAR model is a lumped quasi-physical conceptual rainfall-evaporation-runoff model, with quite distinct water-balance and routing components (Hence its generic name!). Using a number of empirical and assumed relations which are considered to be at least physically plausible, the non-linear water balance (i.e. soil moisture accounting) component ensures satisfaction of the continuity equation, over each time-step, i.e. it preserves the balance between the rainfall, the evaporation, the generated runoff and the changes in the various elements (layers) of soil moisture storage. The routing component, on the other hand, simulates the attenuation and the diffusive effects of the catchment by routing the various generated runoff components, (which are the outputs from the water balance component), through linear time-invariant storage elements. For each time-step, the combined output of the two routing elements adopted (i.e. one for generated 'surface runoff' and the other for generated 'groundwater runoff') becomes the simulated (un-updated) discharge forecast produced by the SMAR model.



Parameter	Description
Z	The combined water storage depth capacity of the layers (mm)
T	A parameter (less than unity) that converts the given evaporation series to the model-estimated potential evaporation series.
C	The evaporation decay parameter, facilitating lower evaporation rates from the deeper soil moisture storage layers
H	The generated 'direct runoff' coefficient
Y	The maximum infiltration capacity depth (mm)
n	The shape parameter of the Nash gamma function 'surface runoff' routing element; a routing parameter
nK	The scale (lag) parameter of the Nash gamma function 'surface runoff' routing element; a routing parameter
g	The weighting parameter, determining the amount of generated 'groundwater' used as input to the 'groundwater' routing element.
K <sub>g</sub>	The storage coefficient of the 'groundwater' (linear reservoir) routing element; a routing parameter

Fig. 2: Schematic diagram of the Liang (1992) version of the SMAR Model and a summary description of its parameters; after Shamseldin *et al.* (1999).

The version of SMAR used in the present study, the schematic structure of which is sketched in Fig. 2, is that which incorporates the suggested modifications of both Khan (1986) and Liang (1992). In the GFFS version presented here, three two-parameter distribution options are available for routing the generated 'surface runoff' component of the SMAR model, namely, the classic gamma distribution (Nash-cascade) model (Nash, 1957), its discrete counterpart, the Negative Binomial distribution (O'Connor, 1976), and the sharp-peaked Inverse Gaussian distribution (Bardsley, 1983) for flashy catchments.

The version of SMAR used in the present study has nine parameters, five of which control the overall operation of the water-budget component, while the remaining four parameters (including a weighting parameter which determines the amount of generated ‘groundwater runoff’) control the operation of the routing component. The SMAR is calibrated to the observed data using the user’s choice optimisation procedure to minimise the selected measure of error between the observed and the model estimated discharges. In the context of the SMAR model, the selected measure of model error used for this study is a weighted combination of the sum of squares of the discharge forecast errors and the corresponding index of volumetric fit (i.e. the ratio of the total volume of the estimated discharge hydrograph to that of the corresponding observed hydrograph). As the Nash-Sutcliffe (1970) model efficiency criterion  $R^2$  is based on the sum of squares of model forecast errors only, it follows that the  $R^2$  value obtained for the SMAR model calibrated using the weighted measure of error will generally be less than that for which the index of volumetric fit is neglected in the calibration process (as is the case for the other models in the GFFS). This should be borne in mind when comparing the  $R^2$  model efficiency values of various other models considered in this study with that of the SMAR model for the same calibration sets of data.

The choice of three automatic optimization algorithms, i.e. the genetic algorithm (Wang, 1991), the Rosenbrock method (Rosenbrock, 1960) and the simplex method of Nelder and Mead (1965) are available for the calibration of the SMAR model. The user may use these individually or sequentially. More details on the structure, operation and applications of various versions of the SMAR model are described in the papers by Kachroo (1992b), Tan and O’Connor (1996), Tan *et al.* (1996) and Shamseldin *et al.* (1997, 1999).

### **The Artificial Neural Network (ANN) Model**

The widely-used artificial neural networks (ANN) provide a flexible non-linear mapping of the network input (or set of inputs) into the network output (or set of outputs) without specifying a priori the mathematical nature of the relation between inputs and outputs. In the GFFS, the ANN can be used in four quite distinct contexts. Firstly, as an option, it may be used as a basic black-box rainfall-runoff model (Shamseldin, 1997) to produce un-updated discharge forecasts (i.e. as an alternative in the GFFS to the SLM, LPM, LVGFM or SMAR models). Secondly, it may be used in the GFFS in the model-output-combination context, wherein the un-updated discharge forecasts of selected basic models are combined by the network to produce better un-updated discharge forecasts than those provided by the individual basic models included in the combination (i.e. as an alternative to either the WAM or SAM forecast combination methods) (Shamseldin *et al.*, 1997). Thirdly, the ANN may be used as a real-time discharge forecast updating technique (Shamseldin and O’Connor, 2001), wherein the ANN operates on both the discharge forecasts and on the recent observed discharge values in order to produce updated forecasts, these input discharge forecasts being either those of an individual basic rainfall-runoff model, or those produced by a forecast combination method (i.e. as an alternative to using an AR model for forecast error updating). Fourthly, the ANN can be used as a real-time rainfall-runoff model having an inbuilt updating structure, using the observed discharges and the traditional input information (i.e. rainfall and /or upstream flow hydrograph data) to directly produce the updated discharge forecasts. It is also planned, as a fourth updating option, to incorporate the Real-Time Model Output

In the context of the ANN as a basic rainfall-runoff model, instead of using the rainfall series  $R_i$  as the input, Shamseldin (1997) used a form of antecedent rainfall index, comprising a weighted sum of the current and immediately previous rainfall values, as the single external input to the network. As the neural network itself does not incorporate storage effects, storage is implicitly accounted for by the use of such an index. Instead of using the classic Antecedent Precipitation Index (API), involving a geometric weighting series, as the rainfall index, Shamseldin used the output series of the naïve SLM, i.e. the convolution summation of the rainfall with a more realistic weighting series, for this purpose. So, the ANN effectively enhances the output forecast of the SLM by means of a suitable non-linear transformation.

In the context of the un-updated forecast combination method (ANNM), the estimated discharge output of each the chosen rainfall runoff models is assigned, at each time-step, to one (and only one) neuron in the input layer, resulting in one neuron in the input layer for each model included (Shamseldin *et al.*, 1997).

In this case, the ANN input-array vector has the form  $Y_i = (\hat{Q}_{i,1}, \hat{Q}_{i,2}, \dots, \hat{Q}_{i,n})^T$ , where  $n$  is the number of individual model forecasts included in the combination. Note that, for network parsimony, the number of

neurons in the hidden layer is usually two or three. Note also that the combination output forecast is still an un-updated forecast.

In the context of using the ANN as a real-time forecasting model having a built-in updating mechanism, involving the production of updated forecasts as new observed discharge values become available, the input array vector has the form  $Y_i = (R_i, R_{i-1}, \dots, R_{i-p}, Q_{i-1}, Q_{i-2}, \dots, Q_{i-q})^T$ , where  $R_i$  and  $Q_i$  are the rainfall and observed discharge series respectively (Xiong *et al.*, 2001).

For a neuron either in the hidden or in the output layer, the received inputs  $y_i$  are transformed to its output  $y_{out}$  by a mathematical transfer function of the form

$$y_{out} = f\left(\sum_{i=1}^M w_i y_i + w_o\right) \quad (5)$$

where  $f()$  denotes the transfer function,  $w_i$  is the input connection pathway weight,  $M$  is the total number of inputs (which usually equals the number of neurons in the preceding layer), and  $w_o$  is the neuron threshold (or bias), i.e. a base-line value independent of the input. In the GFFS, the non-linear transfer function adopted for the neurons of the hidden layer and also that of the output layer is the widely-used logistic function, i.e. a form of sigmoid function, given by

$$f\left(\sum_{i=1}^M w_i y_i + w_o\right) = \frac{1}{1 + e^{-\sigma\left(\sum_{i=1}^M w_i y_i + w_o\right)}} \quad (6)$$

Which is bounded in the range  $[0,1]$ , implying that the network output is likewise bounded in that range,  $\sigma$  being a scaling parameter of the transfer function. The weights  $w_i$ , the threshold  $w_o$  and the  $\sigma$  of the different neurons can all be interpreted as the parameters of the selected network configuration. These parameters may be determined using the method of back-propagation or the conjugate gradient method (Shamseldin, 1997) but, as the Simplex method is used in the GFFS for calibration of the rainfall-runoff models, it is also used for calibrating the ANN in that package.

The effective range of the logistic function is generally less than that indicated by Eq. (6) and in order to facilitate the comparison of the actual observed discharges  $Q_i$  and the network-estimated outputs, the following equation is adopted for training (i.e. calibrating) the ANN;

$$Qs_i = 0.1 + 0.75\left(\frac{Q_i}{Q_{max}}\right) \quad (7)$$

i.e. a rescaling of the observed discharges  $Q_i$  so that the resulting rescaled discharges  $Qs_i$  are bounded between 0.1 and 0.85,  $Q_{max}$  being the maximum observed discharge of the calibration period. The discharge forecast of the ANN is given by the inverse of Eq. (7).

## THE SELECTED CATCHMENTS

Test catchments were used in this study. The first is the Blue Nile up to Eddiem station (254230 km<sup>2</sup>) in Sudan as shown in Fig. 3, and the second is the Upper Awash sub-basin (110000 km<sup>2</sup>) in Ethiopia.

The present modeling work is focusing on the Major tributaries of Koka Reservoir, i.e., Awash River. The most d/s gauging station is Awash at Hombole which has drainage area of 7656 km<sup>2</sup> (69% of koka drainage area) and contributes 90% of total Inflow. This sub-basin originates from the central parts of Ethiopia at an elevation of 3000 m.a.s.l. and flows eastwards along the rift valley and terminates in L.Abe near the Djiboti boarder at an elevation of 250 m.a.s.l. as shown in Fig. 3. These two sub-basins represent the flow behavior of the Ethiopian Plateau of the Eastern part of the River Nile. Eastern Lake Victoria catchments was also represented by Nzoia (12676 km<sup>2</sup>) and Sondu (3450 km<sup>2</sup>) rivers in Kenya as shown in Fig. 3. Topographically, the Blue Nile catchment and the Upper Awash Sub-Basin, Ethiopia are predominantly hilly and mountainous areas. These two catchments having wet climatic conditions with woodland and forests land cover. The Eastern Lake Victoria catchments having a cultivated and grass land cover with a tropical climatic conditions.

# MODEL APPLICATIONS AND DISCUSSION OF RESULTS

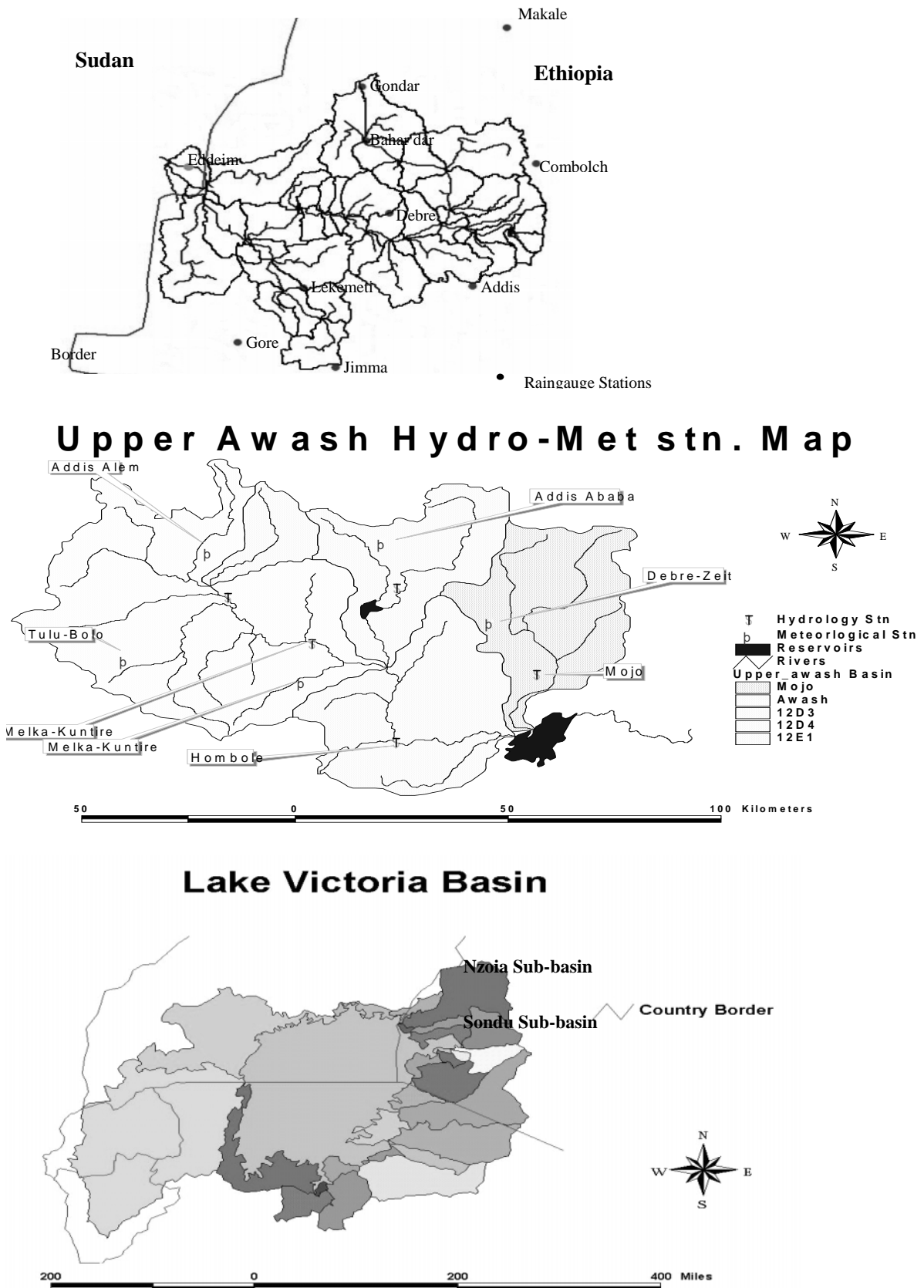


Fig. 3: Location Map of the Upper Awash Sub-Basin in Ethiopia: network (top) and catchments (middle), and of Nzoia and Sondu Sub-Basin in Kenya (bottom).

Each of the five basic models is applied to each of the selected test catchments, using split-record evaluation, involving the use of calibration and verification periods (about two-thirds for calibration and one-third for verification). In terms of increasing complexity, the SLM is the simplest, followed by the LPM and the LVGFM.

These three are system-theoretic in structure, and ordinary least squares solution is used for estimation of the pulse response function. The SMAR model parameters are estimated using the simplex method of optimization. As for the ANNM, the number of weights depends on the number of neurons chosen in the input layer and the hidden layer. If 'l' is the total number of neurons in the input layer and 'm' is that in the hidden layer, then the total number of weights to be estimated is  $(l+1)m + (m+1)$ .

As such, the ANNM is the least parsimonious amongst the models chosen in the study. The simplex method of automatic optimization is also used for calibration of the ANNM. The results of performances of the five substantive models are given for each application as follows:

### Upper Awash Sub-basin–Ethiopia

The climatic and hydrologic conditions of this sub-basin can be described as follows:

Five meteorological stations have been chosen, located within the catchment. Daily Rainfall, mean monthly temperature and evaporation data have been collected from these stations. The mean annual rainfall over the basin is 1200 mm and reaches about 1500 mm at the high lands. 70-75% of the annual rainfall occurs during June-September. The second rain period is Feb-May.

There is a number of flow gauging stations located on main River and on its tributaries. For the present study 4 stations have been collected. Daily flow record for the period of from 1991-2002 have been collected

The present modeling work is focusing on the Major tributaries of Koka Reservoir, i.e., Awash River. The most d/s gauging station is Awash at Hombole which has drainage area of 7656 km<sup>2</sup> (69% of koka drainage area) and contributes 90% of total Inflow. The calibration period is from 1/1/1991 to 31/12/1999 and the verification period is from 1/1/2000 to 30/9/2002. Weighted average of daily rainfall record of the five met. Stations have been used. Long term mean monthly temperature and evaporation data, on daily bases have been used. Fig. 4 shows a comparison between the observed and estimated hydrographs with the input rainfall. It shows also the calibration and the verification periods for the observed and estimated hydrographs with the rainfall input.

It can be seen from the plots and statistical values of model efficiencies as given in Tab.(1), the results of most models are encouraging. At present the PSLM model have better simulated than others. All the models could not well estimate the peak discharges of 1996 and 1999. This might be the effect of water supply reservoir. The other reason could be the high spatial variation of rainfall over the basin.

### Blue Nile River at Eddeim, Sudan

The climatic and hydrologic conditions of this sub-basin can be described as follows:

Ten rain gauge station in and around the study area (MOI and FEWS) have been used. Rainfall data is available from 1987 to 1998. Penman potential evaporation was obtained from USGS FEWS net.

Tab. 1: Summary of the statistical values of model efficiencies for Awash River.

Model	C a l i b r a t i o n				V e r i f i c a t i o n
	I V F	r <sup>2</sup>	d	R <sup>2</sup>	R <sup>2</sup>
N P S L M	1.0899	0.4643	0.7737	0.4612	0.2376
P S L M	0.9292	0.8060	0.9439	0.8046	0.8295
A N N	1.064	0.7205	0.9105	0.7195	0.6117
S M A R	1.0381	0.6626	0.8927	0.6579	0.4477
M O C T _ S A M	1.0043	0.8133	0.9395	0.8077	0.7878
M O C T _ W A M	1.0256	0.8293	0.9507	0.8291	0.8280
M O C T _ N N M	1.0028	0.8275	0.9503	0.8274	0.8235

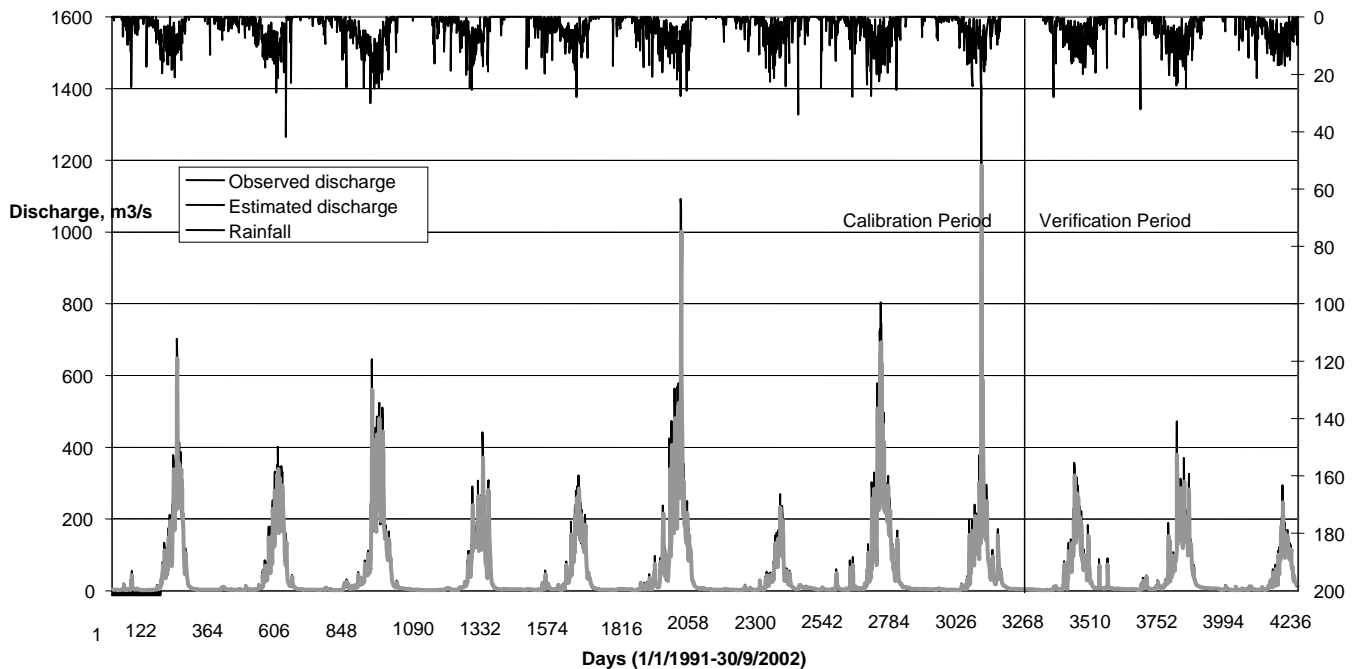
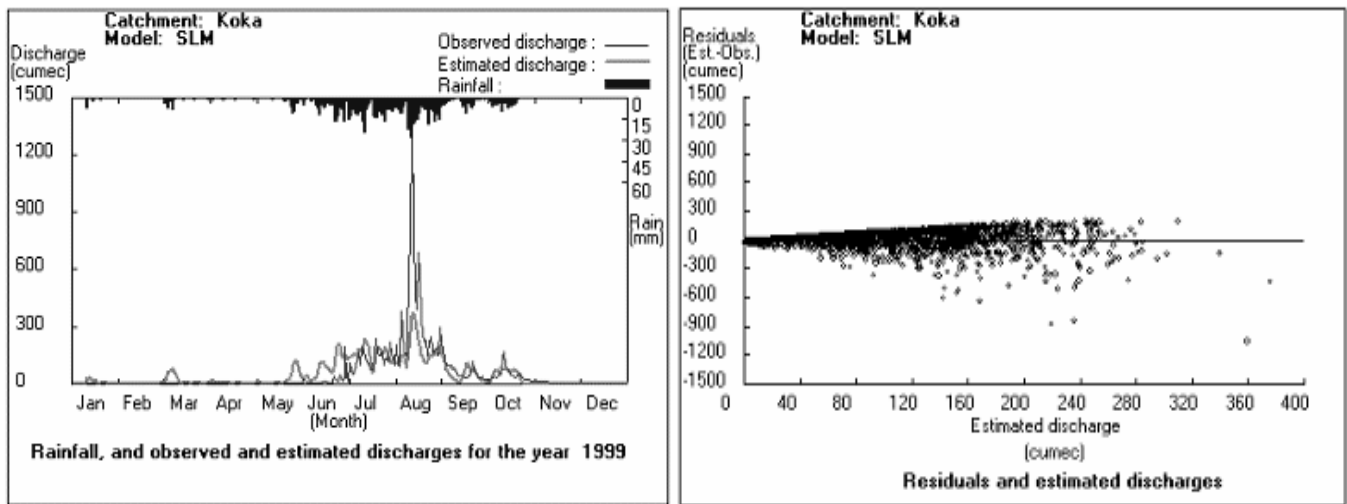


Fig. 4: Rainfall-Runoff Modeling of Koka Reservoir, i.e., Awash River.

Limited amounts of climatic data are available for estimation of potential evaporation in the basin. Data on all parameters that are required in Penman calculations are available for only five years of early nineties. The mean annual Penman evaporation over the catchment was found to be 1400 mm.

The method of Arithmetic Mean was used to estimate time series of Average Daily Rainfall (ADAR) over the catchment (Areal Rainfall). The method calculates ADAR as sum of rainfall observations made on day  $d$  divided by the number of observations made on the day. For ten rain gauges it is not always necessary that on each day all 10 observations were made. If only 8 observations were made on day  $d$ , then the sum of observations made on that day was divided by 8 to give ADAR for that day. The peak of the rainfall occurs on average three weeks before the peak of the flow.

River flow data at Eddeim station from 1964 to 1996 was obtained from MOI Sudan. The flow hydrograph starts to pick up in two weeks time after the start of the effective rainy season

To test the applicability of the GFFS model to the catchment under consideration, it was applied in a non-parametric and parametric constrained by linear transfer function. The parameters are optimized by ols for non parametric form, and by search technique (Rosenbrock's) for the parametric form. For SLM non-

parametric, the data was split in to two parts one for model calibration (5 years) and the other for model verification (2 years). A model efficiency of 78% was obtained during the calibration period and 76% was obtained for the verification period. For SLM parametric, the model efficiency obtained for the calibration period is 98% and that obtained for the verification period is 97% and the results are very impressive.

The Linear Perturbation Model (LPM) was applied as follows to the catchment under consideration using the daily data. Seasonal mean rainfall and seasonal mean discharge were calculated and smoothed for the period of calibration. The smoothed seasonal mean values (xd, yd) were then subtracted from the corresponding observed series for the period of calibration to get the perturbations R and Q. The pulse response was estimated by ols and the resulting pulse response is convoluted with the corresponding rainfall perturbation to obtain the estimated discharge perturbations. The final estimated discharge series of the LPM is calculated by adding the seasonal mean discharge to the estimated outflow perturbation series. The sum of square difference between observed and estimated discharges is obtained and the model efficiency is computed. For the LPM parametric model, it is parameterized using linear transfer function with the following parameters obtained by trail and error:

Model	Calibration			Verification		
	Start	No. days	R <sup>2</sup>	Start	No. days	R <sup>2</sup>
SAM	1/1/1990	1826	89.9	1/1/1995	731	88.4
WAM	1/1/1990	1826	92.4	1/1/1995	731	91.6
ANN	1/1/1990	1826	92.4	1/1/1995	731	91.5

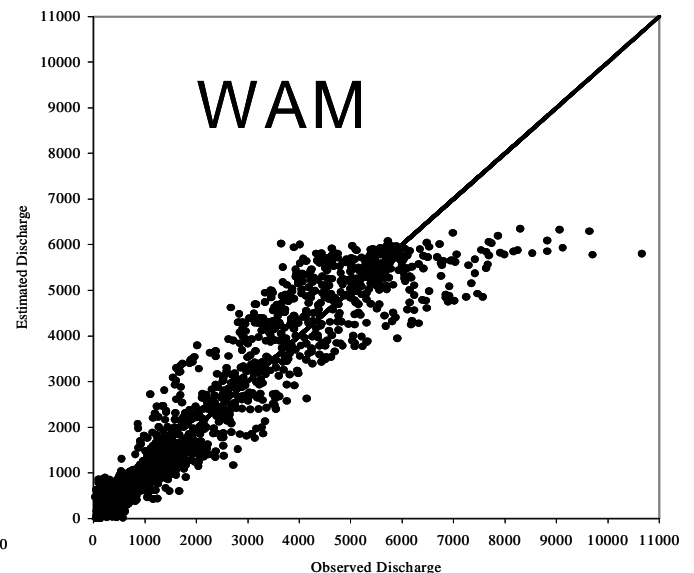
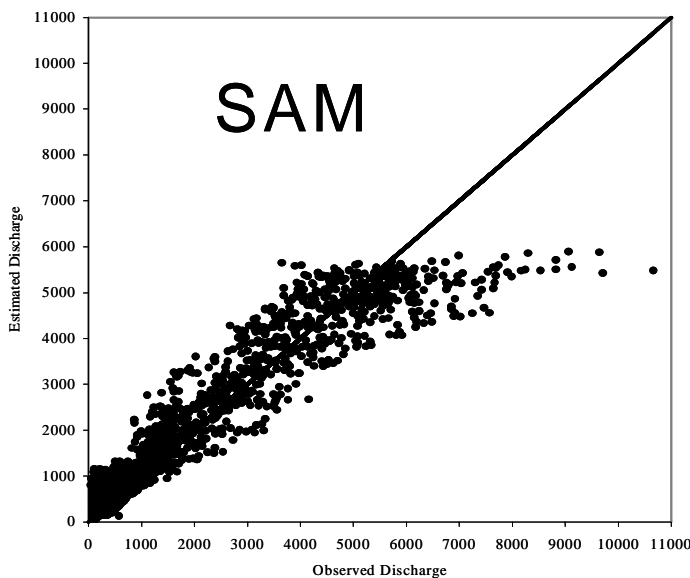
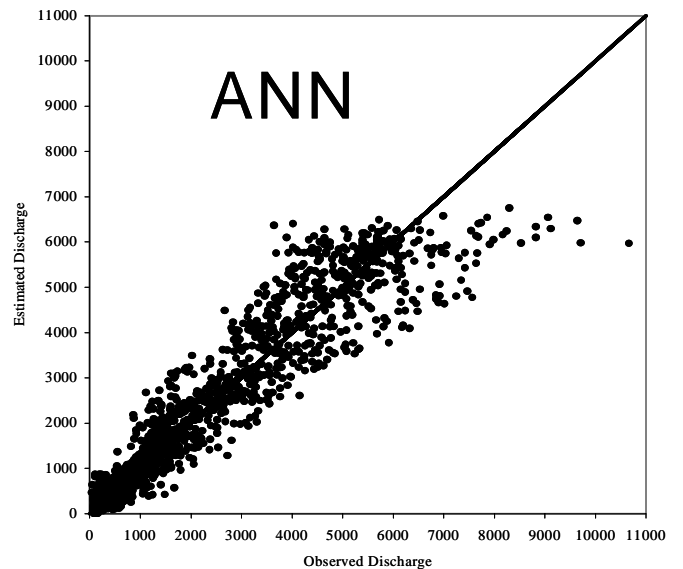
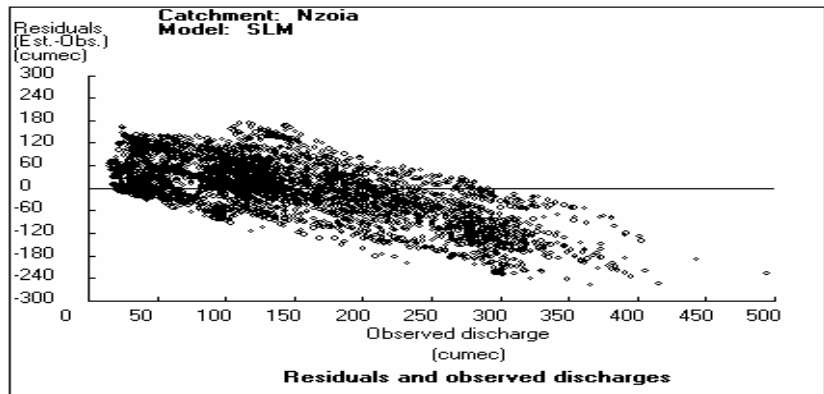
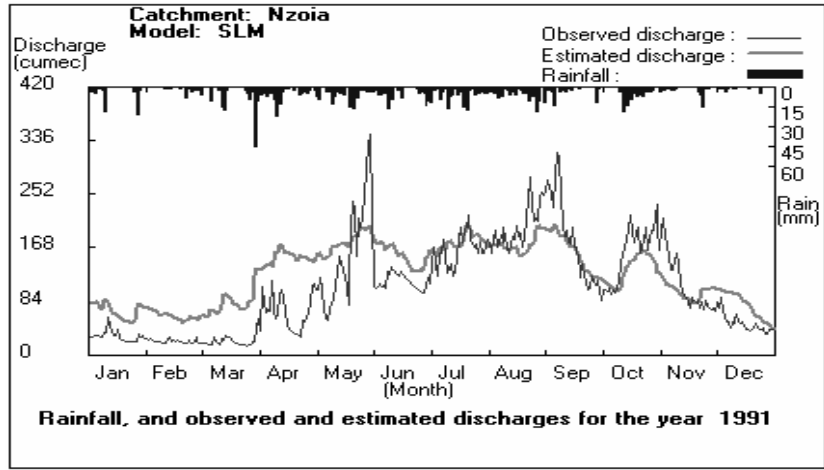


Fig. 5: Rainfall-Runoff Modeling of the Blue Nile at Eddiem by MOCT Model.

- Moving average of 3 days - Pure translation of 1 day - Autoregressive of 3 days.



## Non-parametric



## Parametric (observed $Q_s$ )

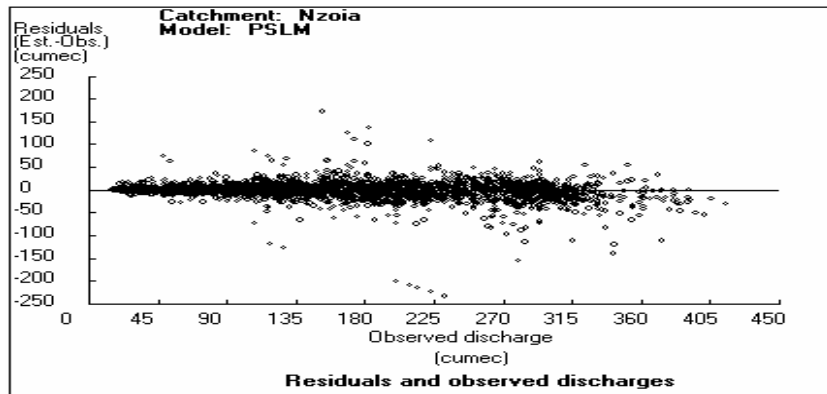
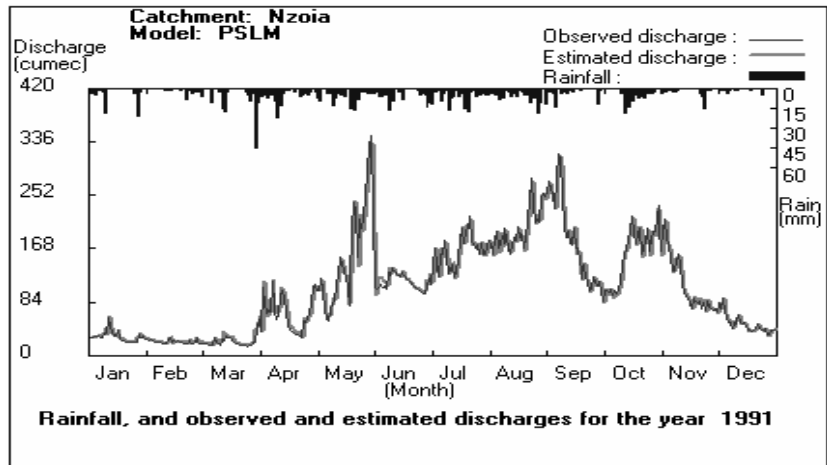


Fig. 6: Linear system models in Nzoia basins in Kenya.

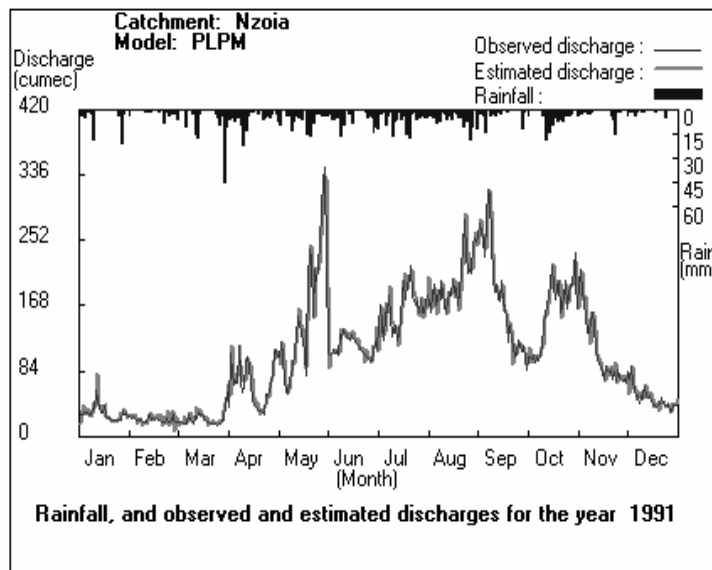
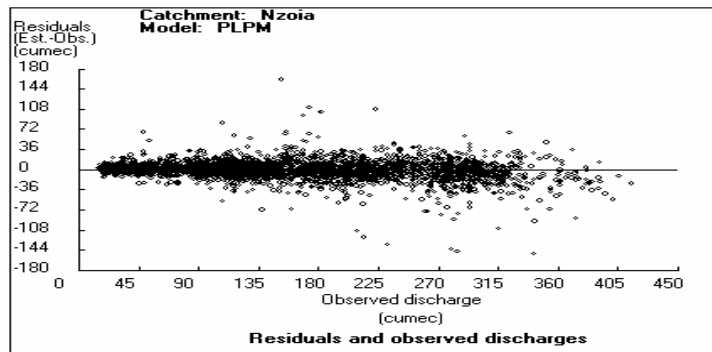
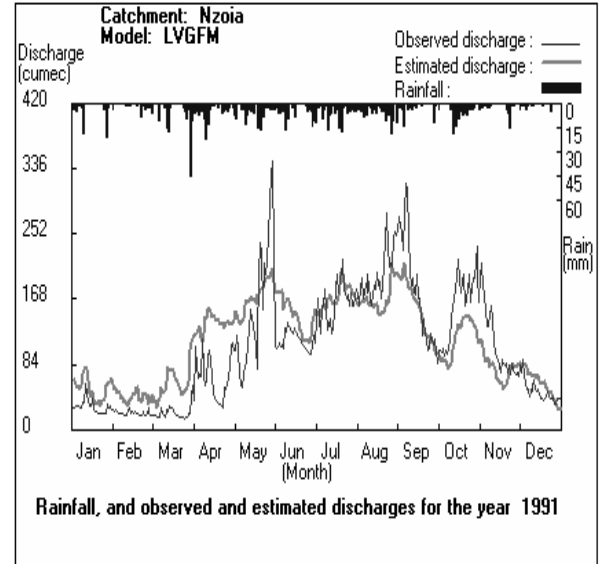
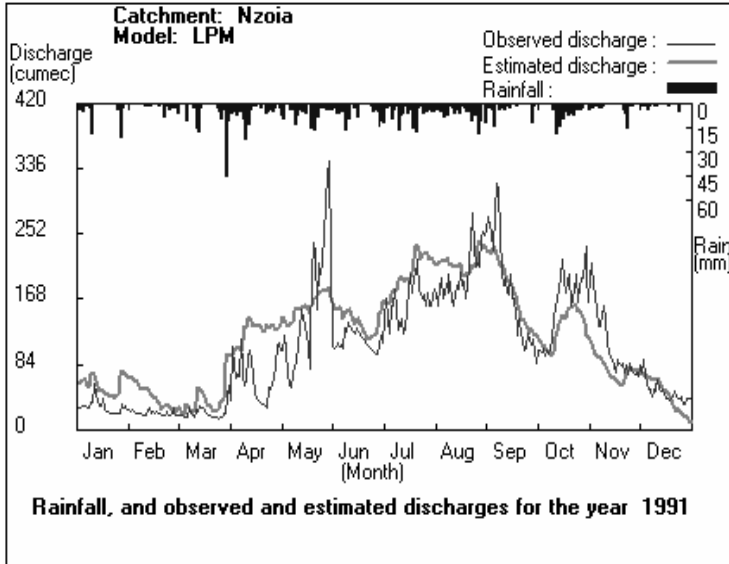
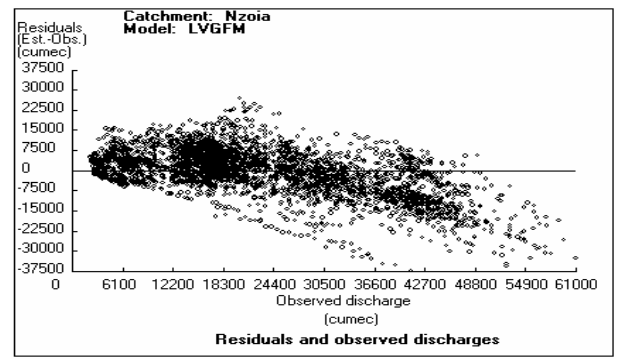
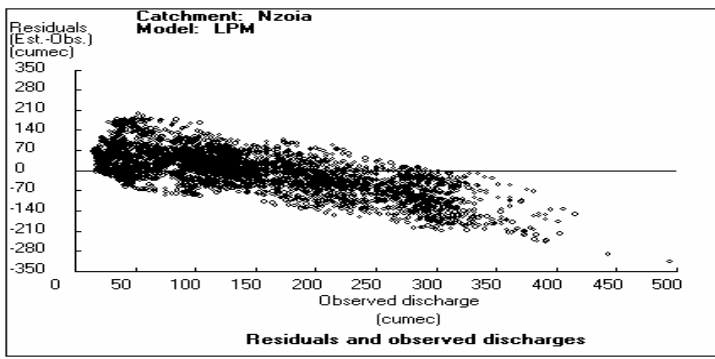


Fig. 7: Non-Linear system models in Nzoia basins in Kenya.

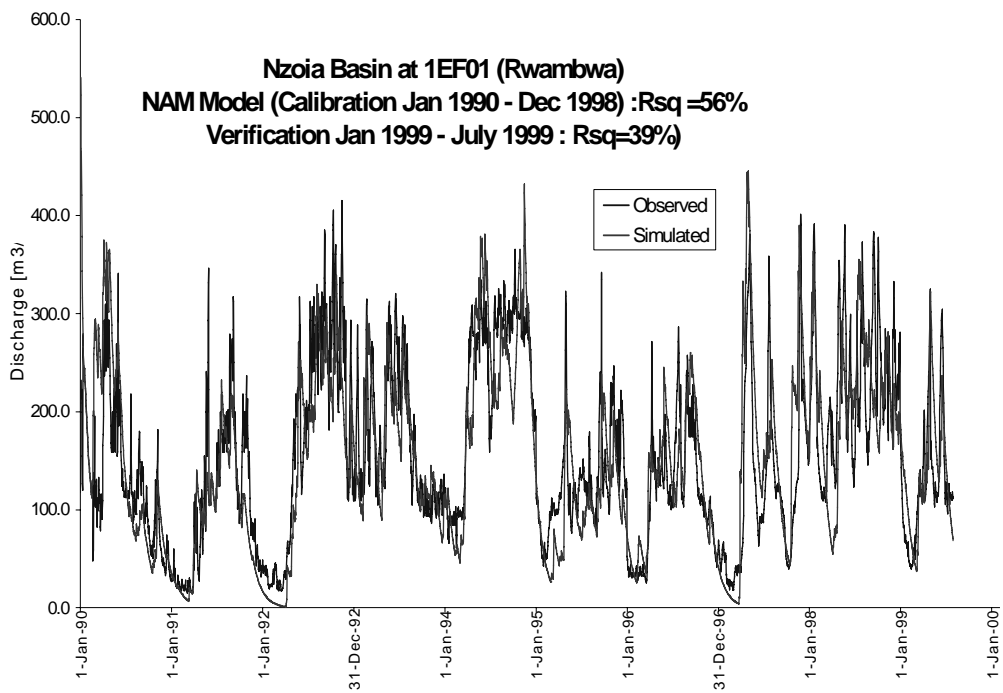
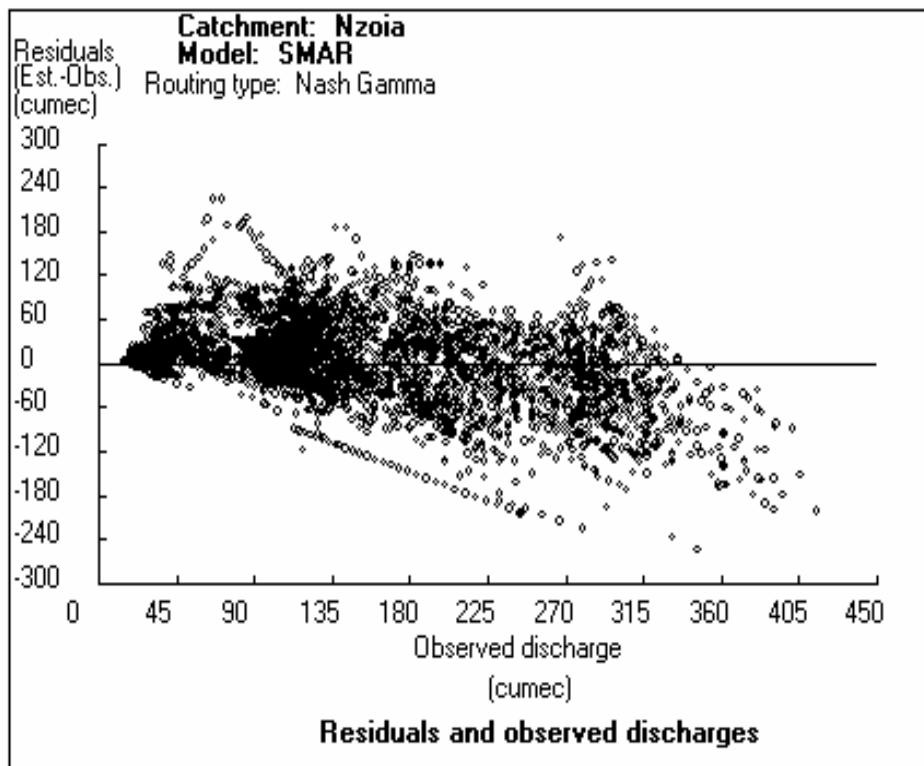


Fig. 8: SMAR and NAM system models in Nzoia basins in Kenya.

Tab. 2: Summary of the statistical values of model efficiencies for Nzoia and Sondu basin.

Period	Basin	Method	Updating	SLM %	LPM %	VGFM %	SMAR %	NAM %
<b>Calibration</b>	Nzoia Jan 90 – Dec 97 2557 days	OLS	No	60	67	64	68	54
		Parametric (Diff. Eq.)	No	52	57	-	-	-
			Yes	96	97	-	-	-
	Sondu Jan 70 – Dec 72 1096 days	OLS	No	44	67	49	68	67
		Parametric (Diff. Eq.)	No	43	65	-	-	-
			Yes	98	99	-	-	-
<b>Verification</b>	Nzoia Jan 98 – Jul 99 943 days	OLS	No	49	44	45	43	41
		Parametric (Diff. Eq.)	No	49	45	-	-	-
			Yes	94	96	-	-	-
	Sondu Jan 73 – Dec 74 721 days	OLS	No	34	42	21	45	68
		Parametric (Diff. Eq.)	No	34	41	-	-	-
			Yes	89	90	-	-	-

## CONCLUSIONS AND RECOMMENDATIONS

It can be concluded from this study that for the Ethiopian plateau, the PSLM model have better simulated than others. All the models could not well estimate the peak discharges of 1996 and 1999. For the Blue Nile in Sudan, the lumped systems models can be used with LPM giving the best performance. Distributed/semi-distributed models such as GeoSFM proved to be very promising. Finally, for Nzoia and Sondu rivers in Kenya, the linear; non-linear; and SMAR and NAM system models give good results.

In conclusion, this study confirms that simpler models for continuous river-flow simulation can surpass their complex counterparts in performance. There is a strong justification, therefore, for the claim that increasing the model complexity, thereby increasing the number of parameters, does not necessarily enhance the model performance. It is suggested that, in practical hydrology, the simpler models, “based largely on exercises in pattern recognition and curve fitting, through analysis of the available data” [O’Connor, 1998], can still play a significant role as effective simulation tools, and that performance enhancement is not guaranteed by the adoption of complex model structures.

## ACKNOWLEDGEMENTS

The authors are pleased to acknowledge the financial assistance of Flemish Government of Belgium and the UNESCO Cairo office in supporting the workshops in the Rainfall–Runoff Modelling Component of the FRIEND/Nile Project that contributed significantly to this paper.

## REFERENCES

- Ahsan, M. and O'Connor, K.M. (1994) A simple nonlinear rainfall-runoff model with a variable gain factor. *J. Hydrol.*, 155, 151- 183.
- Beran, M. (1999) Hydrograph Prediction: How much skill? *Hydrology and Earth System Sciences*, 3, 2, 305-307.
- Clarke, R.T. (1994) *Statistical Modeling in Hydrology*. John Wiley and Sons.
- Kachroo, R.K., Liang, G.C. and O'Connor, K.M. (1988) Application of the linear perturbation model (LPM) to flood routing on the Mekong River. *Hydrol. Sci. J.*, 33, 2-4, 193-214.
- Kachroo, R.K. (1992a) River flow forecasting, Part 1, A discussion of principles, *J. Hydrol.*, 133, 1-15.
- Kachroo, R.K. (1992b) River Flow forecasting, Part 5, Applications of a conceptual model. *J. Hydrol.*, 133, 141-178.
- Khan, H. (1986) *Conceptual Modeling of rainfall runoff systems*. M. Eng. Thesis, National University of Ireland, Galway.
- Legates, D.R. and McCabe Jr., G.J. (1999) Evaluating the use of "goodness-of-fit" measures in hydrologic and hydroclimatic model validation. *Water Resources Research*, 35, 1, 233-241.
- Liang, G.C. (1992) *A note on the revised SMAR model*. Workshop Memorandum, Department of Engineering Hydrology, National University College of Ireland, Galway (Unpublished).
- Liang, G.C., O'Connor, K.M. and Kachroo, R.K. (1994) A multiple-input single-output variable gain factor model. *J. Hydrol.*, 155, 185-198.
- Nash, J.E. and Sutcliffe, J.V. (1970) River flow forecasting through conceptual models, Part 1, A discussion of principles. *J. Hydrol.*, 10, 282-290.
- Nash, J.E. and Foley, J.J. (1982) Linear models of rainfall-runoff systems. In: '*Rainfall-Runoff Relationship*', Proceedings of the International Symposium on Rainfall-Runoff modeling. Mississippi State University, May 1981, USA, Singh V.P. (Ed.), Water Resources Publications, 51-66.
- Nash, J.E. and Barsi, B.I. (1983) A hybrid model for flow forecasting on large catchments. *J. Hydrol.*, 65, 125-137.
- O'Connell, P.E., Nash, J.E. and Farrell, J.P. (1970) River Flow forecasting through conceptual models. art 2. The Brosna catchment at Ferbane. *J. Hydrol.*, 10, 317-329.
- O'Connor, K.M. (1998) *The Education and Training of Hydrologists*. A Discussion Paper submitted to the Unesco Steering Committee of IHPV Project 8.1 in the context of its Draft Education Policy Document (unpublished).
- O'Connor, K.M., Goswami, M., Liang, G.C., Kachroo, R.K. and Shamseldin, A.Y. (2001) The Development of The 'Galway Real-Time River Flow Forecasting System (GFFS). *The proceedings of the 19th European Regional Conference of ICID*, Czech Republic.
- Shamseldin, A. Y. (1997) Application of a neural network technique to rainfall-runoff modeling. *J. Hydrol.*, 199, 272-294.
- Shamseldin, A.Y., O'Connor, K.M. and Liang, G.C. (1997) Methods for combining the outputs of different rainfall-runoff models. *J. Hydrol.*, 197, 203-229.
- Tan, B.Q. and O'Connor, K.M. (1996) Application of an empirical infiltration equation in the SMAR conceptual Model. *J. Hydrol.*, 185, 275-295.
- Willmott, C.J. (1981) On the validation of models. *Phys. Geogr.*, 2, 184-194.
- Xiong, L., O'Connor, K.M. and Goswami, M. (2001) Application of the artificial neural network (ANN) in flood forecasting on a karstic catchment. *The XXIX IAHR Congress*, Beijing.

# CHANGING FLOWS IN SOUTHERN AFRICA AND ITS RELATIONSHIPS TO RAINFALL VARIATIONS

**Patrick VALIMBA, Simon H. MKHANDI**

Department of Water Resources Engineering, Faculty of Civil Engineering and the Built Environment, University of Dar Es Salaam, P.O. Box 35131, Dar Es Salaam, Tanzania.

*pvalimba@hotmail.com*

**Eric SERVAT**

IRD, UMR HydroSciences, Maison de Sciences de l'Eau, Université Montpellier II, BP 64501, 34394 Montpellier Cedex 5, France

**Denis HUGHES**

Institute for Water Research, Rhodes University, P.O. Box 94, Grahamstown, 6140, South Africa.

## ABSTRACT

Flow duration curves (FDCs) were used to study characteristics of daily flows in southern Africa and thereafter used to define the thresholds of low and high flows. Change-point analysis methods were used to identify the existence of any discontinuities in the indices of streamflow. FDCs identified three types of rivers (ephemeral, seasonal and perennial) in southern Africa with ephemeral rivers found mainly in the dry western part of the region. Seasonal streamflow patterns were observed to follow those of rainfall. Change-point analysis indicated significant changes in the river flows regimes in the southern African rivers which have occurred in the 1970s through early-1980s. The changes mainly affected the mean flows with little evidences of high and low flow regime. These changes led to decreases in river flows in western Zambia, Namibia and northeast South Africa considerably affecting the flows during the high flow months in which 34-80% of the annual flow volumes are observed. The results further indicated occurrences of periods of no flow in recent decades in some perennial rivers while lengthening of the no flow period in seasonal rivers. In some parts of southern Africa, alternating increases and decreases in river flow indices were observed which corresponded mainly to interannual patterns of rainfall variation. In other parts like in the eastern Mount Kilimanjaro, the influences of degrading landuse practices contributed significantly to declining flows. However, it was not possible to provide strong links between the identified changes in streamflows and those in rainfall.

**Keywords:** streamflow variations, flow duration curves, flow extremes, change-point analysis, interannual variability

## INTRODUCTION

Surface water resources in southern Africa are declining leading to growing conflicts between different competing users such as agriculturalists, hydropower plants and water suppliers. Dam levels have been reported to decline since the mid 1970s in Namibia (Jury and Engert, 1999), in South Africa since the early 1980s as a reflection of prolonged rainfall deficit in the 1980s and early 1990s (Mason, 1996). Berhanu (1999) found a recent decrease in mean annual runoff in southern African catchments that occurred since 1975, particularly marked in Zambia, Angola, Mozambique and the South African High Veld. The decline is attributed mainly to declining and unreliable rainfall, population increase and changing land and water uses.

It is plausible to hypothesize that identified changes in southern African surface water resources are reflected from changes in rainfall as observed in West Africa (Mahé and Olivry, 1991; Servat *et al.*, 1997a) and their severity is increased by human-related influences. Past studies have identified a mixture of increasing and decreasing rainfall amounts in some parts of southern Africa (Mason *et al.*, 1999; Mkhanda and Ngana, 1999; Mutua, 1999) while in others there was no strong evidence of declining or increasing trends. However, there is evidence of increasing frequency of high rainfall events in some parts of southern Africa (Mason and Joubert, 1997; Smakhtina, 1998; Mason *et al.*, 1999). Such changes in rainfall alone could have serious negative consequences to water resources, the population and properties. Frequent floods have been reported in recent decades in both the humid and dry parts of the region (e.g. the 1984 floods along the Namibian coast; the February 2000 severe floods which hit Mozambique; the November-December 1997 floods in east Africa).

Moreover, the southern African population is dynamic and has been growing rapidly in recent decades with the highest population densities and growth rates in the humid and fertile eastern part. Its rapid growth and consequential increased water demand have led to changes in the land use and water use patterns in the region with more land being cleared for modern agriculture mixed with modern animal husbandry. Consequently large land areas become exposed to actions of the weather and man which may alter soil surface characteristics resulting in increased frequency and/or volumes of flash floods due to poor infiltration. Insufficient groundwater recharge due to poor infiltration during the wet season may further lead to declining dry season flow and hence the danger of severe streamflow droughts.

Therefore, this study investigates changes in flow volumes and flow regimes for selected rivers in southern Africa to highlight their spatio-temporal characteristics and their relationships to changing rainfall and the climate.

## **DATA, METHODS AND STUDY INDICES**

### **Data**

Average daily flow data in rivers in the 11 southern African countries have been acquired from the southern African FRIEND HYDATA database at the Department of Water Resources Engineering (WRE) of the University of Dar Es Salaam. The database was compiled by the Centre for Ecology and Hydrology (formerly the Institute of Hydrology, Wallingford) for the Southern African FRIEND. It comprises time series of average daily river flows for 676 gauging stations. Additional 23 records of average daily flows and updates of the 79 records in the FRIEND database for gauging stations in the Pangani and Rufiji River basins in Tanzania were obtained from the Hydrology Section of the Department of Water Resources in the Ministry of Water and Livestock Development (Tanzania). The spatial distribution of the river flow gauging stations is dense in the eastern, northeastern and southern South Africa, in the eastern and southwestern Zimbabwe, in central-western Namibia and in the two Pangani (northeast) and Rufiji (southwest) basins in Tanzania.

The preliminary data analysis indicates that the southern African region is characterised by short streamflow records. Therefore, the selection criteria of record length, missing data and period of interest were applied to preliminarily screen out unsuitable records. Moreover, Valimba (2004) showed that areas such as part of the southern highlands of Tanzania, northern half of Mozambique and the South Africa lowveld are characterized by intense daily rainfall events and are therefore prone to flooding. The western part of southern Africa is dry and rivers there experience frequent and prolonged dry conditions. Basins whose rivers drain these areas are of particular interest in studying relationships between rainfall and flow variations. The selection process further excluded all gauging stations located downstream of any artificial regulation points. Gauging stations within the selected basins were further selected in such a way to avoid closely located gauges while retaining as many gauges as possible along the river lengths. The overall requirements of analysing long continuous records from unregulated catchments within the selected basins, therefore, retained 38 river flow records (Fig. 1).

### **Methods**

Interannual variability of flow indices was investigated using the change-point analysis methods which identify discontinuities (shifts) in the mean values of a time series. The procedure is described in detail and used in Valimba (2004), Valimba *et al.* (2004a) and Valimba *et al.* (2004b). In summary, the non-parametric test of Pettitt and autosegmentation procedure of Hubert (Lubès-Niel *et al.*, 1998 and references therein) were used with some procedural modification of the Pettitt test, as described in the mentioned articles, to provide multiple segmentation. The interpretation of results of these tests assumed shifts only when segments were at least 5 years long. Segments of less than 5 years were treated as grouped outliers while those comprising single years as isolated outliers.

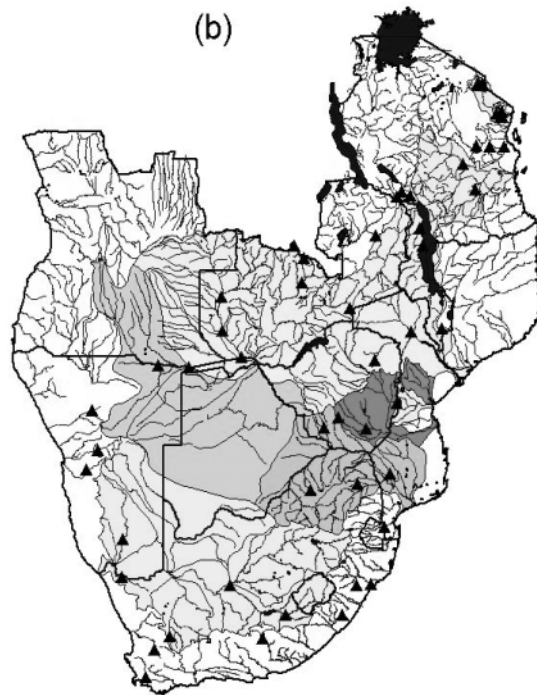


Fig. 1: Spatial distribution of selected flow gauging stations used in the interannual variability analysis in southern Africa. The coloured background indicates some of the important and shared river basins in the region.

### **Study indices and time series reconstruction**

In order to verify the study hypotheses of reduced flows and enhanced frequency and severity of flow extremes (floods and droughts), various indices were extracted from available flow records. Average discharges were appropriate to highlight the flow increase or decrease. The frequency and severity of floods and drought in southern Africa were studied using frequencies and volumes of excess and deficit flows. The excess (deficit) flow frequency was defined as the number of days above (below) the threshold defining the flood (drought) flow while excess (deficit) flow volume was the cumulative flow volume above (below) the respective thresholds (Valimba, 2004; Valimba *et al.*, 2004a).

The analysis of the flow duration curves at various gauging stations indicated that the flows that have been equaled or exceeded 5% (Q5) and 70% (Q70) of the time when it flows appropriately defined the flood and drought flow thresholds respectively. The indices provide a significant number of daily flows above or below them appropriate for interannual variability analysis while avoiding the problem of the frequent zero-drought/flood years, which were apparent when higher (e.g. Q1) or lower (e.g. Q90) thresholds were used.

## **RESULTS**

### **River flow regimes**

The FDCs calculated with zero flows included distinguished i) seasonal rivers from perennial rivers and ii) highly seasonal (or ephemeral) rivers from moderately seasonal rivers. in the southern Africa region. Ephemeral rivers flow when there is rainfall and cease almost immediately afterwards and are found in Botswana, Namibia, western Zimbabwe and South Africa. Moderately seasonal rivers flow continuously during the rainy season and cease sometime after the end of the rains and dry up completely during the dry period. They are a characteristic of small catchments in the Limpopo and in the Western Cape in South Africa and flow continuously between May and December (Western Cape) and November and April-July (other parts of unimodal southern African), the exact end month of the flow between April and July being dependent on catchment characteristics. Perennial rivers flow throughout the year and are a

characteristic of most rivers in southern Africa, particularly the main rivers in the large river basins or their main tributaries in the large river sub-basins. The rivers are characterised by non-zero FDCs indicating residual flows during the dry period and experience periods of high and low flows.

### **Flow seasonality**

Seasonal flow variations in the perennial rivers in southern African are characterised by double flow peaks in northern Tanzania, as well as parts of the southern and Eastern Cape and a single flow peak in the rest of the southern African subcontinent. The peaks correspond to seasonal rainfall variations in the region with double peaks in northern Tanzania corresponding to the bimodal rainfall regime (the short and long rains) and those in the southern South Africa and Eastern Cape in April and December corresponding to early and late summer rainfalls while a single peak in the remaining part corresponding to the unimodal rainfall regime.

A comparison of mean monthly flows ( $\mu_{\text{mon}}$ ) and mean annual flows ( $\mu_{\text{an}}$ ) indicated generally that the periods June-September and January/February-April/May are respective high flow periods in the Western Cape and the rest of the unimodal southern Africa and April-June in northern Tanzania. The highest monthly flows are observed in January-February in most parts of unimodal southern Africa, in August in the Western Cape, in March-April in Zambia and Malawi and in May-June in northeast Tanzania. Similarly, low flows are observed during the dry periods, July-November in unimodal southern Africa, December-March in the Western Cape and both August-October and February-March in bimodal northeast Tanzania. Moreover, mean monthly flows vary greatly between southern African catchments with the highest mean flows observed along the length of the main rivers in the large basins or their main tributaries (e.g. the Zambezi basin or its Luangwa sub-basin; the Okavango basin, etc) which drain the humid part of southern Africa.

### **Interannual variations**

Results (Tab. 1) of change-point analysis performed on seasonal flow indices indicate that excess and deficit flow volumes and frequencies exhibit almost similar patterns of interannual variability. However, for flow extremes, shifts were predominant in the frequency indices than the volume indices. The results further indicated that shifts were predominantly in mean seasonal flows than in the frequencies and volumes of high and low flows and characterised mainly the late summer (February-April, FMA) season. Moreover, shifts in the low flow indices were mostly identified during the the austral winter (June-August, JJA) season. The identified shifts during both the early (November-January, NDJ) and late (FMA) austral summers were predominantly unidirectional and towards a decrease, except in some rivers in northeast Tanzania. These abrupt changes were mainly identified in the 1970s and early-1980s although changes were identified as early as in the late-1950s and early-1960s (Fig. 2).

Tab. 1: Summary of shifts in seasonal flow indices in southern Africa.

	<b><u>Seasonal Flow Index</u></b>								
	<u>Mean flow</u>			<u>Excess Flow Freq.</u>		<u>Deficit Flow Freq.</u>			
	NDJ	FMA	JJA	NDJ	FMA	NDJ	FMA	JJA	
Total number of analysed stations	41	43	43	43	43	42	44	44	
Total number of stations with shifted flows	13	22	14	7	19	12	13	19	
Total number of unidirectional shifts in	12	20	13	7	16	9	8	11	
Total number of upward unidirectional shifts in	4	6	5	1	3	2	3	4	
Total number of downward unidirectional shifts in	8	14	8	6	13	7	5	7	

The cumulative flow volumes during the whole austral summer (November-April) account for 56.7-99.2% of annual flow volumes and the two seasons, NDJ and FMA, account separately for 9.7-59.0% and

34.0-79.9% of annual flow volumes, the largest percentages being for seasonal rivers in the unimodal southern Africa. The mean flow decreases, particularly during the FMA season, were related to changes of up to 50% or higher. This is illustrated by complete declines in the Namibian rivers and abrupt decreases in FMA and JJA seasonal mean flows and deficit flow frequencies in the upper Zambezi in western Zambia (Fig. 2). The start of the declining flows in Namibia is consistent with the start of declining rainfalls (Valimba, 2004) and dam levels (Jury and Engert, 1999) around the mid-1970s. Berhanu (1999) reported declining annual runoff in parts of Zambia and Angola. Furthermore, frequent and lengthening periods of no flows were observed in some of the perennial rivers since the early-1980s suggesting that these rivers are being progressively transformed into seasonal rivers, results which were similarly observed in Zimbabwe (Magadza, 1995).

## DISCUSSION

Changes in river flow regimes may result from a variety of factors such as changes in the climatic parameters (precipitation, temperature) and artificial influences in the catchment, including changing land and water use patterns (Hisdal *et al.*, 2001). The selection of flow records used in this study tried to avoid gauges which were regulated. Since no information on land and water uses patterns were available, a comparison of the interannual patterns of variability of streamflows and rainfalls would indirectly highlight the contributions of artificial influences on the streamflow changes, particularly since the 1960s. In general, NDJ mean flows in southern African rivers have either remained unsegmented or abruptly increased, except for the rivers in Namibia, northeast South Africa and southern Zimbabwe (Fig. 2a). This is identical to changes in early summer (NDJ) seasonal rainfall amounts (Valimba, 2004). Similarly, predominantly decreasing FMA mean flows in unimodal southern Africa correspond to declining overall rainfall amounts in late summer (FMA) (Valimba, 2004). However, the abrupt decreases in FMA overall rainfall amounts in Namibia identified in the 1977-1980 period lagged flow decreases in the mid-1970s (Fig. 2). Due to their seasonal nature, the slight changes in rainfall since the mid-1970s might have caused the early decreases in river flows.

The lack of abrupt decreases in seasonal as well as annual amounts in western Zambia (Valimba, 2004) could be hardly linked to abrupt decreases in mean seasonal flows in the upper Zambezi (western Zambian) catchments, which bordered the Congo River basin. However, the results of linear trends for the 1961-1991 period (not shown) showed decreasing trends in seasonal amounts in these parts of Zambia. Sichingabula (1998) found decreasing annual rainfall in southern and eastern Zambia since 1975, while Bigot (1997) and Bigot *et al.* (1998) identified declining annual rainfall in the Central Africa and the Congo basin since the late-1960s, a decline which was similarly identified in the catchments within the Congo River basin (Laraque *et al.*, 1998, 2001) and which was reflected by decreasing annual flows since the 1970s. The changes in the western Zambian catchments could be partly related to the changes in rainfall identified in the Congo River basin.

Long rainfall records indicate abrupt changes towards persistent wetter conditions in areas around Mount Kilimanjaro (Valimba *et al.*, 2004a, 2004b). Despite a number of existing flow abstractions upstream, mean flows in all months at the most downstream gauge in the Kikuletwa River, which drains the western part of the Kilimanjaro, have increased since 1960/61 (Valimba *et al.*, 2004c), consistent with the reported increases in rainfall amounts. A number of past studies have identified similar increases in rainfall and other hydrological variables such as lake levels since the early-1960s in East Africa which includes Tanzania (Bergonzini, 1998; Nicholson, 1999; Nicholson, 2000). However, the rivers which drain the eastern part of Mount Kilimanjaro were characterised by decreasing flows in all months, contradicting the rainfall increases. A number of studies have linked such flow decreases to the population increase and degrading land and water use practices (Mujwahuzi, 1999; Ngana, 2002; Shishira, 2002; Yanda, 2002; Yanda and Shishira, 1999).

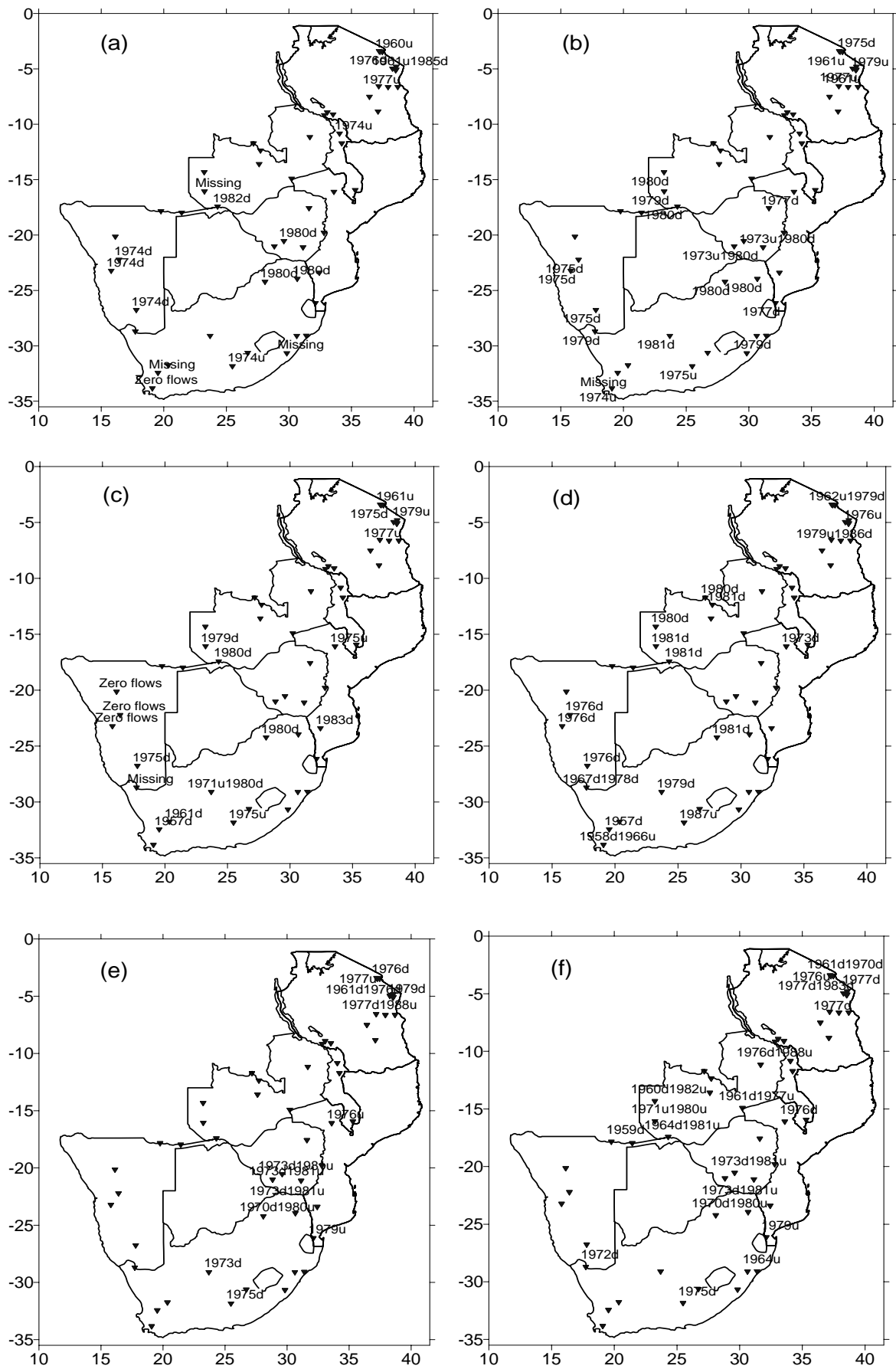


Fig. 2: Dates of shifts in a) NDJ, b) FMA and c) JJA mean seasonal river flows; in the frequencies of d) excess flows (see text for the high flow seasons), e) FMA deficit and f) JJA deficit flows in the southern African rivers. The year indicates the date of shift while the letters indicate the direction of shifts, u for the upward and d for the downward shift.

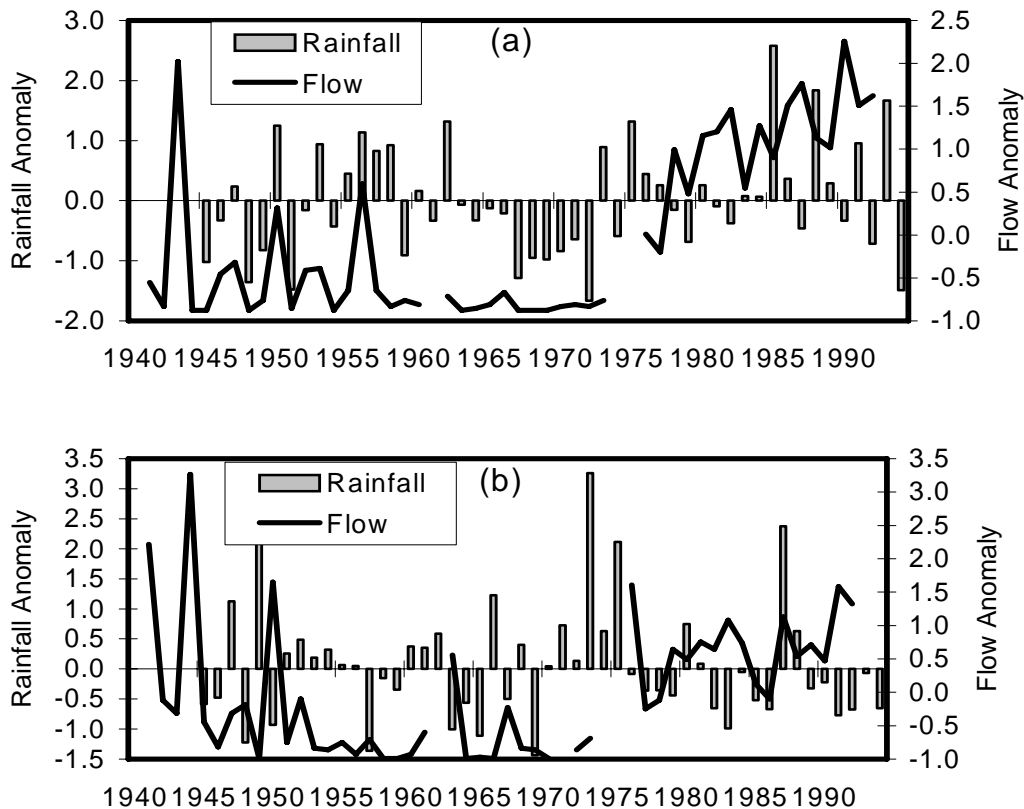


Fig. 3: Time series of anomaly a) NDJ and b) FMA seasonal flows and catchment overall rainfall amounts for the catchment of the gauge 27673901 in the Groot-Vis (Fish) River.

The importance of a thorough knowledge of changes of land and water use pattern within the catchments was illustrated by the flow regime transformation of the Groot-Vis (Fish) River located in the central southern part of South Africa that did not correspond to the pattern of rainfall variability (e.g. Fig. 3). The river has become perennial since around 1974/75. Time series of NDJ seasonal flows are persistently below average before the mid-1970s even during the period of above average rainfall in the 1950s (Fig. 3a) while the FMA rainfall series is predominantly below average after the mid-1970s contradicting the FMA flow series (Fig. 3b). The cause of the observed flow regime change in this river was the water transfer from the Orange River since the completion of the Gariep Dam in 1972.

Changing characteristics of flow extremes are affected partly by changing characteristics of intense rainfalls and changes in the catchment characteristics that affect runoff generation mechanisms. The results (Fig. 2d) show consistent and persistent decreases in the frequency of excess flows in rivers in western and northern Zambia since the early-1980 and in Namibia since the mid-1970s. In other southern African rivers, the changes were heterogeneous as they characterise only a few stations and not persistent as only segments of high or low frequencies were observed, after which, the series returned almost to the pre-change states. The pattern of the changes in the frequencies of excess and deficit flows, therefore, reflected generally the wet and dry periods in southern Africa (Valimba, 2004). Abundant rainfall observed in the 1970s in southern Africa (Chenje and Johnson, 1996) could have caused considerable groundwater recharge which lead to increased groundwater contributions to streamflows and therefore corresponded to decreased frequencies of deficit flow volumes. The rainfall deficits since the early-1980s and low between-the-years flow carry-over in most of the catchments caused a return to the pre-change state and was reflected to an increase of deficit flow frequencies since the early-1980s (Fig. 2e, 2f).

## CONCLUSIONS

Seasonal and interannual variations of streamflows were almost similar to seasonal and interannual variations of rainfall. Seasonally, flow peaks correspond to rainfall peaks and occur mainly during the core of the rainy seasons. Interannually, significant unidirectional abrupt changes in mean flows have occurred mainly since the mid-1970s to early-1980 which i) significantly affected streamflows during the late summer (FMA), ii) led to significant reduction of streamflows in the upper Zambezi basin, Namibia and northeast South Africa, iii) were gradual in the upper Zambezi suggesting that slight changes in rainfall could translate into significant changes in streamflows and iv) indicated little evidence of changes in the flow extremes (high and low flows) except in the upper Zambezi and Namibia.

Since it has been a common practise to calibrate and verify parameters of the hydroclimatological models using long records, the results of this study suggests a revision of the operational and forecasting hydrological models to use pre- or post-change records during model developments to avoid non-stationarities in the 1960s and 1970s. The study found flow changes in Namibia and western Zambia which were consistent with rainfall changes while in other parts it was very difficult to associate changes in streamflows with identified changes in rainfall. Therefore, to accurately quantify the magnitude of the influence of rainfall changes on changes of streamflows, studies at finer spatial scales like catchment scales are recommended. The use of water balance models can assist in quantifying the influence of climate and rainfall changes on streamflows once other model components have been quantified and accounted for.

## REFERENCES

- Bergonzini, L. (1998) Bilans hydriques de lacs (Kivu, Tanganyika, Rukwa et Nyassa) du rift est-Africain, *Ann.-Sciences Geologiques*, Publ. 103, Mus. Roy. Afr. Centr., Tervuren, Belgique, 183 p.
- Berhanu, F.A. (1999) *Development and application of a GIS - based regional hydrological variability and environmental assessment system (RHVEAS) for the southern Africa region*. PhD Thesis, Univ. of Dar Es Salaam, Tanzania.
- Bigot, S. (1997) *Les precipitations et la convection profonde en Afrique Centrale: Cycle saisonnier, variabilité interannuelle et impact sur la végétation*. Thèse de Doctorat, Université de Bourgogne, 283 p.
- Bigot, S., Moron, V., Melice, J.L., Servat, E. and Paturel, J.E. (1998) Fluctuations pluviométriques et analyse fréquentielle de la pluviosité en Afrique centrale. *IAHS Pub.* 252, 71–78.
- Chenje, M. and Johnson, P. (1996) *Water in southern Africa*. Print Holdings (Harare), 238 p.
- Hisdal, H., Stahl, K., Tallaksen, L.M. and Demuth, S. (2001) Have streamflow droughts in Europe become more severe or frequent. *Int. J. Climatol.*, 21, 317–333.
- Jury, M.R. and Engert, S. (1999) Teleconnections modulating inter-annual climate variability over northern Namibia. *Int. J. Climatol.*, 19, 1459–1475.
- Laraque, A., Mahé, G., Orange, D. and Marieu, B. (2001) Spatio-temporal variations in hydrological regimes within central Africa during the XX<sup>th</sup> century. *J. Hydrol.*, 245, 104–117.
- Laraque, A., Orange, D., Maziezoula, B. and Olivry, J.C. (1998) Origine des variations de debits du Congo à Brazzaville durant le XX<sup>ème</sup> siècle. *IAHS Pub.* 252, 171-179.
- Lubès-Niel, H., Masson, J.M., Paturel, J.E. and Servat, E. (1998) Variabilité climatique et statistiques. Etude par simulation de la puissance et de la robustesse de quelques tests utilisés pour vérifier l'homogénéité de chroniques. *Revue des Sciences de l'Eau*, 3, 383–408.
- Magadza, C.H.D. (1995) Special problems in lakes/reservoir management in tropical southern Africa. 6<sup>th</sup> International Conference on the *Conservation and Management of Lakes*, 23<sup>rd</sup>–27<sup>th</sup> October, 1995, Kamisugaura, Ibaraki, Japan.
- Mahé, G. and Olivry J.C. (1991) Changements climatiques et variations des écoulements en Afrique occidentale et centrale, du mensuel à l'interannuel. *IAHS Pub.* 201, 163–171.
- Mason, S.J. (1996) Climate change over the lowveld of South Africa. *Climate Change*, 32, 35–54.
- Mason, S. J., Waylen, P.R., Mimmack, G.M., Rajaratnam, B. and Harrison, J.M. (1999) Changes in extreme rainfall events in South Africa. *Climate Change*, 41, 249–257.
- Mason, S.J. and Joubert, A.M. (1997) Simulated changes in extreme rainfall over southern Africa. *Int. J. Climatol.*, 17, 291–301.

- Mkhandi, S H. and Ngana, J O. (1999) Trend analysis and spatial variability of annual rainfall in Pangani river basin. In Ngana (Ed.): *Water management in Pangani river basin, Challenges and opportunities*. Dar Es Salaam Univ. Press, 11–20.
- Mujwahuzi, M. (1999) Water use conflicts in Pangani basin. In Ngana (Ed.): *Water management in Pangani river basin, Challenges and opportunities*. Dar Es Salaam Univ. Press, 128-137.
- Mutua, F.M., (1999) Comparison of trend and general circulation model based projections of seasonal and annual rainfall in east African region, Proc. of an Interdisciplinary International Conference on *Integrated Drought Management*, Sep 20-22, Pretoria 1999.
- Ngana, J.O. (2002) Diminishing water resources and increasing water demands. In Ngana (Ed.): *Water resources management. The case of Pangani river basin, Issues and approaches*. Dar Es Salaam Univ. Press, 90–100.
- Nicholson, S.E. (2000) The nature of rainfall variability over Africa on time scales of decades to millennia. *Global and Planetary Change*, 26, 137–158.
- Nicholson, S.E. (1999) Historical and modern fluctuations of Lakes Tanganyika and Rukwa and their relationship to rainfall variability. *Climate Change*, 41, 53–71.
- Servat, E., Paturel, J.E., Lubès-Niel, H., Kouame, B., Travaglio, M. and Marieu, B. (1997a) De la diminution des écoulements en Afrique de l'ouest et centrale. *C. R. Acad. Sci. Paris, Sciences de la terre et des planètes*, 325, 679–682.
- Shishira, E. K. (2002) Landuse changes and sustainability of water resources utilisation in the Pangani river basin downstream of the Nyumba ya Mungu dam. In Ngana (Ed.): *Water resources management. The case of Pangani river basin, Issues and approaches*. Dar Es Salaam Univ. Press, 83–89.
- Sichingabula, H.M. (1998) Rainfall variability, drought and implications of its impacts on Zambia, 1886–1996. *IAHS Pub. 252*, 125–134.
- Smakhtina, O. (1998) Historical changes in rainfall pattern in the eastern Cape Province, South Africa. *IAHS Pub. 252*, 135–142.
- Valimba, P. (2004) *Rainfall variability in southern Africa, its influences on streamflow variations and its relationships with climatic variations*. PhD Thesis, Rhodes Univ., South Africa.
- Valimba, P., Servat, E., Mkhandi, S.H. and Camberlin, P. (2004a) Spatio-temporal variations of seasonal and annual rainfall totals in Tanzania. *Submit. to J. Hydrol.*
- Valimba, P., Mkhandi, S.H. and Servat, E. (2004b) Interannual variability of rainfall intensities in Northeast Tanzania and its relation to ENSO and SST variations. *Submit. to Int. J. Climatol.*
- Valimba, P., Mkhandi, S.H., Servat, E. and Hughes, D.A. (2004c) Interannual flow variations in the Pangani Basin in Northeast Tanzania. *Submit. to Hydrol. Sc. J.*
- Yanda, P.Z. (2002) Landuse pressure on the upper slopes of mount Kilimanjaro and progressive colonisation of marginal areas on footslopes. In Ngana (Ed.): *Water resources management. The case of Pangani river basin, Issues and approaches*. Dar Es Salaam Univ. Press, 74–82.
- Yanda, P.Z. and Shishira, E.K. (1999) Forestry conservation and resource utilisation on southern slopes of mount Kilimanjaro: trends, conflicts and resolutions. In Ngana (Ed.): *Water management in Pangani river basin, Challenges and opportunities*. Dar Es Salaam Univ. Press.



# MASS BALANCE AND SNOUT RECESSIOIN MEASUREMENTS (1991-2000) OF DOKRIANI GLACIER, GARHWAL HIMALAYA, INDIA

Prasad DOBHAL, J.G. GERGAN, Renoj J. THAYYEN

Wadia Institute of Himalayan Geology.33, GMS Road, Dehra Dun, India  
*dpdobhal@wihg.res.in*

## ABSTRACT

Dokriani glacier (30°50' to 30°52'N and 78°47' to 78°50'E) is a compound valley type glacier lying to the south-west of Gangotri glacier in Garhwal Himalaya. The glacier occupies an area of 7.0 km<sup>2</sup> of the total catchment area of 15 km<sup>2</sup> and is about 46% of the total glacierized area of the basin. This 5.5 km long glacier extends between 6000 m and 3880 m (amsl) Maximum thickness of glacial ice is 120 m in accumulation zone and minimum thickness 25 m near the snout area as measured (Ground Penetrating Radar Profiling). The lower zone of the glacier is resting over a thick sub-glacial till layer. Lateral moraines are prominent glacial features in the valley, reminiscent of past extent of the glacier.

Annual mass balance and snout measurement of Dokriani glacier was conducted under Himalayan Glaciological programme from 1992/93 to 1999/2000, which provides some of the clearest impressions of continuous recession of glacier volume, area and length. Results of net annual mass balance for six years indicate the continuous negative trend with the maximum deficit of  $-3.19 \times 10^6$  m<sup>3</sup> in 1998/99. Mean annual balance of Dokriani glacier from 1992/93 –1999/2000 was  $-0.32$  m a<sup>-1</sup> w.e. Average reduction of glacial ice thickness by  $2.5$  m a<sup>-1</sup> w.e. is significant, since the Dokriani glacier has average thickness of 50-55 m. Equilibrium line altitude ascended from 5030 m to 5095 m (amsl) and AAR value of the glacier fluctuated between 0.67 and 0.70 during the study period. The mass balance obtained from long term geodetic measurements (19962/63-1995) shows that the average annual mass balance is negative and net volume lost by the glacier during the period amounted to  $-70.11 \times 10^6$  m with an average of  $274$  mm a<sup>-1</sup> while during the period 1992-93-1999-2000 the rate recorded was  $320$  mm a<sup>-1</sup>. The length of Dokriani glacier decreased by 550 m from its position marked in 1962 to 1995 (Survey of India toposheet of 1962-63 and 1995 eds.) with an average rate of  $16.6$  m a<sup>-1</sup>. Frontal area vacated by the glacier is 10% of the total glacier area. The field measurement carried out during the period 1991-2000 show that the glacier has receded by about 161.15 m with an average rate of  $17.9$  m a<sup>-1</sup>. The enhanced rate of  $1.3$  m a<sup>-1</sup> also supports negative balance of the glacier. The studies show that this glacier is highly responsive to negative mass balance regime. This can be related to overall decreasing trend of precipitation in winter as well as high melting in the summer season.

**Keywords:** Dokriani glacier, mass balance, recession, Garhwal, Himalaya

## INTRODUCTION

Glaciers are dynamic and fragile ice mass on the earth; they grow and shrink in response to changing climate. Therefore, they are to be considered as sensitive indicators of climate. Change in climate directly affects glacier mass and thereby, the water resources. Fresh water is a finite and vulnerable resource, essential for sustaining life and development. Water resources in the Himalayas are stored in the form of glaciers. During the winter, most of the high altitude regions experience heavy snow fall. This snow cover plays an important role in the ecology of the region and forms a unique reservoir. Melting from snow bound areas during the summer forms an important source of many perennial rivers originating in the higher Himalaya. Therefore, understanding the pattern of snow accumulation and ablation is important for utilization of the Himalayan water resource. Glacier advancement and recession are thus the most important evidences of change in glacier geometry.

The Mass balance and snout recession studies are important for assessing the volumetric and geometric changes, which occur due to various glaciological processes especially during the advancement and recession of the glaciers. Assessment of the horizontal and vertical shrinkage of valley glaciers provide comprehensive understanding of glacier as to how it has reacted to various changes in the climate over the years. It is a well-established fact that the glaciers are passing through a recessional phase worldwide. Enhanced recession rates of glaciers during the recent years has initiated wide spread discussions, especially in context to global warming and its effects on cryosphere. Himalayan glaciers are also

receding like other glaciers in the world (Mayeswki and Jeschke, 1979; Vohra, 1981; Srivastva and Swroop, 1989; Dobhal, *et al.*, 1995; Shukla and Siddiqui, 1999; Naithani, *et al.*, 2001). However the rate of recession and amount of volume change are irregular for glaciers across the Himalaya. This is mainly due to the variance in climate and change in physiographic features across the Himalayan arc.

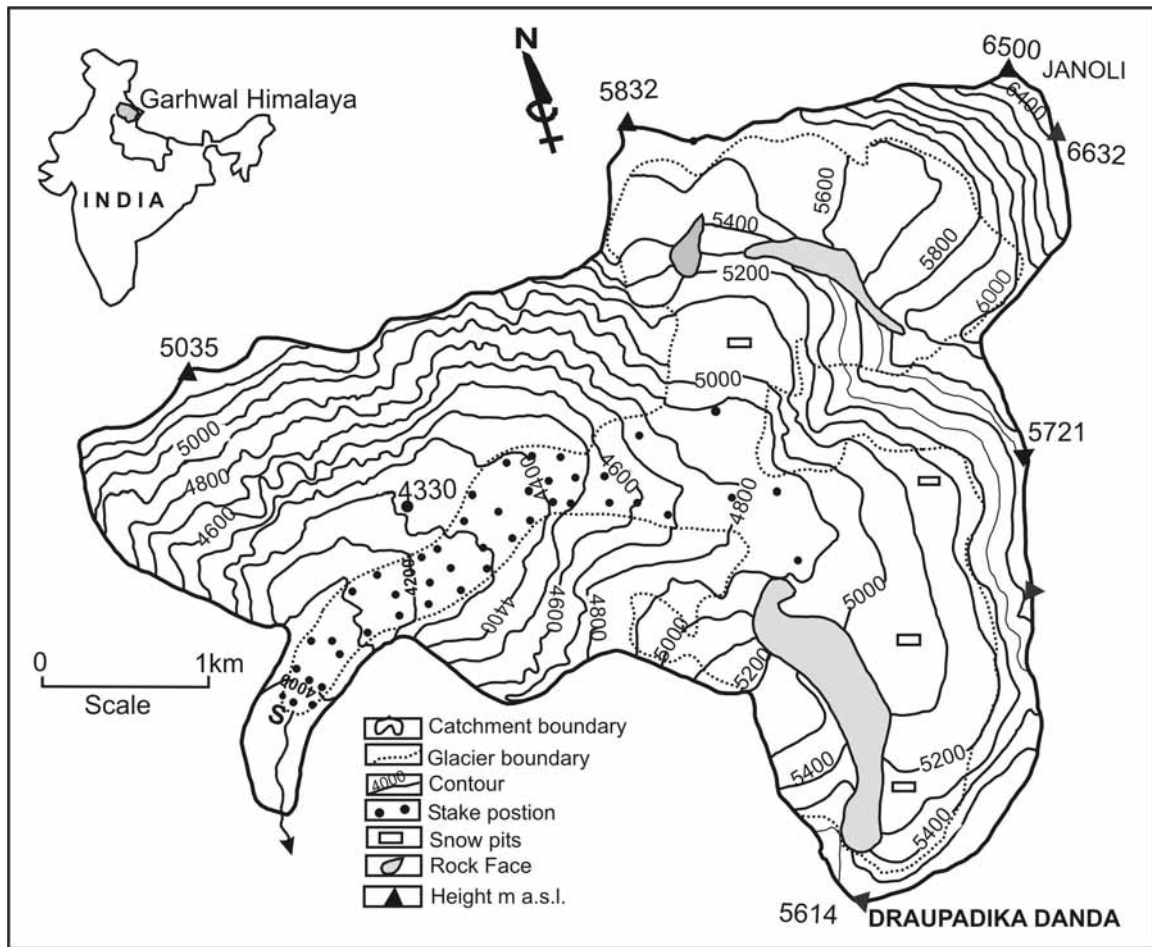


Fig. 1: Location map Dokriani glacier with stake network for Ablation accumulation measurement.

Garhwal Himalaya stretches about 325 km between Nepal in east and Himachal in the west covering an area of 53204 km<sup>2</sup>. About 917 glaciers have been identified in the area which is occupying an area of 3150 km<sup>2</sup> (Geological Survey of India, 1999). Considering the number of glaciers in Garhwal Himalaya very few glaciers have been studied, in this regard contribution of Geological Survey of India is significant. Some of the glaciers which have been studied are Dunagiri glacier, 1984-85 to 1989-90 (Srivastva *et al.* 1999), Tripra Bank, 19981-82 to 1985-86 (Gautam and Mukherjee, 1989) in Alaknanda basin (Ganga basin). A comprehensive morph geometrical study to various related changes of glaciers of Himalayan glaciers is still lacking. The present studies mainly emphasise on annual mass balance and snout recession of Dokriani glacier. Study of this glacier assumes significance because Dokriani is one of few glaciers in the Garhwal Himalaya, where mass balance studies are being carried out on a regular basis from 1991 to 2000. The Dokriani glacier (30°49' to 35°20'N ' and 78°47' to 78°51'E) is a compound valley type glacier located in the Bhagirathi river basin in Garhwal Himalaya. This 5.5 km long glacier extends between 6000 m and 3880 m (amsl) with an average surface slope of 12°. It occupies an area of 7.0 km<sup>2</sup> of the total catchments area of 15 km<sup>2</sup> and is about 46% of the total glacierized area of the basin. The glacier is formed by two cirques, one on the northern slope of Draupadi Ka Danda (5716 m) and second on the Western slope of Jaonli (6632 m) and they join at an altitude of 4800 m (Fig. 1). The glacier flows due NNW for nearly 2.0 km till 4300 m from where it turns WNW and flows for 3 km and terminates at an altitude of 3880 m (amsl). The glacier ice thickness measured by Ground Penetrating Radar (GPR) survey varies from 25 m near the snout in ablation zone to 120 m in accumulation zone (Gergan *et al.* 1999). The lower part of ablation zone of the glacier is resting over a thick layer of sub-

glacial till. Lower part of glacier ablation zone is covered with a thick layer of supraglacial debris. Some salient features of the Dokriani glacier are given in Tab. 1.

## METHODOLOGY

Measurements of mass balance studies were undertaken by traditional method (Osterm and Brugman, 1991). A network of forty stakes was made over the glaciers for ablation measurement (Fig. 1). These stakes were measured with an interval of five to ten days during the entire ablation period to determine daily, monthly and net annual ablation. Accumulation measurements were made by snow pitting at different elevation band (Fig. 1). Repeated transient snow line mapping for each year was done in early summer and the ELA in October for measurement of net residual snow accumulation and net annual mass budget. October is considered as the end of the annual budget year for this glacier as considerable melting occurs in this month. The densities measured from different pits at different altitudes were used for assessing water equivalent measurement. An average density of  $0.56 \text{ g/cm}^3$  and  $0.85 \text{ g/cm}^3$  was calculated for accumulation and ablation respectively. The surface area of each elevation band has been determined from the 1:10,000 surface map of 1995 (Survey of India, 1995). The annual net ablation and accumulation for each 10 m elevation band from snout to accumulation has been computed. The earlier record of Dokriani glacier is available in Survey of India map (1962/63) on a scale of 1:50,000. With the help of this map the northing and easting coordinates of snout position of the glacier in year 1962 were calculated by applying grid values. Since 1991 regular monitoring of snout position and area vacated by the glacier has been studied by fixing the stakes at the center, left and right margins of the glacier snout and measurements were carried out by the EDM (Electronic Distance Meter). The coordinates (grid value) of snout position obtained from Survey of India toposheet (1962-63) was subtracted from the value obtained in 1991 field survey to deduce the total retreat of the snout during the period. The same method was adopted for the years 1992 onwards. The Dokriani glacier has been remapped by Survey of India in 1995 on a scale of 1:10000 and 1:25,000 under the Himalayan Glaciology Programme. Change in glacier geometry, surface elevation and frontal area vacated by the glacier during the period was obtained by comparing the two maps (1962 and 1995). Volume change during the period was calculated by preparing Area- Average thickness maps of both the survey years. The average thickness of the glacier in 1962 was determined from the glacier surface slopes (Nye, 1953). The volume calculation in 1995 is also aided by the GPR thickness profiles of the glacier (Gergan *et al.*, 1999).

## RESULTS MASS BALANCE

A mass balance study of the glaciers is a prime aspect to understand the causes of and nature of changes in glacier mass i.e. relationship between climatic change and fluctuation of glaciers (Meier, 1962). Mass balance measurement of Dokriani glacier has been carried out from 1992-93 to 1994-1995 and 1997-98 to 1999-2000. The data has been acquired by employing glaciological method, including weekly ablation measurement and fixed date accumulation measurement for calculation of net annual mass balance.

### Net ablation measurement

Ablation is an important component in the assessment of net annual mass balance of a glacier, which mainly comprises melting, calving, evaporation and wind erosion. In order to calculate net ablation, a network of ablation stakes was monitored and ablation was measured at an interval of 5 to 10 days in the entire ablation period. The mean monthly ablation and temperatures in each year have been calculated and tabulated in Tab. 2. The total annual ablation was calculated from the entire ablation season from April-May to October. The result shows that in early summer the contributions of snow melting are more than the glacier ice ablation and melting rate calculated was 4.0 to 4.5 cm/day. July and August are peak ablation seasons and ablation recorded was up to 6 cm/day. September onwards the melting gradually decreases and comes down to 2 cm/day to 1 cm/day in the month of October. The ablation pattern of Dokriani glacier clearly shows that the maximum ablation takes place in July and August, where melting, calving, evaporation and rainfall combine to enhance the ablation rate.

Tab. 1: Salient features of Dokriani Glacier, (Source: Geological Survey of India., 1999; Dobhal *et al.*, 2004, Thayyen *et al.*, 2005a, 2005b).

<i>Sl.</i>	<i>Parameters</i>	<i>Dokriani Glacier</i>
1	Identification No	5O13102017
2	Location Drainage system	Central Himalaya, Uttaranchal. Ganga Basin
3	Extension Elevation range Latitude Longitude Length	3880 m to 6000 m , highest 6632 m 30°49' to 35°20'N ' 78°47' to 78°51'E 5.5 km
4	Geometry Catchment area Glacier ice cover Orientation (Flow direction)	15.7 km <sup>2</sup> 7 km <sup>2</sup> NNW to WSW
5	Glacier Zones Accumulation area Ablation area Snout altitude Glacier ice thickness	3.85 km <sup>2</sup> (5000 m-6000 m amsl) 1.19 km <sup>2</sup> (3900 m-5000 m amsl) 3900 m (in 2000) 15 m to 120 m
6	Climate data (Base camp 3760 m amsl, Period May to October) Monthly mean maxi. temp. Monthly mean mani. temp. Lowest temp. recorded Annual Rainfall Relative Humidity Average wind Speed Average slope lapse rate	11.0 °C in July 2.3 °C in October -10 °C in Nov.1995 near ELA 1100 mm to 1350 mm 57% (May and Oct.). 80% June to Aug. 7.2 km/h 0.5- 0.8 °C/100
7	Geology	Crystalline rocks. Biotite Gneisses

Tab. 2: Mean average monthly temperature and Ablation cm/day of Dokriani glacier.

Month	1998		1999		2000	
	Temp. Mean melting		Temp. Mean melting		Temp. Mean melting	
	°C	cm /day	°C	cm/day	°C	cm /day
May	9.4	-	6.8	1.7	9.1	1.9
June	10.0	3.6	8.7	2.9	9.3	3.1
July	11.4	3.5	10.8	3.2	10.2	3.3
Aug	10.9	3.5	10.1	2.9	10.5	3.0
Sept	8.7	2.5	8.7	2.0	7.5	2.0
Oct	5.3	1.1	4.3	0.9	6.1	1.0

### Net accumulation measurement

Accumulation has a strong control over mass balance as it brings positive and negative changes in net annual mass balance of a glacier. Precipitation, avalanches and snow drifting by winds are the main elements of accumulation. Since Dokriani glacier was monitored for the first time, there is no instrumental data on winter snowfall therefore, the estimation of total winter snow accumulation and net annual accumulation (residual snow depth) at the end of budget was measured from the snows pits. The accumulation area was divided into three elevation zones between 5000 m and 5600 m with 200 m contour interval. In higher area above 5600 m which is about 15 to 20% of the total accumulation area, extrapolations have been made for net accumulation measurement. Six snow pits representing different elevation bands in accumulation zone were made for annual accumulation measurements (Fig. 1). The average net accumulation calculated was between 0.70 m and 1.25 m consistent to entire study period except 1998/99 where the amount of snow accumulation was calculated 0.55-0.70 m.

### Net Balance

The net mass balance record determined solely from the field measurements (Tab. 3), yield an average mass balance of 0.32 m a<sup>-1</sup> from 1992 to 2000. The annual net mass balance for six years indicates a negative trend with maximum deficit of  $-3.19 \times 10^6$  m<sup>3</sup> w.e. in 1998-99. The vertical mass balance gradient

was drawn between annual specific balance and altitude (Fig. 2) for the period 1992 to 2000 and it is revealed that the glacier is by and large thinning in the ablation zone by  $-2.50 \text{ m a}^{-1}$  to  $-3.0 \text{ m a}^{-1}$  w.e, while the net accumulation is only  $0.450 \text{ m a}^{-1}$  to  $0.55 \text{ m a}^{-1}$  w.e. This represents a significant thinning of the glacier with an estimated volume of  $13.54 \text{ million m}^3$ . The Equilibrium line altitude (ELA) determined at the end of ablation period was found at altitudes of  $5030 \text{ m}$  in 1993 and  $5095 \text{ m}$  (amsl) in 2000. The AAR value for Dokriani glacier has been calculated with the help of obtained Equilibrium line in each year fluctuates between  $0.70$  and  $0.66$  (Tab. 2). The fluctuation of AAR depends on the ELA and is a variable parameter for mass balance measurement. The estimated AAR value calculated was  $0.73$  for zero mass balance for Dokraini glacier with corresponding ELA at altitude of  $4950 \text{ m}$ .

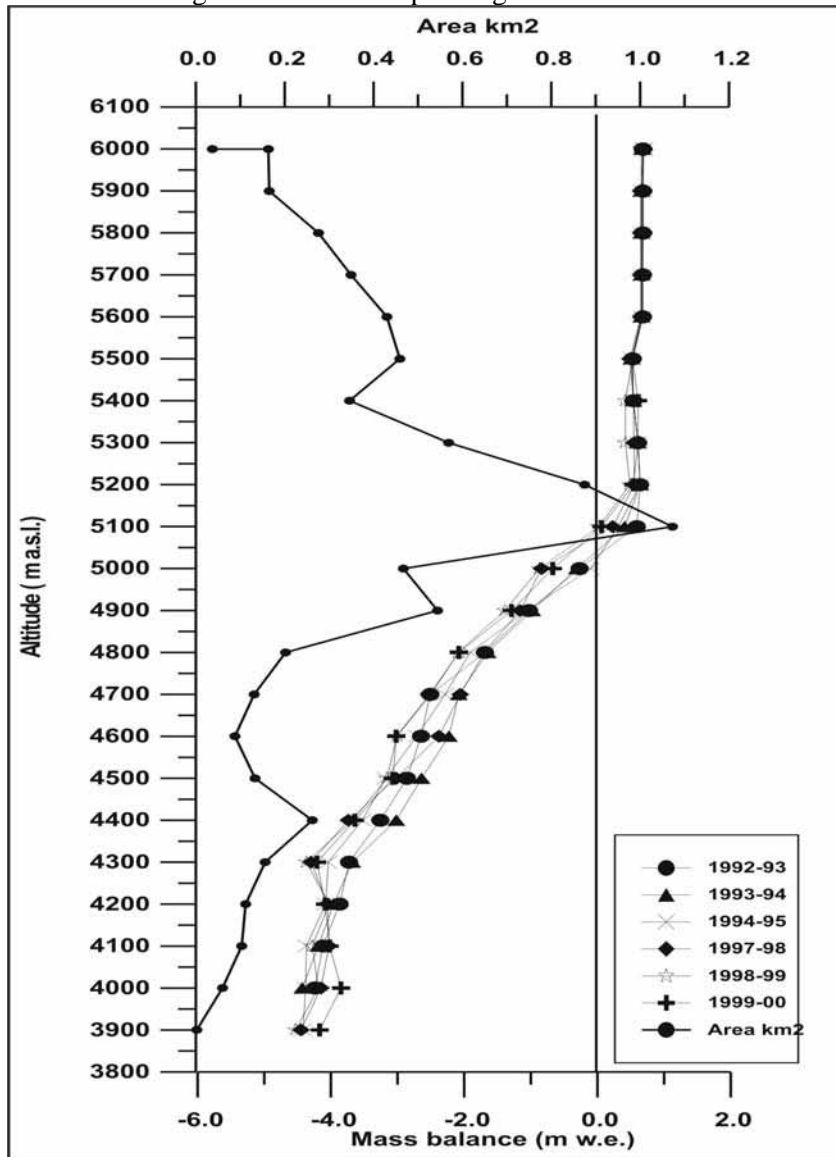


Fig. 2: Altitudinal annual mass balance of Dokriani glacier from 1992/93 to 1999/2000.

The mass balance obtained from long term geodetic measurements (19962/63-1995) shows that the average annual mass balance is negative and corresponds with the recent results (Dobhal *et al.*, 2004). The specific winter and summer balance cannot be determined by geodetic measurement but net volume lost by the glacier during the period was determined which amounted to a gross loss of  $-70.11 \times 10^6 \text{ m}^3$  with an average of  $-0.27 \text{ m a}^{-1}$  w.e. while during the period 1992-93-1999-2000 the rate is recorded  $-0.32 \text{ m a}^{-1}$  w.e.

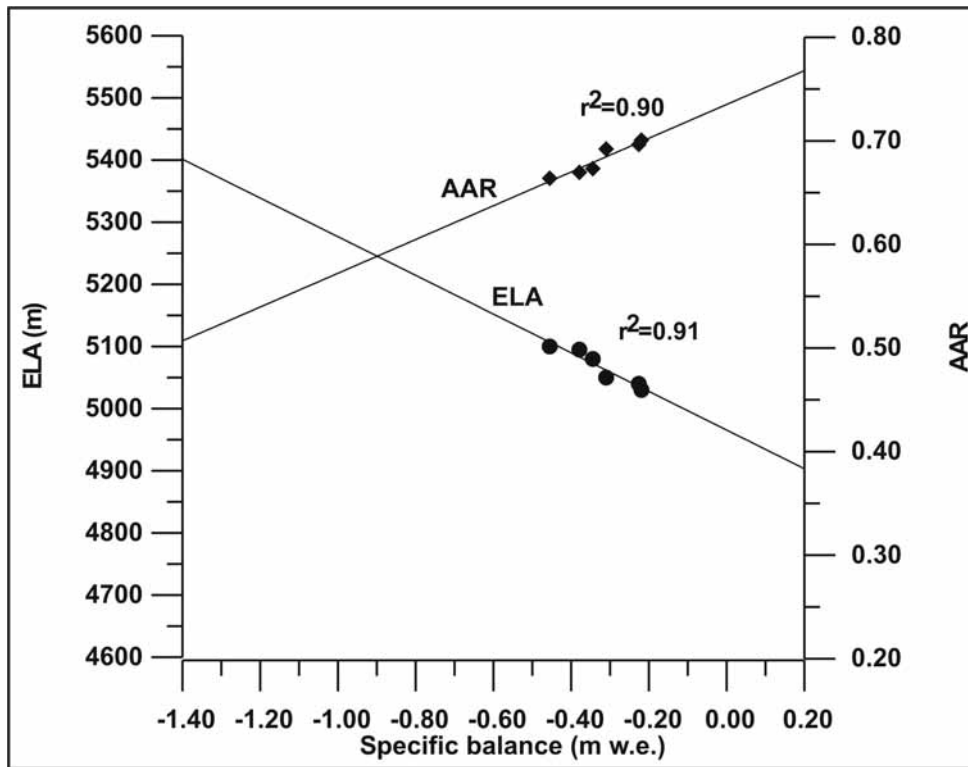


Fig. 3: Relationship between Mass balance AAR and ELA.

The annual mass balance trend of Dokriani glacier during the measurement periods reveals that the high negative balance was recorded  $-3.19 \times 10^6 \text{ m}^3$  of water equivalent in the year 1998-99. Such anomaly of sudden rise in negative balance was also recorded in Tipra Bank glacier in the same region of present study area. Mass balance studies of Tipra Bank glacier during the period 1982/83 - 1987/88 show that highest negative balance ( $-4.24 \times 10^6 \text{ m}^3 \text{ w.e.}$ ) was recorded in 1887/88, while in the remaining years of observations the mass balance was normally fluctuated between  $-0.82 \times 10^6 \text{ m}^3$  and  $-1.87 \times 10^6 \text{ m}^3$  (Gautam and Mukherjee, 1989).

Tab. 3: Net balances for the period 1992-93 to 1999-2000 Relationship between Specific balance, ELA and AAR.

Year	Accu. Km <sup>2</sup>	Abl. Km <sup>2</sup>	Net Accu 10 <sup>6</sup> m <sup>3</sup>	Net Abl. 10 <sup>6</sup> m <sup>3</sup>	Net Bal. 10 <sup>6</sup> m <sup>3</sup> w.e	Sp.Bal m w.e	AAR	ELA m
1992-93	4.90	2.10	2.99	-4.52	-1.54	-0.22	0.70	5030
1993-94	4.88	2.12	2.77	-4.36	-1.58	-0.23	0.69	5040
1994-95	4.84	2.16	2.66	-4.83	-2.17	-0.31	0.68	5050
1997-98	4.71	2.29	2.62	-5.03	-2.41	-0.34	0.67	5080
1998-99	4.65	2.35	2.23	-5.41	-3.19	-0.46	0.66	5100
1999-00	4.69	2.31	2.52	-5.17	-2.65	-0.38	0.67	5095
Average	4.78	2.22	2.63	-4.88	-2.25	0.32	0.66	5065

This reveals that the winter precipitation plays an important role in controlling the annual mass balance. The studies also demonstrate that the present trend of mass balance is moderately negative and increasing each year. The enhanced rate of ice mass depletion by  $-0.32 \text{ m a}^{-1}$  indicates greater percentage contribution of glacial degraded runoff in bulk discharge. Changes in ice volume is the result of changing length, width, surface area of the glacier which is most likely to be altered by changing climate. Relationship between specific mass balance, ELA and AAR were plotted (Fig. 3) and a strong combined relationship of mass balance, AAR and ELA are found. The regression analysis reveals that there is a

good correlation coefficient 0.91 and 0.90. The estimated AAR value calculated was 0.73 for zero mass balance for Dokriani glacier with corresponding ELA at altitudes of 4950 m.

## SNOUT RECESSION

The processes of advancement and recession of glaciers results in the occupation or evacuation of an area glacier depending on the phase through which the glacier is passing in time and space. It is this self-regulating mechanism which controls the glacier's shape, geometry, surface morphology, bedrock topography and climate of the area. The snout of the Dokriani glacier is being monitored since 1991 by fixing the stakes at the centre, left and right margins of the snout glacier. Measurements were carried out by the EDM (Electronic Distance Meter) to measure the rate of recession since 1991 (Fig. 4).

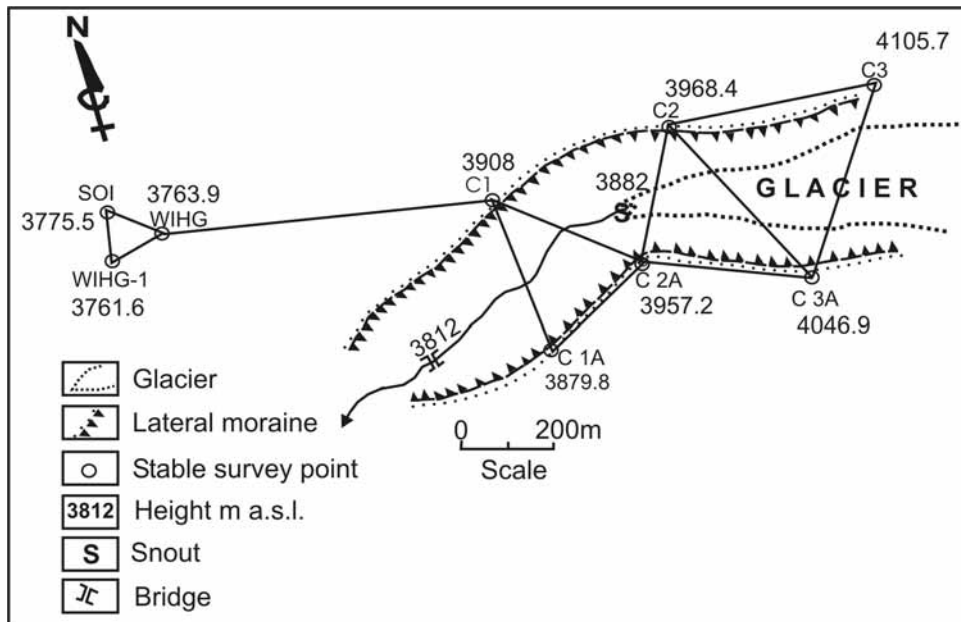


Fig. 4: EDM Survey Network for monitoring of glacier snout.

Total terminal retreat of Dokriani glacier from 1962 to 1991 was about 480 m with an average rate of  $16.6 \text{ m a}^{-1}$  and 10% area of the total area of the glacier vacated during the period (Dobhal *et al.*, 2004). Field observation carried out during the period 1991-2000 showed that glacier has receded about 161.15 m with an average rate of  $17.90 \text{ m a}^{-1}$ . The frontal area vacated by the glacier is estimated to be nearly  $8833 \text{ m}^2$  (Fig. 5, Tab. 4). Based on the above-observed data, it can be assumed that the glacier is continuously retreating with an average annual rate of  $951.4 \text{ m}^2$ . The relationship between the two parameter viz snout recession and area vacation (Tab. 4), clearly indicates that area vacated by the glacier has not always been similar to rise and fall of the rate of snout retreat. This may be due to 1) geometrical readjustment of snout position after its recession and 2) sudden shrinking and breaking of frontal part of glacier. The frontal zone of the glacier always remains in final phase of melting causing thinning of ice mass which changes the slope, shape and geometry, finally resulting in shrinking and breaking of the frontal part of the glacier. This may be one of the causes that produces such anomalies between frontal recession and area vacation. Such type of processes has also observed in others glaciers of adjoining area (Shukla and Siddiqui, 1999). The study also reflects that during the course of study period there is no sign of advancement recorded while glacier showing continuous recession and which is probably attributed to the effect of global warming.

Tab. 4: Snout recession of Dokriani glacier during the period 1962 to 2000.

S.N	Period	Recession (m)	No of Years.	Recession (m a <sup>-1</sup> )	Frontal Area vacated (m <sup>2</sup> )	Altitude m(amsl)
1 2 3	1962-91	480.1 16.2	29 01	16.5 16.2	736043 968	3860
4 5 7	1991-92	16.5 18.5	01 01	16.5 18.5	1187 818 984	3870
8 9	1992-93	18.7 35.0	01 02	18.7 17.5	1882 925 1005	3877
10	1993-94	18.50	01 01	18.5 19.0	1064	3879
	1994-95	19.00	01	18.75		3882
	1995-97	18.75				3886
	1997-98					3888
	1998-99					3891
	1999-2000					3895

In order to study overall changes in Dokriani glacier regime was determined by comparison of two topographic maps (Survey of Indian Toposheet of 1962 and 1995). The results show the glacier has undergone remarkable changes in length, area, surface elevation and ice volume (Tab. 5).

Tab. 5: Morpho-geometrical changes in Dokriani Glacier from 1962-1995. (The glacier was originally mapped in 1962 and remapped in 1995 by Survey of India).

Sl.No.	Parameters	1962	1995
1, 2	Glacierized area Glacier area	11.17 km <sup>2</sup> , 7.78 km <sup>2</sup>	10.20 km <sup>2</sup> , 7.00 km <sup>2</sup>
3	Accumulation area	--	04.84 km <sup>2</sup>
4	Ablation area	-	02.16 km <sup>2</sup>
5	Glacier length	6.0 km	5.5 km
6	Snout position	3810 m	3880 m
7	ELA	-	5050 m
8	Elevation range	3810-6000 m	3880-6000 m
9	Average thickness	55.0 m	50.0 m
10 11	Surface slope - Ice volume (w.e.)	11° - 385.11.8x10 <sup>6</sup> m <sup>3</sup>	12° - 315.0x10 <sup>6</sup> m <sup>3</sup>

## SUMMARY AND DISCUSSION

The mass balance and snout recession studies are capable of providing partial information regarding volumetric and geometrical changes with climatic change. It is a well established fact that the glaciers are in a recessional phase worldwide. Himalayan glaciers also follow the same trend. The Himalaya form the southern limits of Tibetan plateau region and have an enormous influence on the natural environment of adjacent regions. The high plateau causes many changes in the atmospheric column, such as a differential heating effect which is low near the plateau and high above it. It intercepts the sub-tropical planetary high-pressure zone and has a direct effect on the Indian monsoon (Li and Xu, 1984).

The Himalayan glaciers are not only large but they lie at very low latitudes and majority of them are temperate. The major pattern of the glacier regime is controlled by climate and its topography. Climate plays an important role in rapid fluctuation of a glacier mass budget. Glacier melt takes place mainly in summer season occurring both day and night (Kumar and Dobhal 1997). Major amount of solid precipitation falls during the winter and increases with altitude. The summer monsoon precipitation associated with fronts formed between various branches of monsoon currents uplift the air against large orographic obstacles. The glaciers of the Himalayas lie either across or parallel to the mountain range and are valley type. Such peculiar topography influences wind direction that flows generally along the main valley and across the glacier valley. At the junction of two valleys, the wind flows accumulate and form eddy currents that produce higher temperature here than other places. This may be one of the causes of

fast melting at the termination point and rapid recession of glacier snouts of the glaciers (Kumar and Dobhal 1997).

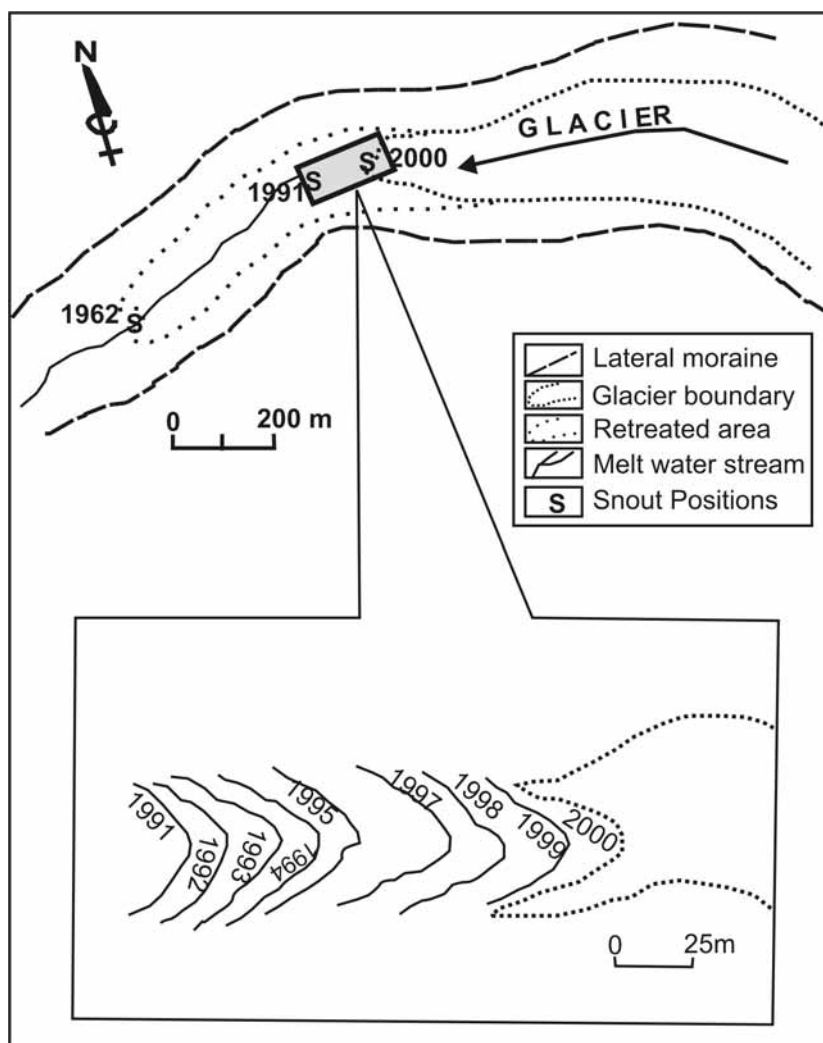


Fig. 5: Different positions and total recession of Dokriani glacier during the period 1991 to 2000.

Calculated mass balance trends of Dokriani glacier is negative in all the measurement periods. The ELA has also ascended by nearly 65 m during the study period, whereas AAR value has fluctuated between 0.63 and 0.70. It is observed that the negative annual mass balance of the glacier is probably attributed to the low accumulation of snow in accumulation area and high ablation in the summer season. The tendency of the continuous retreat of snout position, ELA, AAR and negative net balance in the recent years and its small size of the glacier suggest that the glacier is rapidly reducing its mass volume and may continue to do so in the next decades.

In context to climate change and its impacts on glaciers, it is a well known fact the earth air temperature is rising globally (IPCC report; 2004). It is also observed that nineties was the warmest decade of the twentieth century and year 1998 was the warmest year of the decade. This phenomenon was also observed in parts of the Himalaya like Dokriani glacier. During the period 1998/99 a high negative balance was measured, the frontal recession was also higher and most important the mean monthly air temperature recorded was higher than other measurement years (Tab. 2, 3 and 4). In addition, mass balance trends of other glacier in the region have been carried out during the period 1997-1996, ten glaciers of different climatic and topographic zones were taken up for mass balance studies by glaciological method. A good set of mass balance data has been collected and interpreted. The studies reveal that most of the glaciers have negative mass balance (Tab. 6).

Tab. 6: Mass-balance studies of Himalayan glaciers.

S.No.	Name of the glacier	Location	Period of study	Cumulative Sp.Bn.(m w.e)	Ref.
1	Gara glacier	H.P.	1974-1983	-2.87	1
2	Gor- Garag	H.P.	1977-1985	-3.3	1
3	Shaune Garang	H.P.	1981-1990	-2.87	1
4	Neh Nar	J&K	1978-1984	-2.37	1
5	Cangme Khangpu	Sikkim	1978-1987	-1.86	1
6	Rulung glacier	J&K	1979-1981	-0.21	1
7	Tipra Bank	U.A	1981-1988	-1.34	1
8	Dunagiri	U.A.	1984-1992	-6.26	1
9	Chhota-Shigri	H.P.	1986-1989	-0.21	2
10	Nardu glacier	H. P	1992-1996	-1.47	3
11	Dokriani glacier	U.A.	1992-2000	-1.94	Present

(Sources-Ravishanker, 1999 (1); Dobhal, *et al.*, 1995 (2); Kaul, *e tal.*, 1997 (3) )

The continuing state of recession of Himalayan glaciers and change in snowfall pattern witnessed in recent years are of great concern. The lack of comprehensive data base on Himalayan glaciers and poor understanding of the glacial processes are the major constraints to chalk out a viable management programme for Headwater Rivers. The studies on Dokriani glacier in Din Gad catchment of Garhwal Himalaya is designed to collect the basic data on the various aspects of glacier regime. The study is still continuing to collect long term data on mass balance, climate and fluctuation of Dokriani glacier.

## CONCLUSIONS

Annual net mass balance of Dokriani glacier during the study period was negative with maximum deficit of  $-3.19 \times 10^6 \text{ m}^3$  in 1998/99. The mean annual net balance calculated is  $-0.32 \text{ m a}^{-1} \text{ w.e.}$

Mass balance determined from 1962 to 1995 by geodetic method also show the negative annual balance with an average of  $-0.27 \text{ m a}^{-1} \text{ w.e.}$ , the present studies reveal that the glacier has negative balance trends. Snout of the Dokriani glacier receded about 550 m during the period from 1962 to 1995. Field measurement (1991-2000) study shows that the glacier receded 161.15 m and frontal area vacated by the glacier was  $8833 \text{ m}^2$ .

The study of ablation /accumulation pattern shows that the annual ablation rate recorded 2.5 to  $3.5 \text{ m a}^{-1} \text{ w.e.}$ , while average accumulation rate calculated is  $0.45 \text{ m a}^{-1} \text{ w.e.}$  The tendency of the continuous retreat of glacier snout, ELA, and negative balance in the recent years, combined with small size of the glacier suggests that the Dokriani glacier is receding rapidly. If this trend continues, this glacier will be in a reduced form in the next decades.

## ACKNOWLEDGMENT

Authors are grateful to Prof. B.R. Arora, Director, Wadia Institute of Himalayan Geology, Dehradun for encouragement and providing facilities to carry out the present work. We also thank the Survey of India team for their valuable help during the fieldwork and preparation of large-scale map of the area. Financial assistance by Department of Science and Technology, Govt. of India is dully acknowledged.

## REFERENCES

Dobhal, D.P., Kumar, S. and Mundepi, A.K. (1995) Morphology and Glacier dynamics studies in Monsoon arid transition zone: An example from Chhota Shigri glacier, Himachal Himalaya, India. *Current Science*, 68, 9, 936-944.

- Dobhal, D.P., Gergan, J.T. and Thayyen, R.J. (2004) Recession and morphogeometrical changes of Dokriani glacier (1962-1995) Garhwal Himalaya, India. *Current science*, 86, 5, 692-696.
- Gautam, C.K and Mukherjee, B.P. (1989) Mass-Balance vis-à-vis snout position of Tipra bank glacier District Chamoli, Uttar Pradesh. In: *Proceeding National meeting on Himalayan Glaciology*, 5-6 June 1989, 141-148.
- Gergan, J.T., Dobhal D.P. and Kaushik, R. (1999) Ground penetration radar ice thickness measurement of Dokriani Bamak (Glacier), Garhwal Himalaya. *Current Science*, 77, 1, 169-174.
- Geological Survey of India. (1999) Inventory of the Himalayan glaciers. A contribution to the International Hydrological Program. *Geol. Surv. India*, Spl. Pub. 34 (ed.M.K. Kaul) 165 p.
- Kaul, M.N. Raina, A.K. and Sharma, R.K. (1997) Relationship between mass balance and meteorological parameters of Nardu glacier, Himachal Pradesh. (Abstract), *National Symposium on Himalayan Glaciers and snow cover*, 3-4 March 1997. School of environmental Sciences, J.N.U., New Delhi.
- Kumar, S. and Dobhal, D.P. (1997) Climatic effects and bed rock control on rapid fluctuation of Chhota Shigri glacier, northwest Himalaya, India. *J. Glaciol.*, 43, 467-472.
- LiJijun and Xu Shuying, (1984) The distribution of glaciers on the Qinghai-Xizang plateau and its relationship to atmospheric circulation. In: Miller, K.J., Ed. *The International Karakoram Project*, Proceeding of the International Conference, Cambridge, Cambridge Univ. Press, 1, 84-93.
- Naithani, A.K., Nainwal, H.C., Sati, K.K. and Prasad, C.P. (2001) Geomorphological evidence of retreat of Gangotri glacier and its characteristics. *Current Science*, 80, 87-94.
- Mayeswki, P.A. and Jeschke, P.A. (1979) Himalayan and Trans Himalayan glacier fluctuation since AD 1812. *Arctic and Alpine Research*, 11, 3, 267-287.
- Meier, M.F. (1962) Proposed definition for glacier mass budget terms. *J. Glaciol.*, 4, 33, 252-263.
- Nye, J.F. (1952) The mechanism of glacier flow. *J. Glaciol.*, 5, 12, 82-93.
- Ostrem, G. and Brugman, M. (1991) *Glacier mass balance measurements: A manual for field and office work*, Science report -4. National Hydrological Research Institute, Saskatoon/Norwegian water recourse and electricity board, Oslo, 224 p.
- Ravishanker (1999) Glaciological studies in India, a contribution from Geological Survey of India. *Symp. Snow, Ice and Glacier*, 9-11 March 1999, Abstract Vol.
- Srivastava, D., Swarrop, S., Mukerji, S., Roy, D. and Gautam, C.K. (1999) Mass balance of Dunagiri glacier, Chamoli District, Uttar Pradesh. *Symp. Snow, Ice and Glacier*, 9-11 March 1999, Abstract Vol., 10-11.
- Srivastava, D. and Swaroop, S. (1989) Fluctuation of Dunagiri glacier, District Chamoli, UP. *Pro. National meet on Himalayan Glaciology*, 5-6 June 1989, 153-156.
- Shukla, S.P. and Siddiqui (1999) Recession of snout front of Milam Glacier, Goriganga Valley, District Pithoragarh, Uttar Pradesh. *Symp. Snow, Ice and Glacier*, 9-11 March, 1999, Geol.Surv.Ind. Abstract Vol., 27-29.
- Thayyen, R.J., Gergan, J.T. and Dobhal, D.P. (2005a) Slope lapse rates of temperature in Din Gad (Dokriani Glacier) catchment, Garhwal Himalaya, India. *Bulletin of Glaciological Research*, Japanese Society of snow and ice, 22, 31-37.
- Thayyen, R.J, Gergan, J.T and Dobhal, D.P. (2005b) Monsoonal control on glacier discharge and Hydrographic characteristics, a case study of Dokriani glacier, Garhwal Himalaya, India. *J. Hydrol.*, 36, 1-4, 37-49.
- Vohra, C.P. (1981) Himalayan glaciers, In: *Himalayan aspects of change*, Lall, J.S. and Maddie, A.D. (Ed.). Oxford Univ. Press, Delhi, 138-151.



# CLIMATE CHANGE SIGNALS DETECTED THROUGH MASS BALANCE MEASUREMENTS ON BENCHMARK GLACIER, HIMACHAL PRADESH, INDIA

**Rajesh KUMAR**

Remote Sensing Division, BISR, Statue Circle, Jaipur-302005, India  
*rajeshbhu@yahoo.com*

**Syed I. HASNAIN**

HIGH ICE-India, New Delhi, India

**Patrick WAGNON, Yves ARNAUD, Pierre CHEVALLIER**

UR Great Ice (R032), IRD, Montpellier and Grenoble, France

**Anurag LINDA, Parmanad SHARMA**

PhD Students, Jawaharlal Nehru University, New Delhi, India

## ABSTRACT

In the Indian subcontinent (South Asia), the cryosphere (glaciers and snow covers) provides up to 80% of the low land dry season flows of the Indus, Ganges and Brahmaputra river system through their vast irrigation network. Deglaciation is considered to be a world-wide problem; there is a particular concern at alarming rate of retreat of Himalayan glaciers. The cryosphere retreat is likely to lead a temporary increase followed by reduction in river flows but the quantity, timing and consequences are unknown. It has been estimated in the IPCC report of 2001 that the global temperature rise at the rate of +0.03 °C/year will have a great impact on the sensitive ice mass of the glaciers. The mass balance study started by the initiative of former ICSI, presently known as Commission on Cryospheric Sciences, in 2002 at Chhota Shigri (benchmark) Glacier (32°11' - 32°17' N and 77°30' - 77°32' E), located in the Lahaul and Spiti valley, Himachal Pradesh, India. This glacier is unique as it receives nourishment both by southwest summer monsoon and westerlies. This work is being conducted in collaboration with the Great Ice Research Unit of the *Institut de Recherche pour le Développement*, France and field measurements have been carried out during years 2002-2005.

The study based on the two years of observations shows a negative mass balance of -1.06 and -1.20 m w.e. for the year 2002-03 and 2003-04 respectively. This has increased slightly in hydrological year 2003-04 as compared to hydrological year 2002-03. The glacier is likely to become thinner at lower altitudes, as there is increased negative net mass balance year to year.

The Equilibrium line altitude (ELA) is also shifting upward and stays at an interval of 4800-5100 m, thus reducing the accumulation area. The results clearly indicate the impact of warming in the region.

The work is still continuing and long term mass balance measurements will indicate about the climate signals affecting the cryosphere in the South Asia.

**Keywords:** Himalaya, mass balance, runoff, southwest summer monsoon, Westerlies, ELA

## INTRODUCTION

The Hindu-Kush-Himalaya represents a 'critical region' in terms of glacier melt water contribution to irrigation network for millions of South Asians. The glacier response with the climate is closely associated and has been a central issue in glaciological studies (e.g., Kuhn, 1981; Oerlemans, 1994). Glaciers are so sensitive to climate variations that it can be used as an indicator of climate change, but like a thermometer, the relation between climate change and glacier response needs to be calibrated. This is not only helpful in understanding present climate but is also critical to responding past climate change or predicting future glacier responses. In tropics, glacier-atmosphere interactions are complex because accumulation and ablation are synchronous and ablation is permanent throughout the year (e.g., Hastenrath and Ames, 1995; Kaser, 2001). Changes in glacier length, areal extent or mass balance can also be used as climate indicators in a region where climatic data series (temperature, precipitation) are rare and the climate change signal is not clear (Yadav et al., 2004; Roy and Balling, 2005). Combined glacier mass and energy balance studies on low-latitude glaciers provide valuable knowledge on the tropical and global climate (Wagnon et al., 2001; Francou et al., 2003). As global climate changes, there is an accordant trend towards global recession and wasting of glaciers. Several analyses show that it is not

only increased temperature and/or decreased precipitation that are responsible for these retreats, but also changes in air humidity (Kaser *et al.*, 2002).

In addition, for the people living in the Himalayan valleys, runoff generated by the melting of these glaciers is an important source of water in the perennial rivers originating from Himalaya (WWF, 2005). The problems of water stress are already prevalent in the region due to increasing demands of domestic, agriculture, industry and a growing population. Any reduction in the availability of freshwater could have serious consequences for the economy, the environment and the daily lives of many millions of people within the affected basins and beyond.

Still the importance of looking to the climate change effects on glaciers and its impacts on subsequent freshwater supply has not been addressed in an integrated manner. Lack of which has been reflected in the idleness of the policy makers to look to the matter while dealing with long term sectoral development planning of the region especially in the Hydropower and Agricultural sectors.

Glacier mass balance is a link between climate and glacier dynamics. Mass loss affects the local hydrology because mass is lost generally through melt-water runoff. Thus the prediction of mass balance change is also a prediction of their hydrological effect, which is important for regional water supplies. In the present study an attempt has been made to check climate signals by monitoring mass changes. The sensitivity of the equilibrium line altitude (ELA) is also discussed, which is closely associated with the change in temperature and the precipitation in the glacier valley.

## STUDY AREA

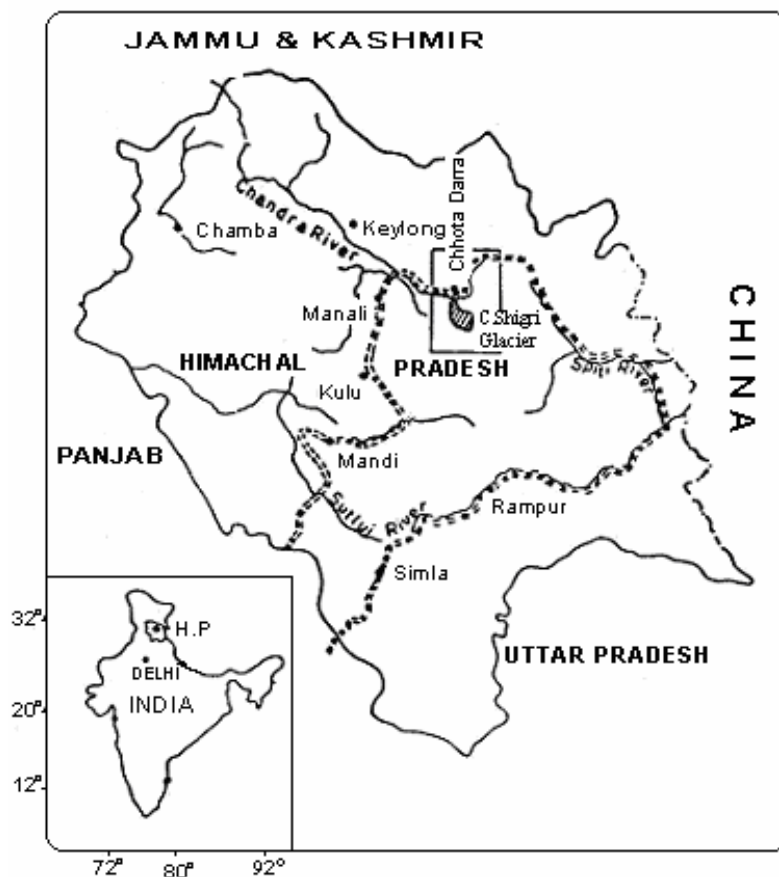


Fig. 1: Location map of the Chhota Shigri (benchmark) glacier, Himachal Pradesh, India.

Chhota Shigri glacier is the study area, which lies in the Himachal Pradesh, India and was selected as benchmark glacier in the HKH region by the International Commission of Snow and Ice (now this is Commission of Cryospheric Science) in 2002. Chhota Shigri glacier lies on the Chandra-Bhaga river basin on the northern ridge of Pir Panjal range in the Lahaul-Spiti valley of Himachal Pradesh. It is included in the upper basin of the Chandra River, which latter joins Bhaga River and together contribute

to the Chenab River, one of the components of the Indus basin, is located about 3 km (glacier terminus) south of Chhota Darra across the left bank of Chandra River (the main river of this region), is trending about N-S to NNE to SSW (Figure 1). This glacier extends between 32°11' - 32°17' N and 77°30' - 77°32' E and occupies an elevation of 4000 to 5660 m a.s.l. It extends for about 9 km in length and the width is varying from 0.3 to 1.5 km (Figure 2). The highest peak (6000 m a.s.l.) is at the eastern side from which four small glaciers feed the main accumulation zone (Nijampurkar *et al.*, 1993).

Alternatively influenced by the Asian Monsoon during the summer, and submitted to the westerlies in the winter, the glacier offers a complex accumulation/ablation regime. The glacier falls in the monsoon-arid transition zone; therefore this glacier is considered to be a potential indicator of the northern limits of the intensity of the monsoon (Krenek and Bhawan, 1945). This glacier is unique in its characteristics as it receives nourishments both by southwest monsoon and westerlies. Melt-water from the glacier surface penetrates the ice body and forms sub glacial channels, and a few surface melt water channels are also observed along the middle of the glacier during the summer months. The total drainage area of the Chhota Shigri basin is about 45 km<sup>2</sup>, with a glacierised area of approx 10 km<sup>2</sup> and the glacier occupies about 22 % of the drainage area (Dobhal *et al.*, 1995). It is a valley glacier and the shape is complex; including two main flows in the central part and several small suspended sub-glaciers in the accumulation zone. The lower portion of the glacier is covered by debris. The thickness of the glacier ice varies from 15 to 130 metres from the snout to the accumulation zone according to the gravity survey (Kumar and Dobhal, 1997).

## **GEOLOGY OF THE AREA**

Chhota Shigri glacier lies within the central Crystallines of the Pir Panjal range of the Himachal Himalaya. This crystalline axis is comprised mostly of meso- to ketazonal metamorphites, migmatites and gneisses. In few places, granitic rocks of different composition and younger age indicate rejuvenation but 3 km upstream of Chhota Dara, in the upper Chandra valley; older Palaeozoic granitic rocks are exposed. The Haimanta formation overlies these with a tectonic break, where black slates, phyllites and fine-grained biotite-schists are exposed. The slates and phyllites show a well developed thrust tectonic contact, which forms the crest of the northern ridge. Box type folds with decollement are quite prominent in the Haimanta Formation. The Haimantas, which rest directly on basement rocks, are highly metamorphosed metasediments and show intense folding and shearing. The brown biotite, with a fine-grained texture, shows intense heating effect, which indicates periodic re-heating of the granite rocks below. The various types of granite and gneiss rocks present in the basement also indicate this. Schistose gneiss and augen gneiss has developed in the granite without any distinct margins. Chhota Shigri glacier rests on the granitic basement rocks. On both sides the ridge tops are at an altitude of 6300 m and the bottom of the Chandra Valley lies at 3300 m and the overall relief is 3000 m.

## **CLIMATE**

The climatic records of the region are not available but the nearest weather station at Keylong records a maximum temperature of not exceeding 24 °C. The region is mainly characterised by the cold winter extending from October to April. The short term meteorological observations (July to September) on the glacier during 1987-1989 showed a temperature ranging between 10.5 °C to -5.2 °C at an elevation of 4600 m while 16 °C to 4 °C near snout (Dobhal *et al.*, 1995). The main valley (3000-7000 m deep), in which the glacier is situated, is dry. The annual precipitation on the glacier is 150-200 cm of snow (~600 kg m<sup>-2</sup> year<sup>-1</sup>). The average environmental lapse rate on Chhota Shigri glacier remained pseudo-adiabatic on most days during the summer and varied from 0.38 °C to 0.67 °C/100 m (Bhutiyan and Sharma, 1989).

## **METHODOLOGY**

This mass balance study was started by the initiative of former International Commission of Snow and Ice (ICSI), presently known as Commission on Cryospheric Sciences, in 2002 (September-October) at Chhota Shigri glacier. Since then the work is being continued in collaboration with Institut de Recherche

pour le Développement (IRD), France and Society for Himalayan Glaciology, Hydrology, Ice, Climate and Environment (HIGHICE –India).

The glacier mass balance study needs to be observed every year during the end of hydrological year, which is from October 1<sup>st</sup> to September 30<sup>th</sup> next year. In this respect the glacier has been revisited annually in September for the measurements of old stakes and installation of new stakes. During the field expedition from September 18 to October 10, 2003, the stake's position of 2002 was re-measured with the help of differential GPS and melting was observed through the differential exposure of stakes measurements. The new stakes were installed on the glacier and the number has been increased to 22 from 14 in order to increase the stake density for better accuracy of the mass balance. Accumulation pits were dug to know the yearly accumulation. The hydrological measurements were also performed at the down stream of snout.

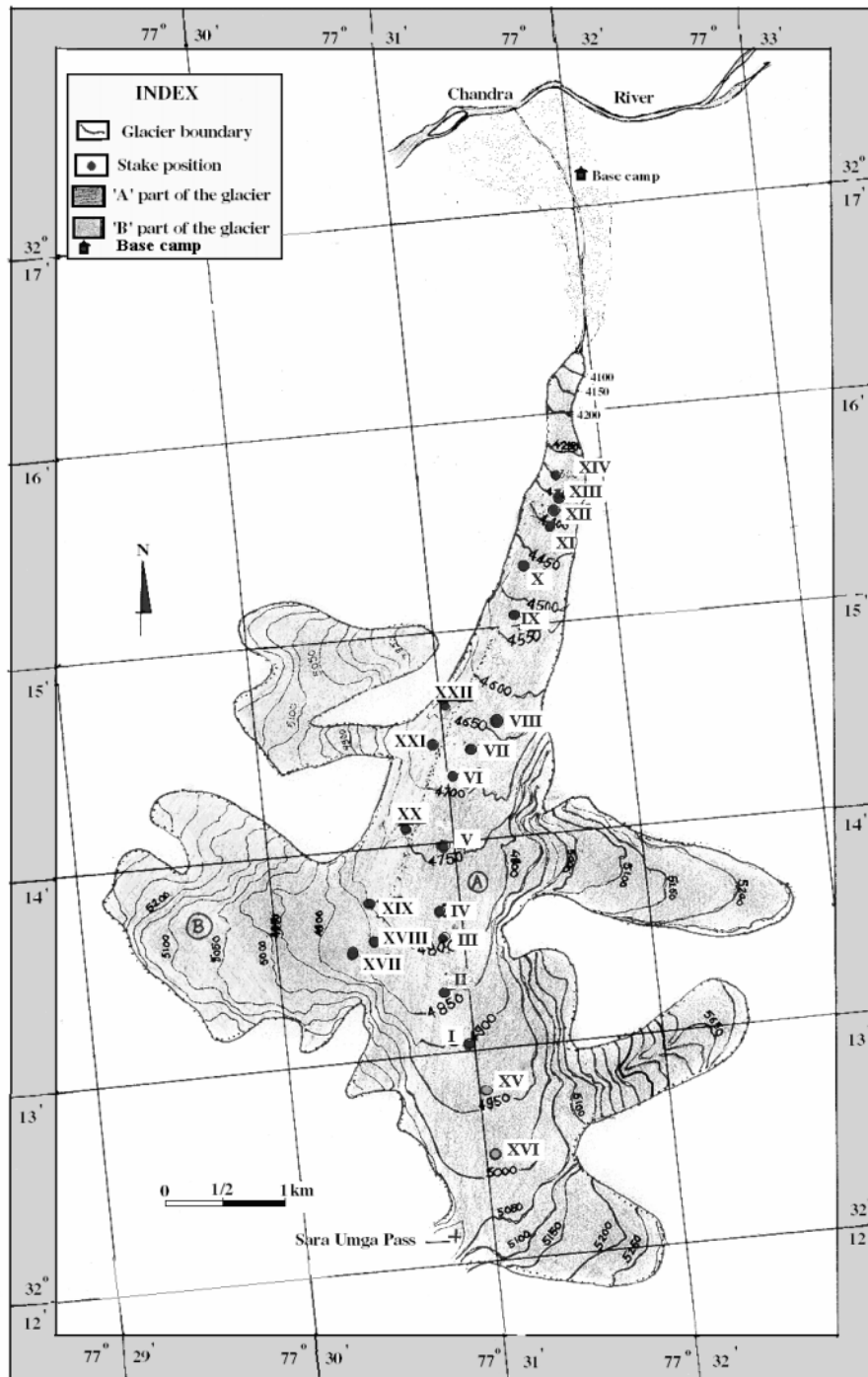


Fig. 2: Stakes installed on the Chhota Shigri glacier during September-October, 2003.

A field campaign during September 14 to 28, 2004 was organised to revisit the glacier for the measurement of 2003 stakes and to put the new stakes on the glacier. The stakes density has been increased further to 27 as compared to 22 in year 2003. Three accumulation pits were dug to know the yearly accumulation at nearly the same place where the last year's observations were performed. The stakes installed in first week of October 2003 is presented on the topographic map of the Chhota Shigri glacier (Figure 2). This clearly shows the distribution of stakes in 2003 on the Chhota Shigri glacier.

### Glacier flow velocity

Differential Geopositioning System (DGPS) was used to measure the coordinates of stakes installed in 2003 and again the same stake in 2004. Displacement of the stakes gave the velocity of the glacier on that altitude. The results so obtained are represented graphically against the altitude (Figure 3). It is observed that the middle ablation zone of the glacier has higher velocity about 40 m/year while the lower ablation and ELA zone shows less velocity of about 25 m/year. The glacier flow velocity reported earlier was 8.1 m/year in the ablation zone to 13.81 m/year at the ELA (Dobhal, 1992). This one year result shows that the glacier flow has increased in last one decade.

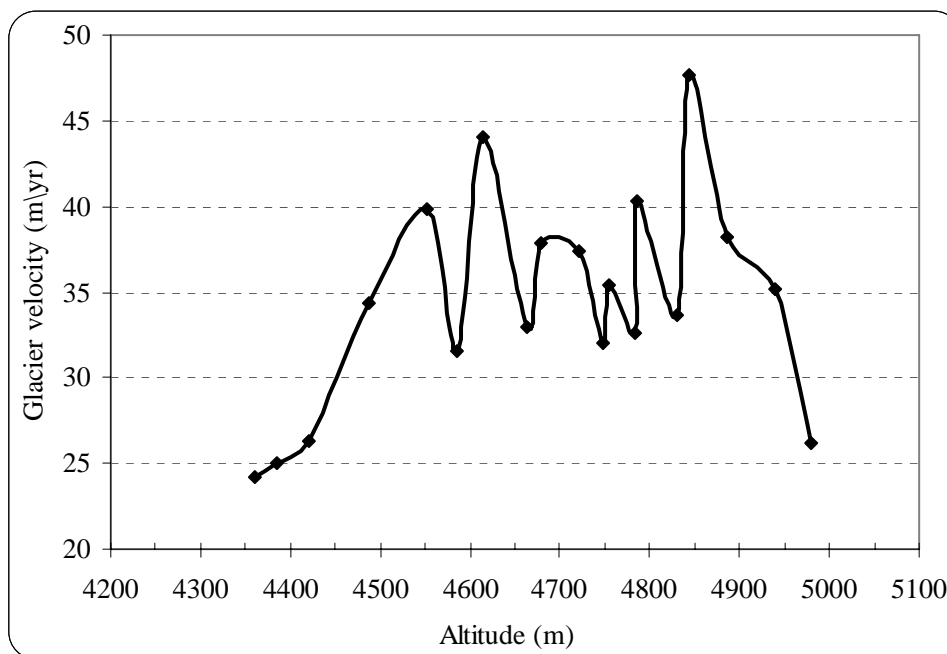


Fig. 3: Annual glacier velocity in the different altitude zone of Chhota Shigri glacier in 2003-04.

### Accumulation measurements

In the accumulation area of Chhota Shigri glacier, three snow/finn pits were dug to obtain information on yearly accumulation of the snow. The only recognisable changes in the stratigraphy were slight differences in the size of the finn grains and few thin ice layers. The ice layers were clear at some places while dirty at the other places.

The vertical density measurements are performed to calculate accurately the water equivalent of snow accumulation in one year. Density profiles of all the three pits are presented for years 2003 and 2004 in Figure 4 and 5 respectively. Very little changes in the density profile have been observed for the first two pits at the elevation of 5200 m and 5405 m in the year 2003. The density first increases and then decreases with depth. The third pit (year 2003) at an elevation of 5500 m shows a large variation in the density profile increasing with depth and reaching to  $0.86 \text{ g cm}^{-3}$  (glacier ice) at the depth range of 300-338 cm. In the year 2004, the pit at 5180 m shows clean ice with bubbles in the depth range of 25 to 165 m showing a density of  $0.79 \text{ g cm}^{-3}$  and thereafter decreased to  $0.58 \text{ g cm}^{-3}$  at the depth of 220 m. The two upper elevation pits (5400 m and 5500 m) are showing the same trend and density reaches up to  $0.8 \text{ g cm}^{-3}$  at several depths as the ice layers were observed.

## Glacier mass balance

Crucial to the survival of a glacier is its mass balance, the difference between glacier ice accumulation and ablation (melting and sublimation). Climate change may cause variations in both temperature and snowfall, causing changes in mass balance. A glacier with a sustained negative balance is out of equilibrium and will retreat. In the ablation area, local net ablation is evaluated using a network of ablation stakes (6 to 10 m-bamboo stakes stuck into the glacier at various altitudes using a steam-drilling device). The emerged part of the stakes is measured every year at the beginning of October together with ice/snow density and the emergence difference gives the annual ablation at that point.

At every point on a glacier, there is a specific net mass balance. In general, this is positive at higher altitudes, where accumulation is more and negative at lower altitudes where the ablation is greater than the accumulation. The net balance of a particular glacier may vary sharply from one year to another. In order to obtain an accurate picture of glacier changes, mass balance programmes, therefore need to be continued for many years. The shape, or geometry, of a glacier may have a significant effect on its mass balance.

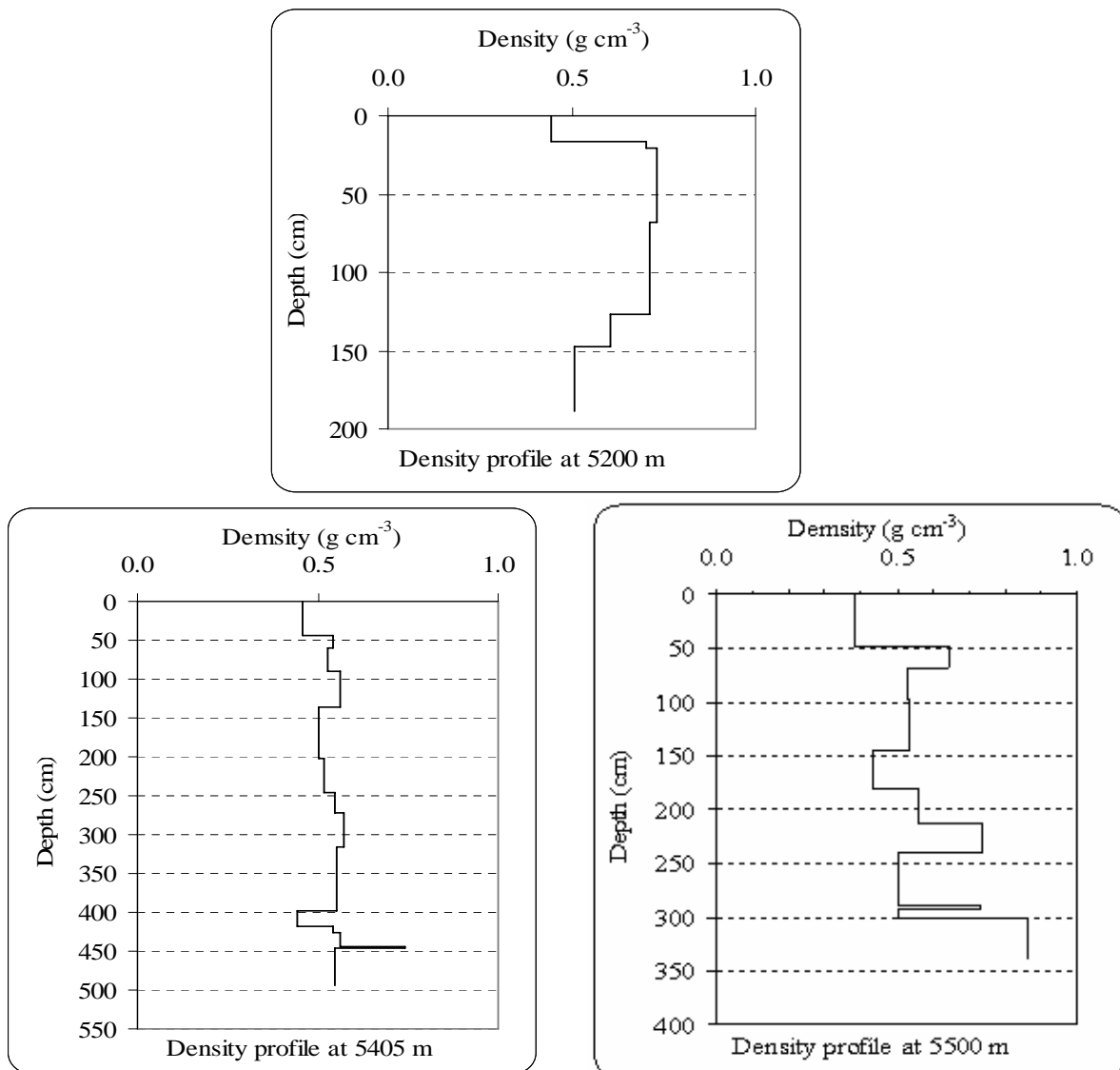


Fig. 4: Vertical density profile of accumulation pits at different elevations in 2003.

The glacier's annual net mass balance is calculated from the measurements of the winter and summer balances but in our case we took only the annual measurements in last week of September every year and calculated the annual balance. The surface area of a glacier is divided into altitudinal zones based on the contours of 50/100 m and stakes and pits features are the representative of the zone in which they are

falling. The average accumulation and ablation is calculated from pits observation and the differential exposure of the stakes respectively on yearly basis. The surface area of each altitudinal zone used in mass balance calculations is based on Survey of India topographic maps.

**Specific net annual mass balance**

Based on the two years of the stake measurements (2002-03 and 2003-04) the specific net mass balance is calculated at every point of stake's and presented in graphical form (Figure 6 and 7) against the representative elevations of the stakes. The glacier melt increases from higher altitude towards lower altitude from 4917 m to 4370 m and suddenly the melting reduces for two stakes in the lower ablation zone. This sudden decrease of melting may be due to the reduction in sunshine hours at this region because of narrowing of the valley, which is observed during the field visit. This reduced ablation may also be due to heavily debris covered zone just above the snout region.

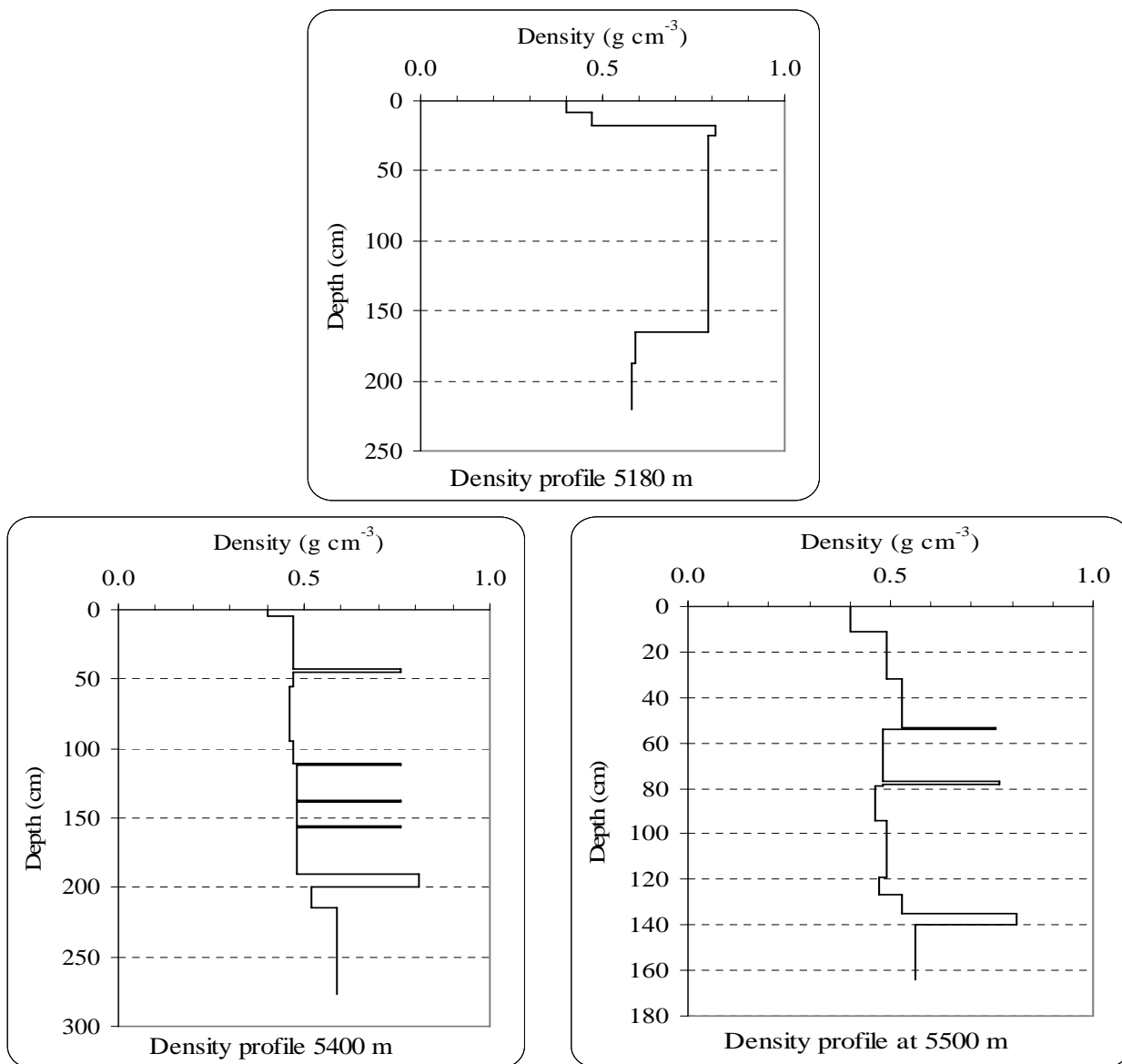


Fig. 5: Vertical density profile of accumulation pits at different elevations in 2004.

**Net mass balance**

The various positions of the snout line monitored during 1987-89 (campaign of Department of Science and Technology, New Delhi) are an indication of the annual climatic variation on the glacier and have been accompanied by three main episodes of advance and retreat. Fluctuations of the equilibrium line, observed during the same period, support the above observations. The snout line of the glacier continued to recede at a rate of  $18.7 \text{ m year}^{-1}$  during 1986-88. This retreat was accompanied by a negative mass balance observed during 1987-88 (Nijampurkar and Rao, 1992).

Our study based on the two years observations (2002-03 and 2003-2004) shows a negative specific mass balance of  $-1.06 \text{ m w.e.}$  and  $-1.20 \text{ m w.e.}$  for 2002-03 and 2003-04 respectively. The increased negative mass balance in 2003-04 reflects more thinning of glacier at lower altitude.

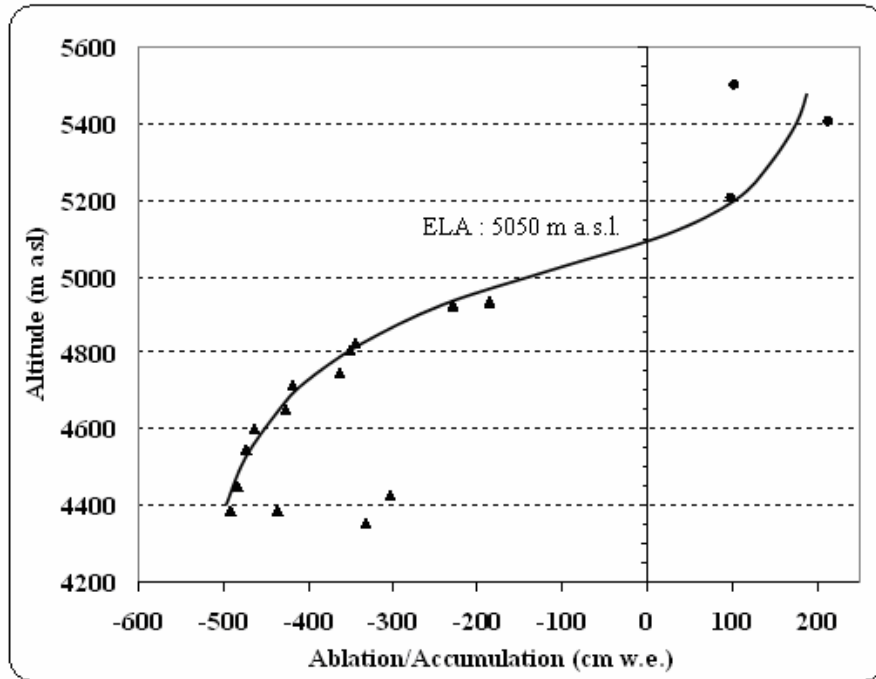


Fig. 6: Specific net annual mass-balance (2002-03) near measurement points averaged against the elevation on Chhota Shigri glacier.

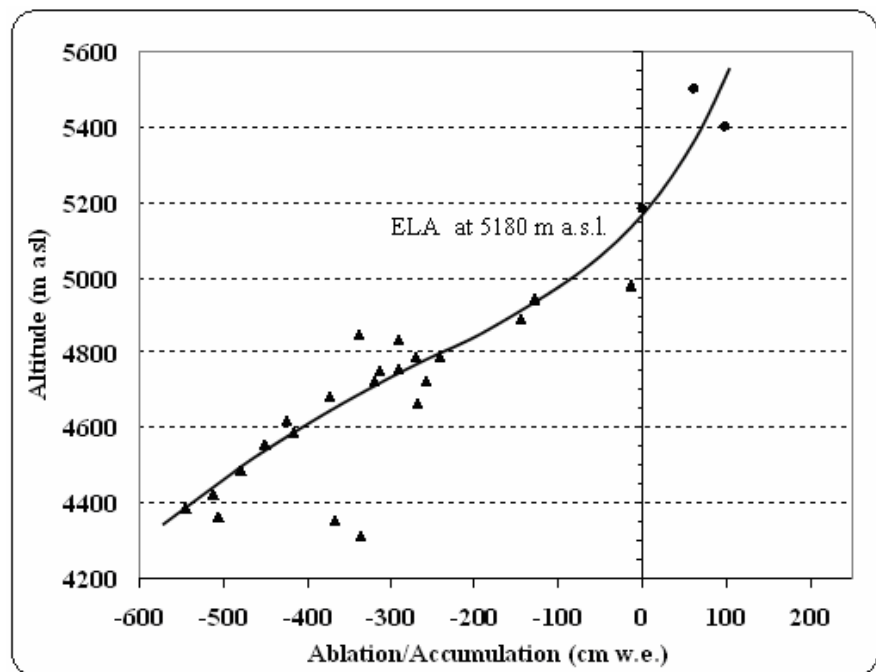


Fig. 7: Specific net annual mass-balance (2003-04) near measurement points averaged against the elevation on Chhota Shigri glacier.

## **Equilibrium line altitude (ELA)**

At the end of the summer, the equilibrium line marks the position at which summer ablation just equals the accumulation of the preceding winter. The equilibrium line altitude (ELA) is the most suitable parameter for interpreting glacier responses to climate variations. The sensitivity of the ELA to climate variations depends on the gradients of the mass balance terms at the respective altitudes. In order to study the sensitivity of the equilibrium lines under the different conditions their mean positions in the respective vertical profiles of specific mass balance has to be determined. Frequently, there is a clear relationship between the equilibrium line altitude (ELA) and the net mass balance of the glacier. The ELA varies from year to year and shows a fluctuating nature.

The ELA during years 1987, 1988, and 1989 were at an altitude of 4650, 4750, and 4840 m a.s.l. respectively (Dobhal *et al.*, 1995). The ELA calculated from the vertical profiles of specific mass balance on Chhota Shigri glacier for years 2003 and 2004 has to be determined and are respectively 5050 and 5180 m a.s.l. (Figure 6 and 7). These comparisons very clearly indicate that the ELA is shifting upward which is not a good sign for the glacier. This upward shift of ELA exposes more ice to the ablation zone for melting. The accumulation area ratio (AAR) has also decreased from 0.40 (in 2003) to 0.31 (in 2004). The earlier study by Dobhal *et al.* (1995) has reported the AAR as 0.73, 0.59 and 0.39 during years 1987, 1988 and 1989 respectively. This decrease in AAR values gave the glacier a threat for the more melting which is also evident from the calculated net mass balance of the glacier for year 2002-03 and 2003-04.

## **CONCLUSIONS**

The climate change impacts are clearly visible on the benchmark glacier (Chhota Shigri) as evident through the increase in the net loss of mass year by year. The glacier is likely to become thinner at lower altitudes, as there is increased negative net mass balance. The ELA variation in 17 years, which was at 4650 m in year 1987, has moved to 5180 in 2004 gives an average rate of upward shifting by 31 m/year. The decrease in AAR value in two years gave the glacier a further threat for the more melting as the accumulation area has reduced and the ablation area has increased in these years. This result is also supported by decrease in net mass balance of the glacier. All together the sharply changing behaviour of ELA shifting upward and reduction in AAR value may be due to the effect of climate change induced warming and the variation in precipitation in the region.

## **ACKNOWLEDGEMENTS**

The authors express sincere thanks to Prof. Georg Kaser, Chairman, Commission of Cryospheric Science (CCS) for his motivation in choosing a bench mark glacier (Chhota Shigri) in 2002 in the HKH region for the glacier mass balance study. The authors are grateful to the Directorate of Mountaineering and Allied Sports (DMAS), Manali, Himachal Pradesh for their support during the field campaign.

## **REFERENCES**

- Bhutiya, M.R. and Sharma, M.C. (1989) *A report on the glaciological studies carried out on Chhota Shigri glacier*, Technical Report of the Multi-disciplinary Glacier Expedition to Chhota Shigri Glacier, Department of Science and Technology, New Delhi, Report No. 3, 203-236.
- Dobhal, D.P. (1992) *Inventory of Himalayan glaciers and glaciological studies of Chhota Shigri glacier, Himachal Pradesh a case History*. Ph.D. thesis H.N.B. Garhwal University, Srinagar, Garhwal, India.
- Dobhal, D.P., Kumar, S. and Mundepe, A.K. (1995) Morphology and glacier dynamics studies in monsoon-arid transition zone: An example from Chhota Shigri glacier, Himachal-Himalaya, India. *Current Science*, 68, 9, 10 May 1995.
- Franco, B., Vuille, M., Wagnon, P., Mendoza J. and Sicart, J.E. (2003) Tropical climate change recorded by a glacier in the central Andes during the last decades of the 20th century: Chacaltaya, Bolivia, 16\_S. *J. Geophys. Res.*, 108(D5), 4154, doi:10.1029/2002JD002959.

- Hastenrath, S., and Ames, A. (1995) Diagnosing the imbalance of Yanamarey Glacier in the Cordillera Blanca of Peru. *J. Geophys. Res.*, 100, 5105– 5112.
- Hock, R. (2004) Glacier melt: A review of processes and their modelling. *Progr. Phys. Geogr.*, in press.
- Kaser, G. (2001) Glacier-climate interaction at low latitudes. *J. Glaciology*, 47(157), 195–204.
- Kaser, G., Fountain, A. and Jansson, P. (2002) *A manual for monitoring the mass balance of mountain glaciers*. IHP-VI, No. 59, 18 p.
- Krenek, L and Bhawan, V. (1945) Recent and past glaciation of Lahaul. *Indian Geogr. Jour.*, 3, 93-102.
- Kuhn, M. (1981) Climate and glaciers, *IAHS Pub.* 131, 3 – 20
- Kumar, S. and Dobhal, D.P. (1997) Climatic effects and bed rock control on rapid fluctuations of Chhota Shigri glacier, northwest Himalaya, India. *J. Glaciology*, 43, 145, 467-72.
- Nijampurkar, V.N. and Rao, D.K. (1992) Accumulation and flow rates of ice on Chhota Shigri glacier, central Himalaya, using radio-active and stable isotopes. *J. Glaciology*, 38, 128, 43-50.
- Nijampurkar, V.N., Sarin, M.M. and Rao, D.K. (1993) Chemical composition of snow and ice from Chhota Shigri glacier, Central Himalaya. *J. Hydrol.*, 151, 19-34.
- Oerlemans, J. (1994) Quantifying global warming from the retreat of glaciers. *Science*, 264, 243-245.
- Rees, H.G., Collins, D.N., Shrestha, A.B., Hasnain, S. I., Kumar, R. and Musgrave, H. (2005) An assessment of the potential impacts of climate change induced glacier retreat on Himalayan river flows. *Mountain Research Development (MRD)*, 25, 4 (In press).
- Roy, S.S. and Balling Jr., R. C. (2005) Analysis of trends in maximum and minimum temperature, diurnal temperature range, and cloud cover over India. *Geophys. Res. Lett.*, 32(12), L12702, doi:10.1029/2004GL022201.
- Wagnon, P., Ribstein, P., Francou, B. and Sicart, J.E. (2001) Anomalous heat and mass budget of Zongo Glacier, Bolivia during the 1997-98 El Niño year. *J. Glaciology.*, 47(156), 21-28.
- WWF (2005) *An overview of glaciers, glacier retreat, and subsequent impacts in Nepal, India and China*. WWF Editions.
- Yadav, R.R., Park, W.K., Singh, J. and Dubey, B. (2004) Do the western Himalayas defy global warming? *Geophys. Res. Lett.*, 31(17), doi: 10.1029/2004GL020201

# DROUGHT ANALYSIS AND THE EFFECT OF CLIMATE CHANGE IN THE WEST BANK / PALESTINE

**Natasha CARMI, Basema BASHIR, Ayman RABI**

Palestinian Hydrology Group, P.O.Box 25220, Jerusalem 97300, West Bank

*natasha@phg.org*

## ABSTRACT

Drought is a frequently occurring natural phenomenon in the semiarid areas, in which rainfall is the only source of recharge. Over the past few years, the West Bank has experienced lower than average annual precipitations. This paper conducts drought analysis in the West Bank and assesses the impact of climate change. The BILAN software package has been used to develop a physically based model and to assess the water balance components in a monthly step. Two sets of simulated time series have been generated; one for the reference situation and one for the conditions of climate change. Analysis of both time series has revealed the impact of climate change on drought characteristics of duration, severity and onset. Given that BILAN has been developed for other bioclimatic zones, this paper will further recommend adapting it to semi-arid zones.

**Keywords:** drought, climate change, West Bank, Palestine

## INTRODUCTION

In the Middle East in general and in Palestine in particular, integrated water resources management is hindered by the complex hydro-political situation, which is characterized by natural water scarcity, shared nature of water resources, conflicting demands, and intensive development and use of resources. In addition, the lack of final regional water agreements defining the exact shares, roles and responsibilities of each riparian, especially the Palestinians, coupled with the lack of adequate water laws, regulations and plans governing water in Palestine make it difficult to manage these resources efficiently, especially under the given uncertainties. Another significant uncertainty is the one related to climate change in general and to drought in particular. Although, it is often assumed that the effect of climate change in the Middle East is insignificant (IPCC-WGII, 1996), yet given the scarcity of water resources and the increased demand, changes in climate over the years are expected to assist in aggravating problems in water quantity and quality. Given that the region is characterized by a high variability in rainfall depth over time and space, the occurrence of a drought event is highly random. In 1998/99, the rainfall record in winter was the lowest in the past 100 year rainfall records. This drought led to water quality deterioration, drop in the groundwater levels and decline in spring discharge. Accordingly, water shortage became very acute and available supply falls short in meeting demand. Under the foreseeable future scenarios of population growth and development needs, this water shortage is expected to intensify. The average population growth rate is estimated at 4%, which, means that the population is expected to double in the coming two decades (Rabi *et al.*, 2003a).

Drought is a natural phenomenon that may have a grave impact on the availability of fresh water resources if it occurs frequently, especially in the semiarid areas. The region lacks alternative water resources and the main source of replenishment is precipitation. Drought, its duration and frequency are the determining factors in setting up sustainable water resources management plans. Although, there is much controversy about the impact of global climate change on the Middle East, yet given the scarcity of resources, any possible change will have a significant effect on the availability of fresh water resources and the stability of the region as a whole.

The possible increased rainfall intensity coupled with an increase in extreme events, and an overall reduction in precipitation will lead to the increased soil erosion, runoff and salinization. This in turn will cause loss of biodiversity and increase desertification. Given that water levels are shallow in the Iskandaroun catchment, the reduction in recharge and the increased salinization will deteriorate the water quality. Palestine already suffers from water shortage and if the available quantities are polluted the situation will be more critical and will likely cause a rise in the incidence of water borne diseases.

On another level, the increased water stress will increase the likelihood for water resource conflicts in the region. This will also increase abstraction from groundwater and will deplete the storage, especially in the northwestern part of the West Bank, where agriculture is the main source of income.

The current paper focuses on the potential impact of climate change on drought incidence and duration and the effect it might have on water resources and water availability in the Iskandaroun catchment in the western part of the West Bank/Palestine,. Derived climatic scenarios for the Middle East region will be used to assess the impacts of climate change on water balance components, including potential evapotranspiration, soil moisture storage, groundwater storage and recharge.

## STUDY AREA

Palestine enjoys typical Mediterranean climate conditions. It has two distinctive seasons; a wet winter, which lasts 5 months (November-March) and a dry summer, which nearly lasts for seven months (May-October). Rabi (1999) demonstrated that the number of rainy days is limited and rarely exceeds 60 days a year. Rainfall depth has a non-uniform distribution and exhibits high spatial and temporal variability.

The presence of hills in the central part of the West Bank-Palestine affects the behaviour of the low-pressure area of the Mediterranean and releases precipitation on the hill ridges. However, the steep gradient of Jordan Rift Valley produces a “lee” effect, which greatly reduces the quantity of precipitation in the Valley (Husary *et al.*, 1995). Moreover, precipitation is considered the main replenishment source of all water resources in the West Bank. However, significant part of it is being lost in the form of evapotranspiration (approx. 67-68%). Surface run-off constitutes only 2-3% leaving nearly 29-30% for infiltration into the subsurface (Rofo and Rafferty, 1963).

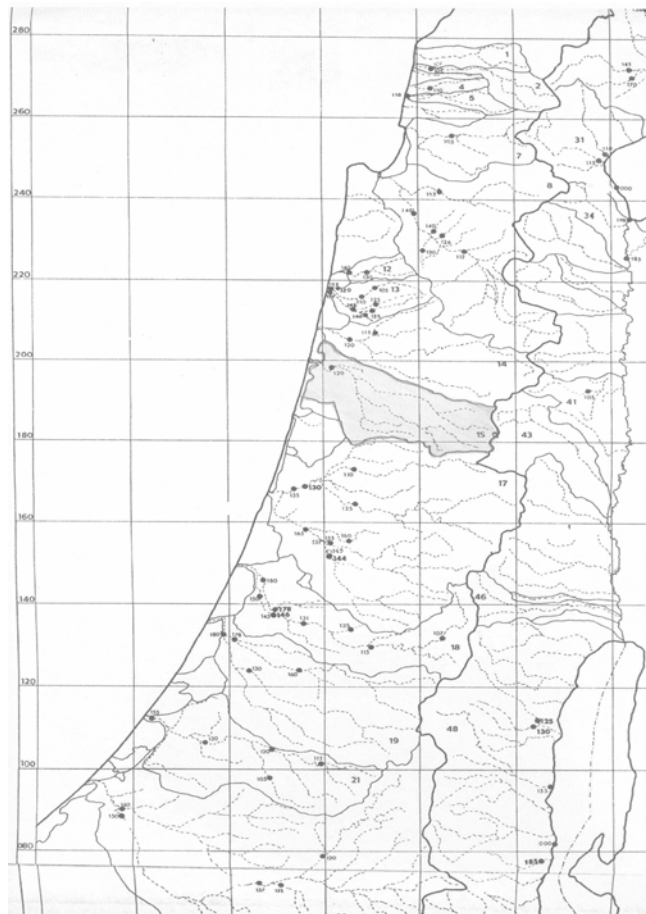


Fig. 1: Location of Iskandaroun catchment.

The study area consists of the two sub-catchments that make up the Iskandaroun catchment; Zeimar and Tin (Fig. 1). The total area is 492 km<sup>2</sup>. The Iskandaroun catchment lies partially in the western part of the West Bank. Mean annual rainfall ranges between 550 and 600 mm, while mean annual evaporation varies

from 1550 to 1750 mm westward. The mean annual temperature ranges from a minimum of 17 to 21°C. The soils are mainly Terra Rossas Brown Rendzinas with areas of Brown Rendzinas, Pales Rendzinas and Grumusols (MOPIC, 1998). The Terra Rossa Brown Rendzinas are originally dolomite and hard limestone, with soil depths varying from shallow to deep (0.5- 2 m). Other parts include loamy or clay reddish brown soils, highly calcareous gray and grayish brown alluvia soil whose parent materials are soft chalk and marl. The aquifer system's unsaturated zone consists of unconfined, fractured and karstic marine sediment composed of limestones, dolomites, chinks and marls (Rofe and Rafferty, 1965) Hence infiltration is high. According to the sensitive recharge areas identified by MOPIC (1998), the area under study is mainly a highly sensitive recharge area. The recharge areas have been classified according to selection criteria, which include hydrogeological characteristics, depth of water table, water quality, lithology and precipitation.

## **DATA AND METHODOLOGY**

### **Hydrological Model**

The BILAN model has been developed to assess the monthly water balance components of a catchment. The model, a lumped physically based model, is based upon a set of relationships, which describe basic principles of water balance both in the unsaturated and saturated zone. The model has eight free parameters and uses an optimization algorithm for their calibration at gauges basins. Input data of the model are monthly time series of areal precipitation, air temperature and either relative air humidity or potential evapotranspiration. In order to calibrate model parameters, a monthly runoff series at the catchment outlet is used. The model simulates time series of monthly potential evapotranspiration, actual evapotranspiration, infiltration to the soil and recharge from the soil to the aquifer. The amount of water that is stored in the snow pack, the soil and aquifer is also simulated for each month. All these hydrological variables apply to the whole catchment. The total runoff consists of three components, direct runoff, interflow and base flow (Kasperek, 1998).

### **Drought estimation**

The EXDEV program selects drought events from flow series and performs statistical analysis including the application of several probability distributions to the annual maximum or partial duration series. Program options include calculation and selection of the threshold discharge, linear interpolation techniques for filling in missing data, calculation of moving average series and its subsequent analysis and graphical interpretation of results (Kasperek and Novicky, 1997). To identify droughts, simulated times series of monthly flow data have been used along with the EXDEV code and log normal distribution (Kasperek and Novicky, 1995). The threshold concept has been used in the derivation of the droughts. The Q90 (90<sup>th</sup> quantile) for the reference situation calculated at 13.15 mm month<sup>-1</sup>, has been taken as a threshold value.

### **Climate scenarios**

General Circulation Model (GCM) simulations for the Middle East, indicate higher future temperatures, increased evapotranspiration and changes in climatic patterns that might reduce rainfall (IPCC-DCC, 1999; IPCC-WGI, 1996). According to Bou Zeid and Fadel (2002), climate change scenarios for the region have large uncertainties and discrepancies between different GCMs. For the purposes of this study, the simulation results from two different GCMs (CGCM, GFDL-R15) for the same set of assumptions - IS92a scenario- (Legett *et al.*, 1992) for climatic change projections in the Middle East have been used. "IS92a is a middle of the range scenario in which population rises to 11.3 billion by 2100, economic growth averages 2.3% year<sup>-1</sup> between 1990 and 2100 and a mix of conventional and renewable energy sources are used. Only those emissions controls internationally agreed upon and national policies enacted into law, e.g., London Amendments to the Montreal Protocol, are included." In these GCMs, both greenhouse gases and sulfur aerosols are accounted for and the projections available are for the 2020s

climate conditions in comparison to the period 1961-1990. Although GCMs have a coarse grid and large scales relative to hydrological systems, yet for the purposes of this study, the climatic scenarios serve in defining possible trends that are used in sustainable future planning. GFDL-R15 is a hot and dry climatic scenario in which temperature increases by 1.2°C between the months of January and March, and by 1.8°C between the months of June and August, without any temperature increase in the remaining 6 months of the year. In addition, precipitation decreases by 0.1 mm/day mainly during the months of November to March. CGCM is a mild-hot climatic scenario in which temperature increases by 1.3°C between the months of January and March, and by 0.8°C between the months of June and August.

A given change in climate will produce different responses as a function of the hydrologic characteristics of each basin. The lack of data on basin characteristics and accurate water balance data hinders the use of advanced hydrologic models. The data set used in this study includes monthly values of air temperature, precipitation, relative humidity and runoff taken from various publications. The runoff series is the only continuous data available at present. The data has been used as given as no information is available regarding the quality of data. One meteorological station, Tulkarem, has been used to represent the rainfall, humidity and temperature for the whole catchment. This is due to the unavailability of data. However, the total annual precipitation observed at Tulkarem station of 575 mm, is 93% of the long mean annual precipitation of 618 mm for the period 1951-1980, as calculated by using the Thiessen method for the whole catchment (Hyo, 1994).

For initial conditions, initial groundwater storage has been set at 1 mm, given that the model does not accept zero values. In a semi-arid region as in Palestine, the groundwater storage is depleted during the summer period. In a previous study (Rabi *et al.*, 2003a), analysis of groundwater level–rainfall depth relationship shows that the best correlation is a one-year model. This means that the groundwater level in any particular year is a function of rainfall during the same year, as well as that of the past year. Once higher time steps are considered, or the number of years of delay time is changed, the correlation coefficient does not improve and the percentage of contribution is negligible. This means that the effect of rainfall on groundwater levels is a yearly event. This can be explained given that the aquifer is mostly karstic; the groundwater flow velocity is relatively high, and/or the storage coefficient is high. In other words, when the rainfall in one cell (during the wet season) is above the average value, groundwater levels will rise. While during the dry season, the aquifer will drain quickly and groundwater levels return to more-or-less the long term average levels. In the case of a deficit year (rainfall below the average), the aquifer will relatively (and naturally) drain until groundwater levels return to the long term average levels (Rabi *et al.*, 2003b).

The eight model parameters have been optimized for the reference situation and have been used to run the climatic scenarios. For the temperature data, two years of data were missing. In addition, eighteen records from the runoff series were missing for the years 1978-1979, 1981-1982, and 1982-1983 for the Iskandaroun catchment station. An attempt was made to correlate with the neighboring Khadera catchment of an area of 519 km<sup>2</sup>, further south. However, the data for the same years was also missing for the Khadera catchment. Hence, it was imperative to estimate the runoff values for the missing period. For each missing record, the average of the previous and following year runoff was used.

In the optimization procedure, normally the standard error of estimate is used as an optimization criterion (standard deviation between observed and simulated runoff). However, in areas of low flow, a good fit is not ensured. Usually the standard procedure in BILAN is to use the standard error of estimate to optimize the parameters that significantly affect the mean runoff, and to use the mean of absolute values of relative deviations to calibrate the remaining four parameters that affect the distribution of runoff into its individual components. In areas of zero flow, as in Palestine, the sum of relative deviations between the observed and simulated runoff series cannot be used. Hence for the purposes of this study, only the standard error of deviations is used. The version of the model used for the purposes of this study accepts zero values.

In addition, the model uses two algorithms; summer and winter ones. The condition controlling the choice of algorithm is the presence or absence of precipitation in the form of snow. Given that in Palestine and for the period under study, all temperatures are above zero and for the period under study, no snow cover occurred, the model uses only “summer algorithm” Hence the parameters for winter and melting conditions have no influence on the results and in fact they are not optimized.

The bioclimatic zones used in BILAN are defined from empirical graphs that represent the conditions in the Northern Hemisphere given in Gidrometeoizdat (1976). Each bioclimatic zone is characterized by characteristic air temperature. The model embodies an interpolation algorithm, which uses catchment long-term average air temperature for interpolating between the zones. The potential evapotranspiration is

estimated from saturation deficits by using functions derived for individual months and zones. The saturation deficit is calculated from data on air temperature and relative air humidity. The bioclimatic zones include Tundra, Coniferous forest, Mixed forest, Deciduous Forest and Steppe. The Steppe bioclimatic zone is characterized by long-term annual temperature more than 12.8°C. There is no upper temperature limit. In the same Russian source, there is a nomogram for desert bioclimatic zone that gives slightly higher potential evapotranspiration values for the same moisture deficit values.

## SIMULATION RESULTS

### Model

Fig. 2 shows the monthly precipitation series, observed and simulated mean monthly flow series. The model overestimates annual flow by 192.68 mm.

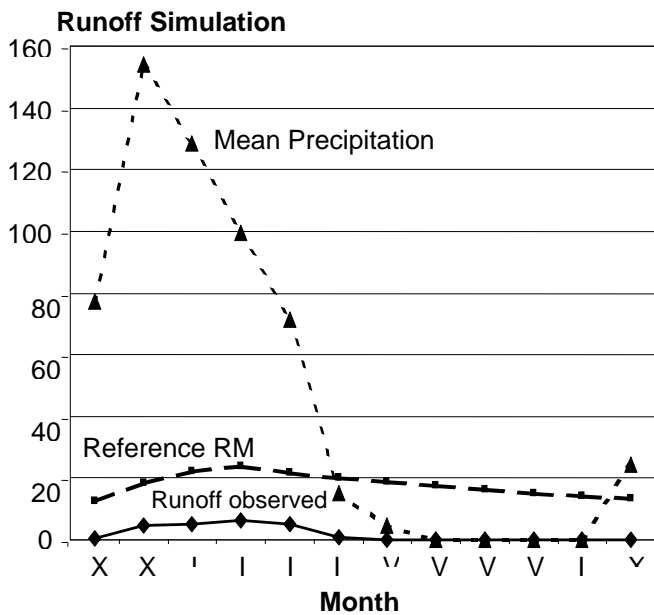


Fig. 2: Monthly precipitation series, observed and simulated mean monthly flow series.

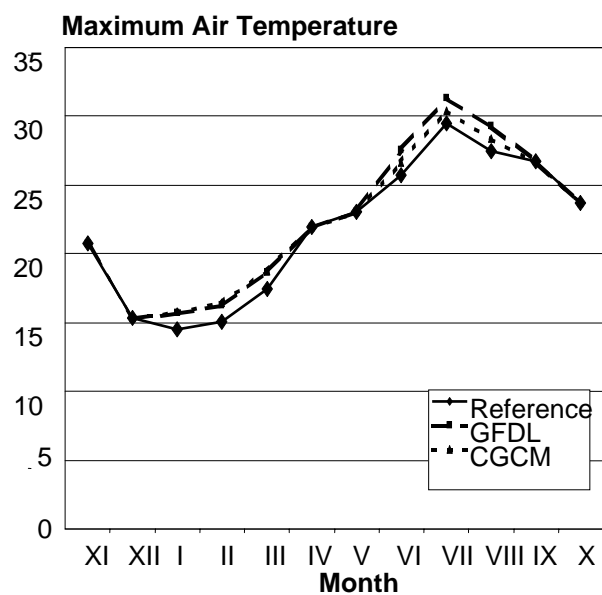


Fig. 3: Maximum air temperature.

### Simulated impact of climate change

As expected, as temperatures increase and precipitation decrease, maximum temperatures and potential evapotranspiration increase in the summer period. (Fig. 3 and 4).

Given that precipitation occurs only during the winter season in the Iskandaroun catchment, actual evaporation  $E$  and soil water storage is reduced in the summer period. Subsequently, infiltration decreases as weather becomes hotter and drier (Fig. 5). The simulations of the climatic scenarios have resulted in a decrease in storage and runoff components. The increase in evapotranspiration reduces both groundwater and soil water storages; more significantly for the hot dry climatic scenario than the dry one (Fig. 6). The depletion in soil water storage starts after the month of January as a result of the increase in the potential evapotranspiration. Direct runoff, interflow and baseflow decrease for both hot and hot dry climatic scenarios, more significantly for the latter scenario (Fig. 7 and 8).

For the hot scenario, the decrease in direct runoff is insignificant given that the precipitation in both reference and CGCM scenarios are the same. The lower baseflow will contribute to lower minimum flows. In terms of water balance components, recharge has decreased for both hot and hot dry climatic scenarios (Fig. 9).

**P, PE, E, R (mm)**

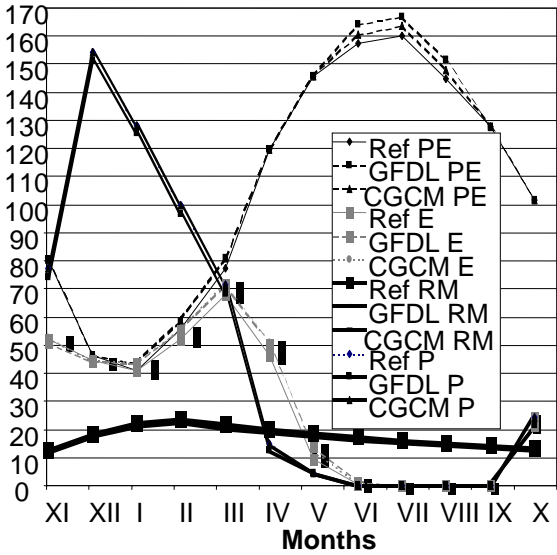


Fig. 4: Monthly variations of water balance components

**PE, Inf, SS (mm)**

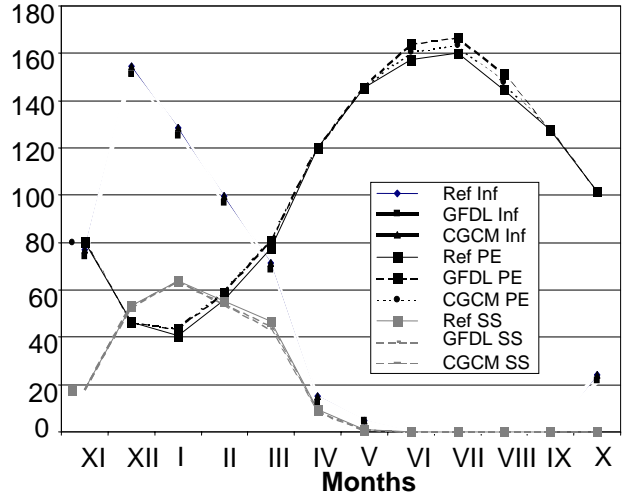


Fig. 5: Monthly variations of infiltration, PE and soil moisture storage

**SS, GS (mm)**

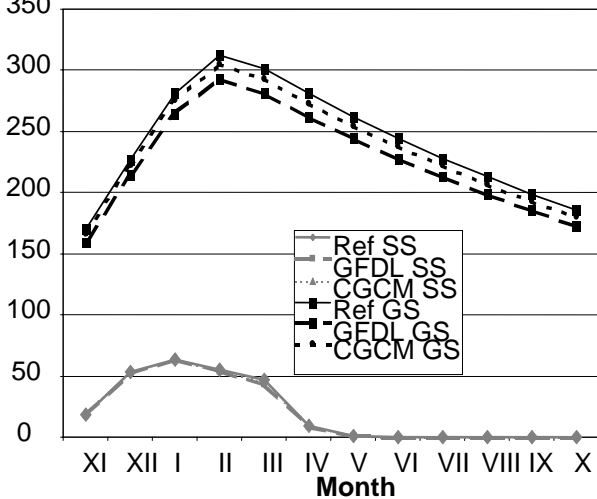


Fig. 4: Monthly variations of water balance components.

**I, BF, DR**

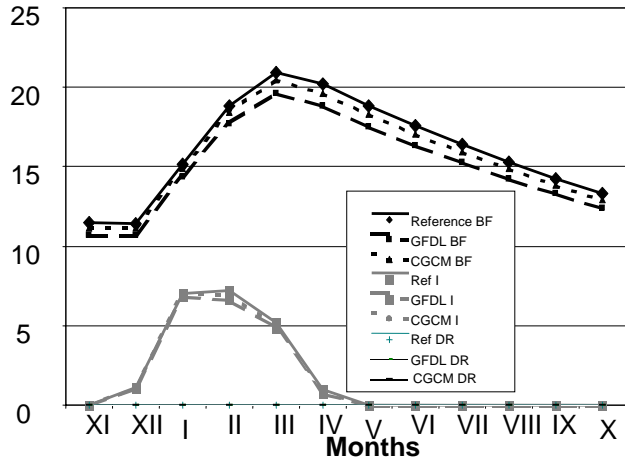


Fig. 5: Monthly variations of infiltration, PE and soil moisture storage.

**SS, GS (mm)**

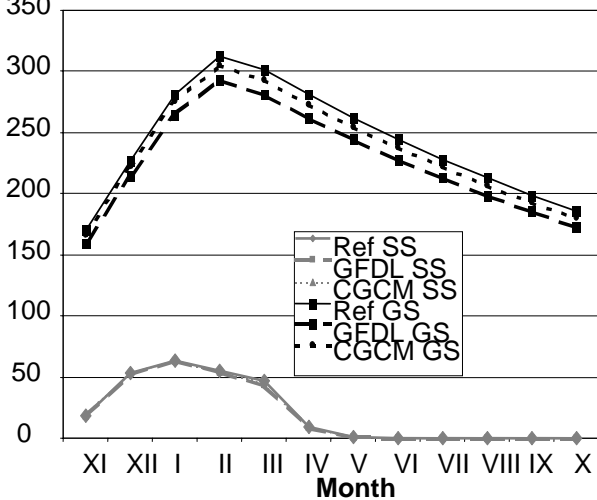


Fig. 6: Monthly variations of water storage components.

**I, BF, DR**

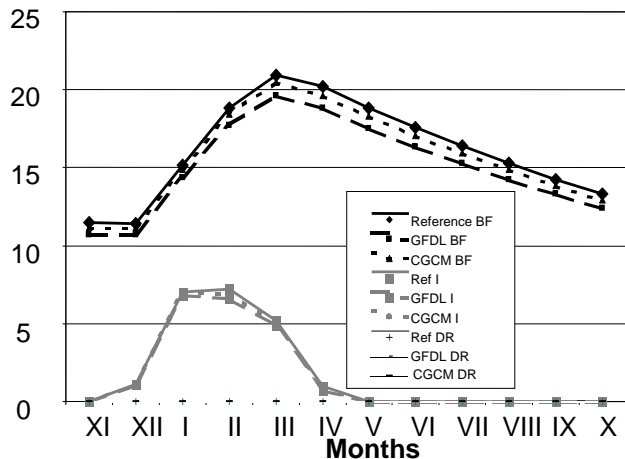


Fig. 7: Monthly variations of runoff components.

The decrease is more significant for the latter scenario though. The recharge feeds the interflow and hence groundwater storage decreases. Pattern of annual recharge of both CGCM and reference scenarios are similar as the only change in parameter is an increased temperature. However for the GFDL, precipitation is reduced during the winter season. Subsequently, the runoff produced is reduced, more significantly with the hot dry climate. The minimum runoff is also reduced, as the weather gets warmer and drier. The decrease in runoff, in comparison, to the reference situation is 6.5% and 2.6% for the hot dry (GFDL) and hot (CGCM) climatic scenarios respectively. The highest deviation in minimum flow is during the month of January (Fig. 10). The increase in temperature (CGCM) will increase potential evapotranspiration and reduce groundwater discharge even further in the summer period. The further decrease in precipitation (GFDL) will enhance the effect. This will subsequently affect the incidence of droughts.

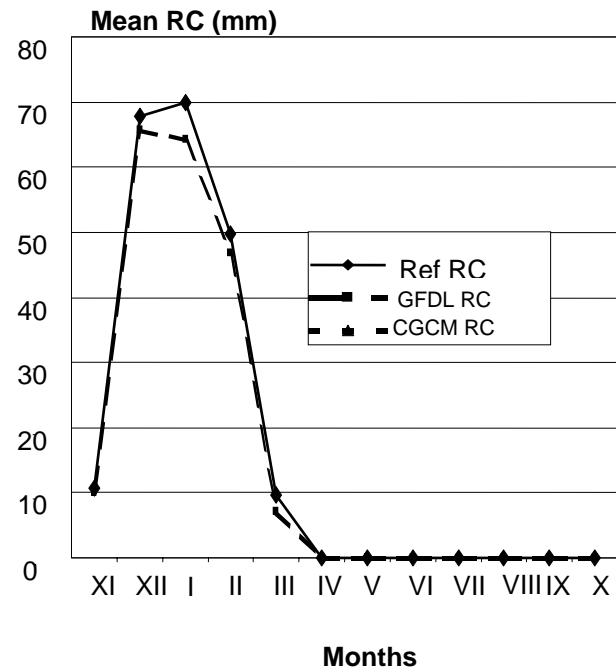
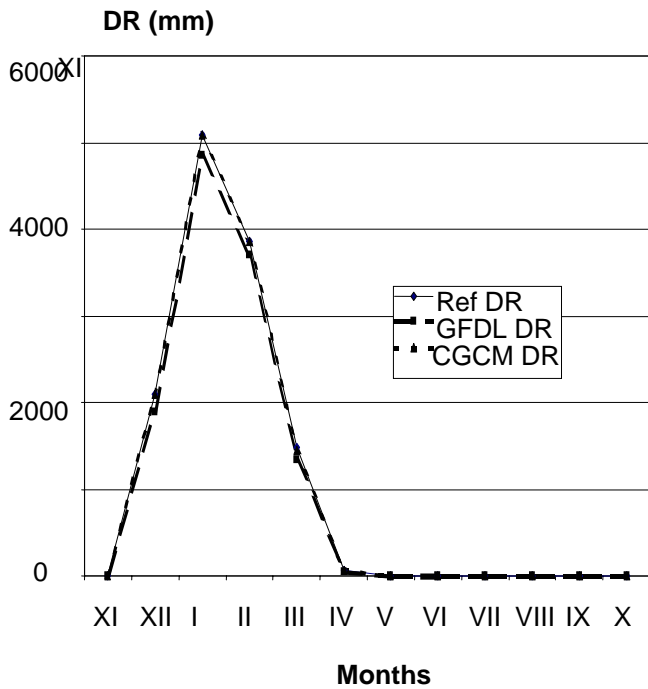


Fig. 8: Monthly variations of direct runoff.

Fig. 9: Monthly variations of recharge.

### Drought Events

For the period of 1977-1989, five drought events are identified. In the related figures, the events are ranked in decreasing order. Fig. 11 shows the impact of climatic change on drought. As temperatures increase and precipitation decrease, droughts become more severe.

The discharge deficit increases by 11.53 mm and 31.50 mm for the hot and hot dry climate change scenarios respectively. Fig. 12 shows the increase in deficit duration, which ranges between one and two months as in event 3 for GFDL. Fig. 13 and 14 show the annual precipitation, its average, the 90<sup>th</sup> quantile and the flow for the scenario GFDL (the figures are nearly identical for the CGCM). Although even the reference situation has few readings above the average annual precipitation, yet comparison of the three figures shows that for the hot dry scenario (*GFDL*), more flow readings fall short of the 90<sup>th</sup> quantile. In all low flow spells, the total annual precipitation is always less than the average annual precipitation. In addition, the figures confirm that drought is a random phenomenon in the West Bank.

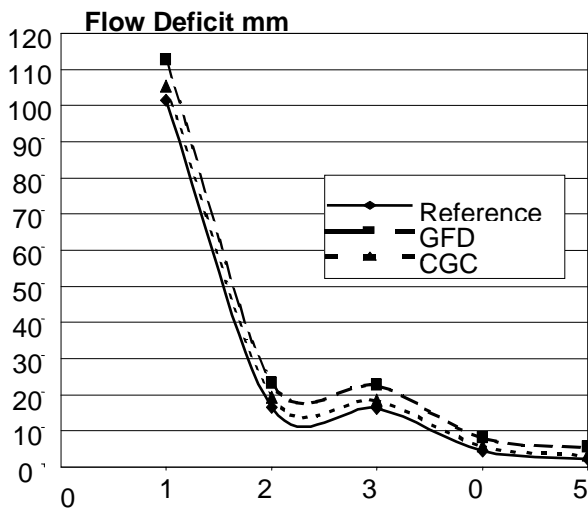


Fig. 10: Monthly variations of flow deficit.

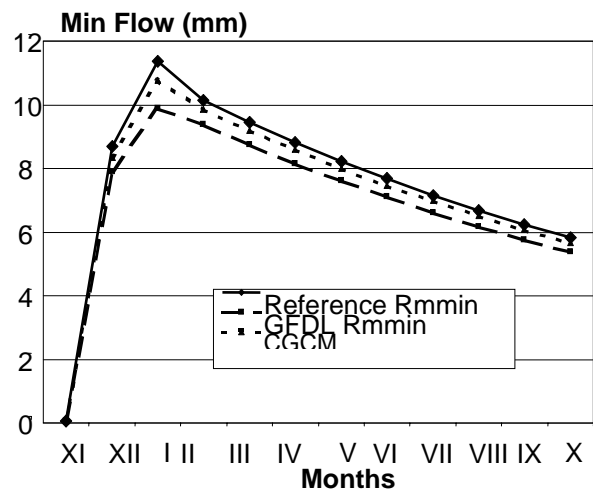


Fig. 11: Monthly variations of minimum simulated flow.

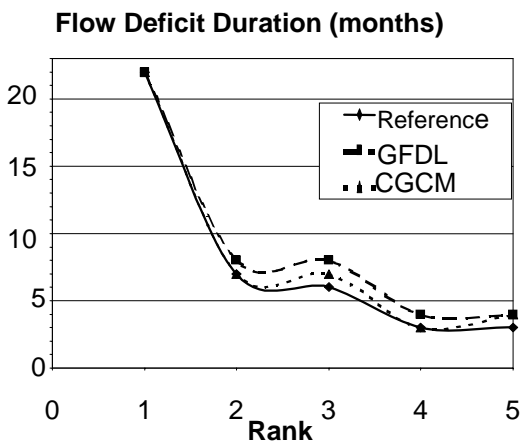


Fig. 12: Flow deficit duration.

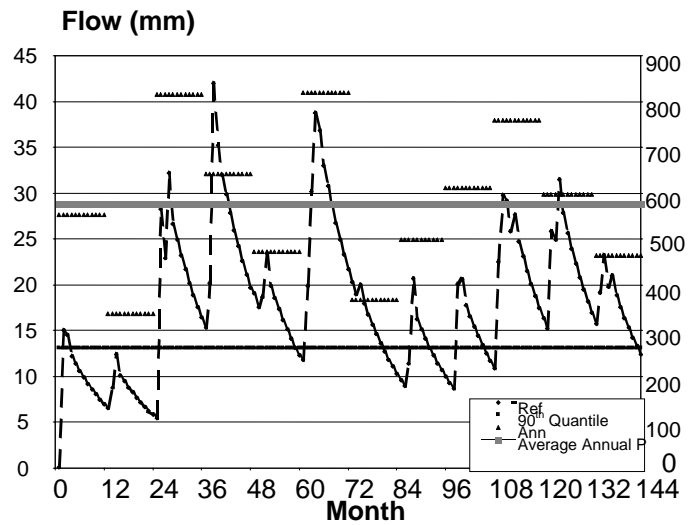


Fig. 13: Reference deficit months.

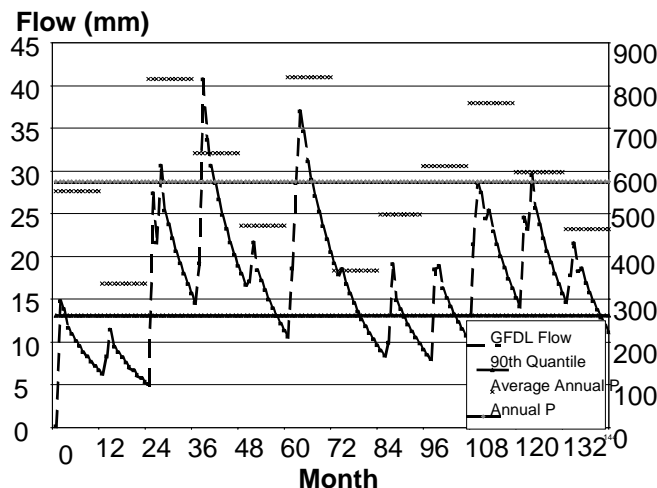


Fig. 14: GFDL deficit months.

## CONCLUSION AND RECOMMENDATIONS

It is imperative to note that the particular climate scenario used has a major role in the assessment of the impact of climate change on drought. Therefore, the assessments made in this study are only expected to

serve as a guideline for future research. However, given the accelerated population growth and the limited water resources, it is important to adopt measures to adapt to possible climate change and reduce the overall impact be it socio-economic, human health or political. The development of non-conventional water resources for agriculture and artificial recharge and sustainable use of water, along with water conservation practices are among the possible adaptation measures adopted. It is also to cooperate regionally in order to develop regional circulation models (RCMs) or local area models that have a higher resolution

The results of the simulations described in this paper cannot be generalized, but can be used as guidelines for a more comprehensive investigation. It is recommended to:

- Use a modified version of the model that incorporates a semi-arid/desert bioclimatic zone and re-run the scenarios in order to study the effect of the use of bioclimatic zones that are more relevant to the Middle East climate. In addition if BILAN is to be modified and used, changes in relative humidity should be included. Scenarios do not take into account the changes in relative humidity. This is one of the dominant factors decreasing minimum flows, as it will contribute to the further increase in potential evapotranspiration if it decreases;
- Use other models and conduct a comparison with the results of BILAN model. The model overestimates runoff and there is a need to use a model that more closely reflects semi-arid conditions;
- Infiltration, as simulated and shown in Fig. 5, is high, and should be verified with another model that does not overestimate runoff as the one used. Hence it is important to study the effect of domestic and industrial effluents, especially which a lot of industries exist in the catchment. Given that the catchment falls within the highly sensitive water recharge areas, it is imperative to develop a comprehensive water management plan.

## ACKNOWLEDGEMENTS

We wish to acknowledge and thank the support and assistance of Mr. Ladislav Kasperek, T.G.M. Water Research Inst., Prague, Czech Rep., whose assistance with the BILAN model has enabled its use in a semi-arid region. We also wish to thank Ms. Lena Tallaksen, Departement of Geosciences, Oslo, Norway, for her valuable comments.

## REFERENCES

- Applied Research Institute- Jerusalem (1997) *The Status of the Environment in the West Bank*. ARIJ, Bethlehem, Palestine.
- Bou Zeid, E. and El-Fadel (2002) Climate Change and Water Resources in Lebanon and the Middle East. *In J. Wat. Res. Planning and Management*, 128, 2 September 1, 2002.
- Husary, S., Najjar, T. and Aliewi, A. (1995) *Analysis of secondary source rainfall data from the Northern West Bank*. Palestinian Hydrology Group, West Bank, Palestine.
- Hyo, I (1994) *Hydrological Year-Book of Israel 1992/1993 and revisions of previous data*. Ministry of Agriculture, Water Commission Hydrological Service, Jerusalem.
- IPCC-WGI (Intergovernmental Panel for Climate Change, Working Group I) (1996) *IPCC workshop on regional climate change projections for impact assessment*. Rep., Geneva.
- IPCC-WGII (Intergovernmental Panel for Climate Change, Working Group II) (1996). *Climate Change 1995: Impacts, adaptation, and mitigation of climate change, scientific-technical analyses*. Cambridge University Press, Cambridge, UK.
- IPCC-DCC (Intergovernmental Panel for Climate Change, Data Distribution Center) (1999) (<http://ipcc-dcc.cru.uae.ac.uk>) (Feb. 24, 2000).
- Kasperek, L. and Novický, O (1995) *Experiments with deficit volumes (EXDEV). Description of the program*. Edn. April 1995. Czech Hydrometeorological Institute, Prague, Czech Republic.
- Kasperek, L. and Novický, O.(1997) Application of a physically-based model to identify factors causing hydrological drought in western and central European basins. *IAHS Pub.* 246, 197-204.
- Kasperek, L. (1998) *Regional study on impacts of climate change on hydrological conditions in the Czech republic*. T.G. Masaryk Water Research Institute, Prague, Czech Republic.

- Leggett, J., Pepper, W.J. and Swart, R.J. (1992) Emissions Scenarios for the IPCC: An Update. In: *Climate Change 1992: The Supplementary Report to the IPCC Scientific Assessment* (Eds. Houghton, J.T., Callander, B.A. and Varney, S.K.). Cambridge University Press, Cambridge, 69-95.
- MOPIC-Ministry of Planning and International Cooperation (1998) Sensitive Water Resources Recharge areas in the West Bank Governorates. In: *Emergency Natural Resources Protection Plan*, Ramallah, Palestine. 2<sup>nd</sup> Edition.
- Rabi, A. (1999) *Optimum intersectoral water allocation in the West Bank*. PhD Thesis Washington International University, Pennsylvania, USA.
- Rabi, A., Khaled, A. and Carmi, N. (2003a) Integrated Water Resources Management Under Complex Hydro-political Conditions–The Palestinian Case Study. In: *Third World Water Forum*, Kyoto.
- Rabi, A., Khaled, A. and Carmi, N. (2003b) Drought occurrence and impact on Eastern Groundwater Basin–West Bank/Palestine. *IAHS Pub.* 273, 263-268.
- Gidrometeoizdat (1976) *Rekomendatsii po roschotu ispareniiia s poverhnosti suchi*. St Peterburg, Russia.
- Rofe and Rafferty (1963) *West Bank Hydrology: Nablus District Water Resources Survey*. Geological and Hydrological report.
- Rofe and Rafferty (1965) *West Bank Hydrology: Analysis 1963-1965*. Hashimite Kingdom of Jordan, Central Water Authority, Jordan.

# INFLUENCE DES VARIATIONS CLIMATIQUES SUR LE REGIME HYDROLOGIQUE DU BASSIN VERSANT DU QSOB (ESSAOUIRA MAROC)

**Nour-Eddine LAFTOUHI**

Laboratoire de géologie appliquée, Faculté des sciences Semlalia, BP. 2930, Marrakech 40000 Maroc.  
*noureddine.laftouhi@ucam.ac.ma*

**Etienne PERSOONS**

Unité de Génie rural, Université Catholique de Louvain, 2, Place Croix du Sud, Boite 2. 1348 Louvain-la-Neuve, Belgique.

## RESUME

Dans ce papier, l'analyse des séries de données hydrologiques sur une trentaine d'années pour les stations d'observations du Qsob (Essaouira-Maroc), a montré une nette corrélation entre conditions pluviométriques et les écoulements. La baisse du régime des pluies moyennes annuelles s'est accompagnée d'une baisse des débits sauf pendant les années "salvatrices", à pluviométrie exceptionnelle, où l'on assiste à un retour vers des régimes d'écoulements plus réguliers. Les épisodes pluvieux, étant précédés par de longues périodes sèches, produisent des écoulements de crue à caractère torrentiel bref et charriant une forte charge solide (blocs, argiles etc.).

**Mots clés :** Qsob-Essaouira, bassin versant, variations climatiques, corrélation, régime hydrologique, précipitations, débit

## INTRODUCTION

Le Maroc a connu depuis le début des années quatre-vingt du siècle passé, une récurrence de périodes sèches qui se sont répercutées sur les disponibilités en eau du pays de manière bien évidente. Malgré l'effort des autorités marocaines à mieux gérer ses ressources en eau et à en mobiliser davantage, les problèmes de raréfaction de l'eau et d'accroissement de la demande se sont accentués. Dans la majorité des cas, le terme entrant du bilan hydrique au niveau du bassin versant hydrologique, se résume aux seules précipitations sous forme de pluie. La baisse dans les apports par cette composante a sérieusement affecté les ressources en eau de surface.

Le bassin versant péri montagneux du Qsob (Essaouira Maroc, Fig. 1) qui servira de site d'étude dans le présent papier, appartient au versant nord du Haut Atlas occidental. Les données hydrologiques disponibles concernent les précipitations et les débits au niveau de trois stations de mesures. Celles-ci fonctionnent depuis le fin des années Soixante et début des années Soixante-dix du siècle passé.

L'intérêt de ce bassin réside notamment dans : (i) la conjugaison des effets anthropiques (déboisement, parcours, etc.) et naturels (sècheresse, aridité) au sein de ce bassin, (ii) l'existence d'une série de données pratiquement complète depuis près d'une trentaine d'années, (iii) le fait qu'il peut servir à comprendre le fonctionnement de bassins versants dans un contexte similaire (à l'échelle marocaine et régionale) et (iv) le fait qu'il constitue une bonne plate-forme pour des études plus détaillées dans le sens de mieux comprendre le fonctionnement de tels bassins.

L'approche adoptée a consisté à confronter par rapport à un axe temps les données de pluie et celles des écoulements engendrés et d'étudier les liens de cause à effet entre ces deux paramètres.

## EXTENDED ABSTRACT

The Qsob basin (Essaouira-Morocco) is located on the extreme Atlantic termination of the Western High Atlas. The whole part of this basin is represented by a succession of low hills with round heads, and a not very deep hydrographic network. The major basin is subdivided in three sub-basins those are: Igrounzar in the North, Zelten in the south and Low Qsob downstream. This last is in fact the result of the junction of both others at the station known as of Zerrar at the entry of the diapir of Tidzi.

## **GEOLOGICAL FRAMEWORK**

The geological formations outcropping in the studied area, start with the clay and marly formations of the terminal Jurassic in the south of Zelten watershed, and end with the sandy and loamy Quaternary in coastal areas in the Low Qsob watershed. The Middle and Upper Cretaceous (marl, fractured limestone, and dolomites) represent the rest of the stratigraphic series especially in the most area of the Igrounzar watershed (up to 85% of the outcrops) and in Zelten (up to 50%).

## **PHYSICAL FEATURES**

In general, the Qsob watershed as defined at Adamna station (Fig. 3), is represented by a lengthened aspect from SE towards NE. The two sub-basins have approximately the same aspects and the same orientation. The main physical characteristics are summarized in Tab. 1 below (Laftouhi, 2002). The absolute altitude difference is about 750 to 1000 m and resumes a mountainous morphology in the three basins. The hypsometry is relatively strong in the upstream parts with an important slope, which becomes softer in the downstream parts.

## **FIELD OCCUPATION**

The field occupation is not very significant. It is summarized approximately to three types: (1) cultures (essentially cereals) where it is possible (on the marly soils of the Cretaceous, the Quaternary and the Eocene), (2) nude areas corresponding to the fissured and karstic limestone outcrops of the Cretaceous and the Jurassic formations and (3) forests (coniferous tree) in the downstream part of the catchments area (Plio-quaternary soils and mountainous reinforcements of the Western High Atlas).

As all of the underprivileged areas of Morocco, the Qsob basin is also subjected to an intensive deforestation (wood for heating and cooking).

## **EXISTING DATA**

All the existing data come from the archives of the General Hydraulic Administration (GHA). For monitoring and evaluating the water resources in the Essaouira basins for water drinking supply, the GHA had installed and is surveying three hydrological stations in the Qsob watershed (Tab. 2). Data collected and used in this study concern precipitations and rivers flow since the middle of the 60's and 70's of the last century.

## **DATA EXPLOITATION**

Data series analysis showed very significant time variability observed also during the same hydrological cycle. Tab. 3 resumes the statistical parameters of the precipitation and river flows during the study period.

Exploiting these data (Fig. 5 to 12) had showed the correlation between the precipitation (as cause) and flow in the rivers (as effect). Selecting significant hydrological cycle with comparison with a mean one (Fekri, 1993, Jalal, 2001, Mennani, 2001, Laftouhi, 1991; Laftouhi, 2002) made it possible to establish the relationship between these two parameters. In this aim, three representative cycles were selected; a mean cycle (1990/91), a dry cycle (1986/87) and a humid cycle (1995/96 for Adamna and 1985/86 for Igrounzar and Zelten).

In a very simplified way, we can note that:

- Precipitations (rainfall) are in all cases, is the only cause generating river flow (Igrounzar, Zelten and Qsob), during the drought cycles. In the humid cycles and those following, there is a groundwater contribution to maintaining river flow during summers.

- According to the physical, morphological features and to the soil occupation, the reaction of the three rivers is torrential and occurs in very short laps of time, especially while occurring after a long drought period.
- The decrease of the mean annual amount of rainfall generally causes a significant decrease in the outflow of watershed. The inter-annual variability is also immediately reflected on river flow.
- Humid cycles contribute highly to the reconstitution of water resources (groundwater and surface water).

## PRESENTATION, CADRE GEOLOGIQUE, STRUCTURAL ET HYDROLOGIQUE

Le secteur de l'étude (Fig. 1) appartient au Bassin Synclinal d'Essaouira-Chichaoua (Ambroggi, 1963 ; Roch, 1930 ; Duffaud, 1960 ; Duffaud *et al.*, 1966 et Ettachfini, 1992). Il constitue la terminaison extrême ouest du flanc nord du Haut Atlas Occidental. Son climat est du type semi-aride à hiver tempéré avec une moyenne des précipitations de l'ordre de 315 mm/an (Fekri, 1993, Jalal, 2001, Mennani, 2001, Laftouhi, 1991, Laftouhi, 2002).

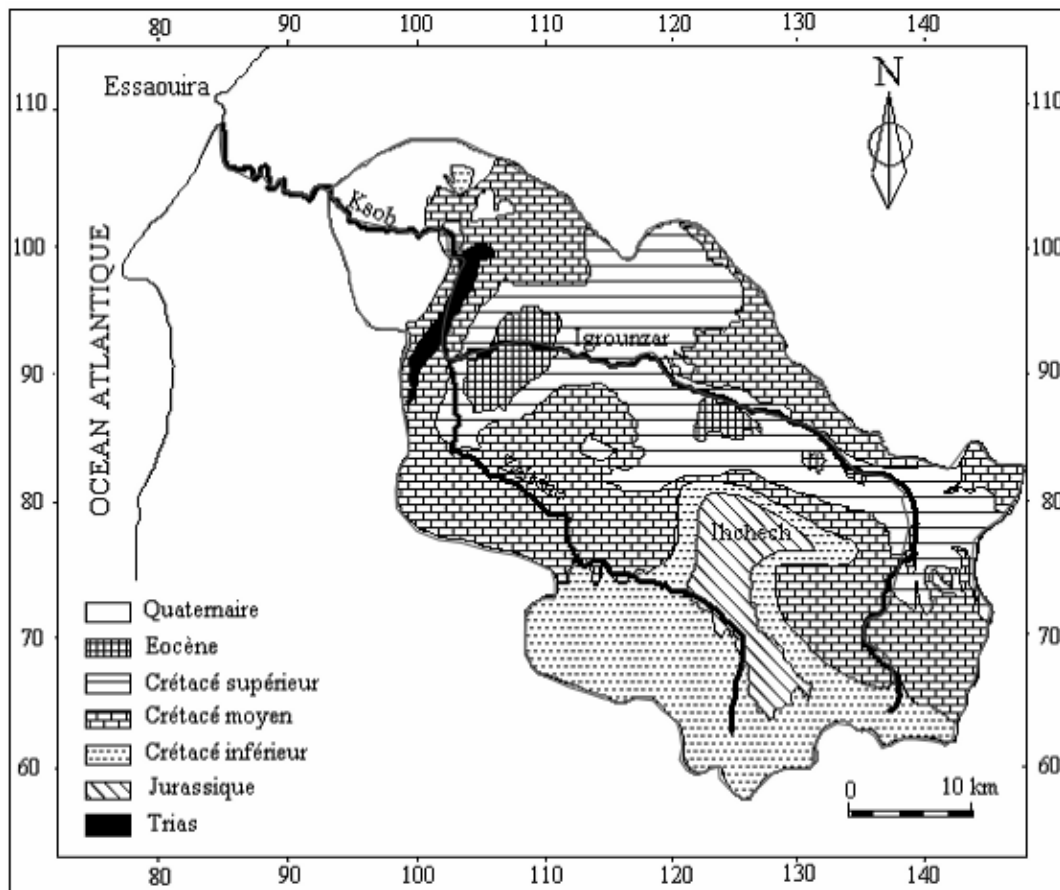


Fig. 1: Secteur de l'étude, cadre géologique et géographique.

Géologiquement, les terrains en affleurement (Fig. 1) sont représentés par le Jurassique terminal, le Crétacé Inférieur sommital (Vraconien), Moyen (Cénomaniens) et Supérieur (Turonien et Sénonien) avec quelques affleurements Eocènes au cœur des unités synclinales. La série se termine par du Plio-quaternaire, sous forme de dunes de sables consolidés ou non, dans la frange côtière. L'ensemble étant perturbé localement par un trait morpho-tectonique particulier ; le diapirisme ayant pour origine les argiles salifères du Trias plus profond. L'histoire tectonique du secteur est complexe. En effet, l'aspect actuel de la zone est le résultat de l'orogénèse alpine (atlasique) avec des directions de raccourcissement N120 à N140 et des directions d'allongement conjuguées. Cette orogénèse a réactivé les anciennes

structures héritées de l'orogénèse hercynienne (raccourcissements méridiens et allongements E-W) en structures inverses.

Le bassin du Qsob constitue la terminaison du Haut Atlas Occidental. Il est représenté par des collines basses à tête arrondie, entaillées par un réseau hydrographique (Fig. 2) généralement peu profond, parfois encaissé. Le bassin est subdivisé en trois sous bassins qui sont : le sous-bassin de l'Igrounzar au nord, du Zelten au sud et du Bas Qsob en aval. Ce dernier est en fait le résultat de la confluence des deux autres à la station dite de Zerrar à l'entrée du diapir de Tidzi.

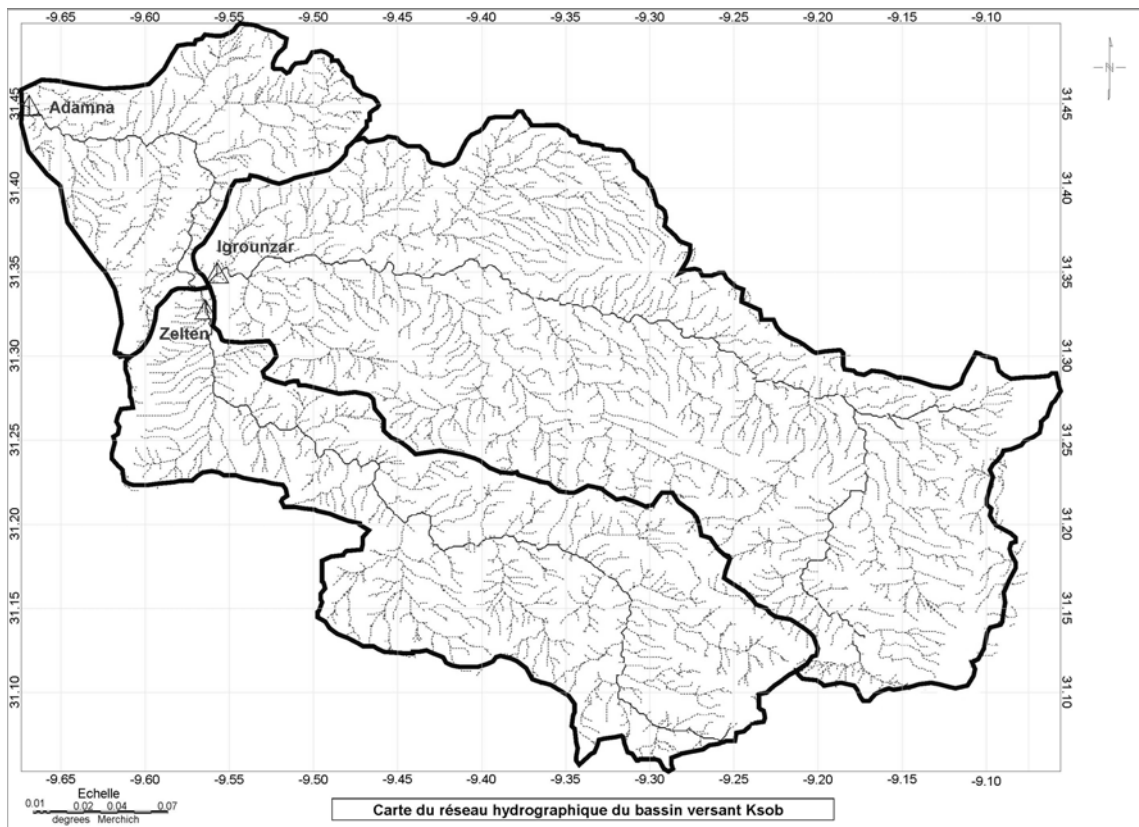


Fig. 2: Carte du réseau hydrographique du Qsob.

Le Jurassique plus prépondérant dans le sous bassin du Zeltene est caractérisé par une dominance des formations plutôt étanches (marnes argiles rouges, etc.). Les formations carbonatées du Crétacé, d'extension spatiale fort dominante, représentent à peu près de 50% de la superficie du Zeltene et presque 85% de celle d'Igrounzar. Il s'agit de calcaires dolomitiques, calcaires marneux et de marno-calcaires et marnes calcaires très fracturés à karstiques. L'Eocène affleure dans la partie médiane du bassin versant, spécialement dans le sous-bassin d'Igrounzar. Il s'agit de formations détritiques généralement en relief. Le Plio-quadernaire affleure uniquement dans la partie aval du Qsob.

La géologie particulière du bassin du Qsob, caractérisée essentiellement par des terrains peu perméables sur d'immenses étendues, associée à ses propriétés physiques relativement accidentées, confèrent à ses écoulements un caractère souvent torrentiel avec de faibles écoulements de base issus des aquifères renfermés dans les formations longeant le son cours principal.

## CARACTERISTIQUES PHYSIQUES

En règle générale, le bassin versant global du Qsob, défini à la station de Adamna (Fig. 2) possède une forme relativement allongée et s'étend sur une direction principale du sud-est vers le nord-ouest. Les deux sous-bassins, Zeltene et Igrounzar bénéficient grossièrement de la même allure. Les principales caractéristiques physiques de ces bassins sont résumées dans le tableau 1 ci-dessous (Laftouhi, 2002). Les trois bassins possèdent une forme allongée (indices de compacité supérieurs à 1). L'écart absolu des

altitudes généralement supérieures à 750 m et voisines de 1000 m, traduirait une morphologie relativement accidentée. La superficie de l'Igrounzar est voisine du double de celle du Zeltene. La pente moyenne au sein du Zeltene est une fois et demie plus forte que celle d'Igrounzar qui reste en moyenne proche de celle du Qsob à Adamna.

L'hypsométrie du bassin (Fig. 3) est relativement accidentée dans les parties amont et médianes et s'estompe vers les parties aval à l'approche de l'exutoire naturel du système situé à quelques 2 km au sud d'Essaouira.

Tab. 1: Principales caractéristiques physiques du bassin versant du Qsob.

Paramètres	Igrounzar	Zeltene	Qsob à Adamna
Superficie (km <sup>2</sup> )	847	439	1479
Périmètre (km)	148	99	246
Indice de compacité $K_c$	1.424	1.323	1.791
Altitude moyenne (m)	1200	1400	1100
Altitude minimale (m)	245	246	76
Altitude maximale (m)	1694	1620	1694
Ecart des altitudes	920	770	960
Indice global de pente	15.6	20.2	8.9
Pente moyenne	0.018	0.026	0.017
Longueur du cours principal (km)	66	54	161
Dénivelée spécifique	463	421	354

Tab. 2: Coordonnées des stations hydrologiques du Qsob.

Coordonnées		Adamna N°IRE 111/51	Igrounzar N°IRE 400/52	Zeltene N°IRE 401/52
	X	092.650	103.500	103.300
	Y	104.200	091.200	90.650
	Z	080.00	260.00	210
Date de mise en service	Juillet 1970	Septembre 1965	Avril 1975	

Tab. 3: Paramètres statistiques des séries d'observations de pluie et débits.

Station	Igrounzar		Adamna		Zeltene	
	Q (m <sup>3</sup> /s)	P (mm)	Q (m <sup>3</sup> /s)	P (mm)	Q (m <sup>3</sup> /s)	P (mm)
Minimum	0.00	0.00	0.00	0.00	0.00	0.00
Maximum	44.40	285.00	476.00	100.00	144.00	285.00
Moyenne	0.32	0.93	1.34	0.87	0.43	0.93
Variance	1.68	37.98	115.66	21.57	12.90	37.98
Ecart type	1.29	6.16	10.75	4.64	3.59	6.16

Tab. 4: Cycles hydrologiques représentatifs des trois stations.

Station	Moyenne (mm)	Min (mm)	Max (mm)	cycle sec	cycle Humide	cycle moyen
Igrounzar et Zeltene	331.87	134.8	823.4	1986/87	1985/86	1990/91
Adamna	326.47	131.6	756.5	1986/87	1995/96	1990/91

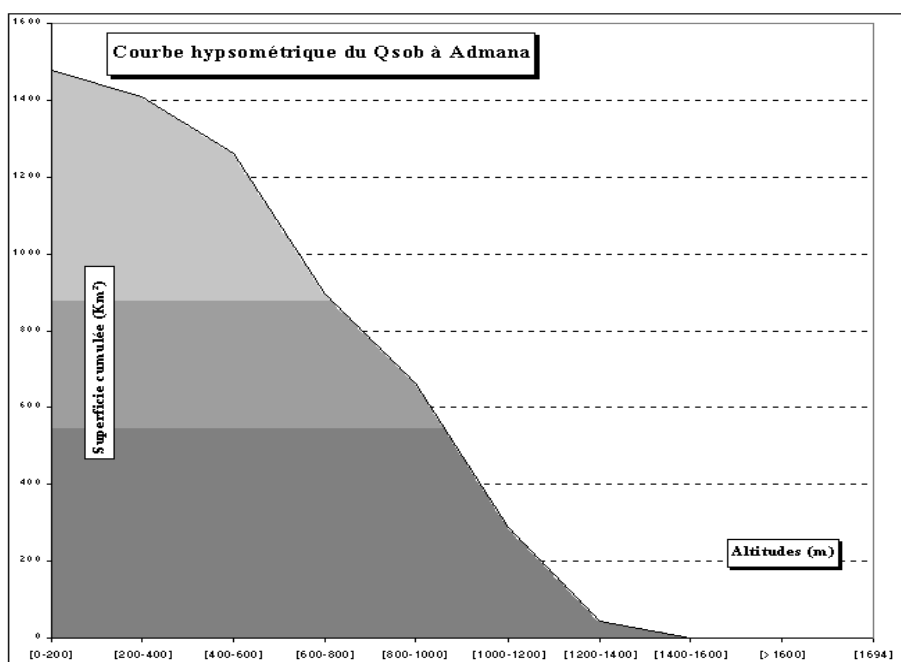


Fig. 3: Hypsométrie du Qsob et de ses sous bassins.

## OCCUPATION DES SOLS

L'occupation des sols est assez sommaire. Elle se résume en gros à trois types de couverts ; (1) des cultures (céréaliculture) sur les terrains marneux d'âge crétacé, sur le Plio-Quaternaire et l'Eocène, (2) des terrains nus correspondant aux affleurements des dalles calcaires fissurées et karstiques du Crétacé et aux formations jurassiques et (3) des forêts (résineux) dans la partie aval du bassin versant sur les terrains d'âge plio-quaternaire et sur les renforts montagneux du Haut Atlas Occidental. Les zones urbanisées sont quasi inexistantes au sein des trois bassins si ce n'est quelques chefs-lieux de communes où les infrastructures susceptibles d'influencer le ruissellement sont très réduites

A l'instar de toutes les régions défavorisées du Royaume, le bassin du Qsob est lui aussi soumis à un déboisement intensif (bois de chauffe et de cuisson).

## DONNEES DISPONIBLES

Celles-ci proviennent de trois stations de surveillance (Tab. 2) appartenant à l'Administration Générale de l'Hydraulique AGH et suivies par l'Agence du Bassin Hydraulique du Tensift. La mise en œuvre de ces stations s'est inscrite dans le cadre de l'évaluation du potentiel hydrique du bassin du Qsob afin de réaliser un barrage pour améliorer l'approvisionnement en eau potable d'Essaouira et des chefs-lieux des centres périurbains et ruraux.

Les données disponibles utilisées dans le cadre de la présente étude portent sur les séries de pluies quotidiennes (mm) pour les stations Adamna et Igrounzar, et de débit moyen quotidiens ( $m^3/s$ ) pour les trois stations considérées (Zeltene et Igrounzar sont distantes de moins de 500 m).

Ces stations sont équipées d'outillage pour la mesure des hauteurs limnimétriques, d'équipements de mesure de la température et des précipitations. La station Adamna est en outre équipée de téléphérique et de moulinet pour la mesure du débit pendant les crues.

A Igrounzar, les données de pluie quotidiennes disponibles commencent régulièrement depuis mars 1969 et continuent à nos jours. Les données de débits quotidiens sont disponibles depuis le début de Septembre 1965. Parallèlement à ces relevés quotidiens, d'autres relevés relatifs aux crues exceptionnelles, bien que très peu nombreux, sont disponibles. A Adamna, les données de pluie disponibles commencent vont de septembre 1977 à nos jours, alors que les données de débits ont commencé depuis juillet 1970.

## EXPLOITATION DES DONNEES

Depuis le début des suivis respectifs, les séries de données montrent une grande variabilité dans le temps. Cette variabilité s'exprime également au cours d'un même cycle hydrologique en fonction des saisons. Le tableau 3 résume les paramètres statistiques de position des séries de données pluviométriques et de débit pour les trois stations.

L'exploitation des données a consisté en la recherche d'une relation de cause à effet entre les précipitations et les débits produits au niveau des trois stations de contrôle et pour des périodes similaires. Ceci a été rendu possible par la confrontation sur un même axe de temps des données de pluie (la cause) à celles de débit (l'effet). Pour illustrer cette relation étroite entre pluie et débit, le choix a été porté essentiellement sur des cycles représentant respectivement des années hydrologiques moyennes, humides et sèches (moins pluvieuses). La définition d'année hydrologique sèche moyenne ou humide est faite par comparaison avec les statistiques des séries des deux stations Igrounzar et Adamna (Tab. 4 ci-dessous).

## DISCUSSIONS ET RESULTATS

### Le régime fluvial du Qsob et des sous bassins

#### Les cycles hydrologiquement déficitaires

Les Fig. 4 et 5 sont relatives au cycle hydrologique de 1986/87 particulièrement déficitaire en précipitation. Elles montrent l'effet des précipitations sur les écoulements de surface aux trois stations. De prime abord, il apparaît clairement que les pics de pluie (bord supérieur des figures) coïncident parfaitement avec les pics d'écoulements. En dehors des périodes de pluie, les écoulements se ramènent à leur plus bas niveau, voire même s'annulent. Ainsi, pour les stations de Zeltene, les pics de pluie et de débit sont superposés et relativement proportionnels. La quantité d'eau produite par ces averses reste limitée aussi bien dans le temps qu'en volumes. Les écoulements ont cessé dès mars 87. Alors que la crue la plus importante (11 février 87) n'a produit qu'une pointe de crue de quelques  $22 \text{ m}^3/\text{s}$ . Tandis qu'à Igrounzar (pour le même cycle), des écoulements bien que très faibles, ont été enregistrés. Ils sont restés la plupart du temps autour de  $0.1$  à  $0.2 \text{ m}^3/\text{s}$ . Avec un débit d'étiage autour de  $0.077 \text{ m}^3/\text{s}$ .

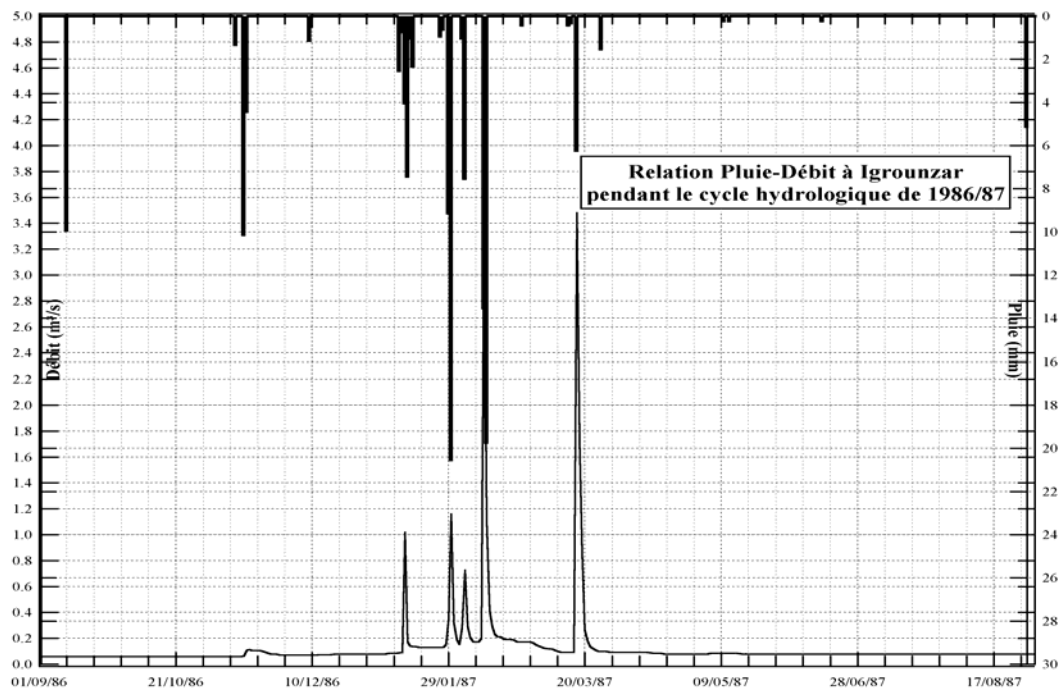


Fig. 4: Relation pluie-débit à la station Igrounzar pendant le cycle hydrologique de 1986/87.

Les pics de pluie coïncident parfaitement avec ceux des écoulements. On note même une décré progressive après chaque événement pluvieux. Pour la station d'Adamna, la Fig. 5 montre que la pointe de crue de 44 m<sup>3</sup>/s intervenue le 02/01/1987, n'a apparemment pas été précédée par une averse importante (en terme de hauteur) alors que d'un autre côté, l'averse suivante du 28/01/1987 (d'une hauteur totale de 15.8 mm), n'a générée qu'une pointe de crue de 16.3 m<sup>3</sup>/s et cela deux jours plus tard.

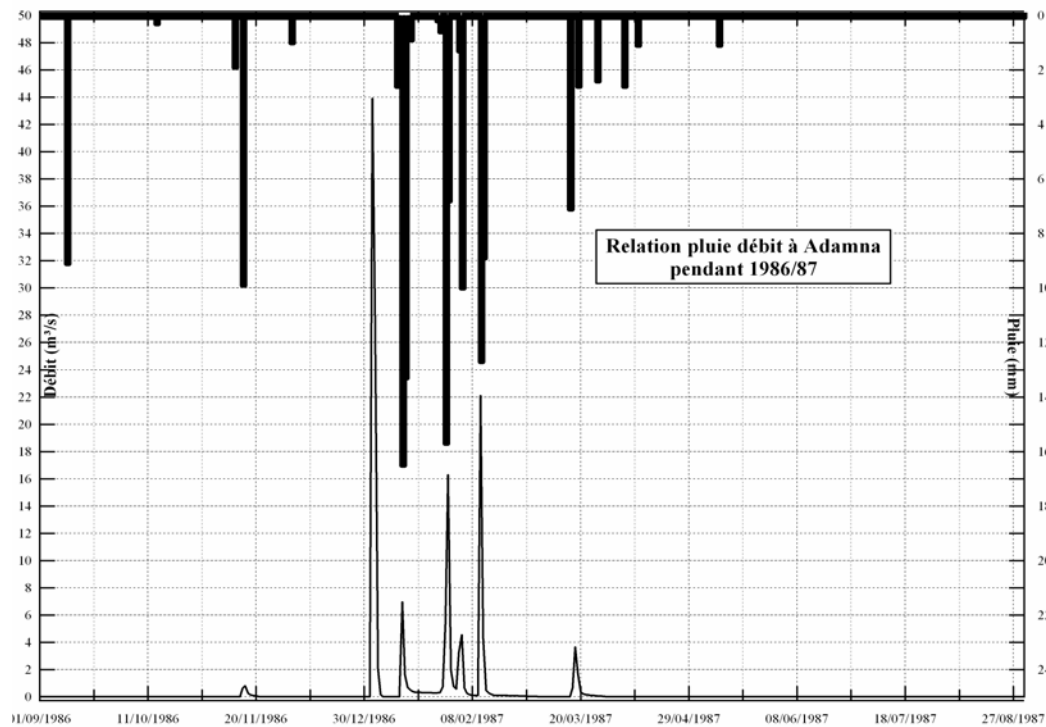


Fig. 5: Relation pluie-débit à la station Adamna pendant le cycle hydrologique de 1986/87.

### Les cycles humides

Les cycles humides choisis sont respectivement 1985/86 à Zeltene et Igrounzar et 1995/96 à Adamna. A Igrounzar (et Zeltene), il a été enregistré un total de 823 mm et à Adamna 756 mm.

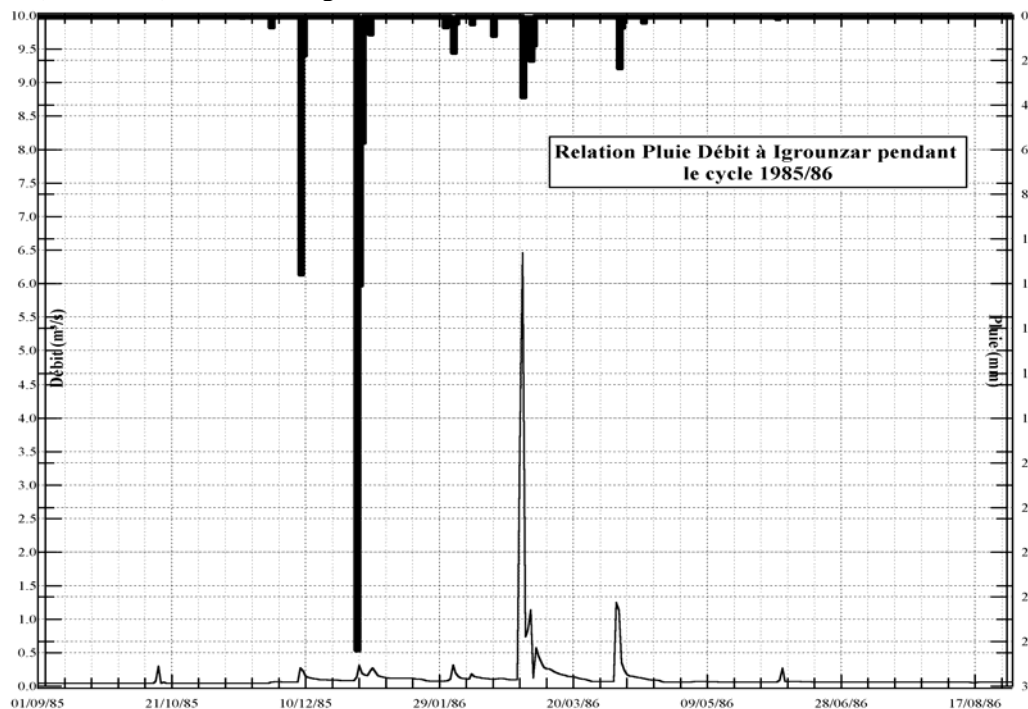


Fig. 6: Relation pluie-débit à Zeltene pendant le cycle hydrologique humide de 1985/86.

A Zeltene, la Fig. 6, montre une coïncidence parfaite entre pics pluviométrique et d'écoulement.

Cependant, ils ne sont pas proportionnels. En effet, le pic de pluie de fin décembre 85-début janvier 86 (30 mm environ) n'a apparemment pas produit beaucoup d'écoulements tandis que celui survenu en février 86 qui n'a enregistré que 35 mm, a produit une pointe de crue beaucoup plus importante (26 m<sup>3</sup>/s). Les débits sont restés en général bien en dessous du m<sup>3</sup>/s. A Igrounzar (Fig. 7), on enregistre un comportement similaire à celui de Zeltene ; c'est à dire, le pic de pluie du 28 décembre 85 (285 mm) n'a produit que peu de variation dans les écoulements tandis que celui survenu le 28 février 86 qui n'a enregistré que 37.6 mm, a produit une pointe de crue beaucoup plus importante (6.5 m<sup>3</sup>/s). Les débits sont restés en général bien en dessous du m<sup>3</sup>/s.

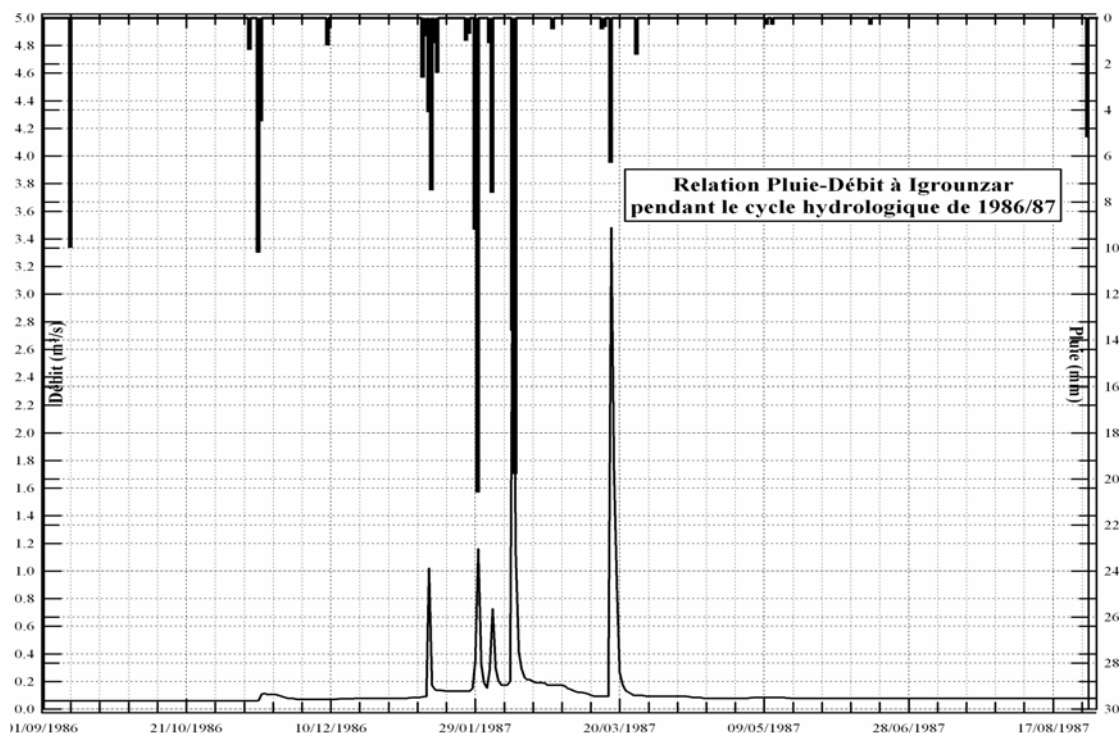


Fig. 7: Relation pluie-débit à Igrounzar pendant le cycle hydrologique humide de 1985/86.

A Adamna, le cycle hydrologique de 1995/96 a été particulièrement humide et a enregistré 756 mm. Les précipitations antérieures à décembre 95 n'ont pas généré de pointe de crue notable. Tandis qu'à partir de cette date, la succession d'événements pluvieux relativement rapprochés pendant la période humide de l'année, a entraîné des crues très importantes dont la plus remarquable est celle du 22 janvier 96 avec 476 m<sup>3</sup>/s pour une précipitation de 100 mm ayant survécu le 21/01/96 suivi le 22/01/96 de 80 mm. Il serait alors possible de dire qu'un tel type d'averses est en mesure de produire d'importants écoulements dans un bassin de la dimension du Qsob à Adamna.

### Les cycles moyens

Comme cycle moyen, le choix a été arbitrairement porté sur celui de 1990/91 qui a enregistré une pluie totale de 339.6 mm à Adamna et 351.7 mm à Igrounzar.

La Fig. 8 montre qu'en décembre 1990 à Adamna, la succession d'épisodes pluvieux croissants a fini par produire une pointe de crue de 28.3 m<sup>3</sup>/s qui a fait suite à une période de sécheresse prolongée (été et automne 1990). Pendant l'hiver et le printemps 1991, deux crues importantes ont été enregistrées et ont atteint 113 et 134 m<sup>3</sup>/s respectivement le 19/02/91 et le 07/03/1991. En dehors de ces périodes, les écoulements ont été réduits si non nuls.

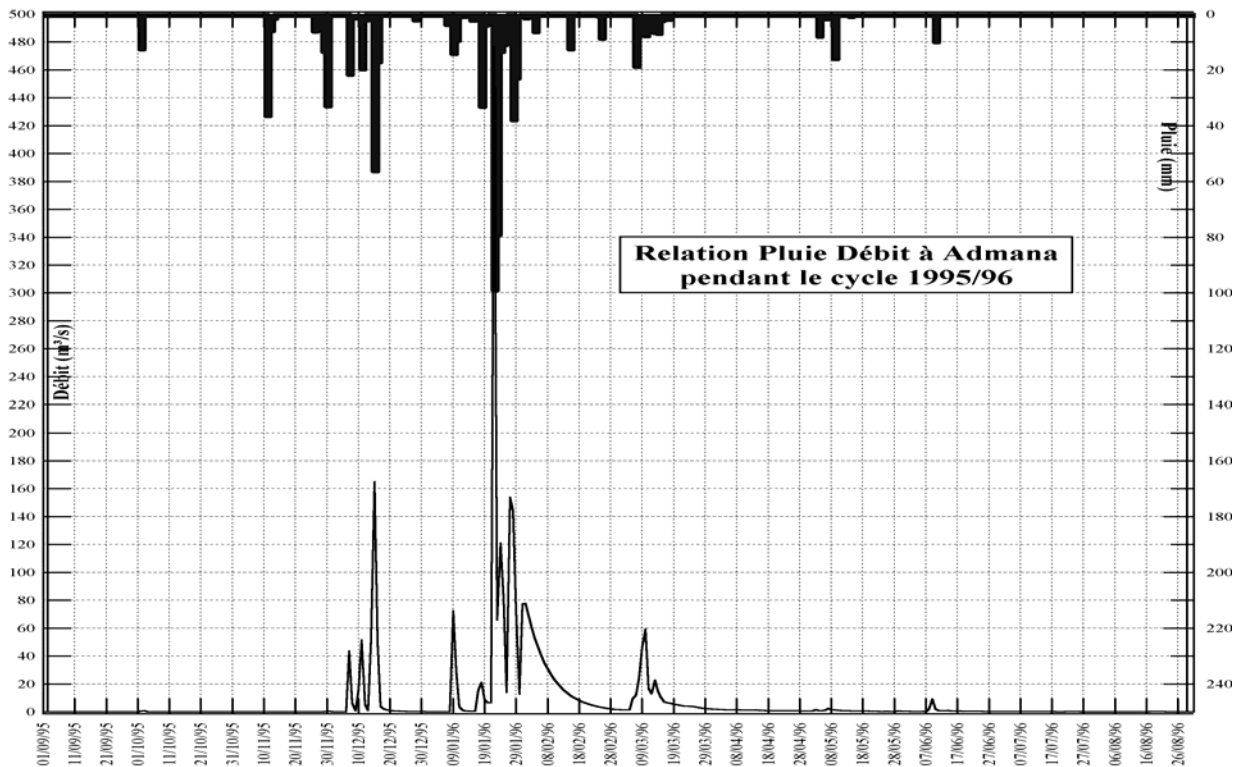


Fig. 8: Relation pluie-débit à la station Adamna pendant le cycle hydrologique humide de 1995/96.

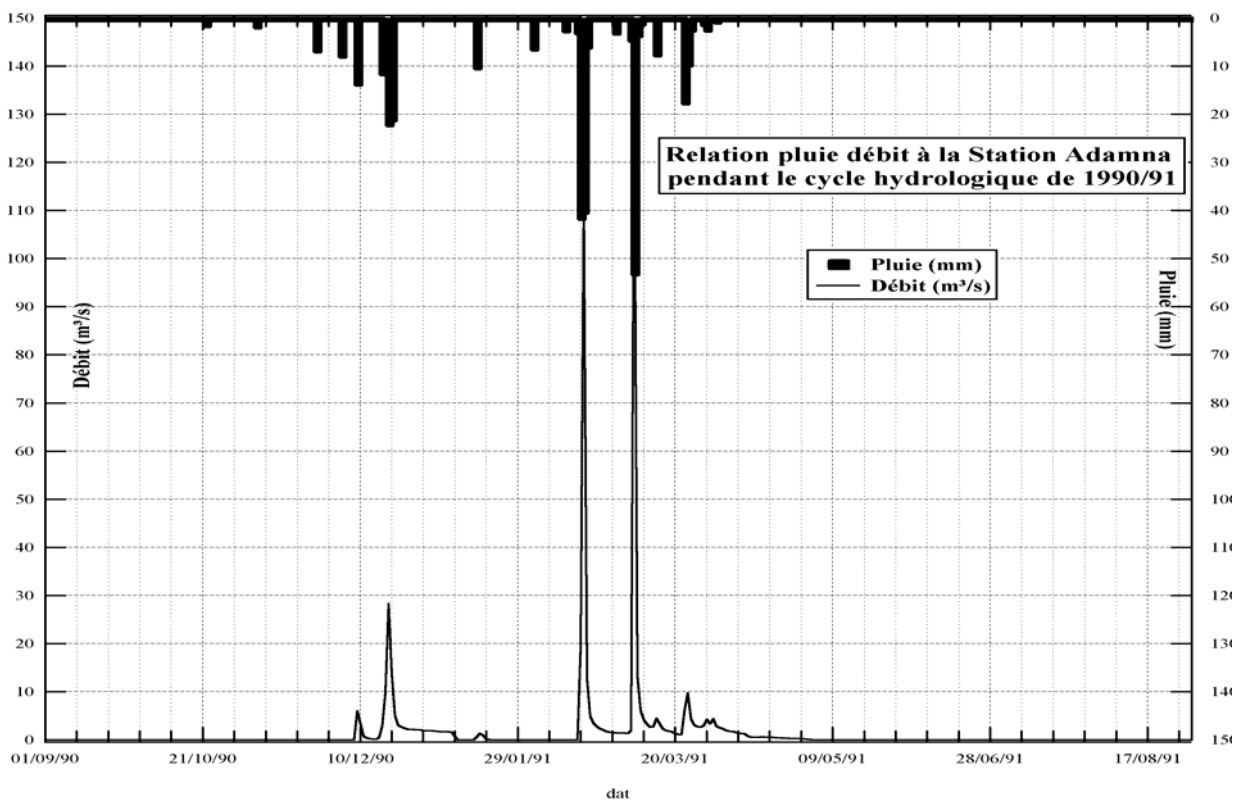


Fig. 9: Relation pluie-débit à la station Adamna pendant le cycle hydrologique de 1990/91.

A Igrounzar (Fig. 9), le cycle 1990/91 a connu une absence quasi généralisée des écoulements pendant l'automne 1990 et une grande partie de l'hiver 90/91 et cela malgré l'occurrence de phénomènes pluvieux ayant dépassé les 10 à 15 mm/jour. Ce n'est qu'entre le 16 et 19/02/1991, qu'une averse de près de 100 mm a résulté en un écoulement qui a approché les 13.5 m<sup>3</sup>/s. Les écoulements sont restés constants

(environ  $0.06 \text{ m}^3/\text{s}$ ) à partir de fin mai 1991. A Zeltene (Fig. 10), le comportement est resté pratiquement identique à celui d'Igrounzar avec cependant une toute légère différence au niveau des valeurs des débits moyens quotidiens (débit d'étiage de l'ordre de  $0.07 \text{ m}^3/\text{s}$ ).

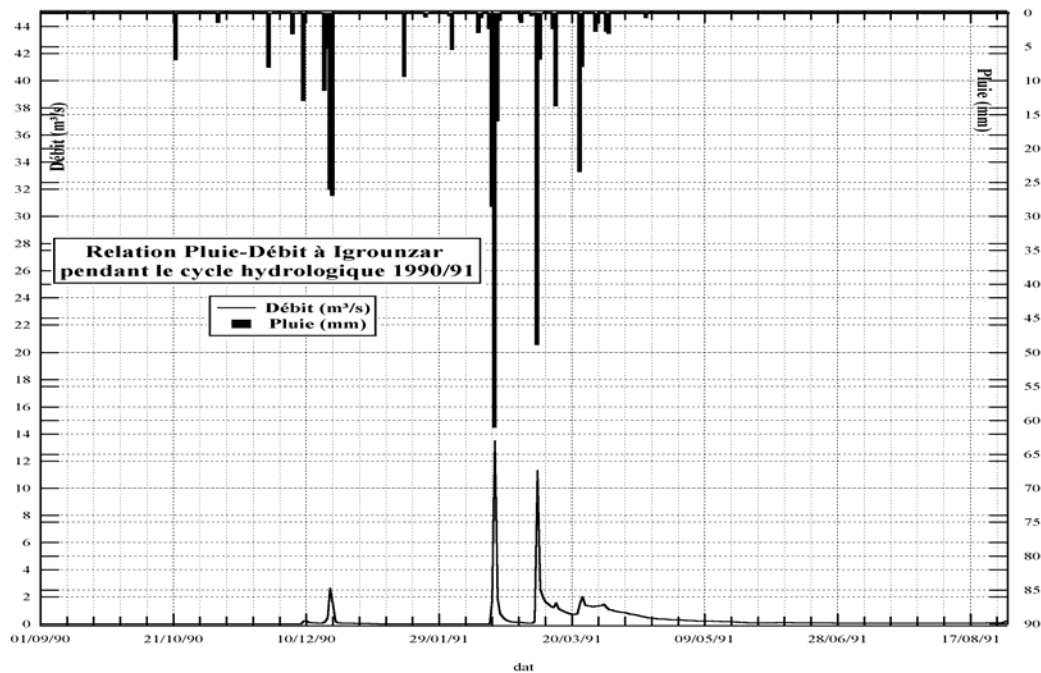


Fig. 10: Relation pluie-débit à la station Igrounzar pendant le cycle hydrologique de 1990/91.

L'exemple particulier du cycle humide de 1995/96 à Igrounzar (Fig. 11), avec un total de 707 mm, montre au contraire de nombreuses averses répétées et successives. Toutefois, la variation des débits, surtout en hiver et printemps, n'obéit pas à la règle générale (pointe de pluie, pointe de crue). L'évolution des débits est progressive mais très lente et s'opère sur les deux saisons. La décrue et le tarissement sont cependant brusques avec un retour à un débit d'étiage de l'ordre de  $0.75 \text{ m}^3/\text{s}$ . Cette valeur est exceptionnelle, mais au regard à la valeur et distribution des pluies, ceci semble normal. Il y a une composante eaux souterraines qui soutient les écoulements à Igrounzar pendant tout l'étiage.

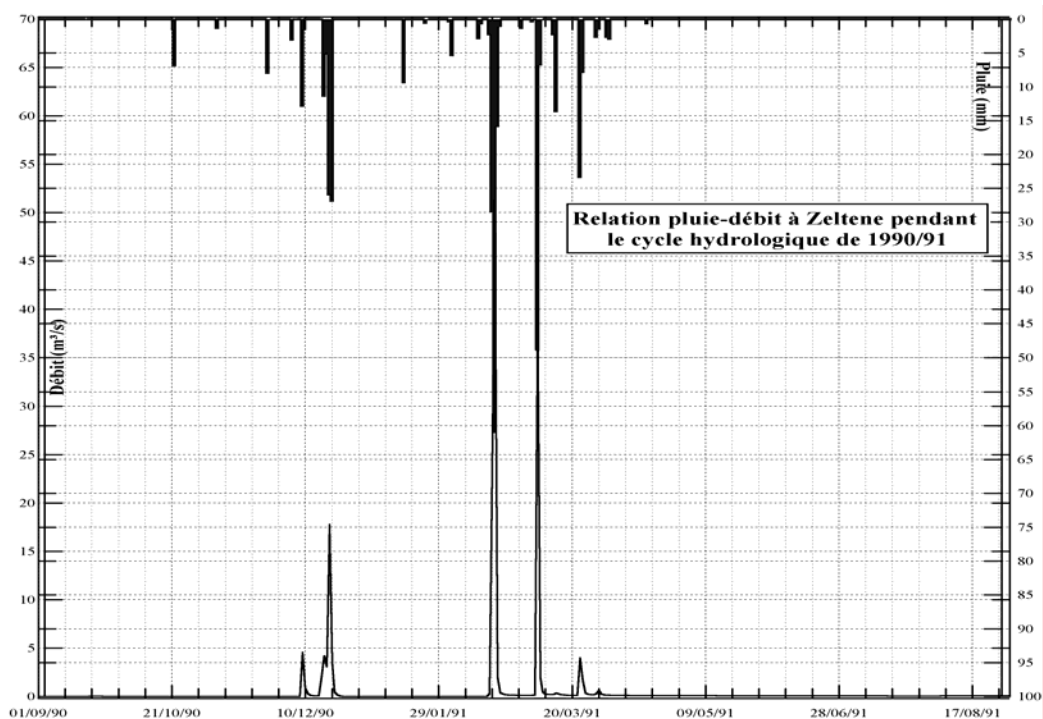


Fig. 11: Relation pluie-débit à la station Zeltene pendant le cycle hydrologique de 1990/91.

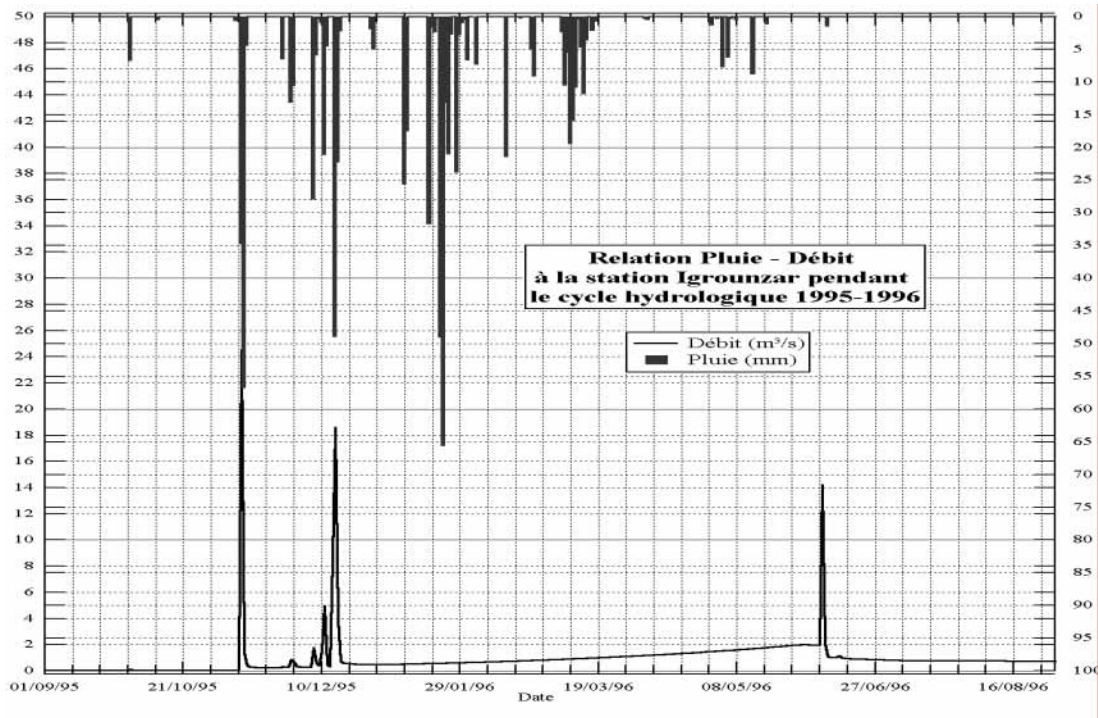


Fig. 12: Pluie débit pendant le cycle hydrologique particulier de 1995/96 à Igrounzar.

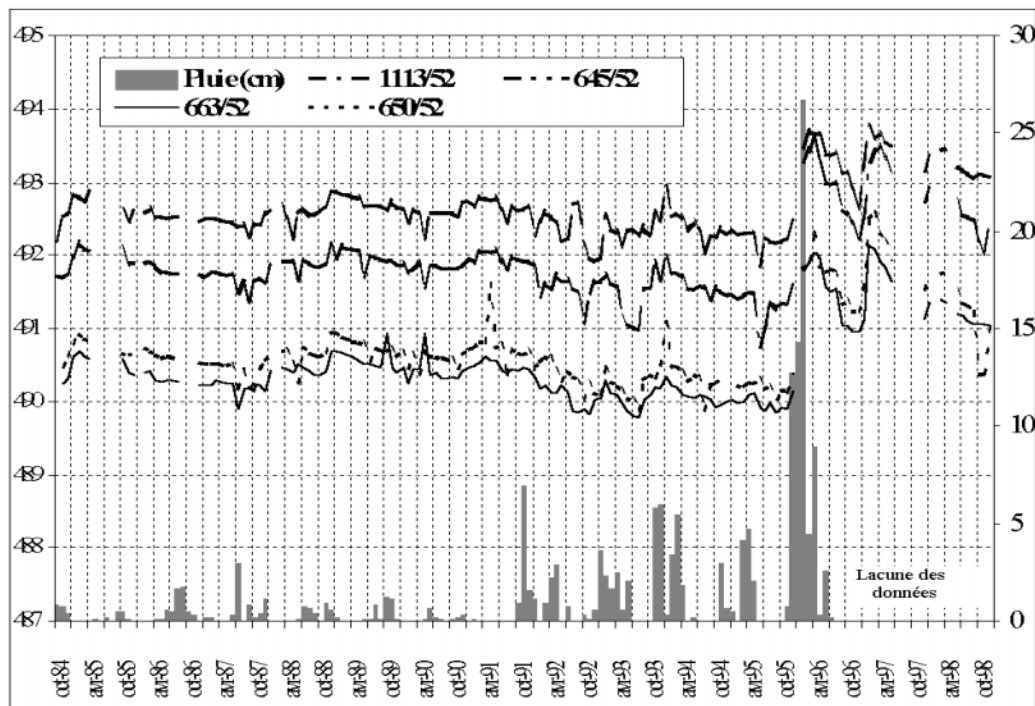


Fig. 13 : Relation pluie- niveau piézométrique dans quelques points de contrôle.

## DISCUSSION

Ainsi donc, que ce soit en année moyenne ou en année extrême, il ressort que les précipitations sont le moteur principal des écoulements aux exutoires d'Igrounzar, de Zeltene et du Qsob à Adamna. Plusieurs remarques concernant la relation pluie-débit ont été relevées :

Les pointes de crues constituent la conséquence d'évènements pluvieux, avec un décalage plus ou moins important. Elles interviennent en règle générale soit le lendemain soit deux jours plus tard. Ceci peut s'expliquer par un temps de concentration de chaque bassin versant plus ou moins long en fonction de la

longueur du cours principal, du lieu où est intervenue la précipitation, des conditions d'humidité initiale du bassin versant (El Idrissi, 1996), ayant prévalu aux averses, des conditions lithologiques du bassin versant et enfin de l'occupation des sols (Révéniéras, 1976, Saidi, 1995).

Les bassins versants ne réagissent pas systématiquement de la même manière, ni au même timing aux épisodes pluvieux. Il faut dire que ceux-ci, malgré la faible distance de 17 km qui sépare Adamna (à l'ouest) d'Igrounzar (plus à l'est), ne sont ni simultanés ni similaires.

Certains épisodes pluvieux, malgré leur volume important, surtout ceux du début du cycle hydrologique, ne génèrent pratiquement pas d'écoulement. En absence de données sur l'intensité de ces épisodes, il paraît spéculatif à ce niveau de renier leur effet. Ce qui corrobore cette thèse, c'est que d'autres épisodes bien moins importants (toujours en terme de lame précipitée) produisent des pointes de crues importantes. Mais, d'une manière presque générale, ces derniers interviennent après les premiers, autrement dit, les conditions d'humidité initiale des terrains du bassin versant ont été modifiées par les premières précipitations. Ce qui favorise la genèse d'écoulements vers les exutoires.

Les crues sont généralement très brusques et disparaissent également très vite en raison notamment des propriétés physiques des bassins versants (Laftouhi, 2002). En effet, ceux-ci se présentent sous forme de cuvettes à bords redressés avec des pentes moyennes relativement fortes.

Par ailleurs, les lithologies des bassins versants sont dominées par les marnes et marno-calcaires peu perméables principalement dans les parties amont.

En outre, les trois bassins versants connaissent une longue période de sécheresse qui s'étale généralement de fin mai à novembre (sauf exception). Pendant cette période, les écoulements que l'on devrait qualifier d'étiage, sont la plupart des temps nuls pour Zeltene, nuls à extrêmement faibles pour Igrounzar et Adamna.

La combinaison de tous ces paramètres fait que les crues de début de saison pluvieuse sont généralement torrentielles alors que celles du milieu de saison (fin hiver et printemps), bien que quelque peu torrentielles, laissent des résidus d'écoulement (tarissement) assez remarquables.

### **Impact sur les eaux souterraines**

La corrélation entre pluies et niveaux piézométriques observée dans une batterie de piézomètres de contrôle installée à cet effet à travers la zone d'étude (Fig. 13) montre une influence nette de la baisse du régime des pluies sur les ressources en eau souterraines. Cependant, les cycles hydrologiquement généreux sont en mesure de rétablir les niveaux des nappes aquifères (exemple du cycle 1995/96). Ce comportement et ces réactions quasi instantanés du système aquifère sont liés à son caractère karstique, ce qui atteste de sa vulnérabilité aussi bien à la recharge (sécheresse) qu'aux pollutions éventuelles.

## **CONCLUSION ET PERSPECTIVES**

Malgré son aspect qualitatif, cette étude a permis de déceler l'existence d'une relation de cause à effet entre les paramètres climatiques (la pluviométrie) et les ressources en eau de surface et souterraines. Elle ouvre cependant les perspectives sur des études détaillées, aussi bien sur des bassins de dimension similaire, que sur des bassins plus grands et dans d'autres latitudes, en prenant en considération la dimension anthropique dans l'évolution des ressources en eau. Ces études déboucheraient sur l'outil modélisation hydrologique dans un objectif de prévision des ressources (sous différents scénarii) à des horizons à moyen et long terme.

## **REFERENCES**

- Ambroggi, R. (1963) *Etude géologique de versant méridional du Haut Atlas Occidental et de la plaine du Souss*. Notes et Mémoires du Service Géologique du Maroc n° 15, 7, 321 p.
- Duffaud, F. (1960) Contribution à l'étude stratigraphique du bassin du Haut Atlas Occidental (Maroc). *Bull. Soc. Géol. de France*, 7, 2, 728-734.
- Duffaud, F., Brun, L. and Fontbote, J.M. (1966) Le bassin du Sud-Ouest marocain. In Reyre D.: *Bassins sédimentaires du littoral africain*. Sympo. New Delhi, Publ. Assoc. Serv. Géol. Afr. Paris, 5-26.

- El Idrissi, A. (1996) *Effet de l'humidité initiale du sol sur le processus de ruissellement à l'échelle de la parcelle et du bassin versant*. Thèse de Doctorat AGRO/SNAP - Institut des sciences naturelles appliquées.
- Ettachfni, E.M. (1992) *Le Vraconien, Cénomaniens et Turonien du bassin d'Essaouira (Haut Atlas Occidental, Maroc). Analyse lithologique, biostratigraphique et sédimentologique, stratigraphie séquentielle*. Thèse d'Université Toulouse.
- Fekri, A. (1993) *Contribution à l'étude hydrogéologique et hydrochimique de la zone synclinale d'Essaouira (Bassin synclinal d'Essaouira - Maroc)*. Thèse de 3ème cycle. UCAM Marrakech, Maroc.
- Jalal, M. (2001) *Potentialités hydrogéologiques du Cénomaniens du Bassin Synclinal de Meskala-Kourimat-Ida Ou Zemzem (Essaouira Maroc)*. Doctorat de l'Université Cadi Ayad de Marrakech, Maroc.
- Laftouhi, N. (1991) *Hydrogéologie et hydrogéochimie de l'aquifère Turonien du bassin synclinal de Meskala-Kourimat Ida Ou Zemzem (Essaouira-Maroc)*. Thèse 3ème cycle. UCAM. Marrakech, Maroc.
- Laftouhi, N. (2002) *Hydrologie, Hydrogéologie et hydrogéochimie de la série carbonatée du Crétacé Moyen et Supérieur du Bassin Synclinal de Meskala-Kourimat-Ida Ou Zemzem (Essaouira-Maroc)*. Thèse de Doctorat d'Etat. UCAM Marrakech, Maroc.
- Mennani, A. (2001) *Apports de l'hydrochimie et de l'isotopie à la connaissance du fonctionnement des aquifères de la zone côtière d'Essaouira (Maroc Occidental)*. Doctorat de l'Université Cadi Ayad de Marrakech, Maroc.
- Réméniéras, G. (1976) *L'Hydrologie de l'Ingénieur*. Eyrolles, 1976, 2nde édition.
- Roch, (1930) *Carte géologique provisoire la zone synclinale de Mogador au 1/200.000*. Notes and Memoires du Service des Mines et Carte Géol. Du Maroc, n° 11.
- Saidi, M. E. (1995) *Contribution à l'hydrologie profonde et superficielle du bassin du Souss (Maroc) : Climatologie, hydrogéologie, crues et bilans hydrologiques en milieu sub aride*. Thèse de Doctorat. Paris-Sorbonne, 197 p.

# LOW FLOW AND DROUGHT STUDIES – THE NORTHERN EUROPEAN (NE) FRIEND EXPERIENCE

**Lena M. TALLAKSEN**

Department of Geosciences, University of Oslo, Norway

*lena.tallaksen@geo.uio.no*

**Siegfried DEMUTH**

IHP/HWRP Secretariat, Federal Institute of Hydrology, Koblenz, Germany

**Henny A.J. VAN LANEN**

Subdepartment of Water Resources, Wageningen University, the Netherlands

## ABSTRACT

The primary objective of the NE-FRIEND Low Flow group has been to characterise the regional behaviour of low flow and drought and to identify the main governing factors at different scales. Focus has been on definitions, extreme characteristics, process understanding, anthropogenic impacts, estimation at the ungauged site, variability in time and space, and synoptic behaviour across Europe. Common to many of the studies is the use of the threshold level method to define drought events from time series of hydrological variables. Two recent pan-European initiatives have been undertaken within the framework of the FRIEND project, the EU-supported ARIDE project, focusing on the spatial and temporal variability of drought in Europe, and the ASTHyDA project aiming at disseminating knowledge on hydrological drought. Scientific achievements as well as dissemination and training activities are summarized in this paper, including the establishment of the European Drought Centre, a virtual centre of European drought research and management organisations.

**Keywords:** low flow; drought; Europe; FRIEND; European Drought Centre

## INTRODUCTION

The Northern European (NE) FRIEND project, a contribution to UNESCO's International Hydrological Programme (IHP), aims to improve the understanding of hydrological variability and similarity across time and space. To achieve this at the European scale it has been essential to carry out hydrological research across national boundaries. The work within the Low Flow group has ranged from statistical multivariate analysis at the regional and pan-European scale to physically based modelling studies at the catchment scale. Comparative analyses have been carried out using a consistent set of definitions and analysing tools, focusing on drought characteristics obtained from observed or simulated time series of streamflow and groundwater variables. Drought is considered a sustained and regionally extensive occurrence of below average natural water availability (Tallaksen and van Lanen, 2004). In other words, drought is seen as a relative and worldwide phenomenon relating a water shortage to what would normally be available in a region at a particular time (e.g. season).

Drought is a complex phenomenon with wide-ranging social, environmental and economic impacts, and drought research and operational applications, e.g. drought forecasting, have been lagging behind the development in flood-related areas. Drought as compared to flood differs in many ways. It develops slowly in time and space and will normally cover a larger area and extend for a longer time period than a flood event. Important aspects of a drought include the spatial extent of the event (climate control), the variability within the affected area (catchment control), the dynamics of the event (growth and decay) and possible recurrent patterns in space. Drought analysis thus often requires that transnational data are available. The NE-FRIEND database, the European Water Archive (EWA) and the FRIEND network have in this respect offered the NE Low Flow group a unique opportunity to study the regional behaviour of streamflow droughts by providing daily streamflow series from 29 countries across Europe. The EWA is considered to be the most comprehensive hydrological database in the world for the issues of low flows (Rees and Demuth, 2000). In addition, time series of precipitation and groundwater recharge, heads and discharge have been analysed for a more detailed process understanding in catchments covering a wide range of hydroclimatological regimes and hydrogeological conditions.

The primary cause of a drought is the lack of precipitation over a large area (meteorological drought). Combined with high evapotranspiration losses, the meteorological drought might give rise to a soil

moisture drought, and subsequently groundwater recharge and streamflow will be reduced causing a hydrological drought to develop. Groundwater is normally the last to react to a drought situation and in deep aquifers only the major meteorological droughts (or clusters of smaller droughts) will finally show up as a groundwater drought. The response in streamflow depends on the storage properties of the catchment and may reveal a high variability within a drought-affected area depending on the heterogeneity of the region. Streamflow variables encompass both low flow and deficit characteristics. Low flow characteristics are particularly suitable for characterising the hydrological regime, e.g. annual minimum series. A method that simultaneously characterises streamflow droughts in terms of deficit volume (severity) and duration is the threshold level method, which defines drought as a period during which the flow is below a certain threshold level. A sequence of drought events can subsequently be obtained from a time series of flow, e.g. streamflow and groundwater recharge and discharge (Hisdal *et al.*, 2004).

A major aim of the NE-FRIEND Low Flow group has been to promote collaboration and capacity building between scientists, operational hydrologists and advanced students working on low flow and drought topics. This has been achieved through the organisation of group meetings, workshops, training activities, student exchanges and by an extensive participation of the consortium at national and international conferences and workshops. Within the Low Flow group co-operation has in recent years evolved around smaller research groups, such as the Eastern European group and the European Union supported projects ARIDE and ASTHyDA. This paper presents these projects briefly, followed by selected examples of scientific achievements and dissemination activities. The paper concludes with recommendations for future research and the need to raise the general awareness of drought as a priority area in research and operational water management.

## RESEARCH AND NETWORK PROJECTS

### Eastern European group

The main objectives of the Eastern European group have been to exchange data and harmonise methods and tools for joint drought analysis across national borders. Common software has been developed, for instance NIZOWKA2003, which analyses drought events based on the threshold level method (Jakubowski and Radczuk, 2004). Focus has been on regional statistical methods, identification of factors influencing severe droughts and long-term fluctuations in time series of drought. This includes a regionalisation of streamflow drought characteristics from the Czech Republic, Poland and Slovakia. The work also encompasses studies on long-term variability of monthly water balance components using the BILAN model; the latter is described in details in Kašpárek and Novický (2004).

### The ARIDE project

The key objectives of the ARIDE<sup>2</sup> project (Assessment of the Regional Impact of Droughts in Europe) were to improve the understanding of processes that control European droughts, and the ability to predict their duration, magnitude and extent for a given frequency. In addition, the sensitivity of droughts to environmental changes was explored (Demuth and Stahl, 2001). Consistent drought definitions were derived to quantify temporal and spatial variations in meteorological droughts in terms of precipitation deficit and hydrological droughts in terms of streamflow and groundwater deficit. The ARIDE studies briefly presented in the following sections, focus on the pan-European dimension of drought as well as on the propagation of drought through the hydrological cycle.

---

<sup>2</sup> <http://www.hydrology.uni-freiburg.de/forsch/aride/>

## **The ASTHyDA project**

The ASTHyDA project<sup>3</sup> (Analysis, Synthesis and Transfer of Knowledge and Tools on Hydrological Drought Assessment through a European Network) was primarily a network project with the aim of disseminating knowledge on hydrological drought and to promote collaboration and capacity building between researchers and practising water managers working on drought topics (Tallaksen and van Lanen, 2005). It responded, through a consortium of international experts, to the need for a concise review and dissemination of knowledge and estimation methods for prediction of streamflow and groundwater in periods of drought. The main focus was Europe, although the diversity in the world's hydroclimatology was considered and streamflow series from around the world were used to evaluate a particular model or estimation procedure (e.g. Fleig *et al.*, 2005).

The outcome and conclusions of the review process, including also new approaches and methods for drought analysis, were compiled in a textbook on hydrological drought (Tallaksen and van Lanen, 2004). Draft versions of the textbook were presented to representatives from water management organisations across Europe and to experts from Mediterranean countries at two *workshops*. The purpose of these expert workshops was to foster cross flow of information between the consortium and the invited experts, and subsequently to incorporate feedback from the discussion into an improved second draft. This was followed by a one-week *international study course* for selected students and professional young hydrologists from all over the world to provide discussions and feedbacks for the final revision of the textbook. Lastly, to ensure a regular exchange of information between scientists, hydrologists, water managers and associated experts beyond the lifetime of the ASTHyDA project, the *European Drought Centre* (EDC) was initiated (see separate section).

## **SCIENTIFIC ACHIEVEMENTS**

### **Pan-European and Regional Studies**

To analyse the spatial and temporal development of past pan-European droughts daily “exceedance” series, indicating the proportion of time the flow on any given day has been equalled or exceeded, have proved useful. The exceedance value gives an immediate indication of how high or low the flow is at a particular time compared with the historic record at that site. Commonly the 90 or 95 percentile is adopted for low flow purposes. The technical feasibility of a pan-European near real-time drought monitoring system based on the concept of flow exceedance was addressed in the ARIDE project. It was, however, concluded that a considerable amount of further development is needed to establish an operational monitoring system for the whole of Europe and in addition, a number of political and non-technical issues would need to be resolved. Despite this, it represented an important first step towards launching a European Drought Watch System, which should consist of both a monitoring and a forecasting component.

The aspect of drought forecasting was addressed in a study on the links between large scale atmospheric driving forces and space-time characteristics of major streamflow droughts in Europe (Stahl, 2001; Stahl *et al.*, 2002). A visualization tool, showing mean sea level pressure distribution (contour map) along with flow exceedances on a given day, was made as a first step towards identifying possible links. Through the introduction of a regional streamflow deficiency index it was possible to relate regional droughts to preceding circulation occurrence. The results demonstrated a stronger relation to a lack of winter precipitation than to summer dryness in Europe. This was supported by an analysis of the relationship between drought series and the North Atlantic Oscillation Index (NAOI) which gave significant correlations for winter values in Northern Europe, Spain and Portugal, whereas a weak relationship was found for Central Europe (Fig. 1). The results suggest that pan-European forecasting of streamflow droughts based on links to atmospheric circulation patterns holds substantial promise.

---

<sup>3</sup> <http://drought.uio.no>

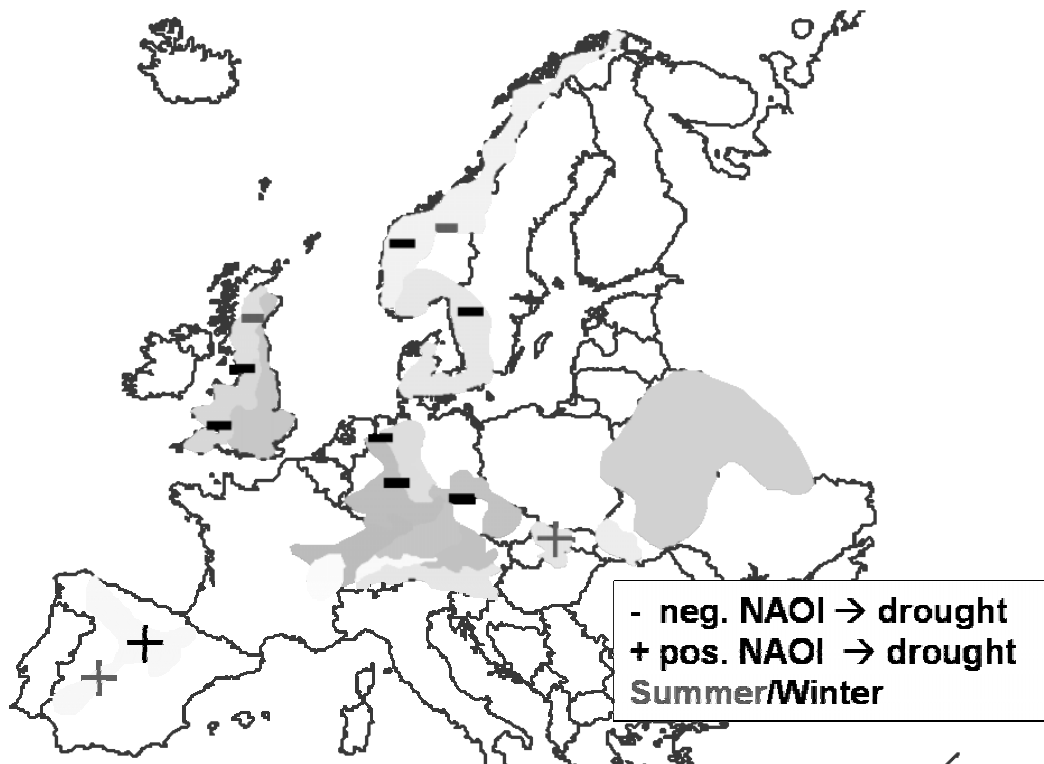


Fig. 1: Correlation of a regional streamflow deficit index with the North Atlantic Oscillation Index. (Regions from which streamflow data were grouped are shaded; data from Demuth & Stahl, 2001).

Hisdal *et al.* (2001) posed the question whether streamflow droughts in Europe have become more severe or frequent. More than 600 daily streamflow series from the EWA were analysed to detect spatial and temporal changes in drought patterns. The results for the period 1962-90 showed that there were no significant changes for most stations. However, distinct regional differences were found, e.g. trends towards more severe droughts in Spain, the western part of Eastern Europe and in large parts of the UK, whereas trends towards less severe droughts occurred in large parts of Central Europe and in the eastern part of Eastern Europe. The trends could, to a large extent, be related to regional changes in precipitation or artificial influences in the catchments. It is important to be aware that the period analysed and also the selection of stations strongly influenced the regional patterns. The former is supported by recent trend studies of long time series in the Czech Republic. Following the catastrophic flood in 2002, extreme hydrological drought occurred in 2003 and 2004 as a result of an increasing trend in air temperature and a long-term decrease in precipitation, in particular during the summer months.

Bower *et al.* (2004) introduced a sensitivity index to assess the river flow regimes' climatic sensitivity. The index provides a mean of assessing the complex linkage between climate drivers and large scale patterns in regimes. Other examples of regional studies include derivation of severity-area-frequency curves for regional drought characteristics (Hisdal and Tallaksen, 2003), a comparison of methods for estimating Q95 from short streamflow records (Laaha and Blöschl, 2005) and a consensus modelling approach that combine different sources of information for estimating annual and seasonal low flow patterns (Laaha *et al.*, 2005).

### **Process-based Studies**

Physically based process models have been used as a tool to define groundwater droughts. Simulated time series of spatially distributed groundwater recharge, levels and discharge were analysed using the threshold level method or the sequent peak algorithm (van Lanen *et al.*, 2004b). Important drought characteristics are the duration and deficit in the groundwater recharge (spatially distributed) and in the groundwater discharge (along a stream). For groundwater level the maximum deviation from a threshold is often preferred (spatially distributed).

The influence of catchment processes and catchment characteristics were investigated based on the effect they have on groundwater drought development. Aquifers that respond quickly to precipitation have many minor droughts as opposed to slowly responding aquifers (e.g. high transmissivity and storage capacity and low drainage density) that have less, but more severe and prolonged droughts (van Lanen *et al.*, 2004a). Peters *et al.* (2005) showed that these differences in the propagation of a meteorological drought through the subsurface are well reflected in the return periods of the drought. For low return periods (e.g. 5 years) the drought in the groundwater discharge is more severe for quickly responding aquifers, whereas for high return periods (e.g. 100 years) it is more severe in areas with slowly responding aquifers.

Process-based studies play a crucial role in analysing the potential impact that anthropogenic influences may have on hydrological drought, including climate and land use change, land drainage, groundwater abstraction, urbanization and surface water transfers (e.g. Querner and van Lanen, 2001; van Lanen *et al.*, 2004b). Fig. 2 shows, as an example, the impact of surface water transfer in the upstream part of the River Elbe catchment. Since 1960 the River Bílina (tributary of River Elbe) has been augmented with surface water from an adjacent catchment. The hydrological model was calibrated with data from 1932-1960 and subsequently used to simulate the discharge from 1961-1990. The observed and simulated time series for the period 1961-1990 were compared to investigate the effect of the augmentation. With the augmentation (real situation) hardly any drought occurred (i.e. three drought events), whereas under natural conditions 22 drought events would have taken place (van Lanen *et al.*, 2004b). Such studies may help to investigate the effects of both re-active and pro-active measures.

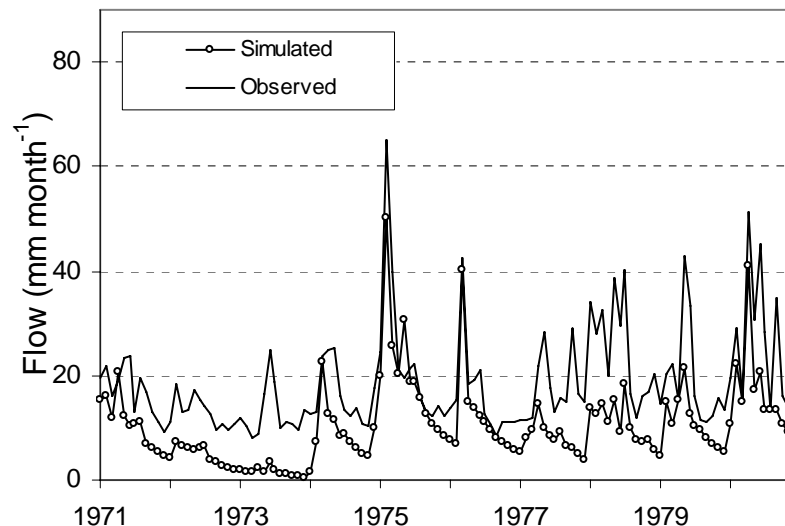


Fig. 2: Observed and simulated discharge (without water transfer) for the River Bílina catchment (Czech Republic).

## DISSEMINATION AND CAPACITY BUILDING

### Textbook

“Hydrological drought—processes and estimation methods for streamflow and groundwater” is a textbook for university students, practising hydrologists and researchers (Tallaksen and van Lanen, 2004). Following its initiation in the NE-FRIEND Low Flow group it was completed with the support of the ASTHyDA project. The main scope of the book is to provide the reader with a comprehensive review of processes and estimation methods for streamflow and groundwater drought. It includes a qualitative conceptual understanding of drought features and processes, a detailed presentation of estimation methods and tools, and concludes with human impacts, ecological issues and key aspects of operational practice. The methods are demonstrated using sample data sets and tools that are provided on the accompanying CD. The drought phenomenon and its diversity across the world are illustrated using a global set of daily streamflow series, whereas regional and local aspects of drought are studied using a combination of

hydrological time series and catchment information. A majority of the examples are taken from regions where the rivers run most of the year. The material presented ranges from well-established knowledge and analysing methods to recent developments in drought research. Its nature varies accordingly, from a more traditional textbook with its clear overview to that of a research paper which introduces new approaches and methodologies.

### **Workshops and Training**

The expert workshops as well as the international study course organised as part of the ASTHyDA project were regarded as successful events that enabled all participants, including the organisers, to benefit from the exchange of information and valuable discussions that took place. The organisation and planning of similar initiatives have therefore been included as a working group activity of the European Drought Centre and the NE-FRIEND Low Flow group. The main objective is to exchange experience, knowledge and tools on drought studies between researchers and water managers with experience from different hydroclimatological regions and water sectors. Present initiatives include international study courses and workshops in Malaysia, Bhutan, the Netherlands (international students at UNESCO-IHE) and in the (semi-)arid regions of North Africa and the Middle East. Furthermore the drought topic will be integrated in international courses and workshops that have a wider scope.

### **European Drought Centre**

The European Drought Centre<sup>4</sup> (EDC) was established in May 2004 as a virtual centre of European drought research and drought management organisations. The main objective is to promote collaboration and capacity building between the scientist and the user community in order to mitigate the impacts of droughts on society, economy and the environment. The establishment of the centre should be seen as a continuation of the work that has been done within the ARIDE and ASTHyDA projects as well as within the framework of the FRIEND project. The centre will create a unique facility for ensuring that advances in understanding drought controlling processes, in forecasting and in prediction lead to benefits to the European society. The EDC will:

- work towards a better understanding of the drought phenomenon and provide the necessary link between science, policy and operational management;
- act as a platform to initiate and discuss scientific progress on drought research within the academic society, including other technical and socio-economic disciplines;
- help to solve society-driven problems by acting as a forum for discussion on policy issues related to sustainable water resources management in a pan-European context, e.g. implications of the WFD on drought management;
- liaise with international organisations and programmes, river commissions and regional drought centres;
- work towards establishing a European Drought Watch System and support the development of national drought mitigation plans based on best practice guidelines.

The centre will have a bottom-up approach and its success will depend on the input and engagement of water experts from a wide range of disciplines. Working groups have been established to focus on priority drought issues and a core group has been identified to co-ordinate the different activities, initiate new actions, promote the centre, seek funding and develop partnerships. Although the key task is to establish the “pan-European dimension”, the centre will build links with other international projects, organisations and experts outside Europe thereby enabling and promoting stronger global co-operation.

## **FUTURE ACTIVITIES**

A joint meeting of the NE and AMHY FRIEND Low Flow groups was held in Bratislava, May 2004. The summary report (Tallaksen, 2004) presents along with the textbook, which concludes with an outline of future research needs (Gustard *et al.*, 2004), a number of recommendations for further research, joint

---

<sup>4</sup> <http://www.geo.uio.no/edc>

activities and co-operation. The call for progress in seasonal drought forecasting and a better understanding of the propagation of drought through the hydrological cycle are highlighted, considering also the impact of land use and climate change on drought development. In addition the need for good quality, long-term data is stressed, along with methods for estimation at the ungauged site. At present it is a major concern that regional data sets, like the EWA, are not regularly updated.

There is further a need for improved coordination of research and operational activities, international collaboration and communication to policy makers and the public. Drought is a natural hazard that cannot be prevented, but its impacts can be reduced through mitigation, i.e. knowledge, preparedness and good management practice. This is also emphasized in a recent discussion document addressing the need for a European drought policy (EurAqua, 2004). The European Drought Centre (EDC) will in this respect interact with the scientific and operational communities as well as policy makers and society to raise awareness of the drought hazard and may represent an important platform for future European drought initiatives. The NE-FRIEND Low Flow group will continue to work actively to ensure continuation and further advances in drought research through the success of the EDC.

## ACKNOWLEDGEMENTS

The authors thank the members of the NE-FRIEND Low Flow group and other partners in the ARIDE and ASTHyDA projects for their co-operation and valuable contribution to the achievements reached. The NE-FRIEND Low Flow group acknowledges the continuous support of UNESCO-IHP Headquarters in Paris and the financial support of EC to the ARIDE (ENV4-CT97-0553) and ASTHyDA (EVK1-CT-2002-80023) projects.

## REFERENCES

- Bower, D., Hannah, D.M. and McGregor, G.R. (2004) Techniques for assessing the climatic sensitivity of river flow regimes. *Hydrol. Proc.*, 18, 13, 2515-2543.
- Demuth, S. and Stahl, K. (2001) *ARIDE - Assessment of the Regional Impact of Droughts in Europe*. Final report, EU contract ENV4-CT-97-0553, Institute of Hydrology, Freiburg, Germany.
- EurAqua (2004) Towards a European Drought Policy. Discussion document prepared by the EurAqua network of Europe's leading freshwater research organisations (<http://www.euraqua.org>).
- Fleig, A.K., Tallaksen, L.M., Hisdal, H. and Demuth, S. (2005) A global evaluation of streamflow drought characteristics. In: *Geophysical Research Abstracts*, Vol. 7, EGU General Assembly 2005, 24-29 April, Vienna, Austria; ISSN 1029-7006.
- Gustard, A., van Lanen, H.A.J. and Tallaksen, L.M. (2004) Outlook. In: L.M. Tallaksen and H.A.J. van Lanen (Eds), *Hydrological Drought-Processes and Estimation Methods for Streamflow and Groundwater*. Developments in Water Sciences 48, Elsevier B.V., 485-498.
- Hisdal, H. and Tallaksen, L.M. (2003) Estimation of regional meteorological and hydrological drought characteristics. *J. Hydrol.*, 28, 3, 230-247.
- Hisdal, H., Stahl, K., Tallaksen, L.M. and Demuth, S. (2001) Have streamflow droughts in Europe become more severe or frequent? *Int. J. Climatol.*, 21, 317-333.
- Hisdal, H., Tallaksen, L.M., Clausen, B., Peters, E. and Gustard, A. (2004) Hydrological Drought Characteristics. In: L.M. Tallaksen and H.A.J. van Lanen (Eds), *Hydrological Drought-Processes and Estimation Methods for Streamflow and Groundwater*. Developments in Water Sciences 48, Elsevier B.V., 139-198.
- Jakubowski, W. and Radczuk, L. (2004) NIZOWKA2003 - Software Manual. In: L.M. Tallaksen and H.A.J. van Lanen (Eds), *Hydrological Drought-Processes and Estimation Methods for Streamflow and Groundwater*. Developments in Water Sciences 48, Elsevier B.V. (Information on CD).
- Kašpárek, L. and Novický, O. (2004) Background information BILAN. In: L.M. Tallaksen and H.A.J. van Lanen (Eds), *Hydrological Drought-Processes and Estimation Methods for Streamflow and Groundwater*. Developments in Water Sciences 48, Elsevier B.V. (Information on CD).
- Laaha, G. and Blöschl, G. (2005) Low flow estimates from short stream flow records—a comparison of methods. *J. Hydrol.*, 306, 264-286.

- Laaha, G., Blöschl, G. and Parajka, J. (2005) Consensus modelling of environmental flows. In: *Geophysical Research Abstracts*, Vol. 7, EGU General Assembly 2005, 24-29 April, Vienna, Austria; ISSN 1029-7006.
- Lanen, H.A.J. van, Fendeková, M., Kupczyk, E., Kasprzyk, A. and Pokojski, W. (2004a) Flow Generating Processes. In: L.M. Tallaksen and H.A.J. van Lanen (Eds), *Hydrological Drought–Processes and Estimation Methods for Streamflow and Groundwater*. Developments in Water Sciences 48, Elsevier B.V., 53-96.
- Lanen, H.A.J. van, Kašpárek, L., Novický, O., Querner, E.P., Fendeková, M. and Kupczyk, E. (2004b) Human Influences. In: L.M. Tallaksen and H.A.J. van Lanen (Eds), *Hydrological Drought–Processes and Estimation Methods for Streamflow and Groundwater*. Developments in Water Sciences 48, Elsevier B.V., 347-410.
- Peters, E., van Lanen, H.A.J., Torfs, P.J.J.F. and Bier, G. (2005) Drought in groundwater–drought distribution and performance criteria. *J. Hydrol.*, 306, 302-317.
- Querner, E.P. and van Lanen, H.A.J. (2001) Impact assessment of drought mitigation measures in two adjacent Dutch basins using simulation modelling. *J. Hydrol.*, 252, 51-64.
- Rees G. and Demuth S. (2000) The application of modern information system technology in the European FRIEND project. *Moderne Hydrologische Informationssysteme, Wasser und Boden*, 52, 13, 9-13.
- Stahl, K. (2001) *Hydrological Drought—a Study across Europe*. PhD Thesis, Albert-Ludwigs-Universität Freiburg, Freiburger Schriften zur Hydrologie no. 15, also available from: <<http://www.freidok.uni-freiburg.de/volltexte/202>>.
- Stahl, K., Hassler, B. and Demuth, S. (2002) Scenarios assessing the influence of climate variability on drought in Europe. *IAHS Pub.* 274, 93-100.
- Tallaksen, L.M. (2004) (Ed.) Northern European FRIEND and AMHY FRIEND Joint Low Flow Meeting, Summary Report. A contribution to the UNESCO IHP-VI program on Hydrological Extremes, 12-15 May, 2004, Bratislava, Slovakia, 30 p.
- Tallaksen, L.M. and van Lanen, H.A.J. (2004) (Eds) *Hydrological Drought–Processes and Estimation Methods for Streamflow and Groundwater*. Developments in Water Sciences 48, Elsevier B.V., the Netherlands, 580 p.
- Tallaksen, L.M. and van Lanen, H.A.J. (2005) ASTHyDA - Final Report: 01 December 2002-30 November 2004. *ASTHyDA Report No 5*, University of Oslo, Norway.

# COMPARATIVE HYDROLOGICAL DROUGHT-FLOOD RISK MODELING AT NORTHERN MEXICO AND WEST AFRICAN SAHEL REGION

**Alfonso GUTIÉRREZ-LÓPEZ**

Instituto Mexicano de Tecnología del Agua, IMTA, Subcoordinación de Hidrología y Mecánica de ríos, Paseo Cuauhnáhuac 8532; C.P. 62550, Jiutepec, Morelos, México  
*agutierrez@tlaloc.imta.mx*

**Hubert ONIBON**

Groupe Afriturible International, GAI, sarl, 02 BP 1567 Cotonou, République du Bénin

## ABSTRACT

West Sahel Africa is a wide stretch of land running from the Atlantic Ocean to Niger; it is a transition zone between the arid Sahara to the north and the wetter more tropical area to the south (15°-25°N). Northwest Mexico is an essentially transition tropical-desert zone (23°-28°N). These both regions are touched by two different rainfall regimes producing either extreme precipitation conditions or severe droughts. This paper presents a stochastic model of rainfall distribution and its regionalisation. The rainfall regime is described by two parameters: the mean event rainfall and the daily mean number of events during a given period (Leak distribution). The method is applied to West Sahel Africa and Northern Mexico and the comparative hydrological drought-flood risk modeling itself is carried out in a geostatistical framework. The results obtained are compared to those obtained by a direct fitting of a Gumbel distribution to series of extreme values.

**Keywords:** flood, drought, Leak distribution, regionalization, West Sahel Africa, Northwest Mexico

## INTRODUCTION

Extending from 15°N to 25°N, West Sahel Africa is a wide stretch of land running from the Atlantic Ocean to Niger; it is a transition zone between the arid Sahara to the north and the wetter more tropical area to the south. In that order, Northwest Mexico is a essentially transition tropical-desert zone located from 15°N to 20°N is characterized by the frequent occurrence of extreme rainfall, causing floods and severe damages to growing and by long periods of drought. The climates of the West Sahel and Northwest Mexico are typically an arid and unstable environment. The Sahel area is a predominately sparse savanna vegetation of grasses and shrubs. Northern Mexico is covered by desert vegetation, including mesquite, cactus, desert scrub, and some grasses. Over the recent years, these both regions are touched by two different rainfall regimes producing either extreme precipitation conditions or severe droughts. In such a context, the development of robust methods of regionalization is needed as a starting point for water resources planning and risk prevention. This paper presents a stochastic model of rainfall distribution and its regionalization. The analytical formulation of the model and some of its main properties are recalled. The rainfall regime is described by two parameters: the average rain depth per event and the mean number of events during a given period (Leak distribution). The method is applied to West Sahel Africa (Fig. 1) and Northern Mexico (Fig. 2) and the comparative hydrological drought-flood risk modeling itself is carried out in a geostatistical framework, focusing on three time scales: annual, monthly and daily. The results obtained by the model are compared to those obtained by a direct fitting of a Gumbel distribution to series of extreme values. This provides an integrated approach for the mapping of the hydrological risk over both gauged and ungauged basins.

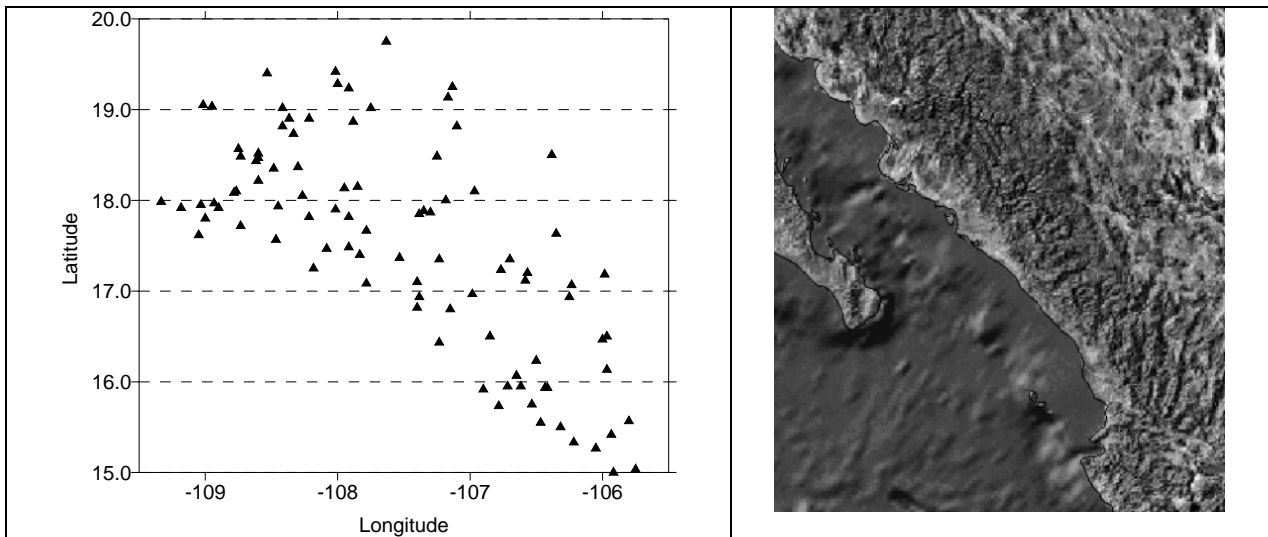


Fig. 1: Recording rain gauge network over the Mexican watershed (95).

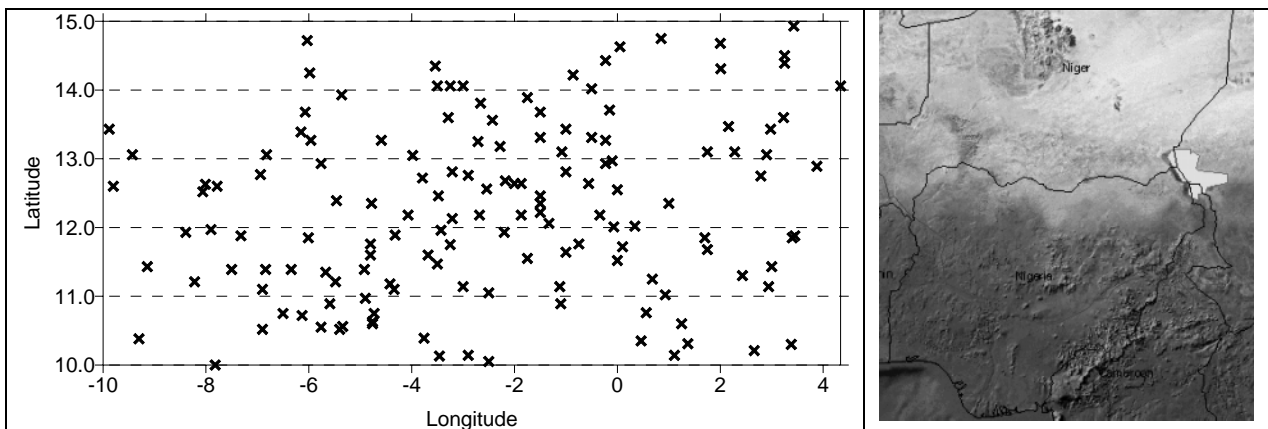


Fig. 2: Recording rain gauge network over the Sahel watershed (145).

## RAINFALL DISTRIBUTION MODEL

The model is based on the hypotheses of a Leak distribution that was developed by Babuziaux, C., (1969), (Electricité de France). This law is commonly used to describe the regime of rainfall in Africa, mainly in Benin (Le Barbé *et al.*, 2002); in Togo (Seguis, 1988) in Nigeria (Le Barbé and Lebel, 1997; Onibon *et al.*, 2002) and in Burkina Faso by Tapsoba, 1993. The Leak distribution is used generally in the study of rainfall data. The main hypotheses to consider are: (a) Rainfall distribution is a process without memory, (b) depth rain of each event, has an exponential distribution and (c) the number of events registered in a measurement station (days with rain), take a Poisson distribution. In addition to the first hypothesis, if the process is stationary, the mean event rain depth,  $\beta$  follows a law of exponential distribution. It is also possible to deduce that over this period  $T$ , the mean number of storms ( $\lambda$ ) assume to be a Poisson distribution. The model itself is basically a Compound Poisson Process with white noise exponential distribution. Therefore the parameter  $\beta$  gives an additional advantage by making possible the deduction of the distribution of the rain over the period  $T' = kT$  from the distribution computed for the period  $T$  ( $\beta' = \beta$  and  $\lambda'_{T'} = k\lambda_T$ ). where,  $I_1$  is the order one Bessel function

$$f(x, \lambda, \beta) = e^{-\lambda - \frac{x}{\beta}} \frac{\lambda}{\beta} \frac{I_1\left(2\sqrt{\frac{\lambda x}{\beta}}\right)}{\sqrt{\frac{\lambda x}{\beta}}} \quad \text{for all } x > 0 \quad (1)$$

### Inference of parameters, Method of Moments

The most effective inference of parameters procedure depends on the average number of dry days, during the period T. For the case  $n_0=0$ , the inference of parameters using the method of moments, can be considered as:

$$\hat{\lambda} = \frac{2\bar{x}^2}{s_x^2} \qquad \hat{\beta} = \frac{s_x^2}{2\bar{x}} \quad (2)$$

If,  $n_0 \neq 0$  the estimation procedure requires, for a correct solution, to take into relation the total observed number  $n$  of sequences of length T in the sample. By this way, the estimators of the parameters can be obtained as:

$$\hat{\lambda} = \left[ 1 - (2 - \sqrt{2}) \sqrt{\frac{n_0}{n}} \right] \left[ \frac{2\bar{x}^2}{s_x^2} - \text{Log}_e \frac{n}{n_0} \right] + \text{Log}_e \frac{n}{n_0} \quad (3)$$

$$\hat{\beta} = \left[ 1 - (2 - \sqrt{2}) \sqrt{\frac{n_0}{n}} \right] \left[ \frac{s_x^2}{2\bar{x}} - \frac{\bar{x}}{\text{Log}_e \frac{n}{n_0}} \right] + \frac{\bar{x}}{\text{Log}_e \frac{n}{n_0}} \quad (4)$$

### Method of maximum likelihood

The logarithm of the probability function, whose maximum must be obtained, is the following:

$$L = -\lambda n + \frac{(n - n_0)}{2} \text{Log}_e \frac{\lambda}{\beta} - \sum_{i=1}^{n-n_0} \frac{x_i}{\beta} - \frac{1}{2} \sum_{i=1}^{n-n_0} \text{Log}_e x_i + \sum_{i=1}^{n-n_0} \text{Log}_e I_1 \left( 2 \sqrt{\frac{\lambda x_i}{\beta}} \right) \quad (5)$$

Simplifying to the partial derived from L, with respect to  $\lambda$  and  $\mu$  leads to an equations system of the form:

$$-n + \frac{n - n_0}{2\lambda} + \sum_{i=1}^{n-n_0} \frac{I_1'(z_i)}{I_1(z_i)} \frac{z_i}{2\lambda} = 0 \quad (6)$$

$$-\frac{n - n_0}{2\beta} + \sum_{i=1}^{n-n_0} \frac{x_i}{\beta^2} - \sum_{i=1}^{n-n_0} \frac{I_1'(z_i)}{I_1(z_i)} \frac{z_i}{2\beta} = 0 \quad (7)$$

where 
$$z_i = 2 \sqrt{\frac{\lambda x_i}{\beta}} \quad (8)$$

$I_1'(z)$  is the first derived of  $I_1(z)$ . Solving the equations system member to member it is obtained:

$$\bar{x} = \hat{\lambda} \hat{\beta} \quad (9)$$

The properties of Bessel function, allow writing the derived of  $I_1$  as:  $I_1'(z) = I_0(z) - \frac{1}{z} I_1(z)$

$I_0$  is the Bessel function of order zero. Using this expression into the equation (6) and by substituting  $\bar{x}$  in equation (8)  $\frac{z_i}{2\lambda} = \sqrt{\frac{x_i}{\bar{x}}}$  :  $g(\lambda) = \sum_{i=1}^{n-n_0} \frac{I_0(z_i)}{I_1(z_i)} \sqrt{x_i} - n\sqrt{\bar{x}} = 0$  whose solution is a single and positive value of  $\hat{\lambda}$ . The function  $g(\lambda)$  is monotonous and decreasing; its solution is in the interval  $[10^{-4}, 5\hat{\lambda}_{mom}]$  where,  $\hat{\lambda}_{mom}$  corresponds to the value of the parameter considered by the method of moments. The value  $\beta$  is obtained from the expression (9). Le Barbé and Lebel (1997), proposed an alternative procedure for inference of parameters of the Leak distribution. This method proposes to use the average number of dry days. This procedure has a singular importance because dry days information, is not used directly in the inference of parameters in both the method of moments and the maximum likelihood one. By this way, the parameters shall be given by:

$$\hat{\lambda} = -\text{Log}_e\left(\frac{n_0}{n}\right) \qquad \hat{\beta} = \frac{\hat{\mu}}{\hat{\lambda}} \qquad (10)$$

where  $\hat{\mu}$  is an estimation parameter of the first moment of the probability function. In 95 raingauge stations within the Mexican hydrological region n°10 and in 145 raingauge stations in the West Sahel region; were taken into account, and the parameters of the Leak distribution were calculated, with the three previously described procedures. For both regions the considered period of May to October are used with a mean available record period data of 35 years (1947-1990) for the Mexican stations and 20 years (1951-1990) for the African region. Based on the statistical  $\chi^2$ , the best adjustments were selected. In the Mexican region, 14 stations were rejected by the test. In 5 of other ones, the method of maximum likelihood was not convergent. 11 stations were adjusted to normal distribution and the frequency analysis of 65 stations followed the Leak distribution. From these 65 stations, 46 stations are considered as being of excellent quality; thus, there were used in this study. A similar procedure was taken in the African stations (Onibon, 2001). According to the methods of inference of parameters, in most of the cases, the method of moments gives the best adjustment to the samples data. Fig. 3 shows the adjustment of daily rainfall in the Mexican Tamazula station (Gutiérrez-López *et al.*, 2005).

## MODEL VALIDATION FOR THE REGIONS OF STUDY

The main advantage of the Leak distribution consists in the possible use of different time intervals. It can be calibrated for different values from  $T$ . The c.d.f. (cumulative distribution function) of the rainfall accumulated over  $k$  time steps is still a Leak distribution, assuming that an average scale parameter  $\lambda$  can be computed over the duration  $kT$ . When daily data are available, it is strongly preferable to chose  $T$  equal to 1 day see Fig. 3. Fig. 4, 5 and 6 show the validation of the model. The considered parameters of the analysis of daily rain, by the method of moments were:  $\lambda = 0.654$  y  $\beta = 12.214$ . In order to estimate the parameters for 10-days cumulative rainfall, we obtain:  $\lambda = 0.654 \times 10$  ;  $\lambda = 6.54$  ;  $\beta = 12.214$ . The real values are:  $\lambda = 7.071$  ;  $\beta = 11.465$ . Then, to obtain the parameters of the monthly rainfall distribution, values are the following ones:  $\lambda = 0.654 \times 31$  ;  $\lambda = 20.274$  ;  $\beta = 12.214$ ; The real values are:  $\lambda = 20.083$  ;  $\beta = 12.33$

## REGIONALISATION OF PARAMETERS

In all the raingauge stations of the Mexican and African regions, the parameters of the Leak distribution day per day during the great wet season from May to October were estimated. This analysis was developed by using an 11 day window (five days before and five after the day N) and enabled us to trace Fig. 7 to 12, for instance for the station Tamazula in Mexico. Also for Kindi, Dedougou, Kamboince, Bilanga, Didir, Boulsa, Botou, Bousse, Bourzanga, Bani, Titao, Tiou-ouahigouya, Pobe stations at Sahel region. Fig. 7 and 8 shows the evolution of these parameters as an interesting variation of number of storms within the hydrological region 10. It is seeable that near the coast, the parameter  $\lambda$  value has a

strong spatial variability. It shows also a great time-variability, during the rainy season. Inversely, in the piedmont and the Sierra Madre, variations are lower. The area of highest values of  $\lambda$  parameter is similar than this of the rainfall annual amount, and is strongly linked to both the topographical pattern and the zonal climate distribution. Thus, the higher values are closer to the coast in the southern region, under a wet tropical climate. In Mexico, at North is located more and more far from the coastal plain, due to the appearance of the dry subtropical climate of the coastal desert (240 mm of annual rainfall at Topolobampo station).

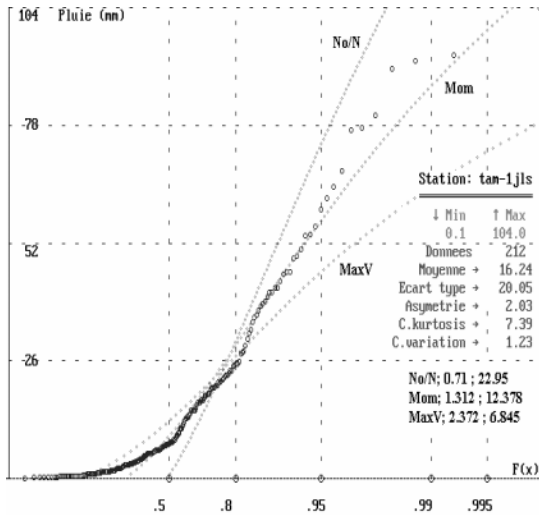


Fig. 3: Tamazula (1961-1985).  
Analysis for 1 July.

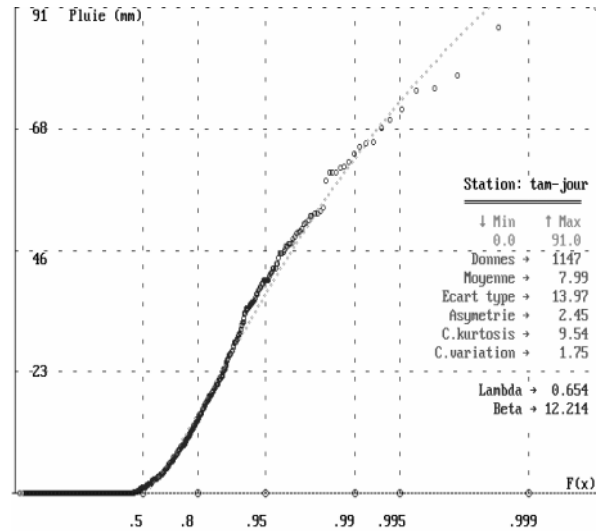


Fig. 4: Tamazula August (1961-1985).  
Daily Rainfall Distribution.

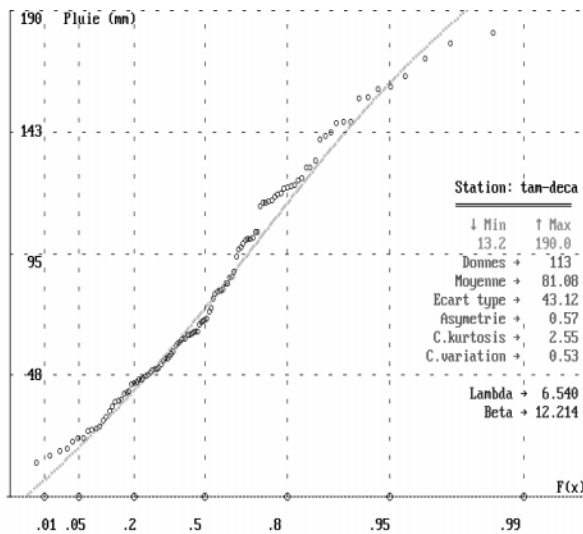


Fig. 5: Tamazula August (1961-1985).  
10-Day Cumulative Rainfall  
Distribution.

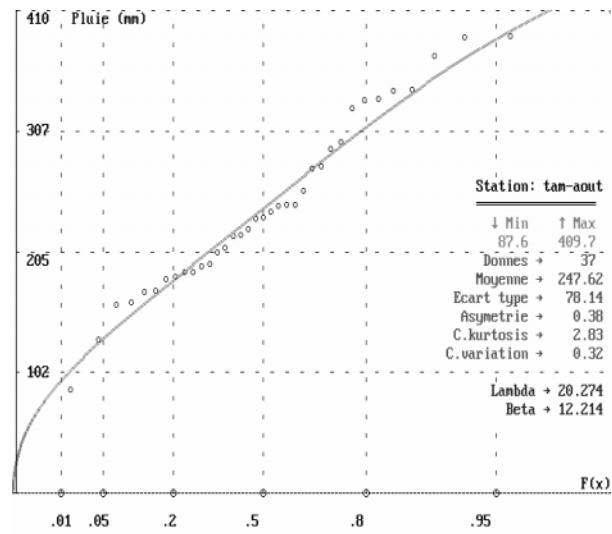


Fig. 6: Tamazula August (1961-1985).  
Monthly Rainfall Distribution.

Therefore, at these higher latitudes, there is a strong relation between rainfall and altitude, while in southern areas, the wettest zones are located on the hills near the Pacific Ocean. This is the reason why the parameter spatial distribution is transverse and across the mountain. Although the obvious parallelism of coast and mountain, rainfall distribution determines its own rules, due to the conjunction of global and zonal influences. At the Sahel region, the decrease of rainfall is closely linked to decrease in the number of rainfall events, except in the extreme south.

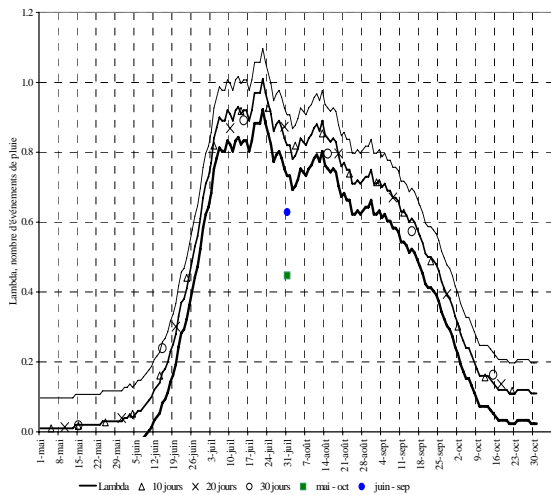


Fig. 7: Tamazula August (1947-1990).  
Daily mean number of events.

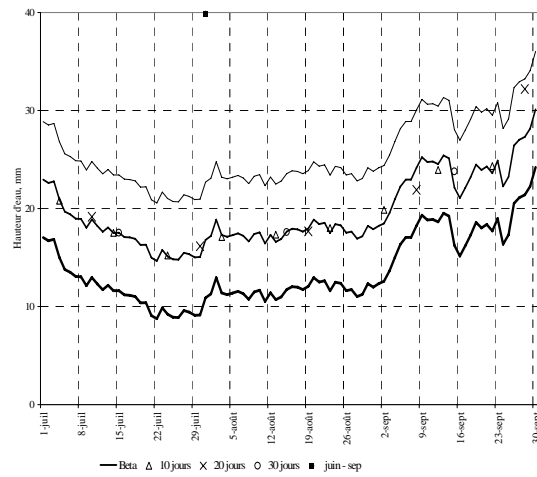


Fig. 8: Tamazula August (1947-1990).  
Mean event rainfall distribution.

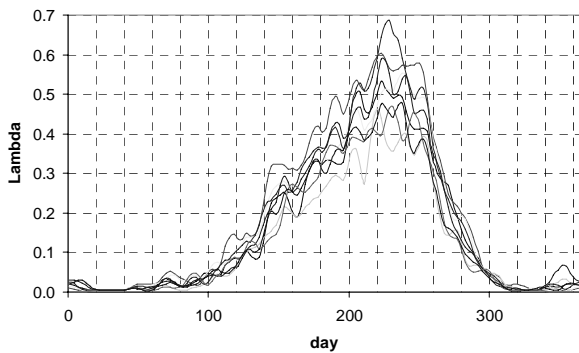


Fig. 9: Kindi, Dedougou, Kamboince, Bilanga, Didir, Boulsa, Botou, Bousse, stations (1951-1990).  
Daily mean number of events.

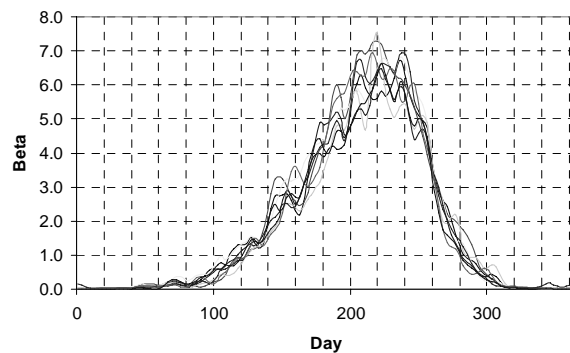


Fig. 10: Kindi, Dedougou, Kamboince, Bilanga, Didir, Boulsa, Botou, Bousse, stations (1951-1990).  
Mean event rainfall distribution.

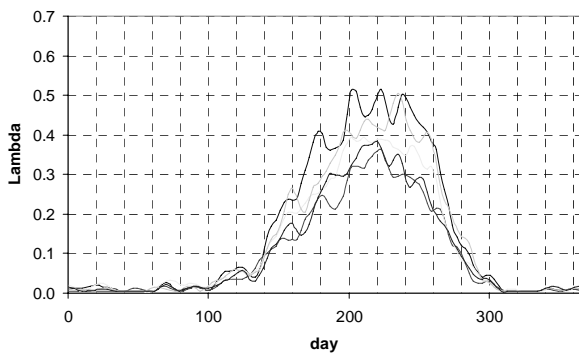


Fig. 11: Bourzanga, Bani, Titao, Tiou-ouahigouya, Pobe, stations (1951-1990).  
Daily mean number of events.

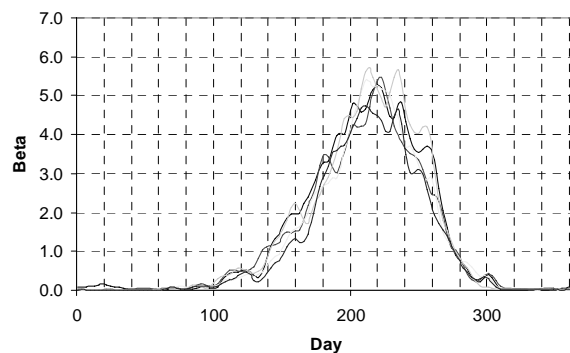


Fig. 12: Bourzanga, Bani, Titao, Tiou-ouahigouya, Pobe, stations (1951-1990).  
Mean event rainfall distribution.

This decrease is especially important for the core of the rainy season (July, August), but in the north (14 to 15°N) it is observed over the whole rainy season. This spatial pattern was detected by Le Barbé and Lebel in 1997. Also two wet periods were detected (1950-1969) and two dry decades (1970-1989).

## MEASURE AND MAPPING OF THE HYDROLOGICAL RISK

The type I distribution (or Gumbel) is often used for maximum type events and results from any initial unlimited distribution of exponential type which converges to an exponential function. Kite (1988), Tapsoba (1997). Examples of this type of distribution include the normal and lognormal distributions. The derivation of the type I distribution for a simple exponential function can be described as: Define  $X_{\max}$  as the maximum value of a series of independent variables  $\varepsilon_i$  with cumulative probability distribution given by:  $P(x) = P(\varepsilon_i \leq y)$  :

$$P(X_{\max} \leq y) = P(\varepsilon_1 \leq y, \varepsilon_2 \leq y, \dots, \varepsilon_n \leq y) \quad (11)$$

$$P(X_{\max} \leq y) = [P(y)]^n \quad (12)$$

Assume that the tail of the distribution  $P(y)$  is exponential such that:  $P(y) = 1 - \beta e^{-y}$  (13)

From (12) if  $\ln(\alpha n)$  is a normalizing constant:  $P[X_{\max} \leq y + \ln(\beta n)] = [P(y + \ln(\beta n))]^n$  and from the equation (13):

$$P[X_{\max} \leq y + \ln(\beta n)] = \left(1 - e^{-y} / n\right)^n \quad (14)$$

If  $n \rightarrow \infty$ , then:

$$\lim_{n \rightarrow \infty} P[X_{\max} \leq y + \ln(\beta n)] = e^{-e^{-y}} \quad (15)$$

This is a reduce form of the cumulative probability distribution. Let  $y = \beta(x - x_0)$ , where  $\beta$  is a concentration parameter (scale) and  $x_0$  is a measure of central tendency, the cumulative probability of the type I extremal distribution becomes:

$$P(x) = e^{-e^{-\beta(x-x_0)}} \quad (16)$$

According of this procedure, Lebel and Laborde (1988), have demonstrated several applications of the scale parameter of Gumbel distribution. Gutiérrez-López *et al.*, (2002), found that the Gumbel extreme value type I distribution, fits the experimental distribution of the point rainfall monthly maxima well. Similarly, Tapsoba (1997), the number of events registered from  $J_1$  day to  $J_2$  day, follows a Poisson distribution with parameter  $\lambda$  (cumulated number of days among this date). If  $Hx_{j_1-j_2}$  is the maximal annual depth of each event observed every year among day's  $j_1$  and  $j_2$ ,  $P(Hx_{j_1-j_2} \leq Hx)$  can be computed from:

$$P(Hx_{j_1-j_2} \leq Hx) = \sum_0^{\infty} \frac{\lambda^i e^{-\lambda}}{i!} \left[1 - e^{\left(\frac{-Hx}{\mu}\right)}\right]^i \quad (17)$$

Moreover, simplifying gives:

$$P(Hx_{j_1-j_2} \leq Hx) = e^{\left[-\lambda e^{(-Hx/\mu)}\right]} \quad (18)$$

$$P(Hx_{j_1-j_2} < 0) = 0 \quad (19)$$

That is the Gumbel extreme distribution, for positive values. Alternatively, if the assumptions are made that events are independent and the mean number of events are independent and the mean number of events in unit time is constant then the Binomial and Poisson distributions can be used to evaluate risk. For a Poisson distribution of event occurrences and a extremal type I distribution of events magnitudes, the design events and risk will be function of  $\lambda$  parameter (expected rate of occurrence of events). Scale

parameter of Gumbel distribution fit, for the maximal annual events in the month of August in Tamazula rain gauge station, is at once the same parameter for the daily August rainfall in the Leak distribution. The study of this scale parameter of the Gumbel distribution is used as an index of the extreme rainfall risk. For the Maximal annual data in August (37 years), Gumbel distribution:  $\beta = 13.28$  and  $x_0 = 45.76$  For daily August rainfall Leak distribution:  $\beta = 12.214$  and  $\lambda = 0.654$ .

## CONCLUSIONS

Rainfall in northern Mexico and in Sahel region is a complex phenomenon to study; nevertheless, results of the application of the Leak distribution in this area have allowed a better knowledge of this phenomenon. The Leak distribution has many advantages and allows the decomposition of the rainfall fluctuations into two terms: the fluctuations of the mean event rainfall, and that of the mean number of rainfall events over any period. The coherent set of these parameters leads to find simple relations with its geographic and physical environment. The model is significantly consistent with the description of changes associated with the extreme phenomenon, according to a normal increase of rainfall during the rainy season; on one the main advance, for the Mexican watershed, is the good knowledge of the hurricane season that gives us the evolution of  $\lambda$ . At the end of September  $\lambda$  shows clearly the decrease and increase of precipitation amount due to the climatic distribution pattern through the hydrological region n°10, and particularly the location of the wettest area, near the coast on the south, and closer to crests on the north (Fig. 13 and 14). The mapping of scale to parameter of Gumbel distribution is a suitable tool to explore the information contained into precipitation series. Hydrological region n°10 and Sahel region show a typical behavior of a region affected by extreme phenomena; the main risks appear in the coastal zones and the zone of high rainfall. Finally, it is considered that recommends methodology and the use of the Leak distribution, is adapted to the necessities of estimation of the hydrologic risk and allows a substantial knowledge of the regional climatology. In general Sahel region shows a regular pattern of daily mean number of events  $0.5 \leq \lambda \leq 1.35$ , with a raining season for middle July to end September. In Mexico, appears a shortening rainy season, but with recent increase of daily events.

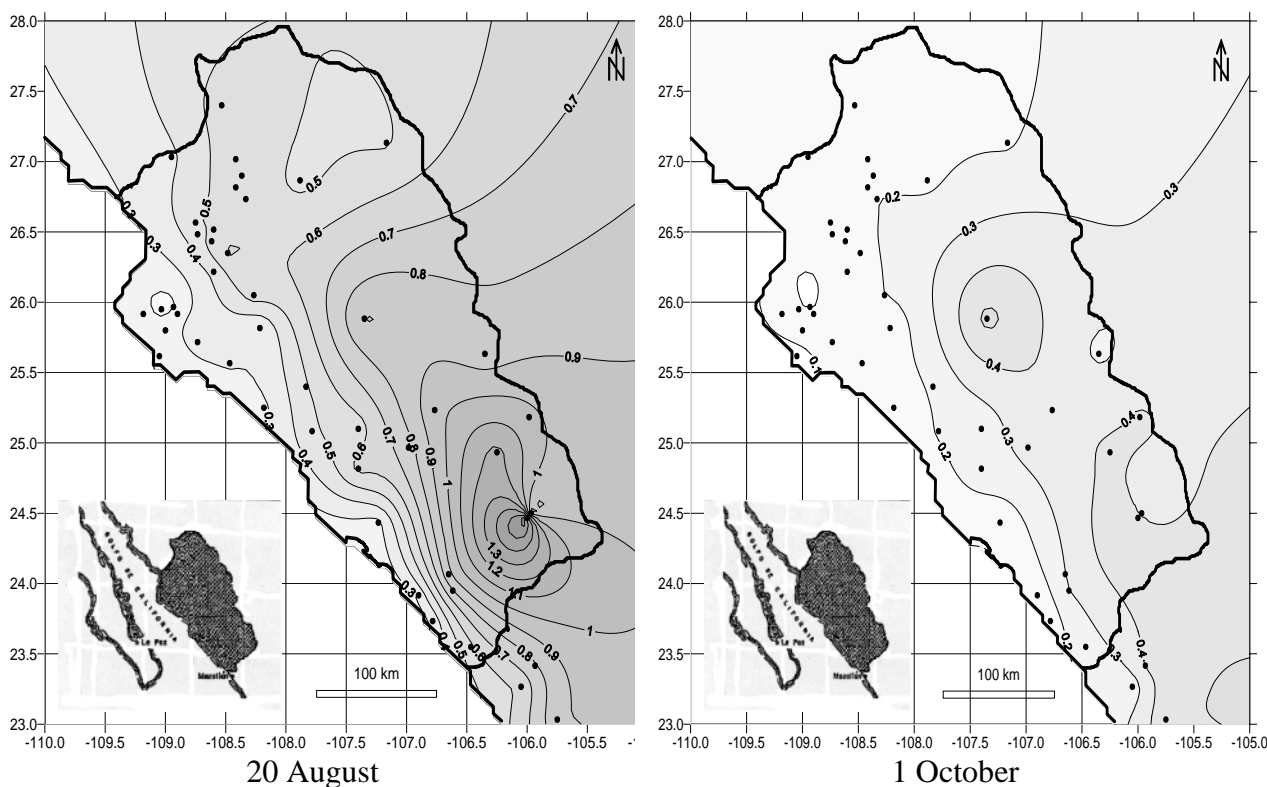


Fig. 13: Spatial - time evolution of mean number of rainy events.

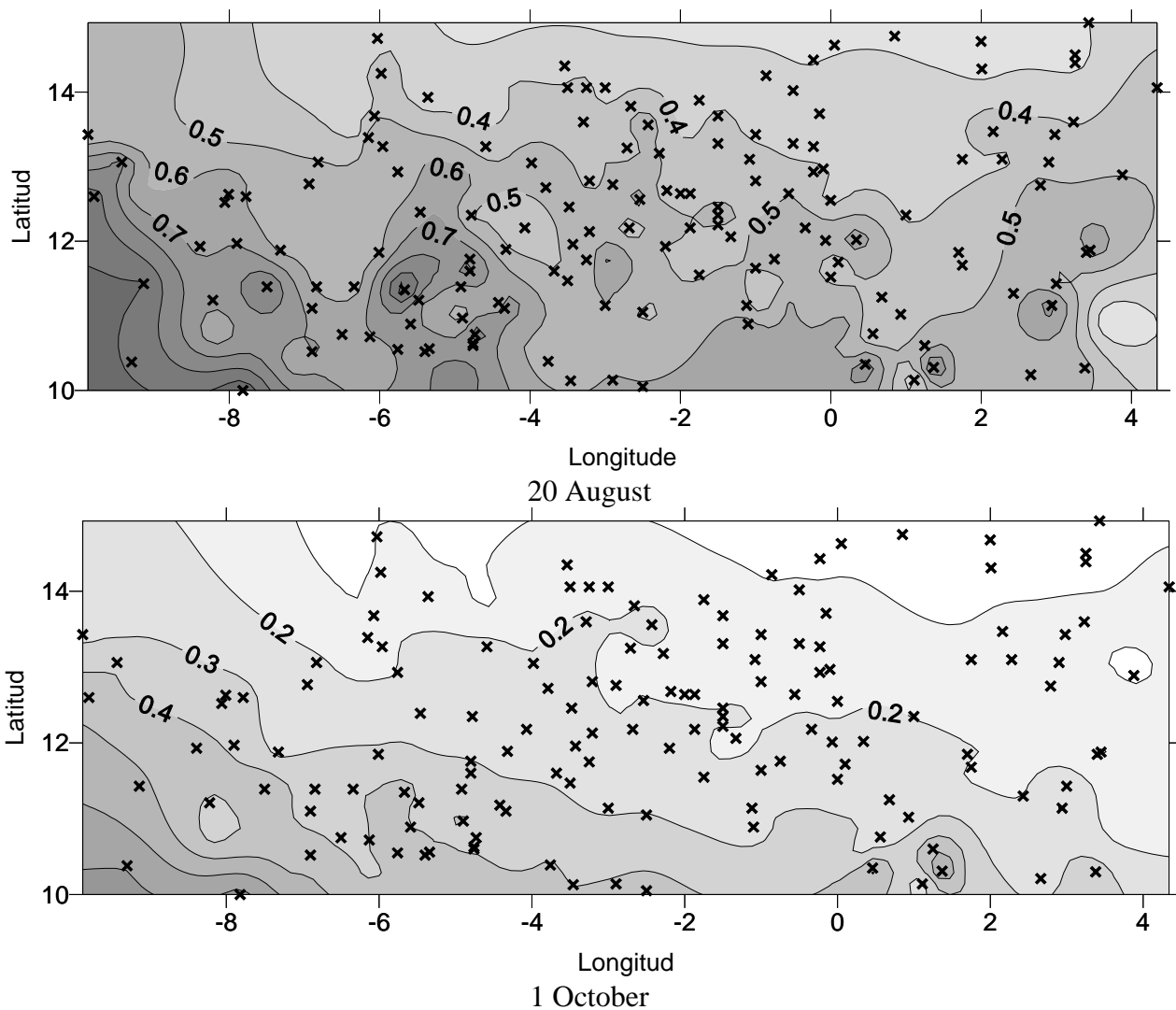


Fig. 14: Spatial - time evolution of mean number of rainy events.

## REFERENCES

- Babuziaux, C. (1969) *Etude statistique de la loi des fuites*. Service des études et recherches nucléaires, thermiques et hydrauliques. Département Laboratoire National d'Hydraulique, Electricité de France, 119 p.
- Gutiérrez-López A., Lebel, T. and Descroix, L. (2002) Statistical Analysis for Modelling the Hydrological Risk in northern Mexico. International Association for Hydraulic Research (IAHR), *Hydraulic and Hydrological Aspects of Reliability and Safety Assessment of Hydraulic Structures*, St. Petersburg, Russia.
- Gutiérrez-López, A., Lebel, T. and Mejía, R. (2005) Estudio espacio-temporal del régimen pluviométrico en la zona meridional de la república mexicana. *Revista Ingeniería Hidráulica en México*, IMTA, 20, 1, 57-65.
- Kite, G. W. (1988) *Frequency and risk analyses in hydrology*. Water Resources Publications USA, 257 p.
- Le Barbé, L. and Lebel, T. (1997) Rainfall climatology of the HAPEX-Sahel region during the years 1950-1990. *J. Hydrol.* 188-189, 43-73.
- Le Barbé, L., Lebel T. and Tapsoba D. (2002) Rainfall variability in West Africa during the years 1950-1990. *J. Climate*, 15, 2 187-202.
- Lebel, T. and Laborde, J.P. (1988) A geostatistical approach for areal rainfall statistics assessment. *Stochastic Hydrology and Hydraulics*, 2, 245-261.

- Onibon, H. (2001) *Simulation conditionnée des champs de pluie événementiels au Sahel : Application de l'algorithme de Gibbs*. Thèse de Doctorat de l'Institut National Polytechnique de Grenoble, France.
- Onibon, H., Lebel, T. and Afouda, A. (2002) Space-time rainfall variability in West Africa derived from observations and GCM's. *IAHS Pub.* 274, 483-490.
- Seguis, L. (1988) *La pluviométrie au Togo: Caractérisation agronomique*. ORSTOM, Centre de Lomé. (Revue interne).
- Tapsoba, D. (1993) *Contribution à l'étude des variations spatio-temporelles des précipitation au Burkina Faso à partir du modèle de la loi des fuites*. Mémoire de DEA de l'Université de Paris XI, Orsay, France, 88 p.
- Tapsoba, D. (1997) *Caractérisation événementielle des régimes pluviométriques ouest africains et de leur récent changement*. Thesis, Université de Paris XI, Orsay, France, 145 p.

# BUSHFIRES AND THEIR IMPLICATIONS FOR MANAGEMENT OF FUTURE WATER SUPPLIES IN THE AUSTRALIAN CAPITAL TERRITORY.

**Trevor DANIELL**

Centre for Applied Modelling in Water Engineering, School of Civil and Environmental Engineering,  
The University of Adelaide, SA, 5005, Australia

*trevord@civeng.adelaide.edu.au*

**Ian WHITE**

Centre for Resource and Environmental Studies, Australian National University, Canberra, ACT,  
0200, Australia.

## ABSTRACT

Periodic, often ENSO-related widespread droughts in eastern Australia frequently generate severe bush fires. These can devastate water supply catchments and have serious impacts on the quality and quantity of domestic water supplies. The implications for water supplies sourced from native forests and their management are profound. The Cotter River Catchment in the Australian Capital Territory (ACT), eastern Australia has been a major source of water for the national capital, Canberra, since 1918. Previous work following the 1939 bushfires in alpine ash (*Eucalyptus Regnans*) catchments in the southern Australia state of Victoria found large decreases in yields (of the order of 30%) for up to 50 years following the fires as forests regrew. It is shown here that the response of catchments with mixed native forests to fires differs from the alpine ash forests in Victoria. Slight increases in yield appear initially over the first 30 months because of the decreases in evapotranspiration. It is thought that as epicormic regeneration of eucalypts continues small decreases in yield of less than 10% could occur for some years but similar results occur after severe droughts without bushfires. Dramatic increases in turbidity, iron, manganese, organic carbon, phosphorous and nitrogen in the reservoirs resulted from the 2003 fires and these persisted for over 12 months. This made water unfit for reticulation as the water needed treatment and forced water restrictions on the ACT for the first time since 1968. The fires revealed problems in the monitoring of catchment water resources and in the management of water resources in the ACT. From our analysis of the aftermath of the fires we suggest changes to the management of water resources in the ACT to improve planning for and response to bush fires and their consequences for domestic water supplies. The relationship between the occurrence and effects of major bush fires with climate and hydrological variables is investigated in this paper.

**Keywords:** drought, bushfires, catchment yield, water quality; water resource management

## INTRODUCTION

Bushfire effects on the catchments of rivers that are used for town water supplies are of great concern. The primary effects are the elimination of the vegetation and the generation of watershed pollution from ash and burnt litter. The secondary effects resulting from the fire are hard to predict and vary from catchment to catchment but can include short-term increase/decrease in runoff and baseflow, and an increase in sediment and ion concentrations in runoff. During the process of recovery this reduction in runoff from the catchment and increase in suspended and dissolved loads are of major concern for the reliability of supply to the city depending on the water.

The Cotter River catchment in the Australian Capital Territory (ACT), eastern Australia has been a major source of water for the national capital, Canberra, since 1918. The Cotter catchment is located along the western edge of the ACT as shown in Fig. 1. Three dams: Corin, Bendora and Cotter (from upper to lower catchments) have been built on the Cotter River and their capacities and relative contributing catchment areas shown in Tab. 1. The other major water source for Canberra is the Googong dam located on the Queanbeyan River (Fig. 1).

Tab.1: Summary of dams in the Cotter catchment.

DAM	Catchment Area (km <sup>2</sup> )	Capacity (GL)	Mean runoff (GL/yr)
Corin	197	76	76
Bendora	91	11	34
Cotter	193	4.7	36

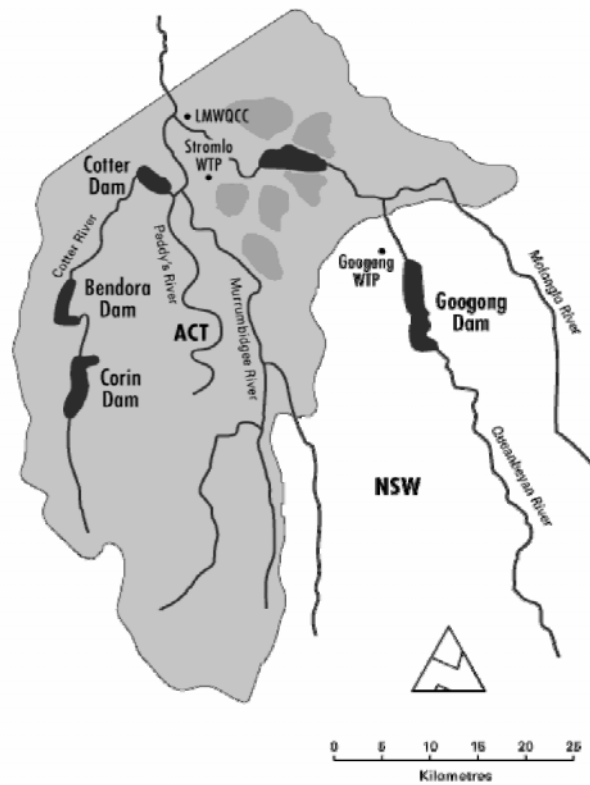


Fig. 1: Location of main dams of the ACT and relevant catchments (ACTEW, 2004b).

Following construction of the Cotter Dam, cleared grazing land in the lower Cotter catchment was quickly replaced with *Pinus Radiata* to improve the quality of water in the Cotter Reservoir but the commercial forestry practices compromised water quality in the lower catchment. Dams in the upper Cotter, completed in 1968, were fed from a near pristine, mixed native forested catchment. Water quality was so good from this source that flocculation and filtration facilities were not installed and water only required chlorination, minor pH adjustment and fluoridation.

Previous work following the 1939 bushfires in alpine ash (*Eucalyptus Regnans*) catchments in the southern Australia state of Victoria found large decreases in yields for up to 50 years following the fires as forests regrew (Langford, 1976; Kuczera, 1985). There were known to be fires in the ACT in 1920, 1926 and 1939. The 1939 fire was exacerbated by weather with strong winds, which resulted in spot-fires up to twenty-four km ahead of the fire-front (Carey *et al.*, 2003).

In January 1983, following a prolonged drought approximately 30% of the upper Cotter catchment was burnt in a bushfire. This was the last major fire in the ACT prior to the fires of December 2001 where 20 000 ha of grasslands and 145 ha of pine plantations were burnt. At the end of the 2002-3 drought, major bushfires swept through the Australian Capital Territory (ACT). These January 2003 fires devastated the national capital, Canberra, and burnt out 165 000 hectares of landscape, caused major loss of private housing, infrastructure including water supply treatment plants, softwood plantation, and publicly owned facilities. Approximately 70% of the ACT, including 90% of Namadgi National Park and, five of the nine ACT river catchments were burnt to varying intensities—all or almost all of the Cotter, Gudgenby–Naas and Paddys River catchments, and parts of the Molonglo and Murrumbidgee River catchments.

In this paper we review the impact of those fires on both the quality and quantity of water from the Cotter catchment and examine the implications for the management of catchments and water resources in the ACT (ACT Government, 2005).

## CLIMATE ISSUES

Droughts are one of the main driving mechanisms for bushfires in that soil moisture levels are lowered significantly due to low rainfall and the forests become stressed. There is evidence of a strong relationship between El Niño Southern Oscillation (ENSO) and The Interdecadal Pacific Oscillation (IPO) severe droughts and subsequent bushfires.

### El Niño Southern Oscillation (ENSO) Effect

ENSO is a natural fluctuation of the tropical Pacific atmosphere and ocean. ENSO variability is defined in terms of the Southern Oscillation Index (SOI) which is the Tahiti minus Darwin mean sea-level pressure difference, normalized with a base period of 1933–1992 (Troup, 1965; Folland *et al.*, 2002). Sea temperatures, winds, and rainfall patterns in the Pacific show a distinct difference between the El Niño and La Niña phases. In the El Niño phase, when the SOI is strongly negative, the key feature is that tropical sea surface temperatures in the central and eastern near-equatorial Pacific can become several degrees warmer than normal. The resulting climate on the East coast of Australia is one of drought. Major bushfires and drought are linked as the natural forested catchments dry and become more prone to bushfires, both natural and human generated.

### The Interdecadal Pacific Oscillation (IPO)

The Interdecadal Pacific Oscillation (IPO) is a natural fluctuation of sea surface temperatures and winds in the Pacific. The IPO has been shown to modulate interannual ENSO-related climate variability over Australia (Power *et al.*, 1999). The key difference is that IPO operates over decades, whereas ENSO operates over 2 to 7 year cycles, and the IPO involves higher latitudes (particularly the North Pacific) as well as the tropics and New Zealand (Salinger *et al.*, 1995). The IPO is characterized using the time series of an Empirical Orthogonal Function of 13 year low pass filtered global Sea Surface Temperatures as shown in Fig. 2 (Folland *et al.*, 1999; Power *et al.*, 1999). Three main phases of the IPO have been identified during the 20<sup>th</sup> century: a positive phase (1922–1944), a negative phase (1946–1977) and another positive phase (1978–2000). The positive phases of the IPO correspond to generally drier periods in eastern Australia.

There is a strong link between the occurrence of ENSO events and positive IPO events as shown in Fig. 2. During positive IPO periods, there are frequent or more intense El Niño events which are highly correlated with drought and risk of fire in the Eastern regions of Australia (Verdon *et al.*, 2004). Bushfires that have occurred in the Canberra region are marked on Fig. 2. The combined effect of natural and human caused severe fires in the Alps in the fire seasons of 1851/52, 1902/03, 1938/1939 and 2002/2003. In the case of most of these wildfires, much of the Cotter catchment was burnt out. These all correspond with positive IPO and the occurrence of an ENSO event. In drought conditions the availability of dry fuel is a major factor in fire spread which is highly likely in the summer January –early February period.

Nevertheless, it is possible to estimate the probability that rainfall and temperature over Australia will be above or below the median for up to a season ahead, using relationships such as IPO and the Southern Oscillation Index (SOI). ENSO has the greatest impact on the Australian region, but it needs to be borne in mind that linear correlation coefficients of SOI with regional rainfall are at most in the range 0.6 to 0.7 (Verdon *et al.*, 2004) and many regions are lower than this. Even where the relationship is strongest, less than 50% of the variation in rainfall is predictable from this source.

ENSO relationships have a strong influence on the seasonal climate of certain parts of Australia, but there are other ocean/atmosphere systems that impact, including the Madden-Julian Oscillation (MJO) in the tropics, (described in <http://envam1.env.uea.ac.uk/~e058/mjo.html>) and Indian Ocean sea surface temperatures (Drosowsky and Chambers, 2001).

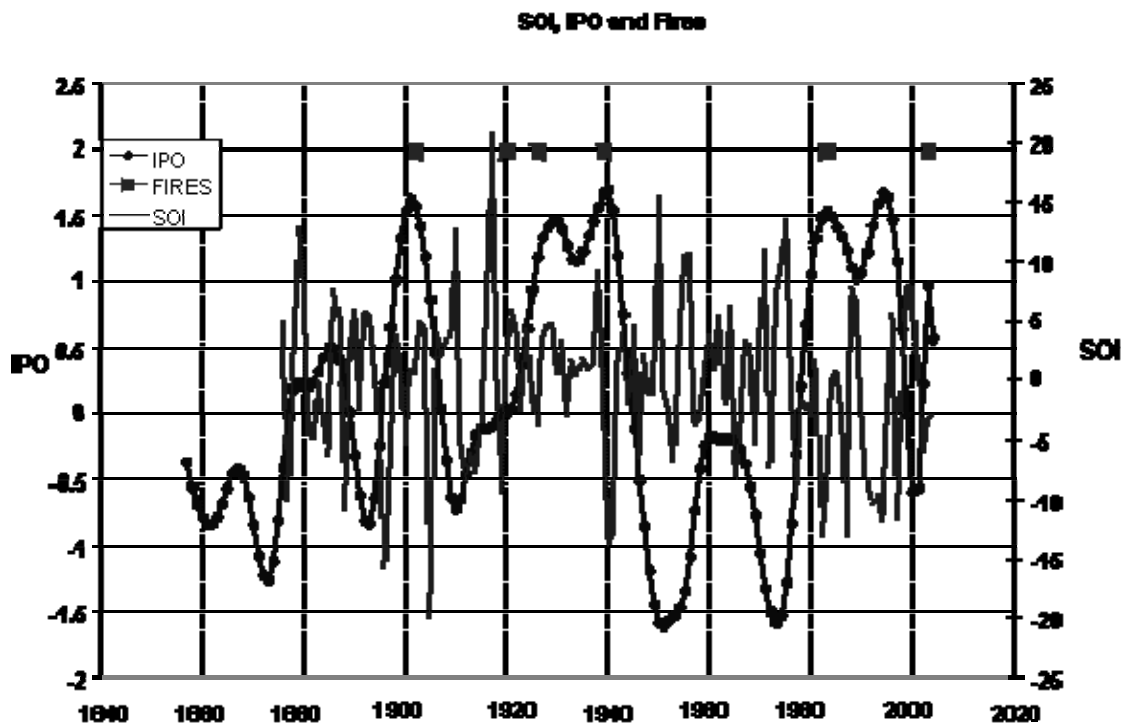


Fig. 2: SOI, Interdecadal Pacific Oscillation (IPO) and Cotter Catchment Bushfire Occurrence.

## SEVERITY OF FIRES

Most of the Cotter catchment was severely burnt in the 2003 fire. The classes of fire intensity classes in eucalypt forests (Cheney, 1981) are shown in Tab. 1 which includes a column (AMOG and EcoGIS, 2005) that relates fire intensities and flame heights to severity effects in eucalypt forests.

The 1983 fire was assumed to be an infrequent mixed severity fire, which equated to High /Very High in Tab. 2. This fire produced soil erosion in both topsoil and sub-soil, mainly from granite derived soils, principally yellow podzolics. The 2003 fire varied in intensity but large areas, particularly steeper eastern slopes had Very High fire intensities. Organic and sediment production in the years following the 1983 fire was about half that of the 2003 fire.

## ISSUES FOR CATCHMENT AND WATER SUPPLY MANAGERS

Following a bushfire in the Cotter Water Supply catchment, a number of impacts affect the operation of Canberra's water supply system. Pristine streamflows from the forested catchment become polluted with the residues of the fire and soils are prone to erosion as there is no vegetative cover. There has been a great deal of conjecture on the changes in yield of streamflow that come from the burnt catchment. The vegetative of the catchment is altered dramatically as is the dynamics of the soil water. Forecasting of fires and the resultant effects both in water runoff and water quality is important to managers of the Canberra water resources for the town supply.

### Runoff Quantity

There were a number of reports and papers written on the Jan 1983 fire (Kulik and Daniell, 1986; Daniell and Kulik, 1988; Kuczera, 1998) and following the Feb 2003 fire (Carey *et al.*, 2003; White *et al.*, 2005). Bushfires usually occur during drought conditions when the vegetation dries out. This creates difficulty in establishing whether any trends in water yield are due to the fire event or due to the drought. The 1983 fire event also corresponded to the most severe short term drought on record further complicating the problem. If the duration of the drought is considered then the present drought from 2000-2005 is the most

severe on record in terms of 24 month rainfall totals, while the 1983 drought is the most severe in terms of 12 month rainfalls.

Tab. 2: Range of Fire Intensities and Flame Heights (Cheney, 1981).

Class	Fire intensity (kw/m)	Max. flame height (m)	Remarks	Severity Effects in Eucalypt Forest
Low	< 500	1.5	Upper limit recommended for fuel-reduction burning.	Partial removal of litter and ground cover layer. Scorch or partial removal of low shrub canopy
Moderate	501-3000	6	Scorch of complete Crown in most forests.	More complete removal of litter layer. Low and medium shrub layer canopy consumed. Partial canopy scorch, depending on tree height.
High	3000-7000	15	Crown fires in low forest types - spotting > 2 km.	Litter layer removed down to mineral soil. 100% canopy scorch of tree layer.
Very High	7000-70000	> 15.0	Crown fire in most forest types - fire storm condition at upper intensities.	Litter and top of soil layer completely burnt. All vegetation layers completely removed.

A simple method used to find whether there was any definitive relationship before or after a bushfire is to use a flow duration curve mapped against an equivalent monthly rainfall exceedance curve as shown in Fig. 3. March 1983 and February 2003 were high rainfall events with low runoff events but this was mainly due to recovery from the drought. Generally after the bush fire, initial moisture levels had recovered an equivalent exceedance runoff corresponded to an equivalent rainfall probability. Note that there were some months immediately after the fire where their exceedances for both rainfall and runoff corresponded very closely as well as some months where they were higher for rainfall and/or for runoff.

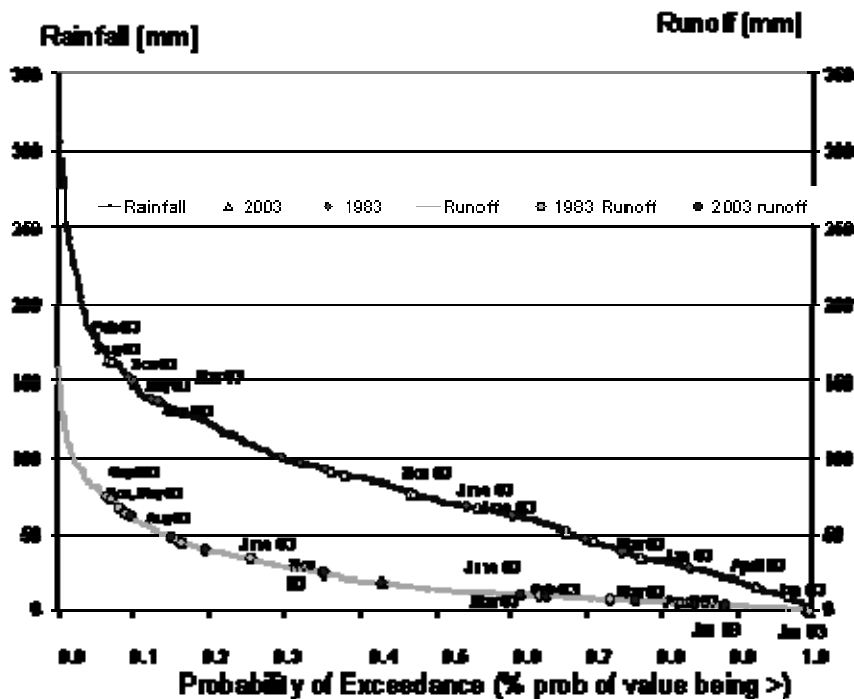


Fig. 3: Corin Catchment Rainfall and Runoff Exceedance Values.

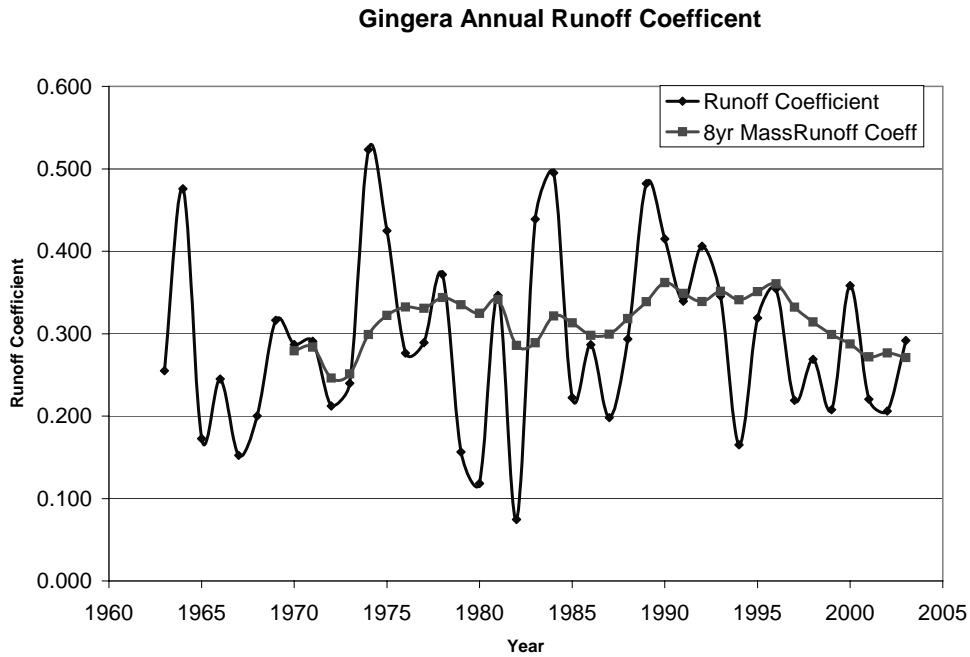


Fig. 4: Plot of Monthly Runoff Coefficient for Gingera Station in Corin Catchment.

Fig. 4 shows the monthly runoff coefficient for the catchment for the 40 years of record for Gingera gauging station upstream of Corin Reservoir. The monthly average runoff coefficient over the period of record is 0.24 i.e. 24%. However if calculated as an average annual runoff coefficient it is 0.292 and if calculated as total runoff coefficient over the period of record (1963 to 2003) it is 0.309 i.e. 30.9%.

When comparing different periods of time pre- and post-bushfire we shall use the total runoff coefficient. There is no appreciable change from the 20 years prior to the 1983 fire which has a runoff average of 29.5% and an average rainfall of 967.8 mm. The 20 years following the fire has a runoff average of 32.3% with an average rainfall of 997.5 mm.

Examination of Fig. 4 suggests that the annual dry periods were not as low post-bushfire as those pre-bushfire. Very low runoff averages occurred in 1968, 1980 and 1982. There is no statistical evidence that the runoff has changed following the bushfire although both the standard deviation of rainfall has dropped from 283 to 183 mm and that of runoff has dropped from 181 mm to 140 mm. Visually in Fig. 5 there is a perceptible increase in runoff following the fire.

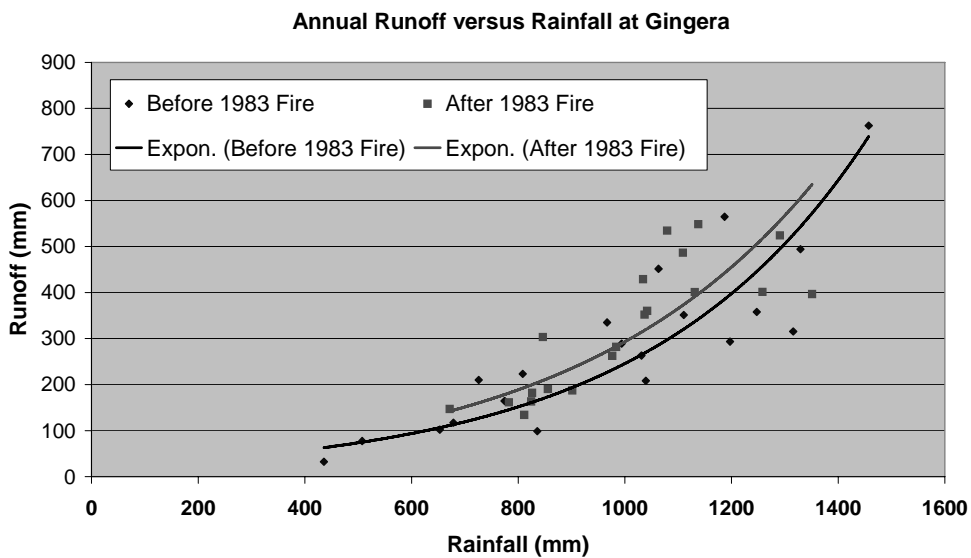


Fig. 5: Curves of rainfall and runoff pre 1983 and post 1983 bushfire.

In order to assess whether there have been significant yield trends following fire, it is necessary to use an approach that is capable of filtering out climate variations. Kuczera (1998) used a daily lumped catchment model to analyse temporal trends in monthly residual catchment yields for the Licking Hole catchment following the 1983 fire. He found that there was an increase in yield which was discernible up to about 36 months after the fire. After that there was no long-term change in catchment yield. This increase in yield was attributed to reductions in interception and evapotranspiration due to vegetation loss. More mature trees largely survived the fire and regenerated by epicormic growth so resulting in no long-term yield reduction.

### Runoff Quality

There have been a number of reports on water quality following the bushfires for both the 1983 and the 2003 events. Water quality data in Bendora dam for the period 1968 to 2003 shows that despite the near pristine conditions of the pre-fire catchment, a build-up in turbidity, and in Fe and Mn occurred annually in the dam in the past. This is due to the release of Mn and Fe from bottom sediments into the increasingly anoxic waters. This mechanism is consistent with the pH and EC profiles in the reservoir. The turbidity in the water is strongly correlated to the iron concentrations. In the pre-fire period, only two major turbid inflows occurred. The first in April 1983 was due to intense rainfall following the 1982-3 drought and the January 1983 bushfire in the upper third of the catchment above Corin Dam. In this event the turbid plume flowed along the bottom of Bendora reservoir. The second was due to intense rains in January 1995 following the 1994 dry period when the turbid plume was injected above the hypolimnion. In March 2003, following the bushfires, the peak turbidity was thirty times that of the 1983 peak. Large quantities of sediment were deposited into the dams from the denuded catchments. After the 2003 fires, the turbid plume flowed along the bottom of the reservoir. (White *et al.*, 2005). In addition after the 2003 fires, Mn, Fe, P and N concentrations were up to one order of magnitude higher than previous peaks. Further sediment flows have led to the construction of a \$40 million Water Treatment Plant.

One of the key questions facing water resource managers in Canberra is the long term implication for water quality. Fig. 6 compares the pre- and post- 2003 fire turbidity exceedance values for the 3 m level in Bendora Dam, close to the off-take level. Taking the guideline level of problem turbidity as 5 NTU, Fig. 6 shows that the pre-fire exceedance value of this limit was 2% compared to a post-fire exceedance of 10%.

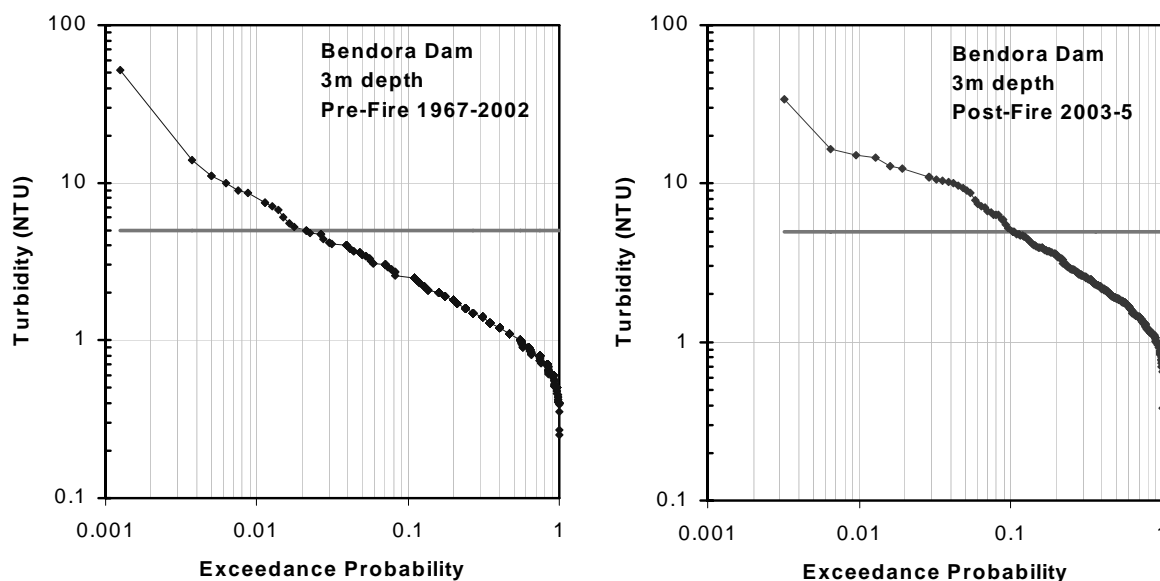


Fig. 6: Pre- and post-fire exceedance probabilities in Bendora Dam at 3 m depth for the 2003 bushfire.

## **Sediment movement and Water quality runoff**

Immediate post fire measurements for both the 1983 and 2003 events of dissolved nutrients, dissolved organic carbon, turbidity, sediment, and dissolved oxygen (Daniell and Kulik, 1988; Wasson *et al.* 2003) showed a shift from pre-fire conditions towards less favourable aquatic living conditions for either aquatic vertebrates, such as fish, or invertebrates. The sediments contain much higher concentrations of particulate matter, lower oxygen levels, and higher concentrations of Manganese and Iron. The first flush appeared to contain higher levels of nutrients, because of the initial higher delivery of organic sediment into streams. A month later similar measurements showed much lower concentrations of organic carbon, sediment, and Manganese and Iron.

The anoxic conditions in reservoirs, caused by increased organic sediments and lower dissolved oxygen, create reducing conditions which led to further release of Manganese and Iron in the storages. Concentrations of Manganese in soil in the upper Cotter catchment is between 0.01 and 0.03 mg per litre (Talsma 1983), and appears to be two to three times higher in granite derived soils compared with that found in soils derived from Ordovician sediments. Post-fire concentrations of dissolved Manganese immediately after storms in 2003 were about two orders of magnitude higher than that found in the soil, which might suggest concentrations of Manganese increased because of the organic-rich sediment reaching streams. Smaller fires which burn less of a catchment than the 1983 and 2003 fires and are of low-to moderate intensity are unlikely to produce similar increases in organic carbon, sediment, and nutrients that were seen with fires of high to severe intensity across most of the catchment.

## **Effects on Water Storages**

It is estimated that 19300 tonnes of inorganic sediment and 1900 tonnes of organic matter were deposited in Bendora Dam (White *et al.*, 2005) in the aftermath of the 2003 fires. The sources of the sediment pre and post fire were found to be mainly from topsoil and these are shown in Tab. 2 (Roach, 2004).

The sediment and organic matter yield were shown to markedly increase within a few weeks after the runoff events and then drop back to pre-fire levels within 2 years post-fire. Examples of event runoff and suspended sediment are shown in Fig. 7 for the 1983 fire indicating that the process of transport of material within an event is not simple and depends on the deposition and availability across the catchment.

Tab. 2: Estimates of sediment and organic matter washed into Corin reservoir for before and after 2003 bushfire (Roach, 2004).

Year	Inorganic sediment (t/yr)	Particulate organic carbon (t/yr)	Sediment yield (t/km <sup>2</sup> /yr)
Annual-from 1968	316	23	2.3
2003	1663	137	9.2

The two peaks of suspended sediment on the rising limbs of the hydrographs demonstrate the erosive mechanism operating. The second rise in sediment runoff also corresponds to an increase in flow in the September event. Many different forms of hysteresis loops for water quality and sediment transport were observed. Overall sediment inflows into the reservoirs in the immediate post-fire period led to a drastic decrease in water quality making the water unfit for reticulation for extended periods.

### Suspended Sediment Licking Hole Creek - 2/05/1983, 28/11/1983

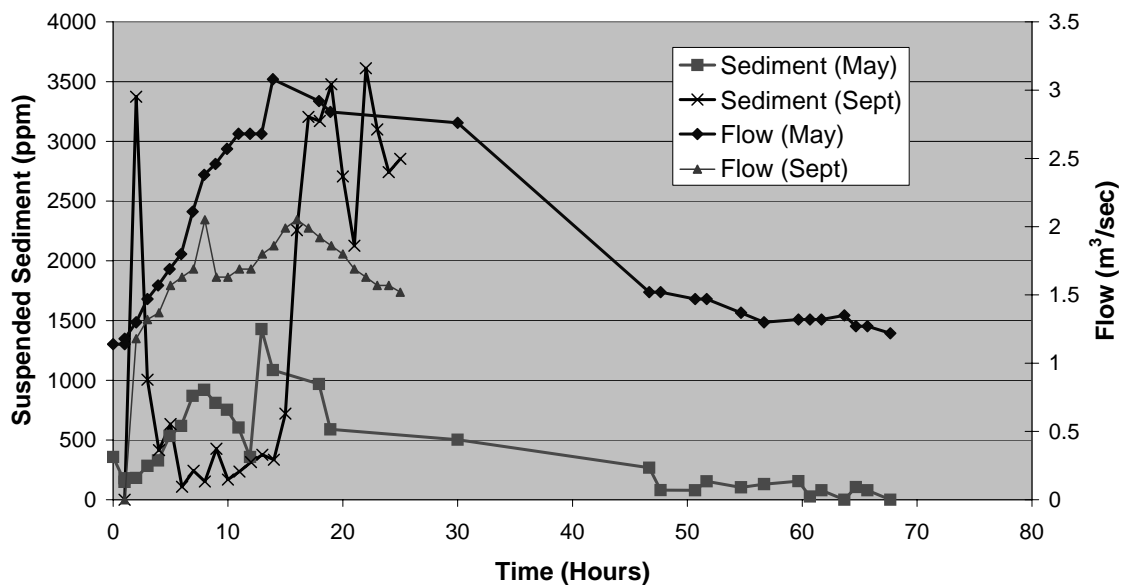


Fig. 7: Suspended Sediment and Flow following 1983 bushfire in Corin Catchment.

## STUDIES UNDERTAKEN

To compare the fire affected period of runoff with non-fire affected period is difficult as only two significant fires have occurred within the Corin catchment during the time that data has been available. The analyses are compounded by the fact that the fires in 1983 and 2003 burnt different proportions of the catchment. The 1983 fire is estimated to have burnt nearly 29% of the Corin catchment (Worthy and Wasson, 2004) with one catchment the Licking Hole Creek Catchment being monitored following the fire (Daniell and Kulik, 1988). The 2003 bushfires damaged almost all the Cotter catchment with 42% of the forest canopy destroyed in the Corin sub-catchment (ACTEW, 2004a). However, these estimates are only approximate.

Bushfires usually occur during drought conditions when the vegetation dries out. This creates difficulty in establishing whether any trends in water yield are due to the fire event or due to the drought. The 1983 fire event also corresponds to the most severe 12 month drought on record further complicating the problem.

Catchments can take years to recover fully from fire events. ACTEW (2004b) suggested that reduced flows could be expected for more than 50 years following a fire event. This was based on experience following the 1939 bushfires in alpine ash (*Eucalyptus Regnans*) catchments in the southern Australia state of Victoria. There is however no scientific evidence to support this assertion for the mixed eucalyptus forests of the Cotter catchment. There is also no evidence to suggest that the Corin catchment had fully recovered from the 1983 Licking Hole Creek fire before the advent of 2003 fire, although Kuczera's (1998) analysis suggests that there was no long-term trend in catchment yield for the period 1986-1998. It is difficult to ascertain the state of growth of the whole catchment before the 1983 fire and what factors cause the variability of streamflow in the catchment (NCDC, 1986). As these factors cannot be established it is difficult to determine whether the effects of the two fire events are overlapping. For example, changes in vegetation structure resulting from the 1983 fire could still have been occurring at the onset of the 2003 fire. Some of the factors and discussion are included in Kulik and Daniell (1986) where the water quality effects from both surface flow and groundwater flow are presented for the 1983 fire.

## CATCHMENT MANAGEMENT

A whole-of-government, Cotter Catchment Management Committee used to oversee management of the Cotter water supply catchment but this was abandoned in the 1980s. Management is now embedded in ACT Urban Services, a federation of customer-focussed businesses. Environment ACT is one of those businesses and ACT Parks and Conservation, within Environment ACT, manages the Namadgi National Park, containing the Cotter Catchment, for a broad range of interests, but concentrating on the preservation of biodiversity.

The ACT's *Water Resources Act 1998* appointed ACT Environment as one of the regulators for water in the ACT (the others are the ACT Prices Commissioner and ACT Public Health). ACT Forests manages the Lower Cotter Plantations and monitors water quality throughout its plantations and reports results to the Environment Protection Authority. Water in dams and pipes in the Cotter is overseen by the multi-utility, ACTEW Corporation, a government-owned holding company with interests in providing water and wastewater services (as well as natural gas, telecommunications and energy) to Canberra and surrounds. The ACT Government through ACTEW Corporation owns the existing water and wastewater network, catchment and treatment infrastructure and associated strategic water and wastewater assets.

ACTEW Corporation formed a joint venture with the private company AGL in 2000. The public-private joint venture company *ActewAGL* is an ACT-based electricity, natural gas, water and sewerage services utility that contracts its services to ACTEW Corporation for a fixed fee. ACTEW Corporation buys bulk water from the ACT Government, and contracts *ActewAGL* to treat water and on-sell it on behalf of ACTEW to communities and industry in the ACT who also pay to have sewerage and wastewater removed and treated by *ActewAGL*. *ActewAGL* returns almost half of the water abstracted from catchments to the Murrumbidgee River as high-quality treated water, part of the environmental flow obligations negotiated by Environment ACT. Because of the fixed fee contract, the major incentive for *ActewAGL*, which has the major concentration of water supply and treatment expertise in the ACT, is for cost minimisation. Monitoring of rainfall, quantity and quality of water in the water supply dams and catchments is contracted to ECOWISE Environmental, a subsidiary of *ActewAGL*.

The ACT Prices Commissioner has ruled that ACTEW should pay the ACT Government a water abstraction fee to cover the environmental costs of for water abstracted from catchments. This abstraction fee is not hypothecated, that is the environmental levee is not exclusively devoted to catchment management and improvements to aquatic environments.

Sydney had a major water crisis in 1998 when *Cryptosporidium* and *Giardia* were detected in Sydney's water supply. Peter McClellan, QC, in a subsequent detailed inquiry, examined the events leading to this water crisis. He found that there was no single authority ultimately responsible for the health of Sydney's water supply catchments and storage reservoirs. The Sydney Catchment Authority was established in 1999 following Mr McClellan's recommendations. The Authority's tasks are to protect catchments, improve water quality, protect and manage Sydney's 21 dams and to educate and involve communities in protecting its catchments.

It is salutary to compare the mission statements of the ACT's water organisations with that of the Sydney Catchment Authority, "*healthy catchments, quality water-always.*" ACT Environment's vision, *environment and heritage -secure, shared sustainable*, reflects its broad responsibilities. ACTEW Corporation's vision is *to be the benchmark multi-utility operating in the private-public partnership model* while the vision of *ActewAGL*, *to connect with customers*, clearly reflects its responsibility to its shareholders. These ACT water organisation vision statements strongly suggest that water is but one of many responsibilities.

Following the 1983 bushfire, a report was submitted to the then ACTEW Board, pointing out the vulnerability of ACT catchments and water supplies and the need for a full water supply treatment plant. The report was not acted on until after the 2003 fire. The immense value of a well-managed catchment as the primary water quality barrier is widely recognised. The formation of an ACT Catchment Authority, dedicated to the protection, wise use, management and planning of the ACT's bulk water supply sources could help avoid future water crises in the ACT.

## CONCLUSIONS

The runoff immediately following the 1983 bushfire in the Corin Catchment seems to increase but then settles down within about 36 months to runoff no different than prior to a bushfire. The small period of

record following the 2003 fire seems to follow the same trend. The natural variability in the catchments of streamflow makes it difficult to discern any trend as recoveries from drought tend to influence the runoff achieved as does the persistence of the effect of one wet year to the next.

It is clear that the 2003 fires were a unique event for the Upper Cotter catchment water reservoirs. The fire and subsequent rainfall appear to be a one in 400 year event. Because of the quality of water when large quantities of sediment were deposited into the reservoirs from the denuded catchments the construction of a water treatment plant was required. Some of the questions on frequency of severe events and the consequences of such events have attempted to be answered by this paper. There will need to be changes in dam operation and catchment management to better respond and enable the systems to be more resilient to such events.

The biggest concern of bushfires is the immediate effects on the water storages and the vulnerability of the catchment to large storms that can severely erode the catchment and create sediment and turbidity problems in downstream storages.

It is imperative that the response of water supply reservoir systems to extreme events is studied. These studies can help identify the frequency of occurrence and recovery times of reservoirs and their catchments, and assist in long term risk evaluation and management strategies for water supply managers. Agencies dedicated to the task of managing water supply catchments for good quality water appear to be desirable.

## REFERENCES

- ACTEW Corporation (2004a) *Options for the Next ACT Water Source*. April. Available: [http://www.actew.com.au/publications/ACTwaterSourceOptions\\_pt1.pdf](http://www.actew.com.au/publications/ACTwaterSourceOptions_pt1.pdf), Accessed: 1 June 2005.
- ACTEW Corporation (2004b) An Assessment of the Need to Increase the ACT's Water Storage. *Future Water Options For the ACT Region in the 21<sup>st</sup> Century*. December 2004.
- ACTEW Corporation (2005). The Cotter Dam Option. *Future Water Options for the ACT Region in the 21<sup>st</sup> Century*, April.
- ACT Government (2005) *ACT Commissioner for the Environment- Fire Indicator*. Available: [www.environmentcommissioner.act.gov.au/text/fire03.html](http://www.environmentcommissioner.act.gov.au/text/fire03.html), Accessed June 2005.
- AMOG and EcoGIS (2005) *ACT Bushfire Summaries Effects of Varying Fire Regimes on Hydrological Processes*. Report No. 5, for The ACT Dept of Urban Services, Jan. 2005.
- Batalla, R. (2001) Hydrological Implications of Forest Fires. *3<sup>rd</sup> International Summer School on the Environment, Fire Landscape and Biodiversity: An Appraisal of the Effects and Effectiveness*. Catalonia (Spain) 9-13 July, 2001. [Online] Available:<http://insma.udg.es/isse2001/papers/Batalla.html>, Accessed 27 June 2005.
- Carey, A., Evans, M., Hann, P., Lintermans, M., MacDonald, T., Ormay, P., Sharp, S., Shorthouse, D. and Webb, N. (2003) *Technical Report 17, Wildfires in the ACT, 2003: Report on initial impacts on natural ecosystems*. Environment ACT, Canberra.
- Cheney, N.P. (1981) *Chapter 7 Fire Behaviour*. In *Fire and the Australian Biota*. Australian Academy of Science, Griffin Press.
- NCDC (1986) Cotter Catchment Resource/Ecological Study Group "Cotter River Catchment Environmental Analysis", National Capital Development Commission. *Technical Paper 45*. Feb.
- Daniell, T.M. and Kulik, V. (1988) Post-Bushfire Hydrochemistry: Simple Graphical Technique of Analysis. *Water International*, 13, 2, 1988, 74-79.
- Drowsdovsky, W. and Chambers L.E. (2001) Near-Global Sea Surface Temperature Anomalies as Predictors of Australian Seasonal Rainfall. *J. Climate*, 14, 1677-1687.
- Folland, C.K., Renwick, J.A., Salinger, M.J. and Mullan, A.B. (2002) Relative influences of the Interdecadal Pacific Oscillation and ENSO on the South Pacific Convergence Zone. *Geophysical Research Letters* 29(13): 10.1029/2001GL014201, 21-1-21-4.
- Folland, C.K., Parker, D.E., Colman, A.W. and Washington, R. (1999) Large scale modes of ocean surface temperature since the late nineteenth century. *Beyond El Niño. Decadal and interdecadal climate variability*, A. Navarra, Ed., Springer-Verlag, 73-102.
- Kulik, V. and Daniell, T.M. (1986) *The effect of a bushfire on Hydrology and Water Quality of Licking Hole Creek, Cotter Catchment, ACT-1*. Techniques of organization, debugging and analysis

- of water quality data. Hydrology and Water Resources Unit, Water Supply, Sewerage and Stormwater Branch Dept of Territories, HWR 86/02, 63 p.
- Kuczera, G. (1985) *Prediction of water yield reduction, following a bushfire in ash-mixed species of eucalypt forest*. Report No. MMW-W-0014. Melbourne and Metropolitan Board of Works, 163 p.
- Kuczera, G. (1998) *Assessment of water yield trends following the 1983 wildfire in Licking Hole catchment*. Ecowise Environmental Ltd., Fyshwick, ACR.
- Langford, K.J. (1976) Change in yield, following a bushfire in forest of E. Regnans. *J. Hydrol.*, 29, 87-114.
- McKee, T., Doesken, N. and Kliest, J. (1993) "The relationship of drought frequency and duration to time scales", *Proceeding of the 8<sup>th</sup> conference on applied Climatology*, Anaheim, CA, American Meteorological Society, Boston, MA, USA, 179-184.
- Office of the Commissioner for the Environment ACT (2003) *State of the environment report 2003*
- Power, S., Casey, T., Folland, C., Colman, A. and Mehta, V. (1999) Inter-decadal modulation of the impact of ENSO on Australia, *Clim. Dyn.* 15, 319-324.
- Roach, I.C. (2004) *Fire as an agent of geomorphic change in southeastern Australia: implications for water quality in the Australian Capital Territory*. Regolith 2004. CRC LEME, 417-418
- Salinger, M.J., Basher, R.E., Fitzharris, B.B., Hay, J.E., Jones, P.D., Macveigh, J.P. and Schmidely-Leleu, I. (1995) Climate trends in the South-west Pacific, *Int. J. Climatol.*, 15, 3, 285– 302.
- Talsma, T. (1983) Soils of the Cotter Catchment Area: Distribution, chemical and physical properties, *Aust. J. Soil Research*, 21.
- Troup, A.J. (1965) The Southern Oscillation. *Q.J.R. Met. Society*, 91, 490– 506.
- Verdon, D.C., Kiem, A.S. and Franks, S.W. (2004) Multi-decadal variability of forest fire risk - eastern Australia. *International Journal of Wildland Fire*, 13, 2, 165-171 DOI: 10.1071/WF03034.
- Worthy, M. and Wasson, R., (2004) Fire as an Agent of Geomorphic Change in Southeastern Australia: Implications for Water Quality in the Australian Capital Territory. In: *Roach I.C. (ed) Regolith 2004*. CRC LEME, 417-418, [Online] Available: <http://crcleme.org.au/Pubs/Monographs/regolith2004/WorthyWasson.pdf>.
- Wasson, R.J., Croke, B.F. and McCulloch M.M. (2003) *Sediment, Particulate and Dissolved Organic Carbon, Iron and Manganese Input to Corin Reservoir*. Report of the Cotter Catchment Fire Remediation Project. ACTEWAGL.
- White, I., Jellett, D., Mueller, N., Wade, A. and Ford, P. (2003) *Preliminary Analysis of Turbidity Profiles Bendora Reservoir, ACT 1993-2003*. Report to ActewAGL, May, CRES, ANU.
- White, I., Govinnage-Wijesekera, D., Worthy, M., Wade, A., Mueller, N. and Wasson, R. (2005) Impacts of the January 2003 bushfires on water supplies in the Australian Capital Territory. In *Water Capital 29<sup>th</sup> Hydrology and Water Resources Symposium* 20–23 February 2005, Canberra. CD Rom ISBN 085 825 8439, Engineers Australia, Canberra.

# CLIMATIC AND HUMAN INFLUENCES ON WATER RESOURCES IN LOW ATOLLS

## **Ian WHITE**

Centre for Resource and Environmental Studies, Australian National University, Canberra, ACT 0200  
Australia  
*ian.white@anu.edu.au*

## **Tony FALKLAND**

Ecowise Environmental, PO Box 1834, Fyshwick ACT 2609, Australia

## **Taboia METUTERA**

Public Utilities Board, PO Box 290, Betio, Tarawa, Republic of Kiribati

## **Eita METAI**

Ministry of Public Works and Utilities, PO Box 498, Betio, Tarawa, Republic of Kiribati.

## **Pascal PEREZ**

CIRAD Montpellier France and Resource Management in the Asia-Pacific Program, Research School of Pacific and Asian Studies, Institute of Advanced Studies, Australian National University, Canberra, ACT 0200, Australia.

## **Anne DRAY, Marc OVERMARS**

South Pacific Applied Geoscience Commission, Private Bag, GPO Suva, Fiji Islands

## ABSTRACT

Low, small islands have water supply problems amongst the most critical in the world. Fresh groundwater, the major source of water in many atolls, is vulnerable to natural and human-induced changes. Storm surges, droughts and over-extraction cause seawater intrusion. Settlements and agricultural activities can rapidly pollute shallow groundwaters. Limited land areas restrict freshwater quantities, which are especially vulnerable during frequent ENSO-related droughts. Demand for freshwater is increasing due to population growth and urbanisation. Water use for traditional crops often competes with water supplies for communities. This paper analyses the impact of frequent severe droughts on the quality and quantity of fresh groundwater in a low, atoll, Tarawa, in the Republic of Kiribati. We also examine the impacts of groundwater harvesting on traditional subsistence crops such as coconuts and of landuse on water quality. Strategies for reducing risks from climate variations and human impacts and increasing resilience are discussed.

**Keywords:** small islands, freshwater supplies, ENSO, drought, pollution, climate variation, risk, adaptation, and resilience

## INTRODUCTION

The Barbados Conference on the Sustainable Development of Small Island States in 1994 focussed world-attention on their fragility and vulnerability. This vulnerability is a product of their remoteness, small size, rapid population growth, restricted capacity and resources and sensitivity to climate variability. Low Gross Domestic Product, limited opportunities and increasing urbanisation are straining traditional support mechanisms (Ward, 1999) and customary traditional approaches to hazard reduction. There are about 8,000 inhabited small tropical islands in the Pacific, Indian and Atlantic Oceans. Many, formed as sand cays, coral atolls or elevated limestone islands, are very small islands, with land areas less than 100 km<sup>2</sup> or with maximum widths less than 3 km. In these islands, surface water resources are usually non-existent because of large soil permeabilities and fresh groundwater resources can be very limited because of restricted land areas and high regolith permeabilities (UNESCO, 1991).

Small island countries face water problems that are amongst the most critical in the world (Carpenter *et al.*, 2002). This is especially so in urban and peri-urban low coral atoll communities (Ward, 1999), on which we concentrate here. Storage of freshwater in atolls to reduce risks during dry periods is constrained by very small land areas, atoll aquifer geology, pressures of human settlements and increasing demand, agricultural activities and waste disposal. Frequent droughts, climate variability and seawater inundation during storms as well as conflicts over traditional resource rights and the demands or urbanised societies add to the difficulties (Falkland, 2002; White *et al.*, 1999b).

The atolls that are most vulnerable to climate variations and human impacts are those with densely populated low islands atolls that rely solely either on thin fresh groundwater lenses for water supplies or those where rainwater is the only water source. In both, limitations in water storage, increase the risk of shortages during dry times. In the past, normal climatic variability in some atoll nations has resulted in declarations of states of emergency and in the evacuation of island populations. In groundwater-dependent atolls traditional, subsistence crops, such as coconuts, swamp taro, breadfruit and pandanus, compete with humans for freshwater (White *et al.*, 2002). Expanding urban atoll communities have the potential to rapidly pollute groundwaters so that water-borne diseases are often endemic. As a consequence, protection of human health is of paramount concern in water supply systems. In populous atolls, land is scarce and the potential to increase wealth through irrigated crops or tourism is restricted. In this paper we examine the impact of ENSO-related droughts on freshwater availability and water quality in a densely populated central Pacific atoll, Tarawa, Republic of Kiribati. We explore the impacts of human settlements on water supply and its quality. Finally we look strategies to protect water resources and reduce risks.

## STUDY LOCATION

Tab. 1 lists the relevant attributes of the central Pacific nation of Kiribati. The country has three key features: the predominance of very low coral atolls; the extent of available freshwater supplies are unknown; and, in its population centres, demand for equals or exceeds supply. In 2000, Tarawa atoll (Fig. 1), the capital and population centre of the Republic of Kiribati, had a population of 36,227 people. Most live in South Tarawa between the islands of Betio and Buota (Fig. 1). North Tarawa is rural with low population density. By 2010 the population of Tarawa is expected to exceed 49,000 with population densities as high as 10,000 km<sup>2</sup>.

In South Tarawa, water supply for the reticulation system is extracted using horizontal infiltration galleries from large freshwater lenses in groundwater reserves on Bonriki (Fig. 2) and Buota islands in the southeastern corner of the atoll. It is then reticulated along the populous South Tarawa as far as the port of Betio in the west. Infiltration galleries minimise the risk of saline intrusion during pumping. Almost all households supplement that supply using dug domestic wells with water of variable quality in both salinity and in contaminants. Some also use rainwater harvesting to supplement supplies.

Although South Tarawa has an average annual rainfall of 2048 mm, it has a high coefficient of variability (CV) of 0.48 (Tab. 1) because of the influence of the migrating Pacific warm pool and has experienced droughts as long as 30 months. In response to the 1998-2001 drought, reverse osmosis desalination units were installed in South Tarawa. These have subsequently failed or are currently not operating. Difficulties in maintaining production from desalination plants is common in many small island countries.

## RELATION BETWEEN RAINFALL, ENSO EVENTS AND GROUNDWATER

### Rainfall

Annual rainfall in Tarawa (Betio) is strongly negatively correlated with the Southern Oscillation Index, SOI (correlation coefficient -0.82). High rainfalls occur during El Niño events and low rainfalls during La Niña episodes. This strong correlation gives rise to frequent severe droughts (approximate frequency 6-7 years) that have major impacts on the availability of freshwater in Tarawa (Falkland, 1992; White *et al.*, 1999a). Fig. 3 shows the strong negative relationship between 12 mth running totals of rainfall at Betio (Fig. 1) and the 12 mth running total SOI. The extreme variability of rainfall and the frequent drought periods are obvious. Tab. 2 shows the significant recorded droughts (rainfall percentile <10%) for 12 mth and 30 mth rainfall totals identified as the period below 40 percentile rainfalls.

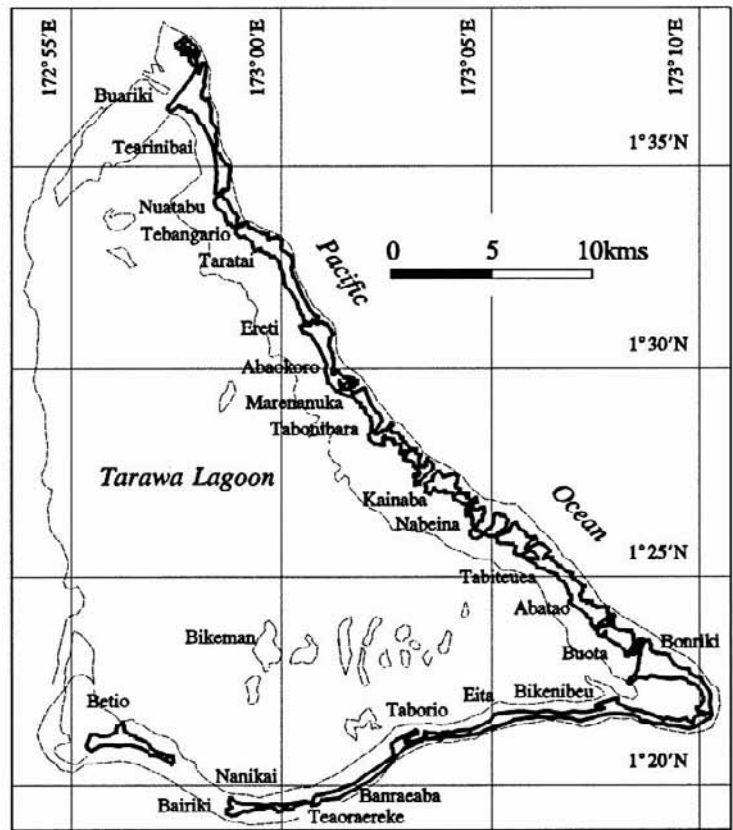


Fig. 1: Tarawa atoll, capital of the Republic of Kiribati.

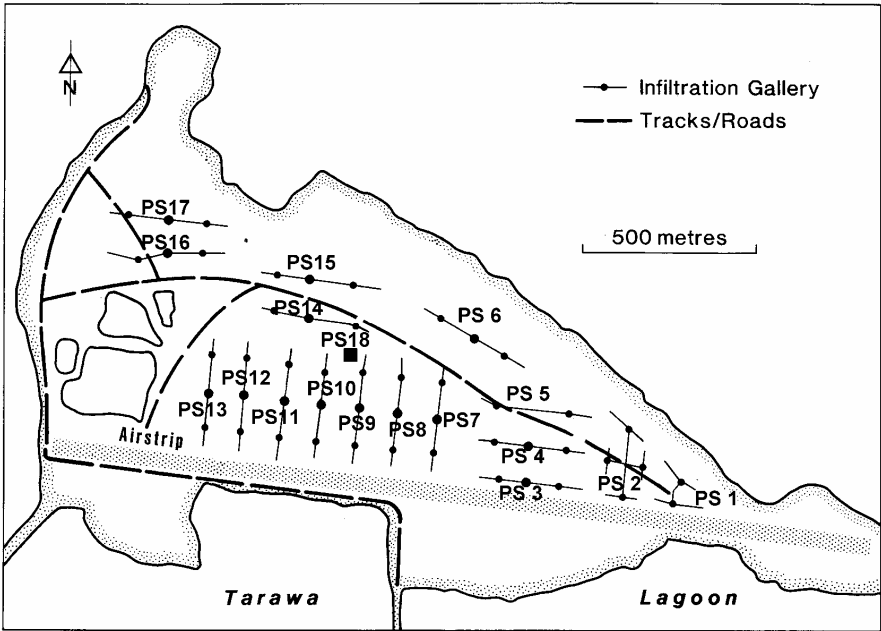


Fig. 2: Distribution of 18 horizontal infiltration gallery pumping stations on Bonriki island.

Tab. 1: Summary of the key features of Kiribati.

Property	Value
Geographic location <sup>1</sup>	1° 25' N 173° E (Tarawa)
Composition <sup>1</sup>	32 coral atolls, 1 raised coral island (Banaba)
Land area (km <sup>2</sup> ) <sup>1</sup>	811
Length of coast (km) <sup>1</sup>	1,143
Length of coast/land area (km <sup>-1</sup> ) <sup>1</sup>	1.41
Highest elevation (m above mean sea level) <sup>1</sup>	81 (Banaba)
Fraction of land elevation < 10 m above msl (%) <sup>2</sup>	99
Climate <sup>1</sup>	Tropical
Cyclones	No
Mean annual rainfall (P mm) <sup>4</sup>	2048 (Tarawa)
Coefficient of variation annual rainfall (CV, %) <sup>3</sup>	48 (Tarawa)
Annual potential evaporation (E mm) <sup>3</sup>	1795 (Tarawa)
Aridity ratio = E/P	0.88 (Tarawa)
Principal water sources <sup>4</sup>	Reticulated groundwater (South Tarawa) Private groundwater wells Public groundwater wells and galleries (outer islands) Private rainwater tanks Desalination* Seawater (washing, toilet flushing)
Estimated per capita demand freshwater (L/cap/day) <sup>4</sup>	50 (Tarawa)
Estimated sustainable yield freshwater (L/cap/day) <sup>5</sup>	49 (Tarawa reticulation system) <sup>†</sup>
Agencies responsible for water supply	PUB (South Tarawa) MPWU (outer islands) Households
Population <sup>1</sup>	103,092 (est. Jul 2005)
Population growth rate (%) <sup>1</sup>	2.25 (est. 2005)
Mean population density (cap/km <sup>2</sup> )	127
Environmental Vulnerability Index (EVI) <sup>2</sup>	3.70
EVI ranking (out of 235 countries) <sup>6</sup>	34/235

<sup>1</sup>CIA The World Factbook (2005), <sup>2</sup>Pratt and Mitchell (2003), <sup>3</sup>Falkland and Woodroffe (1997), <sup>4</sup>Fakland (2005), <sup>5</sup>Alam *et al.* (2002), <sup>6</sup>Kali *et al.* (2003), \*Desalination plants are currently inoperative, <sup>†</sup> Excludes use of private wells or raintanks

It has been shown that 12 mth rainfall percentiles are relevant to domestic wells in islands with thinner freshwater lenses, while 30 mth percentiles are more relevant to islands with thicker lenses (White *et al.*, 1999a). While the Dec 1973 to Apr 1975 drought recorded the lowest 12 mth rainfall amounts on record, the more recent, Nov 1998 to Jun 2002, drought was the most severe for islands with larger freshwater lenses. With the definition of the start (rainfall less than 40 percentile) and end of the drought (rainfall returns to greater than 40 percentile), the average duration of droughts (rainfall <10 percentile) for the 12 mth rainfall totals is 24 months while that for 30 mth totals is 30 mths. The 1998-2001 drought is the longest on record for both rainfall periods. During this drought, almost all raintanks were exhausted, many domestic wells became saline and saline groundwater caused the death or severe die-back of mature (40 year old) breadfruit trees.

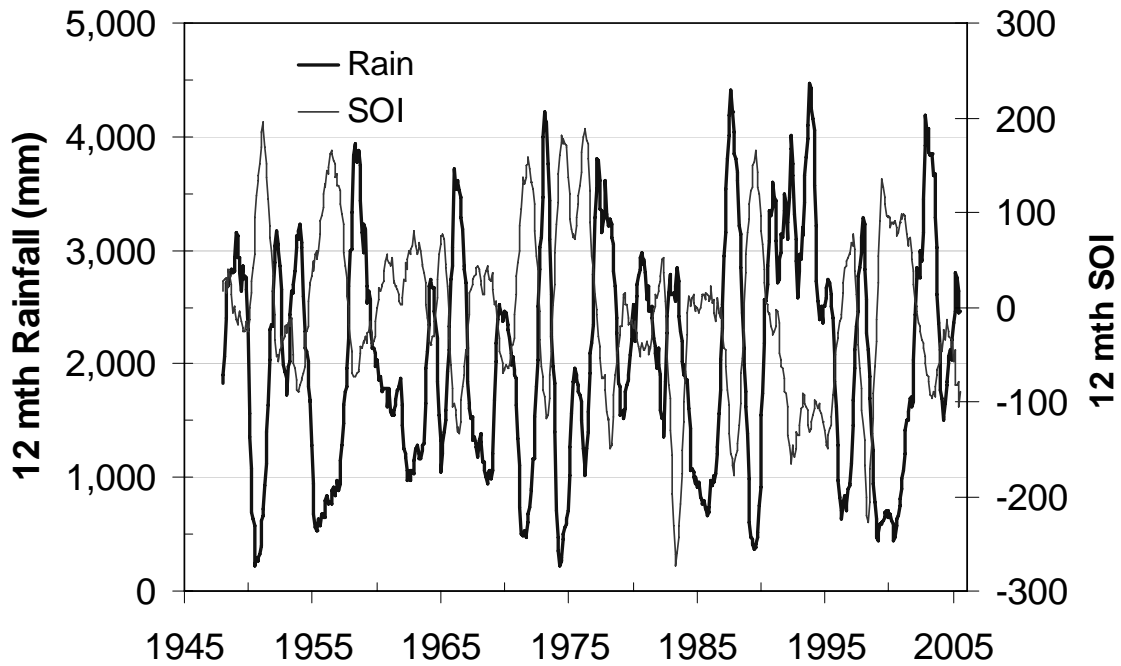


Fig. 3: Relationship between 12 mth running total rainfall and 12 mth running total SOI for Betio, Tarawa atoll, Kiribati.

Tab. 2: Significant droughts in Tarawa for 12 and 30 mth rainfall totals.

12 mth Rainfall				30 mth Rainfall			
Start Date (<40%)	End Date (>40%)	Duration (mths)	Lowest Percentile	Start Date (<40%)	End Date (>40%)	Duration (mths)	Lowest Percentile
Jan-50	Aug-51	19	0.1	Aug-55	Feb-58	30	1.3
Oct-54	Aug-57	34	4.4	Mar-71	Jun-73	27	9.5
Dec-70	Jun-72	18	2.7	Nov-74	Nov-76	24	4.6
Dec-73	Apr-75	16	0.0	Jan-85	Apr-87	27	3.4
May-84	Oct-86	29	9.1	Nov-98	Jun-02	43	0
Oct-88	Mar-90	17	1.3				
Nov-95	Apr-97	17	7.6				
Jul-98	Dec-01	41	2.0				
Mean		24		Mean		30	

## Groundwater

To a first approximation, the maximum thickness of a freshwater lens, from which water is being pumped, to an assumed sharp interface between fresh and saltwater,  $H_p$  (m) is given by the steady state expression (Volker *et al.*, 1985):

$$H_p = \frac{(1-q)^{1/2} W}{2} \left( (1+\alpha) \frac{.R}{2K_0} \right)^{1/2} = (1-q)^{1/2} H_u \quad (1)$$

where  $W$  is the width of the atoll,  $q$  the ratio of pumping rate to recharge rate,  $q = (Q/A)/R$ ,  $Q/A$  (mm) is the annual pumping rate per unit area ( $A$ ),  $R$  (mm) is the net groundwater recharge rate,  $\alpha = (\rho_s - \rho_0)/\rho_0$  where  $\rho_s, \rho_0$  are the densities ( $t/m^3$ ) of sea and freshwater,  $K_0$  is the hydraulic conductivity, (m/y), of freshwater in the Holocene sediments in the horizontal direction and  $H_u$  is the thickness of the unpumped groundwater lens. For Bonriki, the estimated mean groundwater thickness in the absence of pumping is about 15 m.

Eqn (1) can be used to estimate impacts of long term drought on the thickness of the freshwater lens to an assumed sharp interface. The ratio of the freshwater lens thickness during prolonged drought,  $H_d$  to the

long term mean freshwater thickness  $H_m$ , regardless of whether there is pumping or not, follows from eqn (1):

$$H_d = (R_d / R_m)^{1/2} \cdot H_m \quad (2)$$

where  $R_d$  and  $R_m$  are the long term recharges under drought and mean conditions. If we assume that during long term drought the long-term recharge falls from 980 to about 200 mm/year, then eqn (2) predicts that the thickness of the freshwater lens will be reduced to only about 50% of its long term mean. This figure is consistent with measurements at Bonriki during the 1998-2001 drought. This 50% reduction in lens thickness suggests that the watertable elevation could fall by about 400 mm from its long-term mean value during a prolonged drought.

A comparison of the measured watertable elevation in boreholes across Bonriki at the end of the 1998 to 2001 drought with those in more recent, wetter times is given in Tab. 3. This shows that the mean watertable elevation was at least 440 mm lower during the extended 1998 to 2001 drought than in wetter periods.

Fig. 4 shows the change in freshwater depth during wet and dry periods in the groundwater lens on Bonriki island (Fig. 2), in a salinity borehole at the seaward edge of the island, to the 12 mth rainfall deciles. The edge of this thick freshwater lens responds dramatically to long dry periods. Boreholes towards the centre of the island showed relatively smaller decreases in the thickness of the freshwater lens, which in the centre is over 20 m thick.

Tab. 3: Measured change in mean watertable elevation due to drought, Bonriki.

Measurement date	Mean watertable elevation above arbitrary datum (mm)
3-4 November 2001	190
27-28 February 2003	630
Difference	-440

As the lens thin during dry periods, the salinity of the fresh groundwater also increases. Fig. 5 shows the increase in groundwater salinity (electrical conductivity, EC) of groundwater pumped from both Buota and Bonriki groundwater reserves during the severe 1998-2001 drought. Even though the EC peaked at around 1,000  $\mu\text{S}/\text{cm}$  at the end of 2001, the water was still quite acceptable for domestic use. Since this was the worst drought on record for 30 mth rainfalls, this illustrates the robustness of large freshwater lenses in islands that are of widths approaching 1 km.

The impacts shown in Fig. 4 and 5 may not be due to just climate alone, since groundwater is also extracted from these islands at combined rates approaching 1,700  $\text{m}^3/\text{day}$ . The impact of pumping on the freshwater lenses will now be considered.

## IMPACT OF PUMPING ON GROUNDWATER ELEVATION AND THICKNESS

Traditional land owners in islands used as groundwater sources for freshwater reticulation are concerned over the impacts of groundwater pumping on the health and productivity of traditional crops (White *et al.*, 1999b). These concerns have centred on the effects of pumping on lowering unconfined watertables so that taro crops are unproductive or coconut yields are reduced. Pumping in existing fresh groundwater extraction reserves has also been blamed for the unhealthy appearance or death of coconut trees and increasingly brackish domestic wells, possibly through an increase in the salinity of the groundwater. Coconut trees have an unusually high requirement for chlorine and can tolerate a moderate amount of salinity in groundwater provided the saline watertable fluctuates with the tide or is sufficiently deep. However, while they can withstand brief exposures to seawater, permanent exposure to water with salinity of 2000 mg/L TDS or greater (EC above 2,800  $\mu\text{S}/\text{cm}$ ) severely retards growth (Foale, 2003).

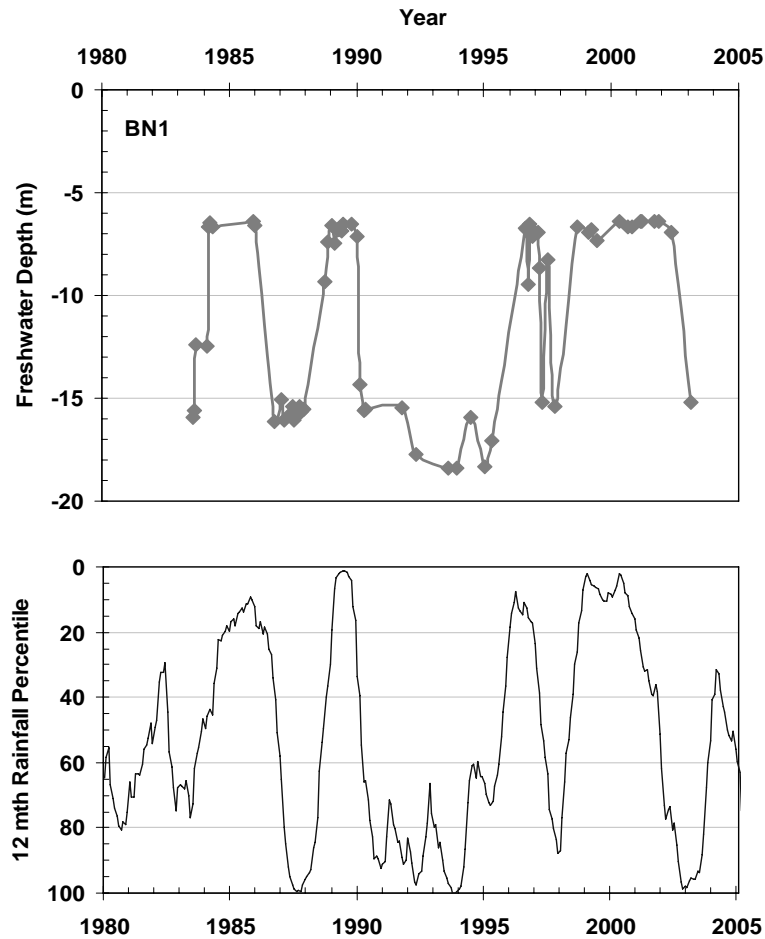


Fig. 4: Change in depth below ground surface of the freshwater/salinity transition zone for a salinity borehole (BN1) at the ocean edge of Bonriki Island, Tarawa atoll and its relation to 12 mth rainfall percentiles.

The annual water balance for a freshwater lens in a low coral atoll in which extraction by pumping is taking place (see Fig. 1) is given by (Falkland, 1992):

$$R = GF + D + Q/A + \Delta S \quad (3)$$

where  $GF$  (mm) is the groundwater discharge to the sea and lagoon,  $D$  (mm) is the mixing or dispersion losses at the base of the lens, and  $\Delta S$  (mm) is the change of freshwater volume per unit area stored in the lens (positive when recharge is greater than the losses, negative when recharge is less than the losses). In the long term,  $\Delta S$  is negligible and recharge equals losses,

$$R = GF + D + Q/A \quad (4)$$

Estimated mean annual components of the water balance in eqn (4) for Bonriki are given in Tab. 4. In Tab. 4, the evapotranspiration component is the water used by vegetation. We have assumed here that this component is unchanged by pumping (White *et al.*, 2002). Eqn (1) suggests that the average mean groundwater thickness of the freshwater lens during pumping at the rate given in Tab. 1 should be about 10.9 m. If  $h_0$  is the height of the watertable above mean sea level ( $h_0 = H_u \alpha / (1 + \alpha)$ ), then, during pumping, the average watertable elevation should drop by about 140 mm (Tab. 1).

Fig. 6 shows that the watertable in Bonriki gallery pump stations fluctuates twice daily in concert with the tidal signal from the Betio tide gauge recorder. This daily fluctuation is caused by the tidal pressure signal transmitted mainly through the karstic Pleistocene limestone aquifer beneath the freshwater lens (Wheatcraft and Buddemeier 1981, Oberdorfer *et al.*, 1990) and transmitted upwards to the groundwater

surface. The results for the watertable in the Bonriki gallery pump station PS 16 show a twice-daily change of up to 170 mm in watertable elevation can be generated by the tidal cycle. In other galleries, tidal amplitudes of up to 300 mm have been measured in the watertable elevation. The impacts of rainfall on watertable elevation are also shown in Fig. 6 where it can be seen that rapid rises as high as 0.65 m can occur during rainfall.

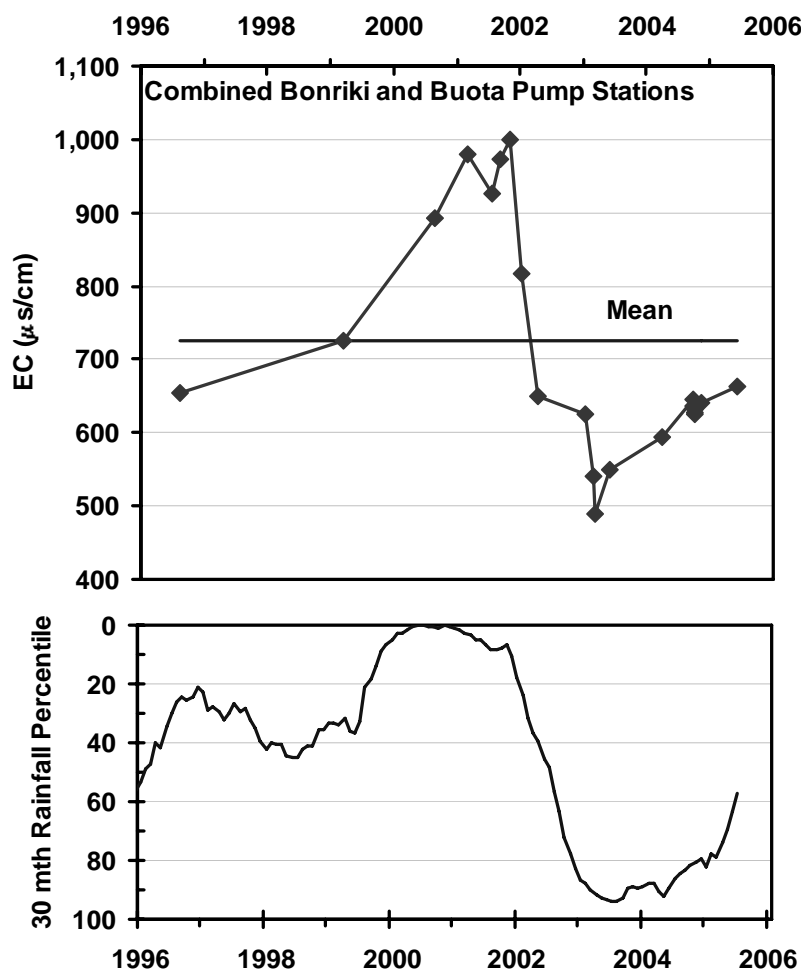


Fig. 5: Impact of the 1998-2001 drought on the groundwater salinity (EC) of combined waters pumped from the freshwater lenses in Buota and Bonriki islands (Fig. 1).

Tab. 4: Principal components of the annual water balance for Bonriki Island.

Component	Estimated depth (mm)	Estimated volume* ( $\text{m}^3$ )
Mean Rainfall, P	2,000	$2.80 \times 10^6$
Mean Actual Evapotranspiration, ET	1,020	$1.43 \times 10^6$
Mean Net Recharge, R	980	$1.37 \times 10^6$
Before Groundwater Pumping		
Mean Outflow and Dispersion, GF+D	980	$1.37 \times 10^6$
Mean Fresh Groundwater Thickness	15,000	$6.3 \times 10^{6\dagger}$
Mean Watertable Height above msl <sup>#</sup>	700	-
After Groundwater Pumping		
Sustainable Pumping Yield, Q	352	$0.49 \times 10^{6\dagger}$
Mean Outflow and Dispersion, GF+D	628	$0.88 \times 10^6$
Mean Fresh Groundwater Thickness	12,000	$5.04 \times 10^6$
Approx. Mean Watertable ht above msl <sup>#</sup>	560	-
Approx. Max. Change in Watertable <sup>#</sup>	140	-

\* Based on the estimated area of Bonriki island of 140 ha, <sup>†</sup> Based on an estimated specific yield of 0.3, <sup>‡</sup> Based on the current estimated sustainable yield of  $1,350 \text{ m}^3/\text{day}$  (Alam *et al.*, 2002), <sup>#</sup> At the centre of the island.

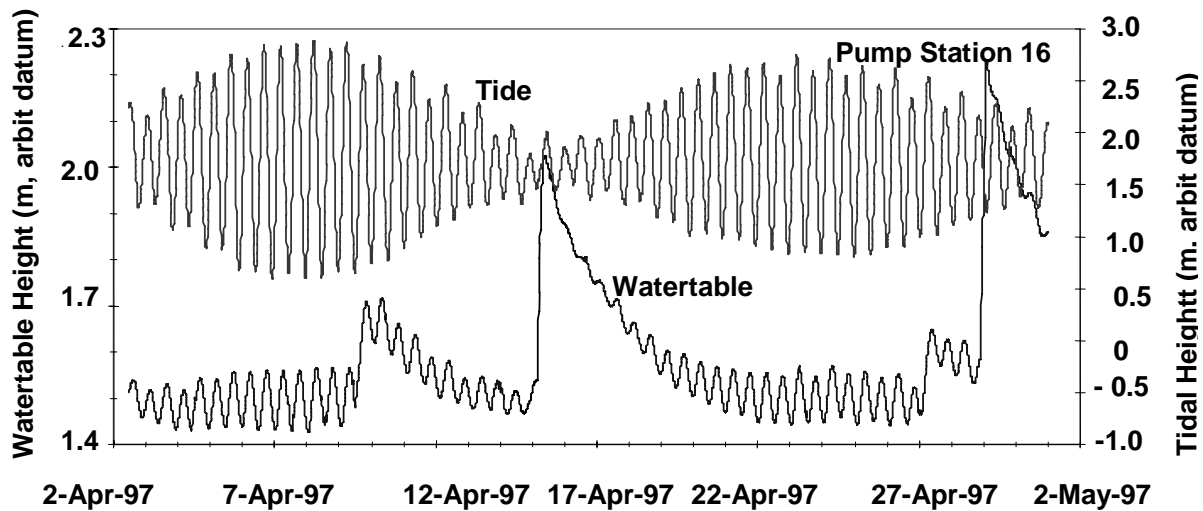


Fig. 6: Influence of the tidal cycle on watertable elevation in a Bonriki infiltration pump station (PS 16).

Tab. 5 compares the magnitude of changes in the watertable elevation in the Bonriki freshwater lens produced by natural processes, long term drought, rainfall and diurnal tidal fluctuations, with the change due to continued pumping. We conclude that the change due to pumping is smaller than changes due to natural processes and that pumping from horizontal infiltration galleries should have a negligible effect on traditional crops such as coconuts and swamp taro.

Tab. 5: Maximum observed changes in watertable elevation at Bonriki due to natural processes compared to that estimated from pumping.

Process	Maximum change in water table elevation (mm)
Natural	
Major Rainfall Events	650
Diurnal Tidal Forcing	300
Prolonged Drought	440 (Tab. 3)
Pumping	
Estimated max decrease	140 (Tab. 4)

## DRAWDOWN DUE TO INFILTRATION GALLERY PUMPING STATIONS

To a first approximation, the maximum unconfined watertable draw down,  $\delta$  (m), for an individual infiltration gallery pumping at a rate  $Q$  can be found by integrating Darcy's law:

$$\delta = W_G Q / (8K_0 H_u L_G) \quad (5)$$

where  $W_G$  (m) is the width of the gallery extraction zone and  $L_G$  is the length of the gallery. Typically values for the pumping galleries in Bonriki (Fig. 2) are  $L_G = 300$  m,  $W_G = 100$  m,  $H_u = 15$  m. Hydraulic conductivities of the unconsolidated Holocene coral sediments vary between about 5 and 50 m/day and individual pumping rates vary from about 40 to 140 m<sup>3</sup>/day. The estimated drawdown using these typical values in eqn (5) is expected in the range of about 2 mm to 80 mm.

Pump drawdowns were measured by switching pumps off and then on again in 16 infiltration gallery pumping stations in Bonriki (Fig. 2) and following the change in watertable elevation with a pressure transducer. A typical measurement is shown in Fig. 7. The mean pumping rate for the galleries was  $96 \pm 27$  m<sup>3</sup>/d and the mean measured draw down was  $33 \pm 46$  mm, with a maximum measured drawdown of 200 mm and a minimum of 2 mm. This clearly indicates that groundwater pumping drawdown has an insignificant impact on traditional crops. Using these measurements in eqn (5), the estimated mean hydraulic conductivity of the Holocene coral sediments is 8.1 m/day.

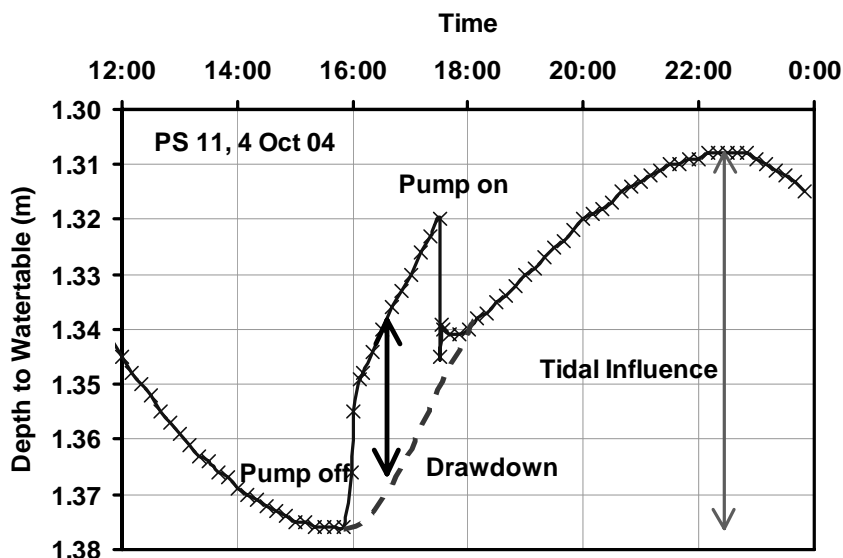


Fig. 7: Pressure transducer record of drawdown tests showing the impact of switching the pump on and off on the depth to the watertable in an infiltration gallery pumping station on Bonriki.

## IMPACTS OF LANDUSE ON WATER QUALITY

In low coral atolls, the watertable is close to the soil surface and superficial contaminants are rapidly translocated into the groundwater. Traditional practices, in low-density populations, have evolved to minimise contamination risk. These include defecation on beaches down gradient from recharge areas, sweeping leaves and debris away from dwellings and domestic wells and keeping pigs on the lagoon side of islands, in groundwater discharge zones. Increasing population is placing significant strains on natural resources, particularly land and water, and has generated tensions between the traditional values and practices of subsistence communities and the demands of urbanised societies (White *et al.*, 1999; Perez *et al.*, 2004).

An important issue in atolls is the impacts of animal wastes, particularly from pigs, on drinking water. In Kiribati there are an estimated 0.32 pigs/person (Saville and Manueli, 2002).

In some large islands used as groundwater sources for reticulation systems, one strategy has been for governments to declare lands overlying groundwater sources to be water reserves and to restrict land uses. Land ownership and use, however, is central to existence in most island communities (Jones, 1997). Declaration of reserves is therefore problematic for the affected landowners, whose landuses and rights are restricted. In some cases, declarations have generated long lasting disputes and have resulted in vandalism of water infrastructure (White *et al.*, 1999). A critical question raised in disputes between landowners and governments concerns the type of landuses that are acceptable in groundwater source areas. With land area severely limited there are significant pressures to maximise land use especially in agricultural production.

Bonriki water reserve (Fig. 2) has been encroached on by squatters who have established market gardens and have pig pens on the water reserve. Water quality testing for the presence of faecal contamination using *E. coli*, and for concentrations of dissolved organic carbon, DOC, total dissolved nitrogen, TDN, and nitrate and phosphate was carried out on all infiltration gallery pump stations in Bonriki (Fig. 2). The results for *E. coli* are shown in Fig. 8. There are extensive, abandoned taro pits, squatter dwellings pig pens, a cemetery and extensive market gardens in the vicinity of the positive galleries. Similar results were found for the other nutrients tested. Ratios of carbon to nitrogen in groundwaters indicated the presence of both microorganisms and added nitrogen.

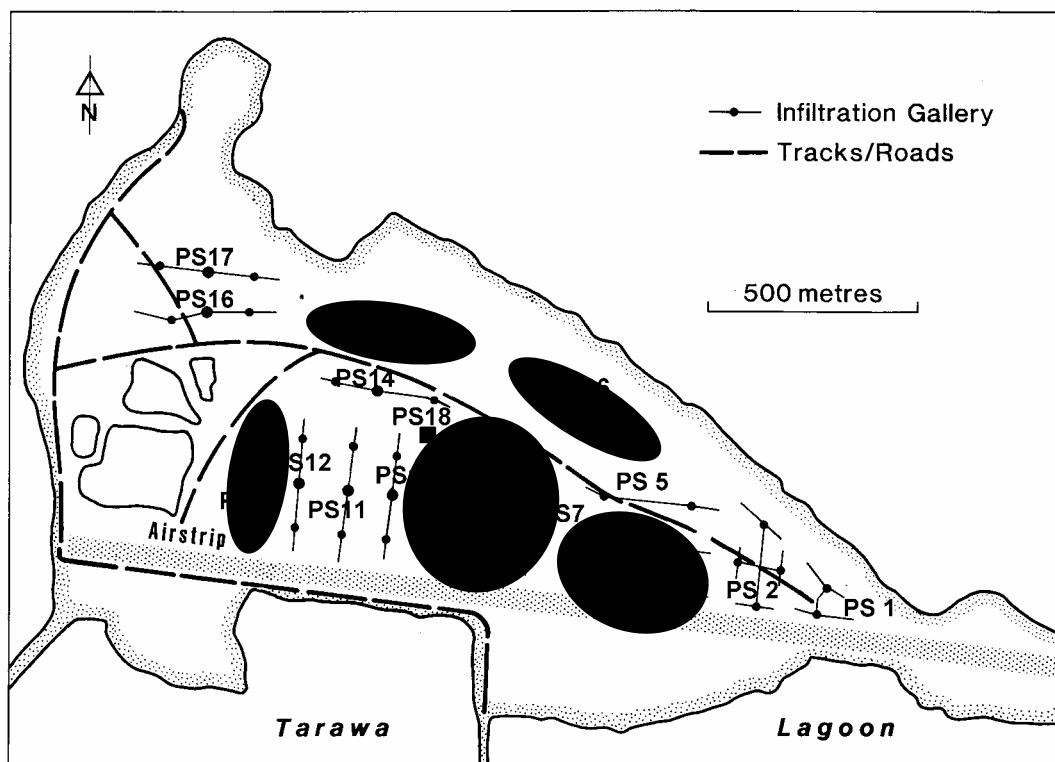


Fig. 8: Distribution of positive *E. Coli* water samples from pumping galleries on Bonriki.

## ADAPTATION STRATEGIES TO DECREASE RISK AND INCREASE RESILIENCE

Locations, such as Tarawa atoll, where demand for water matches or exceeds available water supplies are very vulnerable to climate variations and increasing population pressures. Available adaptation strategies for reducing risks and increasing resilience are limited but a key factor is the provision of appropriate knowledge. In many small islands, meteorological services and water supply agencies are under-resourced and their ability to predict water-related extreme events is limited. The actual amount of water that is available for use and its quality are largely unknown, particularly in outer islands. Monitoring and analysis are also at best spasmodic. As well, there has been a general reluctance to enact national water legislation, defining rights, policies and responsibilities and to involve communities in managing and planning water and related land resources.

Proposed adaptation strategies for small islands can be grouped proposed under 3 main themes, *capacity strengthening, demand management and refurbishment, protection and supplementation of freshwater resources* (Falkland, 2005). Within these themes, at least ten strategies could help increase the resilience of small island communities to water-related climate and human changes (White, 2005):

- Establish a sound institutional basis for the management of water and sanitation (policy, regulations, incentives, plans, organisational reform and assignment of responsibilities).
- Improve community participation in water and related land management and planning and reduce conflicts.
- Increase capacity to manage water and sanitation at the household and community levels.
- Increase capacity to analyse and predict water-related extreme events.
- Improve knowledge of available water resources, their quality and demand for them.
- Improve water conservation and demand management strategies and reduce leakages.
- Increase household and communal rainwater harvesting and storage.
- Protect groundwater source areas from contamination.
- Increase the use of groundwater.
- Improve sanitation systems to minimise water use and pollution.

Australia is currently initiating work to help small island countries in the Pacific implement these strategies in through its Pacific Vulnerability and Adaptation Project.

## ACKNOWLEDGMENTS

This work was initiated under the Humid Tropics Programme of UNESCO IHP V and has been continued with generous support from the Australian Centre for International Agricultural Research and the Government of France.

## REFERENCES

- Alam, K., Falkland, A. and Mueller, N. (2002) *Sustainable Yield of Bonriki and Buota Freshwater Lenses*, SAPHE Project, Hydrogeology Component. Tarawa, Kiribati, February 2002.
- Capenter, C., Stubbs, J. and Overmars, M. (2002) *Proceedings of the Pacific Regional Consultation on Water in Small Island Countries*, Sigatoka, Fiji Islands, 29 July-3 August 2002, Asian Development Bank and South Pacific Applied Geoscience Council, Suva, Fiji.
- CIA (2005) *The World Factbook* (<http://www.cia.gov/cia/publications/factbook/geos>).
- Falkland, A. (1992) *Review of Tarawa Freshwater Lenses, Republic of Kiribati. Report HWR92/681. Hydrology and Water Resources Branch, ACT Electricity and Water*. Prepared for Australian International Development Assistance Bureau.
- Falkland, A. (2002) Tropical island hydrology and water resources: Current knowledge and future needs, In: *Hydrology and Water Resources Management in the Humid Tropics. Proc. Second International Colloquium*, Panama, Republic of Panama, 22-26 March 1999, UNESCO-IHP-V Technical Documents in Hydrology, No 52, UNESCO Paris, 237-298.
- Falkland, T. (2005) *Water resources investments report. Kiribati Adaptation Program*, Preparation for Phase II Project, Government of Kiribati and World Bank, July 2005.
- Falkland, A.C. and Woodroffe, C.D. (1997) Geology and hydrogeology of Tarawa and Christmas Island, Kiribati. Chapter 19, In: *Geology and Hydrogeology of Carbonate Islands. Developments in Sedimentology*. (ed. By H.L Vacher and T. Quinn), Elsevier Science, 577-610.
- Foale, M. (2003) *The coconut odyssey: the bounteous possibilities of the tree of life*. ACIAR, Canberra, 132 p.
- Jones, P. (1997) *The Impact of the Socio-Cultural Order on Urban Management in the Pacific: A Case Study of South Tarawa, Republic of Kiribati*. PhD thesis, Univ Queensland.
- Kaly, U.L., Pratt, C.R., Mitchell, J. and Howorth, R. (2003) The Demonstration, Environmental Vulnerability Index (EVI). *SOPAC Technical Report 356*, SOPAC, Suva, Fiji, 137 p.
- Oberdorfer, J.A., Hogan, P.J. and Buddemeier, R.W. (1990) Atoll island hydrogeology: Flow and fresh water occurrence in a tidally dominated system, *J.Hydrol.*, 120, 327-340, 1990.
- Perez, P., Dray, A., LePage, C., D'Aquino, P. and White, I. (2004) Lagoon, agents and kava: a companion modelling experience in the Pacific. *International Conference on Social Simulation*, Amsterdam, the Netherlands, 18 August 2004.
- Pratt, C. and Mitchell, J. (2003) EVI Country Profile Review–Kiribati. *SOPAC Miscellaneous Report 521*, July 2003, SOPAC, Suva, Fiji, 67 p.
- Saville, P. and Manuelli, P. (2002) Pig production in the Pacific Island Countries and Territories. In: *Priorities for Pig Research in Southeast Asia and the Pacific to 2010*. ACIAR Working Paper No. 53 March 2002, ACIAR Canberra.
- SOPAC (2001). *An integrated approach to rainwater harvesting analysis using GIS and recommendations for roof-catchment legislation in Tuvalu*. SOPAC Technical Report 290, prepared by P.Dawe., SOPAC, Suva, Fiji, 86 p.
- UNESCO (1991) *Hydrology and water resources of small islands, a practical guide*. Studies and reports on hydrology No 49. prepared by A. Falkland (ed.) and E. Custodio. UNESCO, Paris, France, 435 p.
- Volker, R.E., Mariño, M.A. and Rolston, D.E. (1985) Transition zone width in ground water on ocean atolls. *J. Hydraul. Engng.*, 111, 659-676.
- Ward, R.G. (1999) *Widening Worlds, Shrinking Worlds, the Reshaping of Oceania*. Pacific Distinguished Lecture 1999. Centre for the Contemporary Pacific, Australian National University, Canberra.
- Wheatcraft, S.W. and Buddemeier, R.W. (1981) Atoll island hydrology. *Ground Water*, 19, 311–320.

- White, I. (2005) *Pacific Vulnerability and Adaptation Project, Tuvalu Water Management Activity, Background Information*. Report to AusAID, August 2005, CRES, Australian National University, Canberra, 33 p.
- White, I., Falkland, A. and Scott, D. (1999a) Droughts in Small Coral Islands: Case Study, South Tarawa, Kiribati. UNESCO IHP-V, *Technical Documents in Hydrology*, No. 26, UNESCO, Paris, 55 p.
- White, I., Falkland, A., Crennan, L., Jones, P., Etuati, B., Metai, E. and Metutera, T. (1999b) *Issues, Traditions and Conflicts in Groundwater Use and Management*, UNESCO-International Hydrological Programme, Humid Tropics Programme. IHP-V Theme 6. *Technical Documents in Hydrology* No. 25. UNESCO, Paris, 37 p.
- White, I., Falkland, A., Etuati, B., Metai E. and Metutera T. (2002) Recharge of fresh groundwater lenses: Field study, Tarawa atoll, Kiribati, In: *Hydrology and Water Resources Management in the Humid Tropics*. Proc. Second International Colloquium, Panama, Republic of Panama, 22-26 March 1999, UNESCO-IHP-V *Technical Documents in Hydrology*, No 52, UNESCO Paris, 299-322.



# VARIABILITY AND CHANGES IN HYDROLOGICAL VARIABLES AND PERSPECTIVES HYDROLOGICAL SCENARIOS IN THE CARIBBEAN REGION

**Eduardo PLANOS GUTIÉRREZ, Miriam LIMIA MARTÍNEZ**  
Institute of Meteorology of Cuba  
*planos@met.inf.cu*

## ABSTRACT

Based on studies carried out in countries of the Caribbean Region, this paper presents an analysis of the precipitation variability and its impact on the spatial and temporal distribution of the water in the last 60 years. The analysis is carried out using local and regional series of annual rain, annual rainy days series and annual series of maximum rains ; and were used a group of robust statistics tests for the detection of trends and significant changes in the time series. The study takes into account the analysis of the variability of the synoptic patterns associated with the behavior of the rain and the analysis of the ENSO, as important process responsible of the regional climatic variability. Different hydrological scenarios for the next 30 years are presented.

**Keywords:** hydrology, climate change, climate scenarios, Caribbean, ENSO

## INTRODUCTION

The climatic variability has not been sufficiently documented, fundamentally because the series of available data have not, in general, enough records to make such study; and because the hydrometeorological networks have had an unequal development in the world, and in many countries the networks are not well supported by the Government or these are insufficient.

Nevertheless, a growing attention to the study of the trends of the climatic and hydrological variables prevails, because it is observed an anomalous behavior of the climate in many places of the world. For great part of the world scientific community, this anomalous behaviour is linked with the human activity; especially with the disproportionate greenhouse gases emission to the atmosphere. The IPCC, WMO, as well as other institutions of science in the world demonstrate with data and facts the truthfulness of the previous statement. Advances in the study of the temperature and precipitation variability have been obtained; as well as significant results in the long-term climatic predictions, based on the employment of models of general circulation of the atmosphere.

The persistence of climatic anomalies is being observed in the Region of the Caribbean; decrement of the annual precipitation and increment of the droughts, the temperature of the air and the sea level. The current climatic and hydrological scenario in part of Caribbean Region it is a scenario of water deficit. These climatic anomalies affect all the productive sectors, the environment, the economy and the society. Due to insular condition of the Caribbean region, this is a very vulnerable region and therefore one of the world areas more negatively affected by the current climatic and hydrological anomalies.

This article presents an analysis of the observed trends in the synoptic patterns and the annual rain in the Great Antilles, as well as shows an analysis of the more probable climatic scenarios for the future 30 years.

## DATA AND METHODOLOGY

The data of precipitation from Cuba and Dominican Republic that were used in this paper come from the National Meteorological and Hydrological Services, and the data of precipitation from Haiti, Jamaica and Puerto Rico, were obtained from the work of Mike Hulme (<http://www.cru.uea.ac.uk>); these data were used to evaluate the annual rain variability in the Caribbean Region. The use of data of precipitation analyzed in United Kingdom was necessary because the data from the Jamaica Water Authority and from the Haitian Hydrological Service were not available when it was written this paper. In this way, Cuban experts, working in climatic change vulnerability studies in the Region of the Caribbean has had the

opportunity to validate and to use with good results the Hulme's database. The discharge data from Cuba and Jamaica come from the National Hydrological Services.

The regional analysis of the precipitation was elaborated for the period 1931 - 2000; and taking advantage of existence in Cuba of many pluviometers with data of beginnings of the 20<sup>th</sup> Century, from this country were selected pluviometers with longest records (between 1900 to 2000) to analyze the trend and variability of the precipitation in a longest period. Data of annual discharge for three rivers, draining western and eastern Cuba and northern Jamaica were used to quantify the hydrological response to decreased rainfall during the period from 1961 to 2000. Tab. 1 presents the main parameters of the data series used for this paper.

Tab. 1: Parameters of pluviometers and data series used for the variability and trends analysis.

Country	Place	Coordinates		Records	% of missing data
		N	W		
Cuba	Granma	19.88	77.42	1917 - 2000	0.0
Cuba	Holguin	21.00	76.07	1917 - 2000	3.0
Cuba	Pinar del Río	23.34	83.68	1931 - 2000	0.0
Cuba	Habana - Matanzas	22.83	82.03	1924 - 2000	0.0
Dominican Republic	Pimentel	19.18	70.1	1961 - 2000	0.0
Dominican Republic	Santo Domingo	18.48	69.92	1961 - 2000	2.5

For the analysis of the series of data and the precipitation variability, were used several methods:

- To estimate the missing values simple lineal regression models based in nearby station were used, although the most of the selected stations had complete their period of record.
- Composition of the chronological curve of annual rain to analyze the variability and trends through the time. This procedure consist to plot the annual rain from each year against the time and then analyze, firstly, in visual way the serial trend and afterward with statistical methods to confirm if the trend is statistically significant.
- Study of the precipitation anomalies, in which the annual rainfall for individual stations was divided by the median of the series of data and this value was then subtracted from each record and plotted against time.
- The trends were evaluated for 5% of by a group of statistic tests: Wald Walfowitz, Spearman coefficient, Mann-Kendal and Pettit (Sneyers, 1992; Radziejewski and Kundzewicz, 2004). These tests are very well described in texts of mathematical statistic, specially applied to the hydrology in Sneyers (1992). The combined use of these tests in a series can be considered a good methodological focus to check the certainty of the result of each test, because each one evaluates different statistical parameters and serial components, as the randomness of the series, the statistical dependence between the records, the persistence and the trend.

The projections of the future climatic scenario were estimated through the combination of a Simple Climate Model with several Coupled Models of the Atmosphere-Ocean General Circulation (MAGICC/SCENGEN software, v 2.4). Using the MAGICC/SCENGEN, applied in grid-boxes of 5° x 5° latitude-longitude of resolution, were estimated the probable temperature and precipitation changes in each future climatic scenario (Hulme *et al.*, 2000). In each country, the values of change of the temperature and the precipitation, obtained in the SCENGEN grid boxes, were added, in algebraic way, to the selected climatic baseline (1961-1990), under specific greenhouse emission scenarios (IS92a and IS92f); in this way was possible to estimate the future temperature and precipitation patterns, assuming that the structure of the present-day spatial pattern will have no change. This method was applied to each climatological station (Tab. 2).

Tab. 2: Method to apply the index of temperature and precipitation change to climatological stations

**TEMPERATURE**

$$STS_i = BTS_i + CTSB_j \quad i = 1, 2, \dots, n$$

i is a station,  
n is the total number of stations  
j is a SCENGEN box on the area where station is located

Where:

BTS<sub>i</sub> is **B**aseline **T**emperature in the station i

CTSB<sub>j</sub> is **SCENGEN** output **C**hange **T**emperature value (from corresponding j SCENGEN box on the area where station is located)

STS<sub>i</sub> is **S**cenario **T**emperature value in the station i

**PRECIPITATION**

$$SPS_i = BPS_i + CPS_i \quad i = 1, 2, \dots, n$$

i is a station,  
n is the total number of stations  
j is a SCENGEN box on the area where station is located

Where:

BPS<sub>i</sub> is **B**aseline **P**recipitation in the Station i

SPS<sub>i</sub> is **S**cenario **P**recipitation value in the Station i

CPS<sub>i</sub> is the amount of change precipitation in the Station i, according to SCENGEN output Change Precipitation values (from corresponding j SCENGEN box), calculates by:

$$CPS_i = BPS_i * COSB_j$$

Where: COSB<sub>j</sub> is **C**hange **O**utput **SCENGEN** **B**oxes (expressed in percent) on the area where station is located.

## SYNOPTIC AND CLIMATIC FACTORS OF THE CLIMATIC VARIABILITY IN THE NORTH REGION OF THE CARIBBEAN

According with the Dr. Lapinel (pers. com., 2005), in the period 1948-2000 a sustained modification of the atmospheric circulation characteristics is observed in all the troposphere levels on the Caribbean. These modifications are reflected in the topographic configuration of the isobaric surfaces and its vertical structure, causing an increment in the vertical extension of the vertical descendent movements, that increase eastward. The atmospheric circulation has changed, more intensely from the decade of the ninety in last century; this modification have caused unfavourable meteorological conditions for the precipitations, mainly in the eastern region of Cuba and Haiti. On the other hand, the analysis of the behavior of a group of meteorological variables as: geopotential anomalies, vertical pressure changes, long wave radiation, water vapour in the atmosphere and southern wind components, also demonstrate unfavourable conditions for the precipitations in this region. A special interest have the behavior of the vertical pressure changes (Omega), which have a progressive increment of the positive values during important months of the rainy period, which propitiate descending vertical movements in some troposphere levels that cause the inhibition of the normal development of the convection. This Omega behavior causes the increment of the duration of the less rainy period and a shorter rainy period.

Larsen (2000), analysing the rainfall and the streamflow in Puerto Rico during the 20th century and the drought as a regional phenomenon, summarize the opinion of various authors regarding a group of elements responsible for the intensity and frequency of the drought in the Caribbean:

- The variation in the index of the North Atlantic Oscillation (NAO) during winter is inversely related to annual mean precipitation. Conversely, wet periods match times of low NAO (Malmgren *et al.*, 1998; mentioned by Larsen, 2000).

- El Niño-Southern Oscillation (ENSO) events are associated with dry and warm summers in the Caribbean as well as periods of suppressed tropical storm formation (Ropelewski and Halpert, 1987; Kiladis and Diaz, 1989; Diaz, 1996; Poveda and Mesa, 1997; mentioned by Larsen, 2000).
- Over the past 30 years, maximum summer sea surface temperature has increased by 0.7°C (Winter *et al.*, 1998; mentioned by Larsen, 2000).
- Strong ENSO periods have been shown to reduce the number and intensity of hurricanes in the Atlantic (Gray, 1984; mentioned by Larsen, 2000). The 1991-1994 ENSO phenomenon was associated with a 50-year low in Atlantic hurricane frequency (Landsea, 1993; mentioned by Larsen, 2000). Conversely, increased Atlantic hurricane frequency has been correlated with years of enhanced rainfall in the Sahel region of Africa (Landsea and Gray, 1992; mentioned by Larsen, 2000).

## ANALYSIS OF THE PRECIPITATION TRENDS

The behavior of the precipitation in the Great Antilles demonstrates a close relation between the trends observed in the regional atmospheric circulation, specially the strong influence of the Atlantic Anticyclone on the north of the Caribbean area, jointly with the occurrence of another regional phenomena as ENSO and NAO.

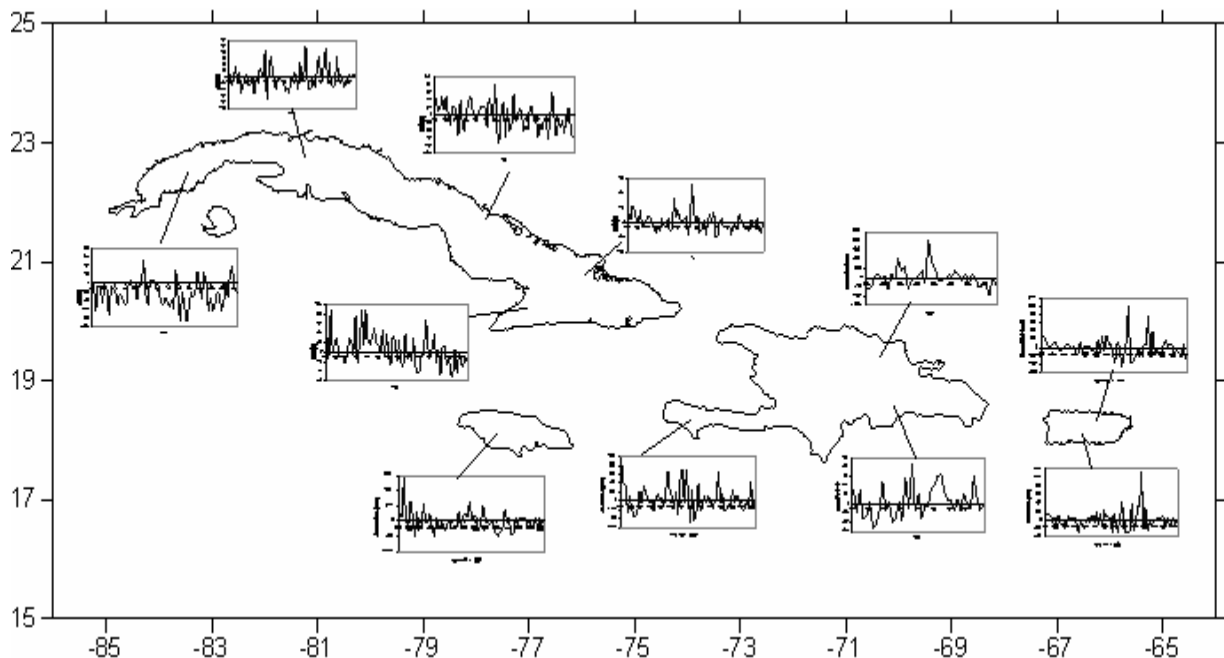


Fig. 1: Precipitation anomalies (period 1931–2000).

The precipitation in the eastern region of Cuba has a significant negative trend since the 1970s of the 20<sup>th</sup> Century; and in some cases since a previous date; while also, negative trends it is observed in Jamaica and in the north of La Hispaniola and Puerto Rico; this behavior is linked mainly with the dominant influence of the Atlantic Anticyclone over these areas. In the central and western part of Cuba and in the south of La Hispaniola and Puerto Rico, where the Atlantic Anticyclone influence is combined with other important meteorological phenomena, is observed a different trend in the annual precipitation.

The Fig. 1 shows the geographical distribution of the annual rain anomalies from 1931 to 2000; in this figure can be appreciated, in the most eastern part of the Caribbean, the negative trend of the precipitation, excepting the Cuban western territory where the continental influence is bigger one. A group of long series of precipitation from Cuba was analyzed to get a more comprehensive approach to the precipitation variability since the beginning of the 20<sup>th</sup> Century. This analysis is based on the study of the trend of the annual precipitation and rainy days and the study of the anomalies of the annual precipitation regarding the median; the trend of the data series was evaluated for 5% of significance with a group of strong statistical tests (Wald Wolfowitz, Spearman coefficient, Mann-Kendall and Pettit). The

selection of the pluviometers to make this study was realized considering that its data series were representative of the regional behavior of the precipitation in the locality where is installed the pluviometer. The criteria to select the regional representative pluviometers was based in the comparison of the annual and seasonal amount of precipitation, the trends observed in the precipitation through the time, the number of rainydays and the meteorological cause of the precipitation in a homogeneous geographical territory. The results of the statistical analysis, based in a rigorous analytical procedure, are presented in the figures and tables. In the areas, where the negative trends are visually and statistically significant can be described the following:

- Reduction of the raining days (Fig. 2). This graph, from a Cuban locality, shows a persistent decrement of the rainy days since the 1930s; which is more remarkable in the rainy days bigger than 50 mm in 24 hours. This behavior is more dramatic in the north eastern Caribbean Region, due to the strongest dominant action of the North Atlantic Anticyclone; in the central and western part of Cuba, the south of La Hispaniola and Jamaica, the rainy days are more variable due to the influence of different meteorological phenomena.



Fig. 2: Annual rainy days in Cuba eastern region.

- A decrease of the amount of the annual precipitation and reduction of the annual precipitation variability in the eastern Caribbean Region, (Fig. 3 to 5, Tab. 3 and 4). The Fig. 3 and 5 show a persistent reduction of the annual precipitation amount in the north eastern Cuba and Dominican Republic; the same behavior is observed in the Fig. 1 in different Caribbean areas where prevail a trend to the reduction of the rain amount since the 1970s. The annual rain anomalies, observed in the Fig. 4 and 5, calculated with the procedure explained in the section of Data and Methodology, confirms the precipitation reduction. In these graphs, it is possible to observe visually the reduction of the variability of the precipitation. Tab. 3 and 4 contain the results of the application of the mentioned statistical methods to the series represented in these graphs; the results demonstrate that the trend to the reduction of the precipitation is statistically significant.
- A remarkable increment of the rain in the dry season and a light reduction of the rain in the rainy season (Fig. 6).
- An increment of the intensity and frequency of drought processes (Fig. 7).

The maximum rains are another important factor for the annual rain behavior in the Caribbean Region. In Cuba, the maximum rains, in 24 hours, shows interesting fluctuations in the last years; Planos and Limia (2005) found changes in the behavior of the maximum rains through the probabilistic analysis (Tab. 5). These authors divided the series of maximum precipitation in 24 hours in smaller series to apply the Gumbel probabilistic analysis. The precipitation calculated to 100 years of return period has decreased in the last years in the northeast of Cuba; in the western region has increased lightly and, in the central region, presents a significant increment, as consequence of an exceptional phenomenon that produced an amount 867 mm, in 24 hours.

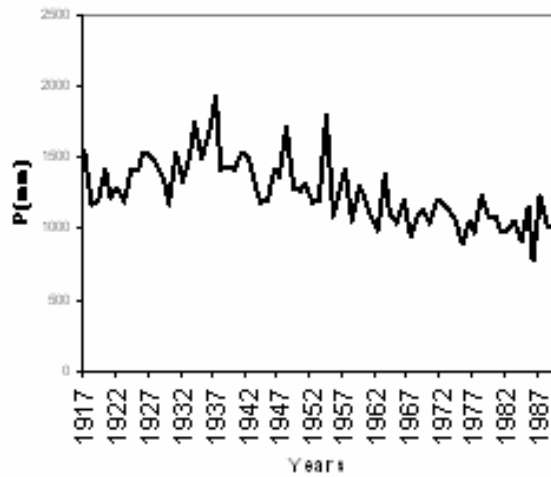


Fig. 3: Annual rain in the North of Cuba eastern region.

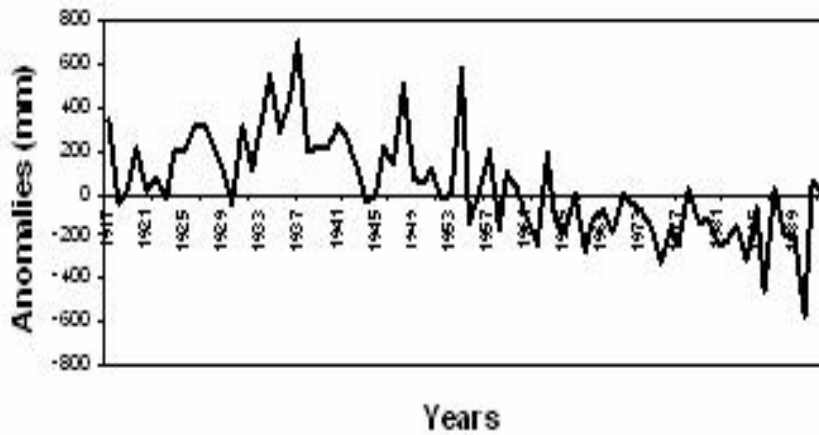


Fig. 4: Annual rain anomalies. North of Cuba eastern region.

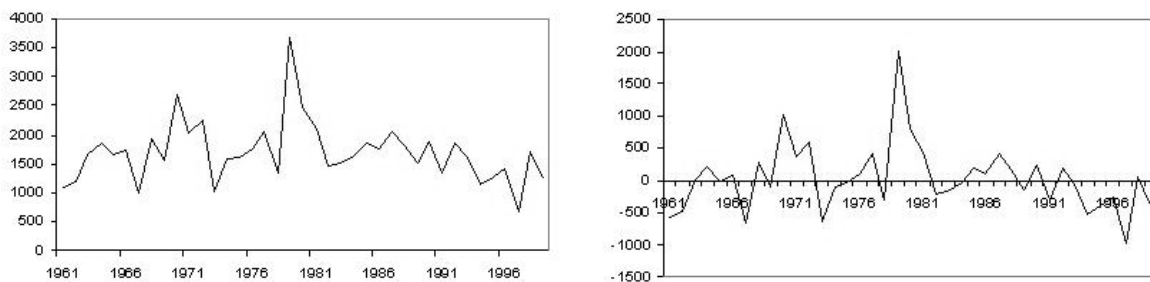


Fig. 5: Annual rain (left) and anomaly (right) in Dominican Republic, north region.

Tab. 3: Results of the statistic analytical procedure to Annual rain. North of the Cuba eastern region. Significance level 0.05%.

Test	Result	Evaluation
Wald-Wolfowitz	4.322.786	Alfa1 = 0.0000 < Alfa 0 = 0.0500
Spearman	-5.947.053	Alfa1 = 0.0000 < Alfa 0 = 0.0500
Mann-Kendall	-6.200.562	Alfa1 = 0.0000 < Alfa 0 = 0.0500
Pettit	1136.0	Alfa1 = 0.0000 < Alfa 0 = 0.0500

Tab. 4: Results of the statistic analytical procedure to Annual rain. Dominican Republic, North region. Significance level 0.05%.

Test	Result	Evaluation
Wald-Wolfowitz	0.692677	Alfa1 = 0.2443 > Alfa 0 = 0.0500
Spearman	-2.628449	Alfa1 = 0.0086 < Alfa 0 = 0.0500
Mann-Kendall	-2.595.543	Alfa1 = 0.0094 < Alfa 0 = 0.0500
Pettit	2000.0	Alfa1 = 0.0273 < Alfa 0 = 0.0500

Tab. 5: 24 hours maxima rain in Cuba. Return period 100 yrs, estimated with Gumbel.

Locality	Record 1930-1949	Record 1950-1969	Record 1970-1989	Record 1930-1990
Western Cuba region (Habana Matanzas)	323	218	392	297
Central Cuba region (Cienfuegos)	701	274	634	509
Eastern Cuba region (Holguín)	233	671	334	341

This result is not conclusive for several reasons; first because the absolute maximum values are very influenced by the form like the statistical sample is made to build the series and, particularly, for the way like are considered the outliers in the probabilistic analysis. The Tab. 5 show that the sub-series 1930-1949 and 1970-1989 have a similar behavior, but it is not a reason to speak a priori of significant changes in the last years. However, like part of the general conditions that is observing in the behavior of the climate, is necessary to study the decrease of the maximum precipitation amount in the last years, to identify if it could be consequence of changes in the meteorological system responsible of the intensive and high precipitation. The frequency of the precipitations that produce amount bigger than 50 mm reveals also a marked negative trend in the areas where the trend of the annual rain is negative (Fig. 8).

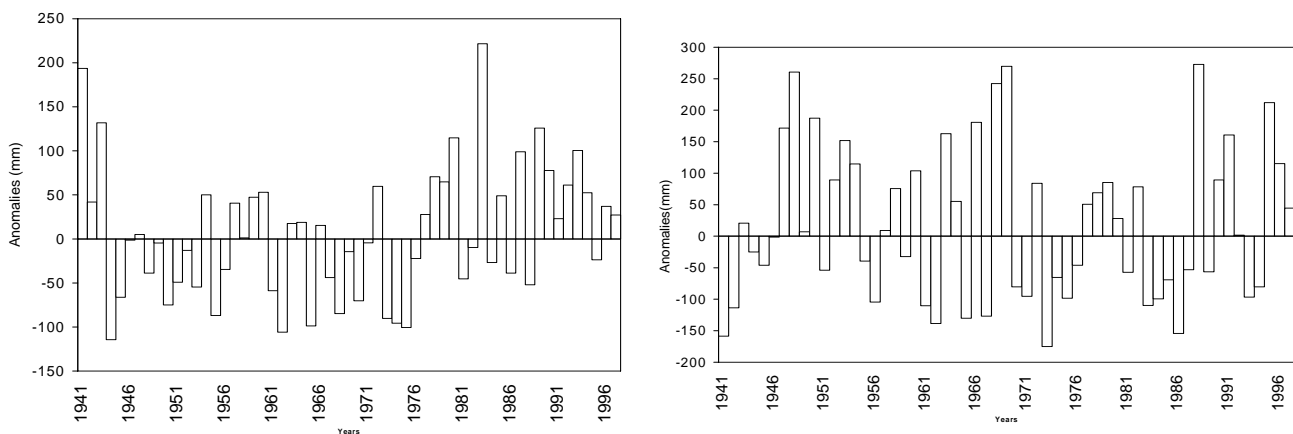


Fig. 6: Precipitation anomalies less raining months (left), and raining months (right). Period 1941–1996 respect to period 1961–1990.

In the Caribbean Region, the rain is the only source of production of water, and of course, the runoff has a similar behavior of the rain, although more or less accentuated by the specific characteristics of each place. The Fig. 9 and 10 shows as the runoff in Cuba and Jamaica have similar trends to the described in this paper for the rain and Fig. 11 show the runoff station locality. The above mentioned, means that in Cuba and Jamaica a negative trend in the annual runoff values prevails, with a decrement of the runoff variability in the 1990s decade.

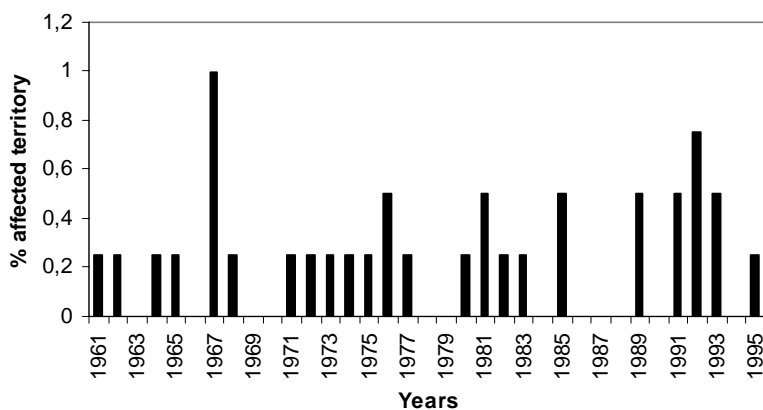


Fig. 7: Frequency of drought processes in the North of the Caribbean region.

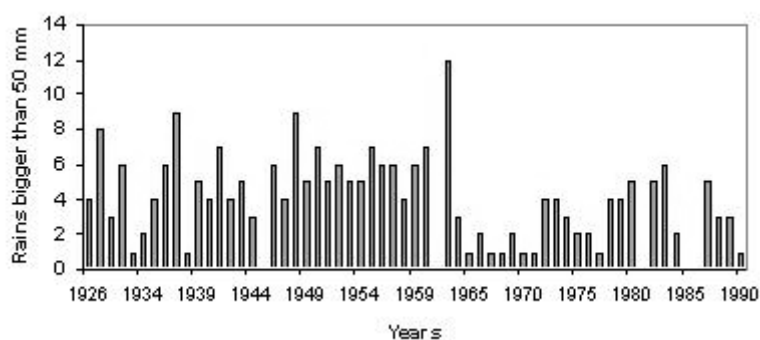


Fig. 8: Annual Frequency of Rains bigger than 50 mm in Cuba eastern area.

## CLIMATE CHANGE SCENARIOS

The climate change scenarios are obtained through 3 procedures:

- Determination of a global scenario of greenhouse gases emission
- Determination of the influence of the greenhouse gases in the global warming of the atmosphere.
- Association of the global warming of the atmosphere with a regional pattern of climate change (Centella *et al.*, 1999).

For this paper, the first two procedures were developed with MAGICC and the third one was obtained with SCENGEN. In this way, the IS92a emission scenario, defined by IPCC (Leggett *et al.*, 1992), it was applied in the northern part of the Caribbean Region: Cuba, Haiti and Dominican Republic (Centella *et al.*, 1999; Centella, 2002; Limia, 2001). The IS92a is a mid-range estimation of the future emissions with a very modest reduction intervention action. This emission scenario has been widely used in other regions of the World and had been adopted as a standard scenario for studies of impact assessment (IPCC-TGCI, 1999). The values of global warming and sea level rise were computed for a climate sensitivity of 2.5°C with the emissions of SO<sub>2</sub> stable since 1990, values that have been common in the most Caribbean countries studies of vulnerability assessment. The IS92f emission scenario was selected with 4.5°C of climate sensitivity; and this scenario was evaluated for water resource assessment study under more severe climate conditions in one country as example. The Tab. 6 show the projection of greenhouse gases concentrations for the year 2030 as is projected in the emission scenarios IS92a and IS92f. The Tab. 7 shows the temperature increment and sea level rise under emission scenarios IS92a and IS92f for the year 2030.

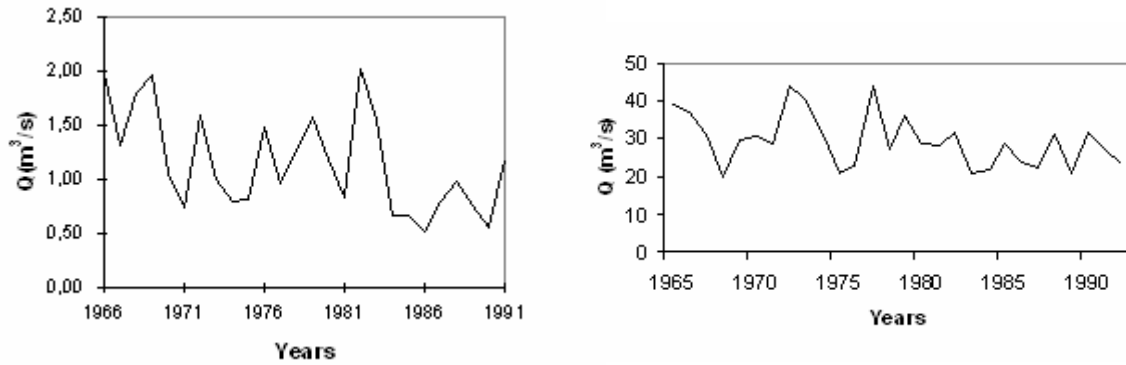


Fig. 9: Annual runoff. Santa Cruz, Santa Ana River, Cuba western region (left), and Toa River, Cuba eastern region (right).

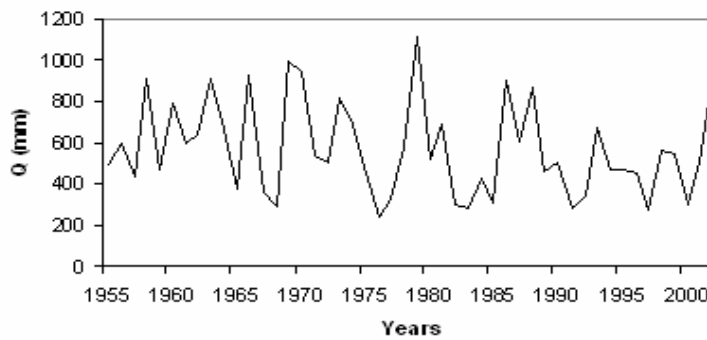


Fig. 10: Annual runoff. Cobre River, Jamaica.

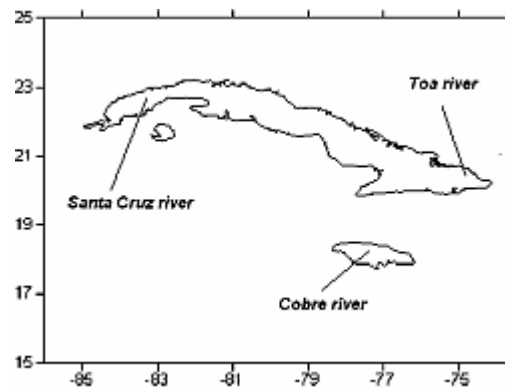


Fig. 11: Runoff station location.

Tab. 6: Emissions of CO<sub>2</sub>, CH<sub>4</sub> and N<sub>2</sub>O, based on the assumptions of the IS92a and IS92f scenarios for 2030 year.

SCENARIO	YEAR	2030	
	CO <sub>2</sub> (Pg)	CH <sub>4</sub> (Tg)	N <sub>2</sub> O (Tg)
<b>IS92a</b>	13.70	756.8	19.21
<b>IS92f</b>	14.96	793.4	19.65

Tab. 7: Temperature increments and sea level rise emission scenarios IS92a and IS92f. 2030 respect 1990.

Year 2030	Global Temperature	Sea Level Rise
<b>IS92a</b>	0.76	12.33
<b>IS92f</b>	1.17	26.73

# PROJECTION OF CLIMATE CHANGE PATTERNS

The Model of Global Circulation HADCM2 was selected among all the available models in SCENGEN, to obtain the climate change patterns. This is an ensemble of four "warm-start" transient simulations, consisting of a 19-layer high resolution (2.5deg. latitude by 3.75deg. longitude) atmospheric Global Circulation Model coupled to a 20-layer ocean model. This coupled model yields a global precipitation sensitivity of 1.6% per degree Celsius warming (Mitchell *et al.*, 1999) and has a very good global monthly precipitation pattern correlation (0.76).

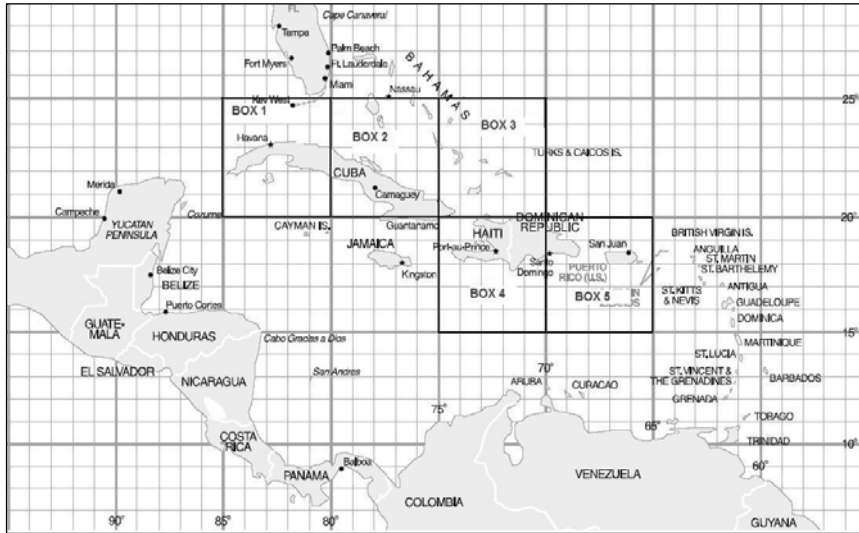


Fig. 12: The five 5° x 5° latitude-longitude SCENGEN grid boxes on the North of the Caribbean region.

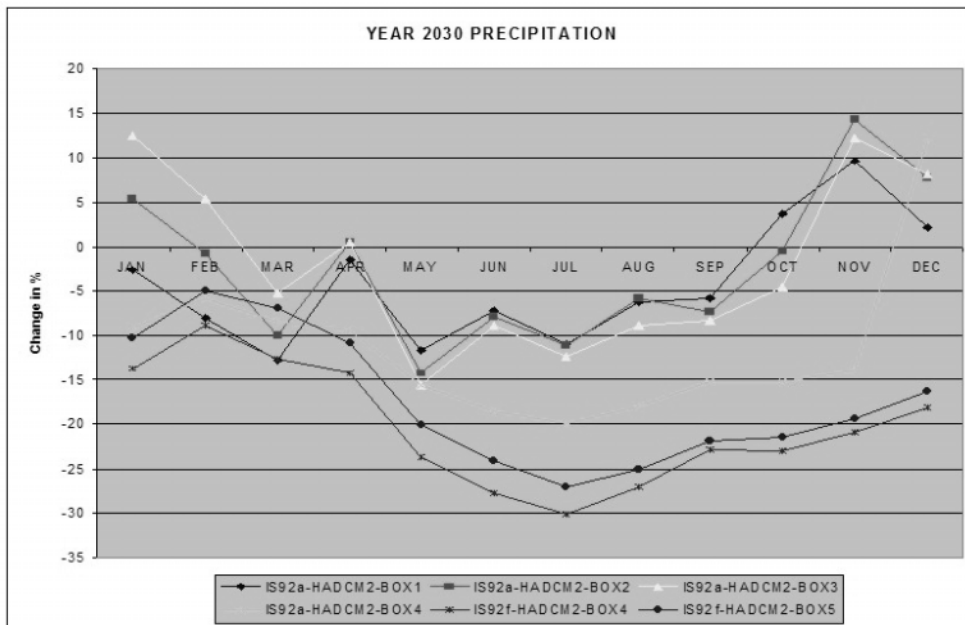


Fig. 13: Percentage change in annual rainfall in 2030 (with respect to 1961-1990 baseline). HADCM2 model under IS92a in boxes from 1 to 4 and IS92f in boxes 4 and 5.

On other hand, the simulation reached with Model HADCM2 agree well with the climatic trend observed in the Caribbean area and, with this model, has been feasible to consider the islands of Cuba and La Hispaniola as land in the Caribbean sea; while other models consider the Caribbean like a great sea without islands. Because of this consideration, the values in SCENGEN output on the Caribbean Region

are valid for the islands. The Fig. 12 shows the five SCENGEN boxes available on the north of the Caribbean Region.

The HADCM2 model, for the emission scenario IS92a projects an increment of the annual temperature and a reduction of the annual rainfall. Nevertheless, in the boxes 1 to 4 (Fig. 13), the annual variation pattern reflects an increment of the rainfall in several months of the less rainy season and a decrement of the precipitation during the rainy season. Under the emission scenario IS92f, the HADCM2 model reflects a decrement of the rainfall in all the year, but the decrease in the rainy season is smaller than in non-rainy season (boxes 4 and 5 Fig. 13). This indicates the occurrence of a warmer and drier climate than the present climate condition, and a trend to a more homogenous annual rainfall pattern in the future. These climatic scenarios have a high level of uncertainty, due to the complexity of the atmospheric system and the available data; an additional element of this uncertainty is the models inability to express the scenarios in probabilistic terms. For the studies realized in each Caribbean country, were used several Models of General Circulation to obtain several climatic responses to the increment of temperature, these models are, for example: CSRT and ECH4 for Dominican Republic and OSU and UKTR for Cuba.

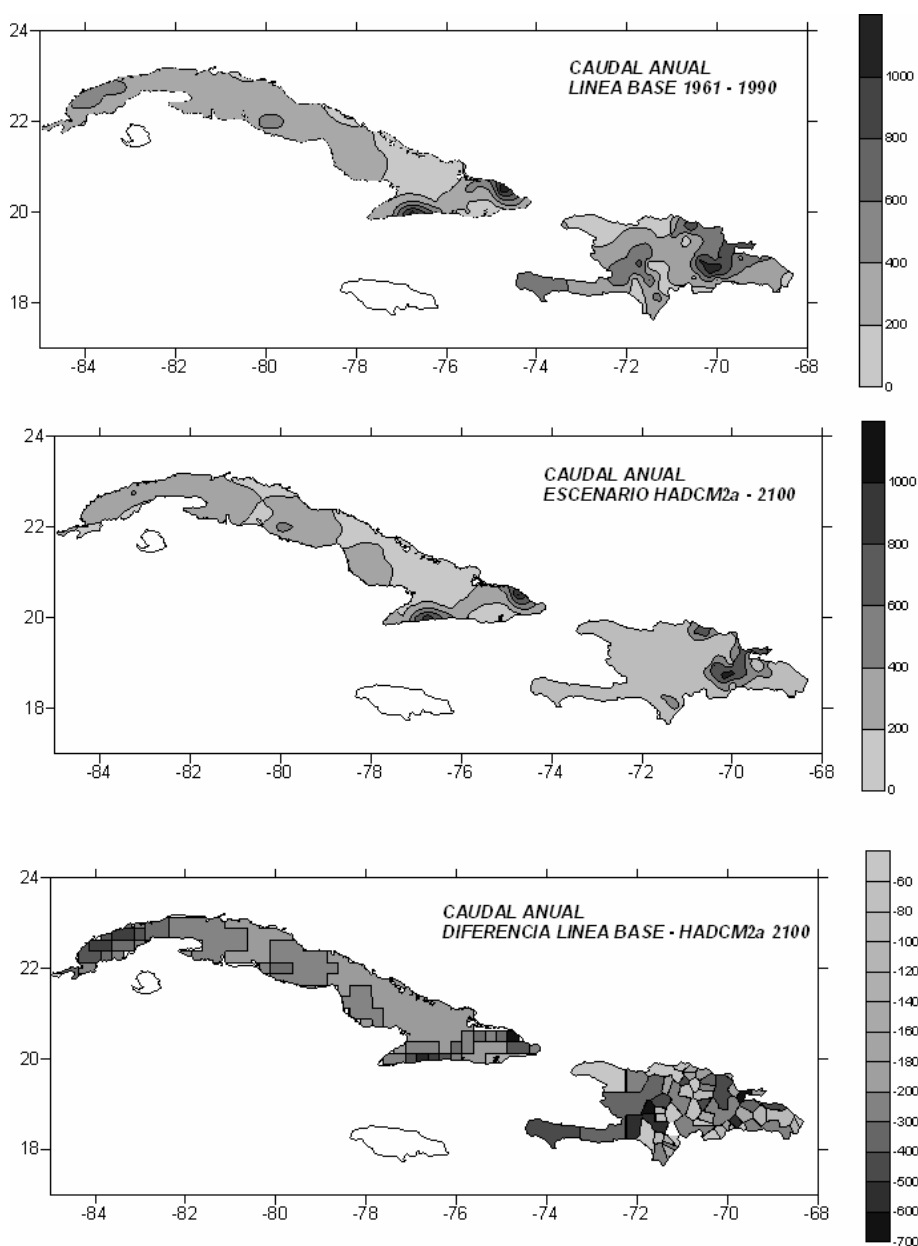


Fig. 14: Cuba and Hispaniola water scenarios 2100. Hadcm2 models.

However, from the practical point of view, the best model is the one that reflects better the behavior of the climate in the past and whose predictions (short terms) can be observed through the hydrometeorological networks. In this way, the HADCM model has reflected very well the climatic behavior in Cuba, Haiti

and Dominican Republic, and for that reason the authors say that the climatological and hydrological scenarios that were obtained with this model are more plausible.

Fig. 14 shows the water scenario for Cuba and La Hispaniola in 2100. According to this consideration and taking into account also that the hurricanes' response to the increment of temperature could cause a 15% of precipitation increment; and considering that the high frequency of the hurricanes that it is being observed nowadays in Caribbean Region would extend for 30 or more years, the authors' opinion is that more probable climate and hydrological scenarios in the Caribbean Region should be more variable regarding the extreme meteorological phenomena and, in general, drier than the present conditions.

## CONCLUSION

The data demonstrate that in the last 30 years have been observed an important modification in the vertical structure of the atmosphere on the Region of the Caribbean that rebound in the general circulation of the atmosphere in this geographical area and in the behavior of the variables of the hydrological cycle. The climatic scenario is favorable for the reinforcement of the hydrological extremes and a more variable climate. On the northeast of the Caribbean region has been strengthened the influence of the Anticyclone of the Atlantic and is observed a decrement of the precipitation and an increment of the droughts. The series of precipitation longest than 50 years, reflect a persistent decrease of this element of the climate in the last 30 years.

The climate and hydrological scenarios in north of the Caribbean region have a marked trend to the increment of the frequency of the droughts, a reduction of the annual precipitation. An extreme climate, the prevalence of climatic and hydrological trends toward the aridity and the increment of the water demand, characterize the future hydrological scenarios in this region as scenarios of deficit of water.

## REFERENCES

- Centella, A., Gutiérrez, G., Limia, M. and Rivero, R. (1999) Climate Change Scenarios for Impact Assessment in Cuba, *Climate Research*, 12, 223-230.
- Centella, A. (2002) *Escenarios climáticos para Haití*. Informe de consultoría. Secretaria de Medio Ambiente, 9 p.
- IPCC-TGCI (1999) *Guidelines on the Use of Scenario Data for Climate Impact and Adaptation Assessment. Version 1*. Prepared by Carter, T.R., M. Hulme and M. Lal, Intergovernmental Panel on Climate Change, Task Group on Scenarios for Climate Impact Assessment, 69 p.
- Larsen, M. (2000). Analysis of 20<sup>th</sup> century rainfall and streamflow to characterize drought and water resources in Puerto Rico. *Physical Geography*, 21, 6, 494-521.
- Leggett J., Pepper W.J., Swart R.J. (1992) Emissions scenarios for the IPCC: an update. In: *Houghton JT, Callander BA, Varney SK (eds) Climate change 1992: the supplementary report to the IPCC scientific assessment*. Cambridge University Press, Cambridge, p 75-95.
- Limia, M. (2001) *Escenarios Climáticos para la República Dominicana*. Informe de Consultoría, Secretaría de Medio Ambiente, 29 p.
- Mitchell, J.F.B., Johns, T.C., Eagles, M., Ingram, W.J. and Davis, R.A. (1999) Towards the construction of climate change scenarios. *Climatic Change*, 41, 547-581.
- Murphy, J.M. and Mitchell, J.F.B. (1995) Transient response of the Hadley Centre coupled ocean-atmosphere model to increasing carbon dioxide. Part 2. Spatial and temporal structure of the response. *J. Climate*, 8, 57-80.
- Planos, E. and Limia, M. (2005) Cambio climático, escenarios de déficit de agua y precipitaciones máximas. *Revista Cubana de Meteorología*, 12, 1, 53-64.
- Radziejewski, M. and Kundzewicz, Z. (2004). *Development, use and application of the hydrospect data analysis system for the detection of change in hydrological time series for use in WPC-water and national hydrological services- WCASP-65*. WMO/TD-No 1240, Poznan, June 2004.
- Sneyers, R. (1990) On the statistical analysis of series of observations, *Techn. Note 143*, World Meteorological Organization, Geneva, 192 p.

# PREVISION DES RESSOURCES EN EAU EN AFRIQUE AU 21<sup>EME</sup> SIECLE.

**Sandra ARDOIN-BARDIN, Jean-François BOYER, Alain DEZETTER, Claudine DIEULIN, Gil MAHÉ, Jean-Emmanuel PATUREL, Eric SERVAT**  
UMR HydroSciences Montpellier, IRD, BP 64501, F-34394 Montpellier cedex 5, France  
*ardoin@msem.univ-montp2.fr*

## ABSTRACT

We evaluate the impact of climate change on the runoff of great rivers of West and Central Africa. We develop climatic scenarios for rainfall and PE from HadCM3-A2 projection data for the XXIst century, and we simulate the runoff with two hydrological conceptual models: GR2M and WBM. Results show that future runoff depends mainly on precipitation. Locally the prediction is an increase for the Chari and the Sassandra rivers, and a decrease for the Senegal and the Gambia rivers. It seems that the continuous increase of PE have little effect on runoff in West and Central Africa. These results also demonstrate the differences in the results according to the use of one or another of the hydrological models: with the GR2M model, simulated runoff variations are amplified in regard to those simulated by WBM.

**Keywords:** Climatic scenarios, water resources, General Climate Models, hydrological modelling, west and central Africa

## INTRODUCTION

Le changement climatique annoncé pour le XXI<sup>ème</sup> siècle par les Modèles de Circulation Générale (ou GCM) ne peut être sans conséquence sur les ressources en eau. L'estimation quantitative des impacts sur les systèmes hydrologiques est essentielle pour comprendre et prévenir les problèmes potentiels sur les ressources en eau et leur gestion future. La modélisation du système climatique est complexe et trois problèmes majeurs relatifs à l'utilisation des GCM peuvent être soulevés (IPCC, 2001) : leur résolution n'est pas adaptée à celle de la modélisation hydrologique ; les différences entre les projections climatiques produites par les GCM sont très marquées ; les précipitations sont généralement peu réalistes. Cependant, ces GCM, même imparfaits, sont les seuls outils à notre disposition pour simuler les conditions climatiques futures.

Cette étude propose une méthodologie pour évaluer les impacts du changement climatique sur les écoulements de grands fleuves en Afrique de l'Ouest. Les séries chronologiques de précipitations et d'évapotranspiration potentielle représentant les conditions climatiques futures sont construites à partir de deux scénarii climatiques, en utilisant les prévisions du modèle HadCM3-A2. Les débits mensuels sont simulés à l'aide de deux modèles hydrologiques conceptuels, préalablement calés et validés, puis comparés aux observations. Il convient donc d'être extrêmement prudent quant à l'interprétation des résultats obtenus. En particulier parce que nous sommes amenés à utiliser des modèles conceptuels avec des séries chronologiques issues d'un travail de prospective, censées refléter ce qui devrait se produire au cours du siècle à venir. Nous devons donc faire l'hypothèse que la relation pluie-débit ne sera pas modifiée par rapport à celle établie à partir des chroniques d'observations. Cette hypothèse est probablement très simplificatrice. Néanmoins, elle nous permet de proposer des ordres de grandeur et de faire correspondre évolution climatique et évolution hydrologique.

## DESCRIPTION DES DONNÉES

### Données climatiques spatialisées

Les données climatiques utilisées dans cette étude sont spatialisées sous forme de grilles à la résolution du demi-degré carré. Nous utilisons deux types de données : celles observées et celles simulées par les

modèles de climat, communément appelés GCM. Les données climatiques observées couvrent la période 1950-1995 et ont été obtenues auprès du Climatic Research Unit (CRU) de l'Université d'East Anglia. Il s'agit de grille de données pluviométriques mensuelles, construites par interpolation (fonction Spline) de séries pluviométriques sélectionnées pour la qualité et la longueur de leurs observations (New *et al.*, 1999 et 2000), et de données d'évapotranspiration potentielle (ou ETP), calculées à partir de la formule de Penman (1956). Les données climatiques simulées proviennent des GCM et sont extraites des archives du Data Distribution Centre de l'IPCC. Il existe de nombreux GCM mais seulement sept d'entre eux sont recommandés par l'IPCC (2001). Notre choix s'est porté sur les simulations du HadCM3 conduites avec le scénario d'émission de gaz à effets de serre A2. Ce choix est d'abord motivé par le fait que les données de précipitation et des variables nécessaires au calcul de l'ETP sont disponibles sur la période 1950-2099, qui couvre bien la période d'observations. Cette disponibilité des données a permis d'évaluer la qualité des simulations du modèle HadCM3-A2 au regard des précipitations et des températures (Casenave, 2004 ; Lucio, 2004 ; Salathé, 2005).

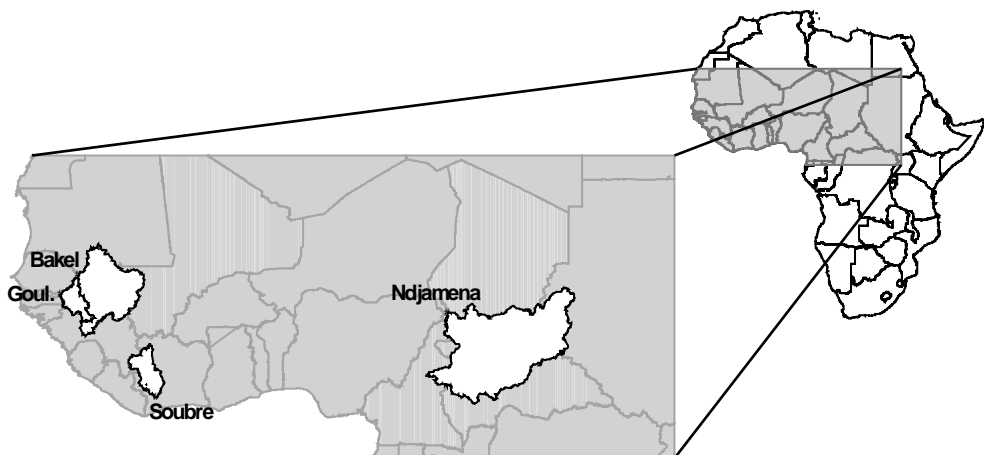


Fig. 1 : Situation des bassins versants sur la fenêtre d'étude (20°W-32°E et 1°N-24°N).

### **Bassins versants**

Pour cette étude, quatre unités hydrographiques situées en Afrique de l'Ouest et Centrale ont été retenues (Fig. 1). Elles correspondent à des bassins versants de plusieurs dizaines à plusieurs centaines de kilomètres carrés, découpés en une quarantaine de sous-bassins. Ce choix s'est effectué en fonction de plusieurs critères : caractéristiques climatiques, localisation géographique, disponibilité et qualité des données. Il s'agit de bassins versants situés en zone soudano-sahélienne (Sénégal, Gambie, Chari) et d'un bassin situé en zone plus « humide », le Sassandra. Les données hydrologiques mensuelles proviennent des données collectées par l'IRD, complétées auprès des Services Hydrologiques Nationaux et rassemblées au sein du Système d'Informations Environnementales SIEREM développé par HydroSciences Montpellier. La longueur des séries dépend du bassin versant considéré : 1908-1998 le Sénégal, 1971-1996 pour la Gambie, 1953-1998 pour le Sassandra et 1933-1999 pour le Chari.

### **Modèles hydrologiques**

Les deux modèles retenus pour cette étude sont des modèles de bilan d'eau fonctionnant au pas de temps mensuel et utilisant les mêmes données d'entrée (pluie, ETP, débit et capacité de rétention en eau des sols) : GR2M du CEMAGREF et Water Balance Model (WBM). Les écoulements mensuels ont été simulés avec ces deux modèles conceptuels en utilisant une distribution du bassin versant en un maillage régulier au demi-degré carré. Seule une brève description des modèles est donnée ici, les détails de leur fonctionnement pouvant être consultés dans Paturel *et al.* (1995) et Conway (1997). Sur chaque cellule du réseau et à chaque pas de temps, une fraction de la pluie participe à l'écoulement direct. Le niveau d'un réservoir qui représente le stock d'eau évolue en fonction de la fraction de pluie restante et de l'ETP. La vidange progressive de ce réservoir produit l'écoulement retardé. L'écoulement à l'exutoire du bassin versant est obtenu par la sommation des contributions des différentes cellules du réseau. Le remplissage

maximal du réservoir sol correspond à la capacité en eau du sol, dont les données sont estimées à partir de la carte des sols de la FAO (Dieulin, 2005). Avec la perspective d'utiliser ce modèle hydrologique dans la continuité chronologique des observations pour simuler les écoulements dans le futur, les paramètres du modèle sont calés pour les conditions déficitaires, installées depuis la fin des années 60 et qui perdurent aujourd'hui (L'hôte *et al.*, 2002 ; Ardoin *et al.*, 2003). Pour chaque bassin versant, les deux paramètres du modèle sont estimés à partir d'un calage sur la période 1971–1987 et validés sur la période 1988–1995 (Ardoin-Bardin, 2004).

## MÉTHODE D'ÉVALUATION DES IMPACTS DU CHANGEMENT CLIMATIQUE

### Principe

La méthode employée pour étudier l'impact du changement climatique sur les ressources en eau se divise en trois étapes : (a) les modèles conceptuels GR2M et WBM sont calés pour chaque bassin versant en utilisant les séries hydrologiques et climatiques observées (période 1971-1995) ; (b) les séries climatiques futures (période 2006–2095) sont construites à partir des séries observées sur une période de référence et de scénarii climatiques exprimant un changement dans les précipitations et l'ETP ; (c) les modèles conceptuels GR2M et WBM avec les paramètres calés à l'étape (a) simulent les écoulements avec les séries chronologiques construites à l'étape (b).

### Génération de scénarii climatique

D'après l'étude comparative de Casenave (2004) sur l'Afrique de l'Ouest, les GCM s'avèrent relativement performants dans la zone soudano-sahélienne en termes de dynamique saisonnière mais ils sont en revanche incapables de reproduire les cumuls pluviométriques ainsi que la variabilité interannuelle des précipitations. Les précipitations simulées par les GCM ne sont donc pas suffisamment fiables à l'échelle régionale pour être utilisées directement dans les études d'impact, il est recommandé d'établir les champs de variations entre le climat futur et une période de référence (IPCC, 2001). Les scénarii climatiques sont établis pour les précipitations mais également pour les ETP, car les températures extrêmes simulées par le modèle HadCM3-A2 ne sont pas géostatistiquement réalistes (Lucio, 2004). Les différences entre le climat (précipitations et ETP) représentatif de la période de référence et du climat futur sont calculées pour chaque cellule du GCM et à chaque pas de temps (mois  $i$ , année  $j$  de la période de référence, année  $k$  de la période 2006-2095). Elles sont alors exprimées en anomalies standardisées (scénario *Anomalies–suffixe Ano*) ou en taux de variations (scénario *Horizons–suffixe Horiz*) en fonction d'une climatologie moyenne tirée des simulations du HadCM3-A2 sur la période de référence 1969–1998:

Scénario *Anomalies* :

$$Ano_{GCM,i,k} = (X_{GCM,i,k} - \overline{X}_{GCM,i}) / \sigma_{GCM,i} \quad (1)$$

où  $X_{GCM}$  est la valeur mensuelle simulée par le GCM,  $\overline{X}_{GCM}$  est la moyenne de la série simulée sur la période de référence,  $\sigma_{GCM}$  est l'écart-type de la série simulée sur la période de référence.

Scénario *Horizons* :

$$\Delta_{horiz,i} = 100 \times (\overline{X}_{horiz,i} - \overline{X}_{ref,i}) / \overline{X}_{ref,i} \quad (2)$$

où  $\overline{X}_{horiz}$  est la valeur moyenne de la série simulée calculée sur un horizon donné (2020, 2050 ou 2080),  $\overline{X}_{ref}$  est la valeur moyenne de la série simulée calculée sur la période de référence.

Les séries chronologiques représentant le climat futur (période 2006–2095) sont construites en combinant les séries chronologiques observées sur la période de référence et les deux scénarii de changement climatique, selon les formules suivantes:

avec le scénario *Anomalies* :

$$X_{SCEN,i,k} = \overline{X}_{CRU,i} + (Ano_{GCM,i,k} \times \sigma_{CRU,i}) \quad (3)$$

où  $\overline{X}_{CRU}$  est la valeur moyenne de la série observée sur la période de référence,  $\sigma_{CRU}$  est l'écart-type de la série observée sur la période de référence.

avec le scénario *Horizons* :

$$X_{SCEN,i,k} = X_{CRU,i,j} \times \Delta_{horiz,i} \quad (4)$$

où  $X_{CRU}$  est la valeur mensuelle observée d'une année tirée aléatoirement sur la période de référence.

### Application des scénarii climatiques à la modélisation hydrologique

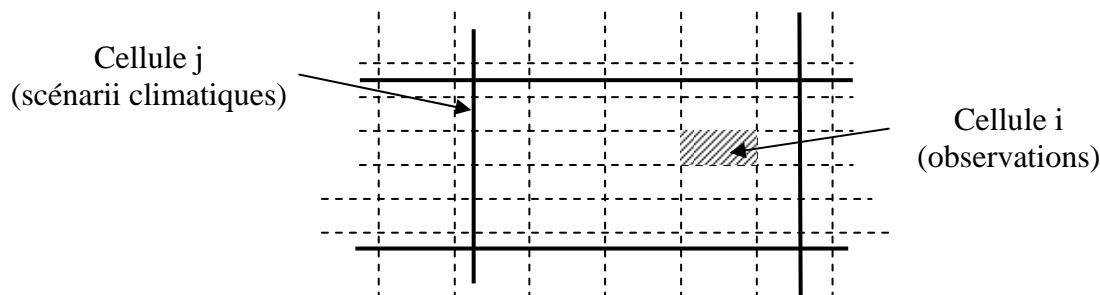


Fig. 2 : Superposition schématique des grilles scénarii climatiques avec les grilles de données observées (grilles CRU à 0,5°x0,5°).

Les données simulées par les GCM fournissent donc une base pour développer les scénarii climatiques. Cependant l'information issue du modèle HadCM3-A2 est à la résolution 2.5°x3.75°. Cette résolution spatiale est donc à première vue une limitation principale de l'application des scénarii climatiques dans les modèles hydrologiques. Une méthode simple est la désagrégation des scénarii climatiques à la résolution du fonctionnement des modèles hydrologiques, c'est-à-dire 0.5°x0.5°. La technique consiste à superposer le réseau du GCM à celui du CRU et d'appliquer la valeur d'une cellule de GCM à l'ensemble des cellules observées concernées (Fig. 2). L'indice  $i$  correspond au réseau de référence et l'indice  $j$  au réseau à désagréger. En utilisant un Système d'Information Géographique, on calcule la proportion de chaque cellule  $i$  incluse dans une cellule  $j$ . Cette proportion est notée  $coeff(i)$ . On utilise la formule suivante pour désagréger les données de précipitations et d'ETP des scénarii climatiques à l'échelle du demi-degré carré :

Désagrégation : 
$$X(i) = X(j) \times coeff(i) \quad (5)$$

où  $X(i)$  est la variable désagrégée sur la cellule  $i$ ,  $X(j)$  est la variable du scénario climatique sur la cellule  $j$  et  $coeff(i)$  est le coefficient d'intersection d'une cellule  $i$  dans une cellule  $j$ .

Cette approche est suffisante pour permettre l'évaluation des impacts du changement climatique sur les ressources en eau. Facile à appliquer, elle permet aux modèles hydrologiques d'utiliser des scénarii climatiques à une résolution qu'il serait autrement difficile à obtenir. Ainsi, les séries désagrégées de précipitations et d'ETP mensuelles issues des scénarii climatiques *Ano* et *Horiz* sont utilisées en entrées des deux modèles hydrologiques, GR2M et WBM, pour simuler les écoulements de chaque bassin versant. On suppose donc que la relation pluie-débit reste identique à celle formulée dans les modèles hydrologiques calés. Les paramètres ont donc été maintenus constants, depuis le calage initial avec les données climatiques observées, pour tout le XXI<sup>ème</sup> siècle.

## PRÉVISIONS DES RESSOURCES EN EAU POUR LE 21<sup>ÈME</sup> SIÈCLE

### Évolution climatique : précipitations et ETP

L'évaluation des précipitations pour les décennies à venir est très importante du fait de la sensibilité des modèles hydrologiques à cette variable. La Fig. 3 montre les taux de variations moyennes des précipitations *Ano* annuelles aux horizons 2020, 2050 et 2080, exprimés en un pourcentage par rapport à la moyenne observée 1969-1998.

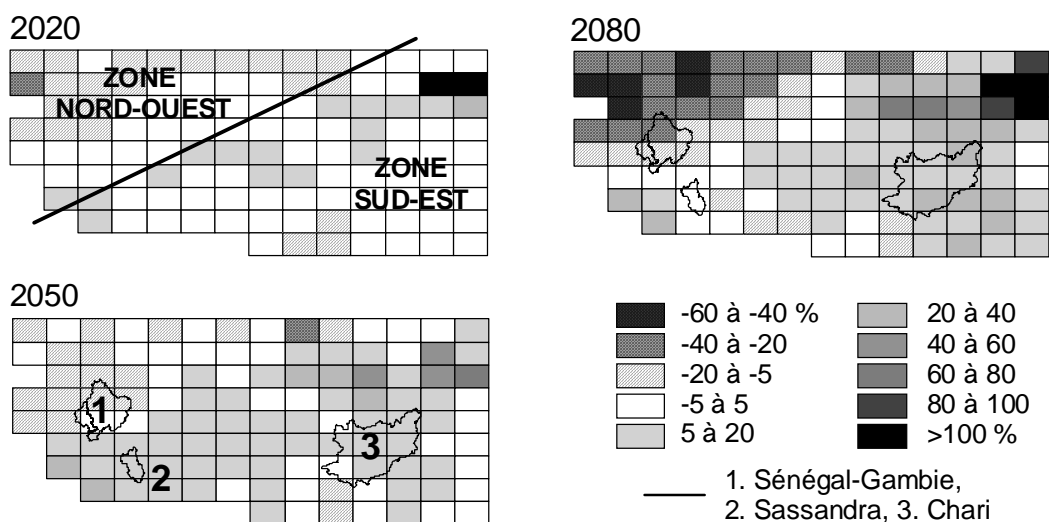


Fig. 3 : Variations des précipitations moyennes (scénario Anomalies) aux trois horizons par rapport aux précipitations moyennes observées sur la période 1969–1998 (en %). Les taux de variations entre les deux scénarii sont du même ordre de grandeur.

Les résultats sont similaires avec les précipitations *Horiz* et donc non présentés sur cette figure. Les variations aux trois horizons ne sont pas uniformes sur l'ensemble de la fenêtre étudiée. Deux zones se distinguent de part et d'autre d'un axe orienté sud-ouest / nord-est. On identifie également un petit groupe de cellules au nord-est de la fenêtre d'étude dont les variations sont supérieures à 100 % quelle que soit la série de précipitations étudiées (*Ano* ou *Horiz*) et quel que soit l'horizon considéré. Ces cellules sont toutes situées au Tchad ou au Soudan au-delà de 15° N, là où les précipitations annuelles sont très faibles et où le modèle HadCM3-A2 atteint ses limites. Au nord-ouest de cet axe, les précipitations moyennes annuelles diminuent, tandis qu'elles augmentent au sud-est de l'axe (Tab. 1). Pour les bassins du Sénégal et de la Gambie, les conditions pluviométriques déficitaires observées sur la période 1969–1998 semblent se maintenir, puis se dégrader à l'horizon 2080. Au contraire, les bassins versants du Sassandra et du Chari sont situés dans la zone où les conditions pluviométriques s'améliorent. On note que pour le bassin du Sassandra les taux de variations sont maximums à l'horizon 2050.

Tab. 1 : Taux de variations moyens des précipitations aux trois horizons, calculés par rapport à la période de référence 1969–1998 sur les deux zones identifiées (exprimés en %).

	Zone Nord-Ouest		Zone Sud-Est	
	<i>Ano</i>	<i>Horiz</i>	<i>Ano</i>	<i>Horiz</i>
2020	-5.4	-8.8	+1.6	+0.5
2050	-4.6	-2.1	+6.5	+6.8
2080	-28.9	-41.2	+11.4	+12.7

Tab. 2 : Taux de variations (en %) aux horizons 2020, 2050 et 2080 calculés pour les ETP\_ *Ano* et ETP\_ *Horiz* sur chaque unité hydrographique ; l'ETP moyenne observées est exprimée en 1/10e de millimètres.

Unités hydro.	ETP moy observée	Taux variation ETP_ <i>Ano</i>			Taux variation ETP_ <i>Horiz</i>		
		2020	2050	2080	2020	2050	2080
Sénégal -Gambie	19055	0.8	1.8	4.9	3.9	8.0	22.9
Sassandra	14147	1.5	4.5	10.6	2.4	6.2	15.7
Chari	17870	2.1	6.0	11.6	3.3	10.8	23.1
<b>moyenne</b>	17024	1.5	4.1	9	3.2	8.3	20.6

Comme tous les GCM prévoient un accroissement de la température pour les décennies à venir (jusqu'à 4°C avec le modèle HadCM3-A2), on constate une augmentation de l'ETP sur l'ensemble de l'Afrique de l'Ouest et Centrale. Cette augmentation, relativement faible à l'horizon 2020, atteint plus de 30 % à l'horizon 2080 (Tab. 2). L'Afrique Centrale et les pays en bordure du Golfe de Guinée sont touchés dès

l'horizon 2020 par cette hausse et montre les plus fort taux d'accroissement. Entre les deux séries élaborées, l'ETP\_Horiz montrent des taux de variations plus élevés par rapport à l'ETP\_Ano et ce, dès l'horizon 2020. Les taux de variations aux trois horizons pour chacun des quatre unités hydrographiques sont donnés dans le tableau 2. Les ETP moyennes observées sont exprimées en 1/10<sup>e</sup> de millimètres et constituent la valeur de référence. En moyenne sur ces quatre cellules, l'ETP augmente de 1.5 % à 3.2 % à l'horizon 2020, de 4.1 % à 8.3 % à l'horizon 2050 et de 9 % à 20.6 % à l'horizon 2080. Pour l'ETP\_Ano, les taux de variation les plus faibles sont observés pour la cellule 32LAT94LON, et les plus forts pour la cellule 34LAT05LON. Pour l'ETP\_Horiz, la cellule 34LAT95LON présente les taux de variation les plus faibles et la cellule 34LAT06LON les plus forts.

Associées à une ETP croissante, des précipitations réduites (accrues) laissent présager une réduction (augmentation) des écoulements. L'introduction des séries de précipitations et d'ETP issues des scénarii climatiques au sein des modèles hydrologiques retenus constitue l'étape ultime pour étudier l'impact du changement climatique sur les ressources en eau.

### **Évolution des écoulements**

Pour chaque bassin versant, les séries de précipitations et d'ETP mensuelles issues des scénarii climatiques *Ano* et *Horizons* sont utilisées en entrée des modèles hydrologiques, GR2M et WBM, pour simuler les écoulements. Les valeurs de débits mensuels ainsi simulés peuvent être considérées comme des valeurs "réalistes" permettant d'aboutir à des ordres de grandeur et traitées en terme de séries chronologiques, ou peuvent être comparées aux observations pour évaluer les changements en terme de taux de variation, exprimés en pourcentage. L'ensemble des tracés de débits moyens annuels entre 2006 et 2095 n'est pas représenté ici. En effet, nous disposons de quatre séries de débits simulés pour chaque bassin versant (2 modèles x 2 scénarii climatiques), correspondant à 168 graphiques au total.

Outre le volume que cela représente, certains de ces graphiques n'apporteraient aucune information supplémentaire. Toutefois, l'examen visuel de l'ensemble des tracés montre que les évolutions des débits moyens annuels simulés sous les conditions climatiques des scénarii "*Anomalies*" et "*Horizons*" sont semblables. Les différences majeures résident dans l'utilisation des modèles hydrologiques. On distingue trois situations d'évolution du débit moyen annuel sur la période 2006-2095 : (i) diminution plus ou moins importante des écoulements : bassins du Sénégal et de la Gambie ; (ii) augmentation, puis diminution des écoulements : bassins du Sassandra ; (iii) augmentation des écoulements : bassins du Chari.

Cette répartition découle directement de celle observée pour les précipitations issues des scénarii climatiques. Les écoulements sont plus sensibles aux variations sur les précipitations qu'aux variations sur les températures via celles de l'ETP. À vrai dire, les études menées par l'IPCC (2001) ont établi le même constat : les variations des débits simulés suivent largement les variations des précipitations pour le futur. Dans l'ensemble, un excès (un déficit) de précipitations selon les scénarii climatiques "*Anomalies*" ou "*Horizons*" se traduit par une augmentation (une diminution) des débits pour la majorité des bassins versants, quelle que soit l'évolution de l'ETP et donc des températures.

Du fait des jeux de paramètres retenus pour simuler les écoulements futurs, la période de référence retenue ici, pour évaluer les variations des écoulements aux horizons 2020, 2050 et 2080, est 1971-1995. Certes, elle ne comprend que 25 années mais elle est jugée significative des conditions observées ces trente dernières années. La Fig. 4 montre les taux de variation des débits moyens annuels *Ano* et *Horiz* simulés par les modèles WBM et GR2M pour quatre bassins versants jugés représentatifs des unités hydrographiques étudiées. Les variations des écoulements entre le scénario "*Anomalies*" et le scénario "*Horizons*" sont de même signe, même si les écarts entre les taux peuvent être importants, en particulier aux horizons 2050 et 2080.

Pour les bassins versants du Sénégal et de la Gambie, la tendance est à la diminution des écoulements. Aux horizons 2020 et 2050, le Sénégal présente des taux de variations positifs alors qu'ils sont négatifs pour la Gambie. Ces différences s'expliquent par la répartition des cellules du HadCM3-A2 au-dessus des bassins versants. En 2020, la Gambie est alimentée en précipitations par une cellule déficitaire (-1.7 %) et le Sénégal par une cellule excédentaire (+4.6 %). Mais à l'horizon 2080, selon le scénario climatique choisi, les déficits moyens annuels varient entre -3.6 % et -38.1 % pour les bassins du Sénégal et entre -19.4 % et -62.2 % pour les bassins de la Gambie (Tab. 3). Cette diminution est plus conséquente pour les séries simulées par le modèle GR2M\_Horiz.

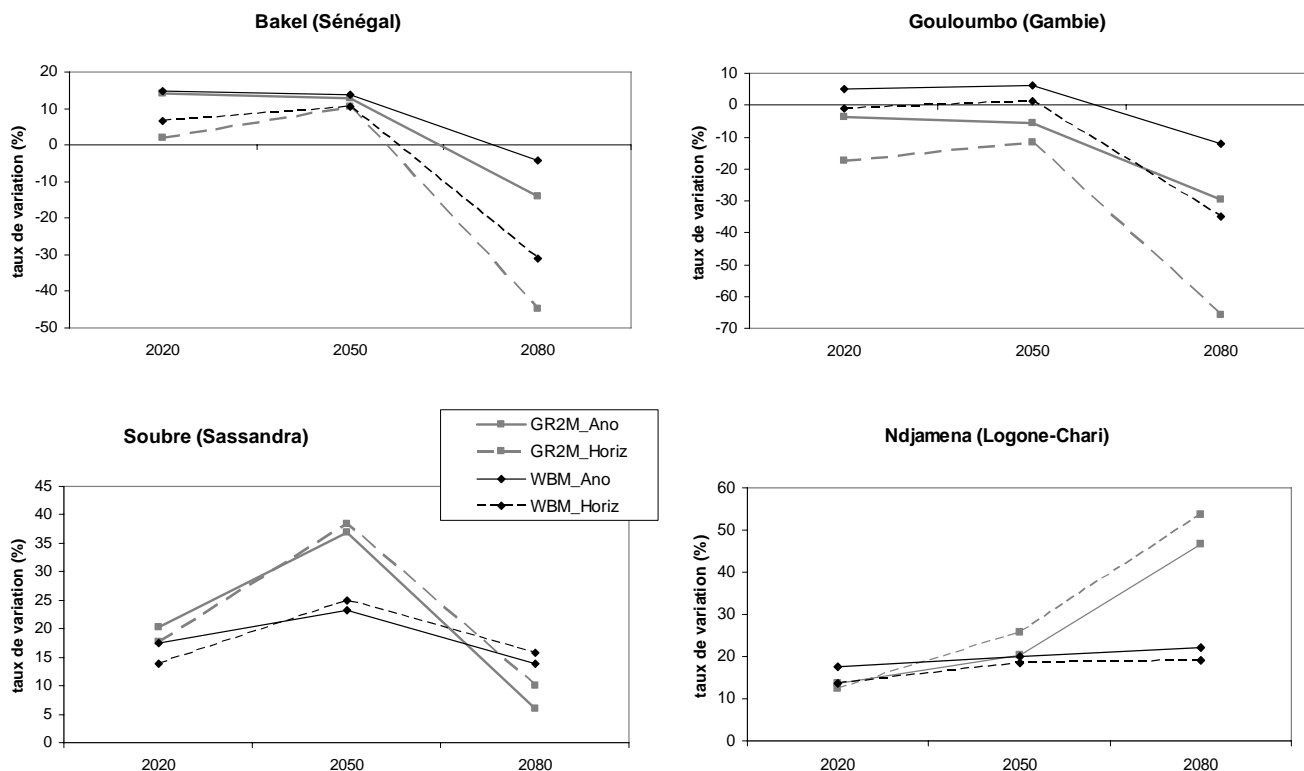


Fig. 4: Évolution des taux de variations des débits moyens annuels calculés aux trois horizons 2020, 2050 et 2080, pour quatre bassins versants représentatifs de chaque unité hydrographique.

Les débits moyens annuels simulés sur les dernières décennies du XXI<sup>ème</sup> siècle seraient donc plus faibles que ceux observés sur la période 1971–1995. Au contraire, les projections climatiques du modèle HadCM3-A2 conduisent à l'augmentation des écoulements pour les bassins du Chari et du Sassandra. Pour le Chari, les débits moyens annuels augmenteraient progressivement tout au long du XXI<sup>ème</sup> siècle : +10 % à +19.6% à l'horizon 2020 et de +22.3 % à +48.9 % à l'horizon 2080 (Tab. 3). Pour le Sassandra, les taux de variations à l'horizon 2080 (-14.2% à +13%) sont plus faibles qu'à l'horizon 2050 (+10.6 % à +22.7%) (Tab. 3). Malgré cette tendance à l'augmentation, les écoulements ne semblent pas retrouver les niveaux observés avant la mise en place de la sécheresse sur l'Afrique de l'Ouest et Centrale.

Tab. 3 : Taux de variation moyen par unité hydrographique des débits moyens annuels simulés aux horizons 2020-2050-2080 et exprimés en pourcentage par rapport à la période 1971-1995.

Unités hydro.	Horizon	GR2M_Ano	GR2M_Horiz	WBM_Ano	WBM_Horiz
Sénégal	2020	16,2	6,0	13,9	8,7
	2050	15,6	15,9	13,9	14,1
	2080	-10,4	-38,1	-3,6	-24,2
Gambie	2020	-6,6	-18,6	-1,7	-6,4
	2050	-8,0	-12,0	-0,7	-3,5
	2080	-29,6	-62,2	-19,4	-41,6
Sassandra	2020	-1,8	-4,5	15,5	12,3
	2050	10,6	13,2	20,7	22,7
	2080	-14,2	-13,5	11,8	13,0
Chari	2020	12,2	10,0	19,6	16,3
	2050	18,6	22,8	21,1	20,9
	2080	46,5	48,9	23,2	22,3

## CONCLUSION

Cette étude décrit une approche pour évaluer les changements possibles du climat et ses impacts potentiels sur les ressources en eau. La méthodologie mise en œuvre utilise des scénarii climatiques basés sur les projections du modèle HadCM3-A2 avec les modèles hydrologiques conceptuels GR2M et WBM pour simuler les écoulements futurs de quatre unités hydrographiques en Afrique de l'Ouest. Dans l'ensemble, les variations vont toutes dans le même sens, quels que soient le modèle et le scénario climatique utilisé. L'évolution de ces taux est à rapprocher de celle des précipitations *Ano* et *Horiz*. L'augmentation des précipitations sur la zone sud-est conduit à l'augmentation des débits sur les bassins versants du Logone et du Chari. Au contraire, la diminution des précipitations sur la zone nord-ouest entraîne une réduction de l'écoulement sur les bassins versants du Sénégal et de la Gambie. Il semble que l'augmentation continue de l'ETP affecte peu la production des écoulements en Afrique de l'Ouest et Centrale.

Cependant, deux remarques principales se dégagent de cette étude :

- les écarts entre les taux de variation sont importants, alors qu'on utilise au départ les mêmes données de précipitations et de température issues du modèle HadCM3-A2. Les séries de débit moyen annuel *Horiz* simulées par le modèle GR2M sont celles qui présentent les plus forts taux de variations aux trois horizons. À l'opposé, les séries *WBM\_Ano* sont celles qui présentent les taux de variations les plus faibles ;

- à l'horizon 2080 pour les bassins du Sénégal, de la Gambie et du Logone-Chari et à l'horizon 2050 pour le bassin du Sassandra, il y a eu une très grande différence d'amplitude entre les modèles pour un même scénario climatique *Ano* ou *Horiz*.

L'examen des séries de débits moyens annuels souligne les différences dérivant de l'utilisation de l'un ou l'autre des deux modèles hydrologiques retenus. Les débits moyens annuels simulés avec le modèle GR2M présentent des valeurs extrêmes et des dispersions supérieures à celles simulés par le modèle WBM et permet donc de classer les bassins versants en deux catégories :

- les bassins versants pour lesquels les débits moyens annuels simulés sont identiques quelle que soit la série *Ano* ou *Horiz* considérée, mais ils diffèrent selon les modèles hydrologiques utilisés. Ce sont des sous-bassins versants du Sénégal et de la Gambie ;

- les bassins versants pour lesquels les débits moyens annuels sont identiques quel que soit le modèle hydrologique considéré mais diffèrent selon la série *Ano* ou *Horiz*. Ce sont des sous-bassins versants du Chari et du Sassandra.

Ces résultats sont spécifiques au secteur étudié avec les projections du modèle HadCM3-A2 et ne peuvent être transposés ailleurs. Ils constituent un exemple d'utilisation des sorties des modèles climatiques pour évaluer les impacts sur les ressources en eau et doivent être utilisés avec précaution. Les simulations des écoulements au cours du XXIème siècle dépendent essentiellement du modèle hydrologique utilisé mais également des projections climatiques, et donc du choix du GCM. Si les prévisions des GCM convergent vers une augmentation significative de la température, l'étendue des situations rencontrées pour les précipitations en Afrique de l'Ouest (Casenave, 2004) suggère de prendre en compte les prévisions de plusieurs GCM pour évaluer la gamme des impacts potentiels.

## RÉFÉRENCES

- Ardoin, S., Lubes-Niel, H., Servat, E., Dezette, A., Boyer, J.F., Mahé, G. and Paturel, J.E. (2003) Analyse de la persistance de la sécheresse en Afrique de l'Ouest : caractérisation de la situation de la décennie 1990. *IAHS Pub.* 278, 223-228.
- Ardoin-Bardin, S. (2004) *Variabilité hydroclimatique et impacts sur les ressources en eau de grands bassins hydrographiques en zone soudano-sahélienne*. Thèse de Doctorat en Sciences de l'Eau. Université Montpellier II, France.
- Casenave, L. (2004) *Hydro-climatic variability: comparison of different global circulation model in western Africa*. Master thesis. University of Chalmers, Sweden.
- Conway, D. (1997) A water balance model of the Upper Blue Nile in Ethiopia. *Hydrol. Sci. J.* 42, 2, 265-286.

- Dieulin, C. (2005) Calcul des capacités en eau des sols (WHC) à partir de la carte des sols de la FAO. *Note technique*, UMR HydroSciences Montpellier.
- IPCC (2001) *Climate Change 2001: Impacts, Adaptation and Vulnerability*. Contribution of Working Group II to the Third Assessment Report of the IPCC. (Ed. by McCarthy J.J, Canziani O.F., Leary N.A., Dokken D.J., White K.S.) Cambridge University Press, Cambridge, UK.
- L'Hôte, Y., Mahé, G., Somé, B. and Triboulet, J.P. (2002) Analysis of a Sahelian annual rainfall index from 1896 to 2000; the drought continues. *Hydrol. Sci. J.* 47, 4, 563-572.
- Lucio, P.S. (2004) Geostatistical assessment of HadCM3 simulations via NCEP reanalyses over Europe. *Atmos. Sci. Let.* 5, 118-133.
- New, M., Hulme, M. and Jones, P. (1999) Representing twentieth century space-time climate variability. Part I: development of a 1961-1990 mean monthly terrestrial climatology. *J. Climate*, 12, 3, 829-856.
- New, M., Hulme, M. and Jones, P. (2000) Representing twentieth century space-time climate variability. Part II: development of a 1901-1996 monthly grids of terrestrial surface climate. *J. Climate*, 13, 13, 2217-2238.
- Paturel, J.E., Servat, E. and Vassiliadis, A. (1995) Sensitivity of conceptual rainfall-runoff algorithms to errors in input data. Case of the GR2M model. *J. Hydrol.* 168, 111-125.
- Penman, H.L. (1956) Evaporation: an introduction survey. *J. Agric. Sci.* 1, 9-29.
- Salathé, E. (2005) Downscaling simulations of future global climate with application to hydrologic modelling. *Int. J. Climatol.* 25, 419-436.



# CLIMATE CHANGE SCENARIOS AND IMPACTS ON THE SURFACE WATER RESOURCES OF THE VOLTA RIVER BASIN

**Yaw OPOKU-ANKOMAH**

CSIR-Water Research Institute, P.O. Box M.32, Accra, Ghana;  
y\_ankomah@yahoo.com

**Zinede MINIA**

Meteorological Services Agency, P.O. Box 87, Legon, Accra, Ghana

## ABSTRACT

A study was carried out in the Volta basin for assessment of impact of climate change on water resources. Two sets of climate change scenarios were used and these were synthetic scenarios and scenarios based on general circulation models (GCMs). The parameters modelled in the scenarios were temperature and rainfall. Two GCMs were used for the scenario generation. A water balance model WATBAL was used to assess the impact of climate change on runoff.

The modelling using the synthetic scenarios showed that runoffs or discharges are sensitive to changes in precipitation and temperatures and thus to climate change. A ten percentage reduction in precipitation or a rise of 1°C in temperature can cause a reduction in runoff of not less than 10%. Runoff simulations using GCM-based climate change scenarios indicated reduction in flows of about 16% and 37% for the year 2020 and 2050 respectively in the basin.

**Keywords:** Volta basin, GCM, runoff, precipitation, climate change

## INTRODUCTION

Water resources of the Volta River Basin are needed for the socio-economic development of the inhabitants of the basin. Development in the basin is low where Gross National Product of the six riparian countries is between \$190 and \$710 (World Development Report 2000/2001). There is a rapid population increase in the basin and water resources are needed for domestic and industrial water use, sanitation, irrigation of crops, generation of hydropower and navigation.

Available water resources in the basin have been on the decline for the past two decades in the basin and other sub-saharan region in general (Servat *et al*, 1998; Ardoin *et al*, 2003). In Ardoin-Bardin *et al*. (2005), predicted flow variations follow the rainfall variations and positive and negative rainfall and runoff anomalies were predicted in some parts of west and central Africa. Available potential water resources in the basin may be a limiting factor for development. Thus, the assessment of impacts of climate change on the water resources of the basin is crucial for its socio-economic development.

In assessing the impact of climate change on water resources of the Volta basin, a sub-basin was chosen as representative of the whole basin for the analysis (Fig. 1). The representative sub-basin is the White Volta basin which covers an area of about 105,000 km<sup>2</sup> of the total 400,000 km<sup>2</sup> of the whole Volta basin. Climate change scenarios were developed and used to simulate potential available water resources under climate change. The paper considers the development of the climate change scenarios and the simulations of the flows using the latter. The potential impacts of climate change on water resources are then assessed.

## MODELLING OF SYNTHETIC CLIMATE CHANGE SCENARIOS

Climate change scenarios were modeled using two approaches. In the first one referred to as synthetic scenarios, historical data sets between 1961 and 1990 were used as the base data. The synthetic scenarios were developed by uniformly increasing or decreasing the base data. Temperatures were increased by 1°C or 2°C and rainfall were decreased or increased by 10% or 20% of the base values.

# MODELLING OF CLIMATE CHANGE SCENARIOS USING GCM OUTPUTS

## Method

The second method and the most detailed used the output of General Circulation Models (GCMs). The method after Hulme and Jenkins (1998) and Hulme *et al.* (1999) was adopted. The method takes into account only the consequences of anthropogenic interference with the climate system through emission of Greenhouse Gases into the atmosphere. Also considered, is the cooling effect of anthropogenic sulphate aerosols in the atmosphere on future global and regional temperature. Scenarios for change in mean daily temperature and rainfall with respect to 1961 to 1990 baseline means for the thirty-year periods centered on 2020, 2050 and 2080 were constructed.

In the method, the response patterns of GCMs to various greenhouse gas emission path ways were first standardized. These standardized values were then scaled by the global warming values of user specified emission scenarios, calculated using a simple climate model. The pattern scaling method was based on the separation of the global-mean and spatial-pattern components of future climate change, and the further separation of the latter into greenhouse-gas and aerosol components. The simple climate model employed here is known as MAGICC (Model for the Assessment of Greenhouse gas Induced Climate Change) developed at the Climatic Research Unit (CRU) of the University of East Anglia (UEA). MAGICC is a coupled gas-cycle/climate model that drives a spatial climate-change scenario generator (SCENGEN). The main advantage of MAGICC and its inbuilt Scenario generator known as SCENGEN, is that, it allows for user defined emission scenarios and choice of atmospheric sensitivity, as well as choice of GCM results that are contained in its database. This makes it possible to compare the global warming potential of different GCMs under the same greenhouse gas forcing specifications. An important feature in MAGICC, is the inclusion in its carbon cycle model of climate feedbacks, which has been taken into account, in developing these scenarios.

## Climate Models, Atmospheric Sensitivity and Emission Scenarios

The outputs of two GCMs, the European Centre Hamburg Model (ECHAM4) and the Commonwealth Scientific and Industrial Research Organization (CSIRO) model, were used in the construction of the scenarios. Atmospheric sensitivities of 2.6°C and 4.5°C, respectively while MAGICC parameter and aerosol effect, were set at medium values in both cases, were used to scale the two GCM results. Two sets of scenarios were thus developed, one set for mid-range values and the other, the upper boundary values.

The greenhouse gas emission scenario that was used is known as A1FI, and is a member of the A1 scenario family of the recently published IPCC emission scenarios in the Special Report on Emission Scenarios (Nakicenovic *et al.*, 2000). The A1 scenario family describes a future world of very rapid economic growth, a global population that peaks in about 2150 and declines thereafter, and the rapid introduction of new and more efficient technologies. The A1FI option assumes fossil intensive energy sources for production.

## Data

Observed climatological data from the globally-complete CMAP (Xie and Arkin, 1997-updated) precipitation and CRU (New *et al.*, 1999) temperature climatologies used in the MAGICC/SCENGEN model, served a major purpose in the construction of these scenarios. Additional information on temperature and rainfall, was obtained from the Ghana Meteorological Agency for the period 1961 to 2000. Climatological means for the period 1961 to 1990 calculated from these data sets were used to define the baseline climates for six eco-climatic zones of the basin. Also in order to appreciate the changes that anthropogenic interference with climate system by way of greenhouse gas emissions could cause the climate of the basin, the observed time series of temperature and rainfall, were analyzed for each eco-climatic zone. This made it possible to look at trends in these variables during the period 1961 to 1990 and compare such with the projected trends captured in the scenarios.

## **Climate Change Scenarios**

Plots of historical time series of temperature and rainfall showed increasing temperatures in all zones during the 1961 to 1990 period (Fig. 2 and 3). This is consistent with global trends for the same period. For precipitation, however, the trend has been towards decreasing annual totals during the same period. The climate scenarios constructed using the mean of the outputs of the two GCMs, follow the trends inherent in the observed past climate record in all the zones. It must however, be noted that these projections are based solely on the effect of anthropogenic signal. This is essential in climate change impacts assessments, as it is the effects of human action on the climate system, that relevant policy initiatives could be directed to address. The scenarios do indeed indicate that, by the 2050s for example, annual mean temperatures could have risen by about 2°C while rainfall amounts could reduce by above 12% over the baseline values. These scenarios are however, based on a mid-range estimate of the sensitivity of the atmosphere to anthropogenic greenhouse gas forcing. A higher estimate of the value of the atmospheric sensitivity did produce much higher estimates of the changes in temperature and precipitation in the future, in all zones. For example, when an atmospheric sensitivity of 4.5°C was used, temperatures by the 2050s were higher by about 2.5°C and rainfall totals becoming only about 84% of the baseline values in all the zones.

## **HYDROLOGICAL MODELLING**

### **Model Description**

A water balance model WATBAL (Yates, 1994) was used to assess the response of catchment runoff to potential climate change. The model consists of two components: the water balance component and a component that calculates the potential evapotranspiration (PE) which is very critical in assessing climate change impact on water resources. The PE is calculated by Priestly-Taylor method. The water balance component of the model has five parameters related to direct runoff, surface runoff, subsurface runoff, maximum catchment holding capacity and base flow.

### **Baseline Data**

The following monthly mean data sets were collected for the hydrological modelling and simulation: rainfall, temperature, sunshine duration, relative humidities and river discharges. The data collected cover the period 1961-1990. The hydrometeorological stations are shown in Fig. 1. The basin area rainfall was computed by the Thiessen polygon method from five stations evenly distributed in the basin. The discharge data used were taken from Nawuni in the downstream part of the basin. Historical data sets of temperature, rainfall and runoff in the basin were analyzed as indicated earlier, to check any trend or changes in the time series. Plot of the mean annual temperature trend is shown in Fig. 2 and the rainfall and runoff trends in Fig. 3. In Fig. 2, there was an observed rising trend in the temperature of about 1°C over the 30 year period. The rise in temperatures is associated with climate change linked to atmospheric warming. Concurrent reductions were however observed in rainfall and runoff especially beyond 1970 (Fig. 3) as in Opoku-Ankomah and Amisigo (1998) for the south-western river system of Ghana and in Servat *et al* (1998). The White Volta basin mean annual rainfall from 1961 to 1970 was about 1003 mm and the mean for 1971 to 1990 was 863 mm. The magnitude of the latter rainfall was 86% of the former showing a reduction of about 14%. Similarly, reductions in runoffs were observed and mean annual runoff estimated for the 1961-70 and 1971-90 periods were 84 and 57 mm respectively. The latter mean runoff was just 68% of the former showing a reduction of 32%. The reductions in historical rainfall and runoff point to climate variability and possible impacts of climate change.

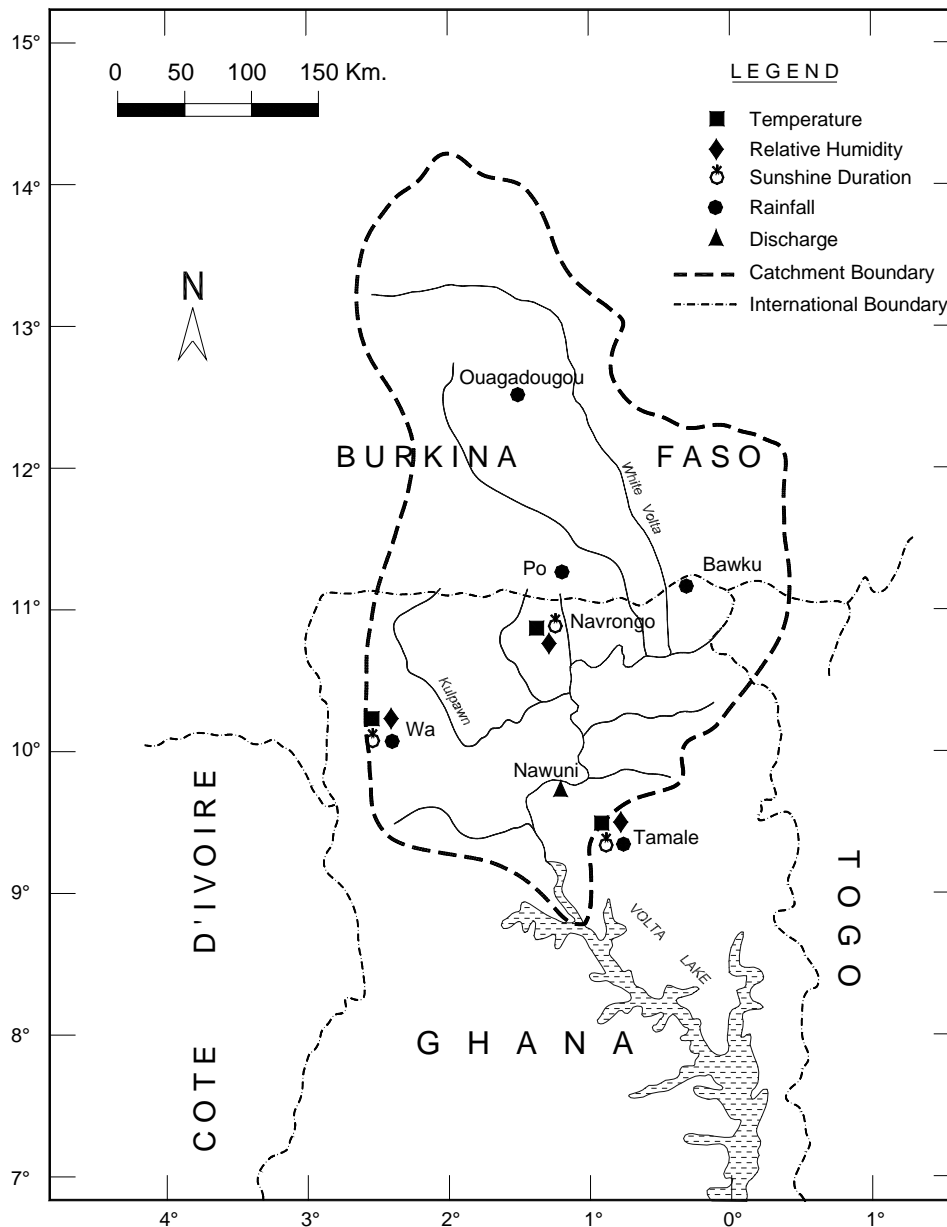


Fig. 1: White Volta Basin Showing Some Hydrometeorological Stations.

### **Calibration of the Model**

The model was calibrated using the following hydro-climatic variables: effective precipitation, temperature, relative humidity, sunshine duration and runoff. Effective precipitation was pre-defined and entered into the model. In its determination, seasonal characteristics of the basin's rainfall and wetness of catchment were taken into consideration.

The parameters for initial relative storage, direct runoff coefficient, base flow, the power term associated with the sub-surface runoff coefficient were pre-defined. In the calibration, several runs of the model were carried out for minimum error. The data used for the calibration was from 1961 to 1974. The model was run in a monthly time step (30.4 days).

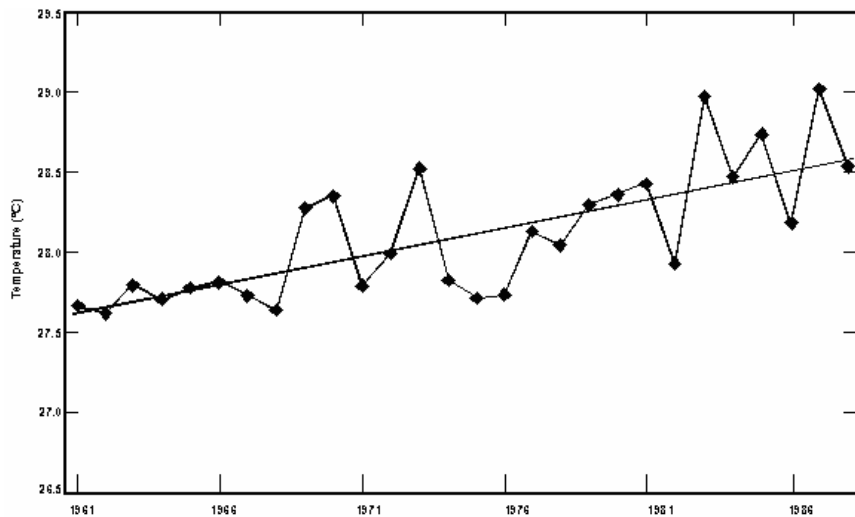


Fig. 2: Temperature trend in the White Volta basin over the years 1961-1988.

### **Validation of the Model**

The model was validated using data from 1975 to 1988 which were available. During the validation, optimized parameters obtained from the calibration were used. The correlation coefficient for the calibration and validation were 0.88 and 0.80 respectively. Plots (not presented) showed good fits for both the calibrated and the validated series. The model, however, slightly overestimated the minimum flows and also underestimated the peak flows.

## **MODEL SIMULATION USING SYNTHETIC CLIMATE SCENARIOS**

Synthetic climate scenarios were initially simulated to check the sensitivity of the model to climate change. Simulation of synthetic scenarios offers further opportunity to examine a wide range of possible climate change and their impacts on runoffs. Certain critical runoffs and changes in climatic conditions that may give rise to them could be assessed in making decisions for water resources development and management.

Historical rainfall data, temperature, sunshine hours and relative humidity within the period 1961-1990 were used as base data. The percentage changes in modelled runoffs of the synthetic scenarios with respect to the runoff of the base data were tabulated and plotted. The plot is shown in Fig. 4. The method assumes that the historical data series will repeat itself with uniform increment or reduction over the time period and this may be a limitation to the real life situation.

It is observed from the plot that runoff is sensitive to both precipitation and temperature changes. This means that there are corresponding changes in runoffs when temperature and precipitation change. The changes are however not uniform over the whole temperature and precipitation ranges. For example, 10% change in precipitation at constant temperature produced between 10% and 22% change in runoff depending on the magnitudes of precipitation and temperature at which the changes occurred.

Similarly, for 1°C rise in temperature, there is a reduction of 10% to 23% change in runoff. These non-uniform changes are observed in the plots as slight convergence of the curves at the bottom left or divergence at the top right.

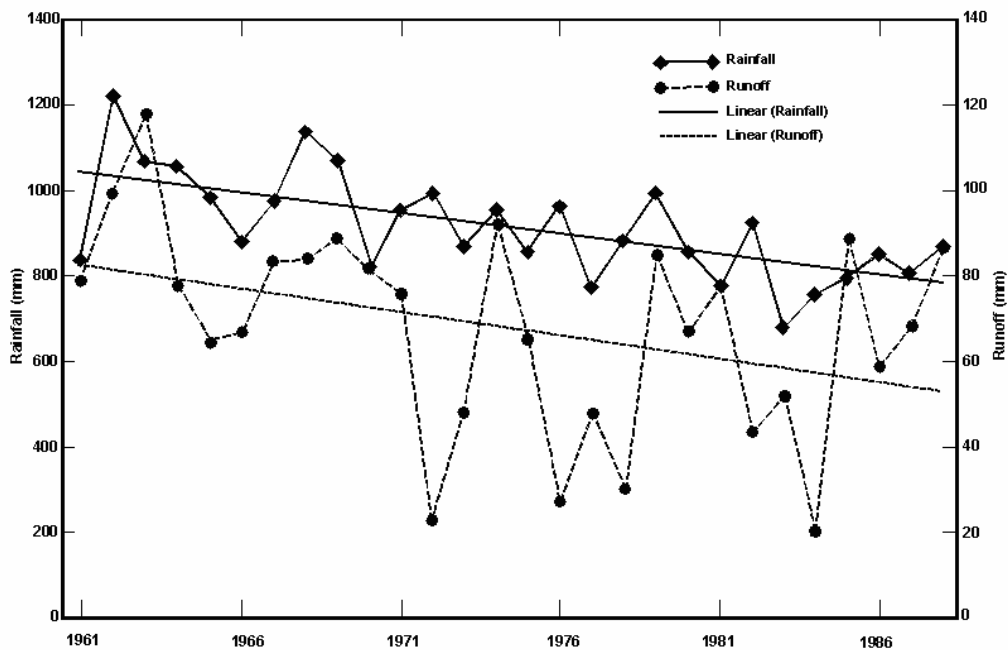


Fig. 3: Rainfall and runoff trends in the White Volta basin over the years 1961-1988.

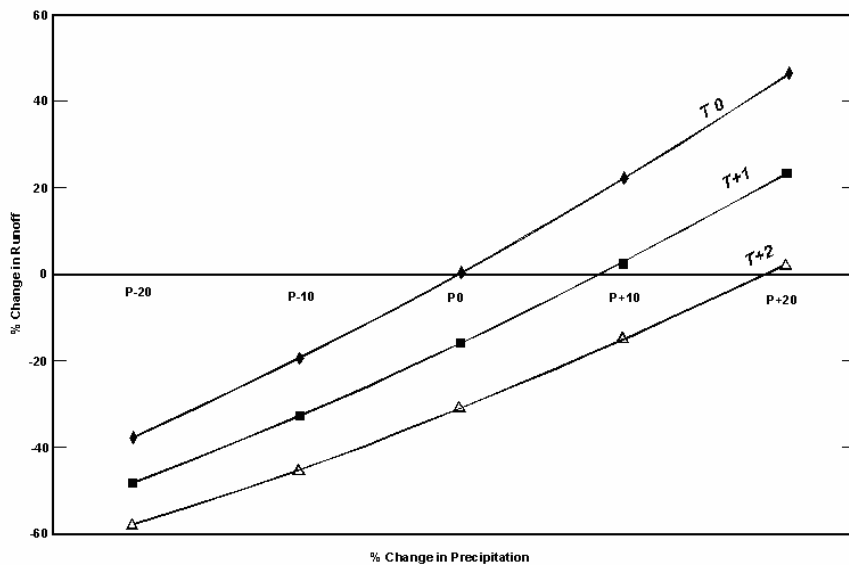


Fig. 4: Percentage change in runoff with respect to the precipitation and temperature (White Volta basin).

## MODEL SIMULATION USING GCM-BASED CLIMATE SCENARIOS

Temperature and rainfall changes were extracted from the constructed climate scenarios for the basin for the year 2020 and 2050 and used for the simulations. The changes in rainfall and temperature were applied to the base scenario to develop climate change scenarios. Six scenarios were generated for the two time periods using three levels of sensitivity.

The model was run using the optimized parameters selected after the calibration and validation of the model. The modelled runoffs using the generated climate scenarios were compared with the modelled runoffs of the base climate scenarios. The percentage changes in runoffs were computed and tabulated in Tab. 1 below.

Tab. 1 : Percentage change in runoff in the White Volta basin using the result of GCM-based climate change.

	Low Sensitivity	Medium Sensitivity	High Sensitivity
2020	-8.8	-15.8	-22.9
2050	-24.0	-37.1	-50.9

The results shown in the table indicate reduction in runoff for the two time periods. The low and the high sensitivity values give an indication of the range of values. The medium sensitivity values indicate that runoff could decrease by 15.8% and 37.1% by the year 2020 and 2050 respectively. These reductions are to be associated with greenhouse gas induced climate change. These results have implications for the future water resource availability in the basin.

The reduction in runoffs identified in the historical data sets for the same 30-year period are greater than the reduction in runoffs simulated from greenhouse gas induced climate change scenarios. In the basin, the historical series indicated a reduction of about 30% in runoff as compared to the reduction in the range of 9 to 23% in simulated runoffs as shown in Tab. 1. The increase in historical temperature and reduction in rainfall over a 30-year period were approximately 1°C and 20% respectively while the changes projected under greenhouse gas induced climate change were about 1°C and 5% for temperature and precipitation respectively. Thus the change in historical rainfall series was much greater than the change projected by the climate scenarios which was only 5%. The change in temperature is approximately the same and thus the high reduction in historical runoff must be due to the corresponding high reduction in rainfall. Groundwater abstraction is not very significant to cause these high changes in runoffs.

The high reduction in rainfall and runoff is not due to only the effect of greenhouse gas induced climate change but other factors such as land-use and climate variation. Climate variation is normally part of the hydrological cycle and further studies will be needed to model these factors.

The results of the runoff simulation using the GCM-based climate scenarios and regional climate models are consistent with the result using the synthetic scenarios. The curves derived from the synthetic scenarios can therefore be used to estimate the probable change in runoff if the change in temperature and the percentage change in precipitation are known. Thus results of the study (Fig. 4) provide a rapid method for assessing future probable changes in runoff when changes in temperature and precipitation are known. Improved results from GCM outputs for assessing changes in temperature and rainfall could easily be used in assessing changes in runoff.

## CONCLUSION

The climate scenarios presented here have been constructed applying appropriate techniques and methods and while acknowledging the many uncertainties usually associated with climate scenarios, in particular those developed using GCM outputs, they are appropriate for use in assessing climate change impacts in the areas for which they have been developed.

The hydrologic model was found to be sensitive to potential climate change and the model when applied showed reduction in future runoff in the basin. The potential reductions in runoff are of the orders of 16% and 37% by the years 2020 and 2050. These results have far reaching implications for water resources development and management in the basin.

## REFERENCES

- Ardoin, S., Lubes-Niel, H., Servat, E., Dezetter, A., Boyer, J. F., Mahé, G. and Paturel, J.E. (2003) Analyse de la persistance de la sécheresse en Afrique de l'Ouest: caractérisation de la situation de la décennie 1990. *IAHS Pub.* 278, 223-228.
- Ardoin-Bardin, S., Dezetter, A., Servat, E., Mahé, G., Paturel, J.E., Dieulin, C. and Casenave, L. (2005) Evaluation des impacts du changement climatique sur les ressources en eau d'Afrique de l'Ouest et Centrale. *IAHS Pub.* 296, 194-202.

- Hulme, M. and Jenkins, G.J. (1998) Climate change scenarios for the United Kingdom. *UKCIP Technical Note No. 1*. Climate Research Unit, Norwich, UK, 80 p.
- Hulme, M., Mitchell, J.F.B., Ingram, W., Johns, T.C., Lowe, J.A., New, M.G. and Viner, D. (1999) Climate change scenarios for global impacts studies. *Global Environ. Change*, 9, S3-S19.
- Nakicenovic, N., Alcamo, J., Davis, G., de Vries, H.J.M., Fenhann, J., Gaffin, S., Gregory, K., Grubler, A., Jung, T.Y., Kram, T., La Rovere, E.L., Michaelis, L., Mori, S., Morita, T., Papper, W., Pitcher, H., Price, L., Riahi, K., Roehrl, A., Rogner H.H., Sankovski, A., Schlesinger, M., Shukla, P., Smith, S., Swart, R., van Rooijen, S., Victor, N. and Dadi, Z. (2000) *Special Report on Emission Scenarios*. Intergovernmental Panel on Climate Change. Cambridge University Press, Cambridge.
- New, M., Hulme M. and Jones, P.D. (2000) Representing twentieth century space-time climate variability. Part2: Development of 1901-96 monthly grids of terrestrial surface climate. *J. Climate*, 13, 13, 2217-2238.
- Opoku-Ankomah, Y. and Amisigo, B.A. (1998) Rainfall and runoff variability in the south-western river system of Ghana. *IAHS Pub.* 252, 307-314.
- Servat, E., Paturel, J.E., Kouame, B., Travaglio, M., Ouedraogo, M., Boyer, J.F., Lubes-Niel, H., Fristch, J.M., Masson, J.M. and Marieu, B. (1998) Identification, caractérisation et conséquences d'une variabilité hydrologique en Afrique de l'Ouest et Centrale. *IAHS Pub.* 252, 323-338.
- World Bank (2001). *World Development Report 2000/2001*.
- Xie, P. and Arkin, P.A. (1997) Global precipitation: A 17-year monthly analysis based on gauge observations, satellite estimates, and numerical model outputs. *Bulletin of the American Meteorological Society*, 78, 2539-2558.
- Yates, D. (1994) *WATBAL—An integrated water balance model for Climate Impact Assessment of River Basin Runoff*. WP-94-64. Yates, D. (ed.). International Institute for Applied Systems Analysis. Laxemburg, Austria.

# IMPACTS DES FLUCTUATIONS CLIMATIQUES SUR LE REGIME DES ECOULEMENTS DU FLEUVE SANAGA AU CAMEROUN, PROSPECTIVES POUR LE XXI<sup>EME</sup> SIECLE

**Daniel SIGHOMNOU, Luc SIGHA NKAMDJOU, Gaston LIENOU**

Centre de Recherches Hydrologiques, BP 4110 Yaoundé, Cameroun

*danielsighomnou@yahoo.fr*

**Alain DEZETTER, Gil MAHE, Eric Servat, Jean Emmanuel PATUREL, Jean-Claude OLIVRY**

Institut de Recherche pour le Développement, Montpellier, France

**Félix TCHOUA, Georges Emmanuel EKODECK**

Département des sciences de la terre, Université de Yaoundé I, Yaoundé, Cameroun

## RESUME

Les performances de deux modèles hydrologiques (GR2M et Yates) ont été analysées en utilisant les données d'observation du bassin versant de la Sanaga à Edéa. La meilleure reconstitution des débits est obtenue avec le modèle GR2M qui est alors utilisé pour simuler les futurs écoulements du fleuve à Edéa. Deux jeux de données construits à partir des données brutes du modèle climatique HadCM3 sont utilisés. Par rapport à la période 1971-2000, les deux scénarii prévoient une augmentation de précipitations moyennes annuelles sur le bassin pouvant atteindre +7,4 % dans le courant du XXI<sup>ème</sup> siècle et dans le même temps une augmentation graduelle de l'évapotranspiration moyenne annuelle qui atteint 30% vers 2100. Par rapport à la même période de référence, les écoulements varient entre +4 et -20% (+18 à -93 mm/an en terme de lame écoulée sur le bassin) suivant le scénario. Si l'on se réfère aux débits non régulés de la période 1943-1969 par ailleurs reconnue pour son caractère humide dans la région, les deux scénarii testés montrent qu'une période comparable ne sera jamais retrouvée durant tout le XXI<sup>ème</sup> siècle. Ils prévoient des débits annuels globalement inférieurs (-10 à -32%) tout au long de ce siècle, soit -52 à -162 mm/an en terme de lame écoulée. La planification des usages futurs des ressources en eau du bassin de la Sanaga devrait tenir compte de cette situation.

**Mots clefs :** changement climatique, modélisation hydrologique, GR2M, Cameroun, Sanaga, scénario climatique

## INTRODUCTION

En raison de ses répercussions sur le milieu naturel et le développement socio-économique, les questions de variabilité climatique et leurs implications sur les ressources en eau sont placées depuis quelques temps au centre des préoccupations des scientifiques et des décideurs politiques dans le monde. Prévoir et caractériser l'impact de ces fluctuations sur les disponibilités en eau dans l'espace et dans le temps deviennent alors indispensables pour proposer des solutions adaptées aux projets de développement et à une gestion durable de l'environnement. De ce point de vue, les ressources en eau du bassin versant du fleuve Sanaga jouent un rôle très important sur le plan de l'économie du Cameroun. La Sanaga draine à elle toute seule le quart des ressources en eau du pays, produit maintenant près de 90% de l'énergie hydroélectrique du pays et dispose encore d'un important potentiel énergétique non exploité. Les autres usages de ses ressources vont des besoins *in situ* du milieu naturel, à l'agriculture irriguée et pluviale, l'eau potable, la navigation, l'industrie, la dilution d'effluents, les loisirs, etc.. Ces demandes sont différentes par leurs besoins en terme de degré de sensibilité aux variations, la saisonnalité des besoins, les exigences de qualité, etc. Dans ces conditions, il serait intéressant d'anticiper les impacts des fluctuations climatiques pour la planification et l'organisation des usages futurs.

Deux modèles de bilans hydrologiques (Yates et GR2M) calés et validés sur la base des observations de la période sans régulation (1943-1969) des écoulements de la Sanaga permettent une simulation fiable des écoulements de la période récente non jaugés et de se faire une idée de l'impact du changement climatique sur le régime hydrologique dans le courant du XXI<sup>ème</sup> siècle. Les prévisions de précipitations et d'évapotranspiration pour le XXI<sup>ème</sup> siècle fournies par le modèle climatique HadCM3 sont utilisées pour des analyses prospectives. Des simulations à partir de deux jeux de données issus des prévisions de

ce modèle montrent une baisse croissante des écoulements moyens annuels par rapport à ceux de cette période connue pour son caractère humide dans la région.

## PRESENTATION DU BASSIN VERSANT DE LA SANAGA A EDEA, DONNEES ET METHODES

Avec un bassin versant dont la superficie est évaluée à 133 000 km<sup>2</sup>, le fleuve Sanaga compte parmi les grands cours d'eau de l'Afrique tropicale et constitue le plus grand fleuve du Cameroun dont il couvre près du tiers de la superficie et draine près du quart (65 000 km<sup>3</sup>/an) des ressources en eau. Presque entièrement camerounais, son bassin versant s'étend entre les parallèles 3°30 et 7°30 et couvre ainsi des régions passant du climat équatorial (à 4 saisons et une pluviométrie comprise entre 1600 et 4000 mm), au climat tropical à 2 saisons et une pluviométrie comprise entre 1600 à 1400 mm (Fig. 1).

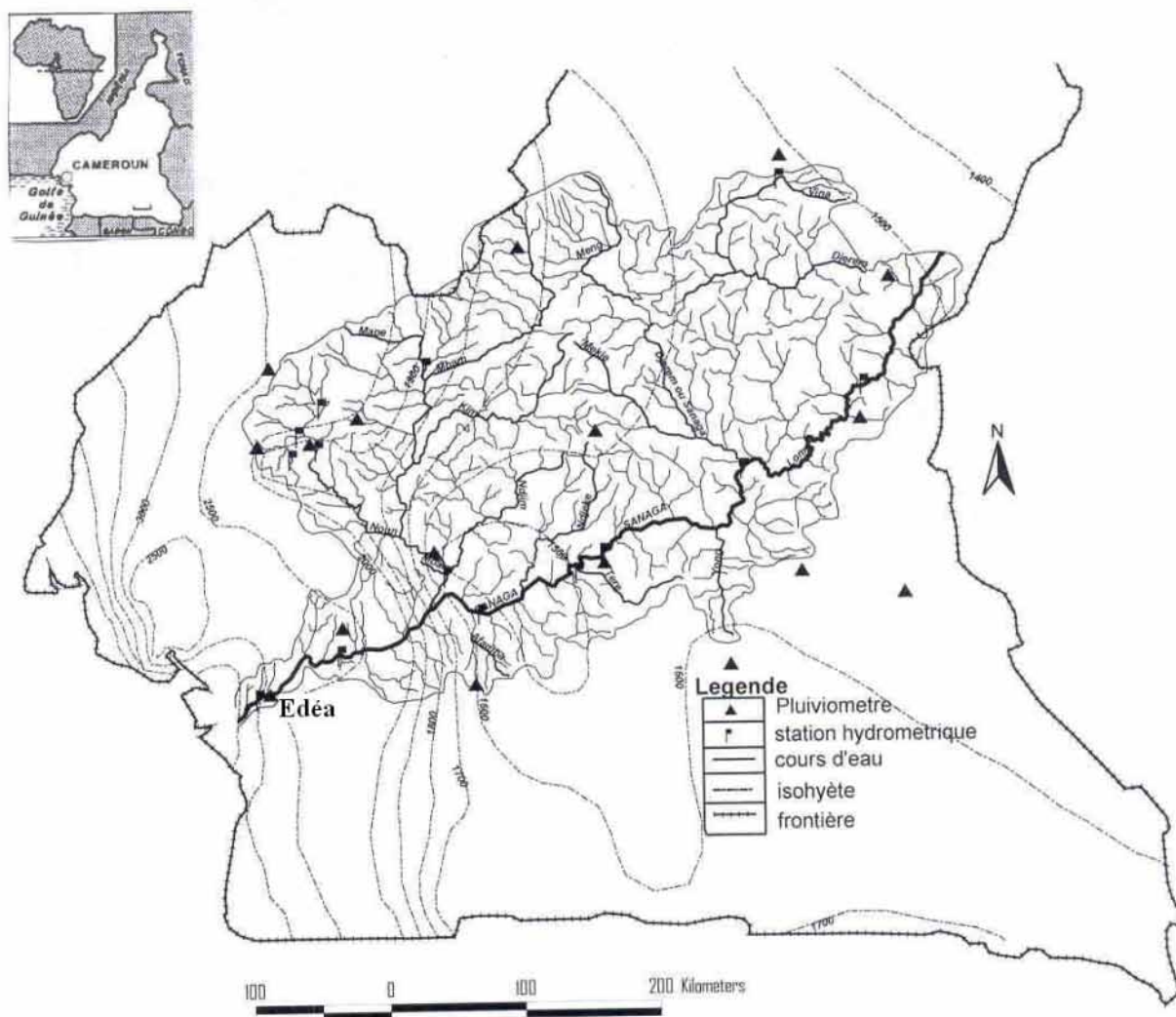


Fig. 1 : Bassin versant de la Sanaga à Edéa.

Les sols ferrallitiques qui occupent la quasi-totalité du bassin supportent une végétation qui passe de la savane arbustive (près des 2/3 du bassin versant) dans le Nord, à la forêt dense humide dans le Sud. La densité des populations y est tout aussi variée. Elle va des hauts plateaux de l'Ouest du pays où elle dépasse 200 habitants au km<sup>2</sup>, aux régions presque vides de populations dans le centre du bassin (région de Yoko), en passant par les zones d'exploitations agro-industrielles (plantations de cannes à sucre) de la

région de Mbandjok. Les pôles de grandes activités socio-économiques sont quant à eux situés aux marges du bassin versant, notamment à Edéa du côté de l'exutoire. L'importance de ce fleuve sur le plan de l'économie du Cameroun est également considérable, puisqu'il dispose d'un potentiel énergétique extraordinaire et produit maintenant près de 90% de l'énergie hydroélectrique du pays.

Outre l'information hydropluviométrique, l'étude utilise des données d'évapotranspirations (ETP) et des données sur la capacité de rétention en eau des sols. Plus d'une vingtaine de stations hydrométriques ont été suivies sur la Sanaga, dont certaines depuis le début des années 1940. Ces observations, généralement de bonne qualité, se sont poursuivies régulièrement jusqu'au début des années 1980, mais elles sont arrêtées depuis près de deux décennies ou au mieux, se limitent à la seule période d'étiage à quelques stations jugées d'intérêt pour l'exploitation hydroélectrique. Trois barrages de retenue d'une capacité totale de 7 600 km<sup>3</sup> sont actuellement en fonction sur son bassin, dont le premier depuis la fin des années 1960. Ils permettent la régulation du débit en vue d'une production énergétique efficiente, ce qui conduit à la modification du régime des écoulements naturels. Les observations hydrométriques utilisées dans l'étude sont celles de la station d'Edéa (un bassin versant de 131 500 km<sup>2</sup>) qui couvrent la période 1943-1983. Elles seront complétées jusqu'en 2000 par les données de simulation du modèle GR2M au moyen des données d'observation de précipitations et d'ETP déterminées par le Climatic Research Unit (CRU) à partir des données d'observation de températures. Si le suivi pluviométrique a commencé beaucoup plus tôt sur le bassin, les données d'observations utilisées dans l'étude (14 stations) se sont limitées à la période 1950-2000, par souci d'homogénéité des séries. Il en va de même pour les données d'observation de températures (une douzaine de postes) utilisées dans les calculs de l'ETP. Les données sur la capacité de rétention en eau des sols ont été tirées de la classification fournie par la FAO (Dunne and Willmott, 1996), suivant une méthodologie mise au point par le groupe *Vahyne* de l'IRD (Ouedraogo, 2001). Pour permettre de faire des comparaisons, des données d'ETP, de précipitations et de capacité en eau des sols issues du Climatic Research Unit ont été également utilisées.

## LES MODELES PLUIE-DEBITS

La typologie des modèles mathématiques utilisés en hydrologie de nos jours est très variée. Les modèles distribués (ou maillés) et ceux dérivés de l'analyse des systèmes comptent parmi les plus évolués. Les modèles GR2M et de Yates utilisés dans notre étude appartiennent à ces deux groupes. Ils ont déjà été utilisés avec succès sur de nombreux bassins versants de la région tropicale africaine (Ouedraogo, 2001 ; Nkankam Kamga, 2001 ; Ardoin, 2004 ; Sighomnou, 2004). Les performances des deux modèles sur le bassin versant de la Sanaga à Edéa sont satisfaisantes, avec un avantage pour GR2M. On se réfèrera à Makhoulf (1994) et Yates (1997) pour la description des modèles et leur schéma de fonctionnement qui peut se résumer comme suit : le bassin versant est discrétisé en unités spatiales (mailles d'un demi-degré carré, soit environ 55 x 55 km) considérées comme homogènes, qui se vident les unes dans les autres de l'amont vers l'aval. Les lames d'eau écoulées mensuelles en tout point de l'espace sont estimées à partir d'informations disponibles sur la région considérée. A partir de grilles de précipitations, d'évapotranspiration potentielle et de données liées au stockage de l'eau dans le sol, on simule par le modèle les variations de l'humidité du sol, de l'évapotranspiration réelle et de l'écoulement. Celles-ci sont calculées pour chaque maille, indépendamment les unes des autres, et chaque mois. L'écoulement total à l'exutoire de chacun des bassins est obtenu par sommation des contributions élémentaires pondérées des différentes mailles qui les constituent.

Pour permettre de faire des comparaisons, trois grilles mensuelles de pluies construites à partir de données pluviométriques de deux origines différentes ont été utilisées dans le modèle. Un premier échantillon est constitué des grilles de pluie mensuelle fournies par le Climatic Research Unit (CRU), alors que les deux autres sont obtenues à partir de l'ensemble des données d'observation des pluies ponctuelles enregistrées au niveau des 14 postes d'observation signalés plus haut. Une première grille établie par la méthode de spatialisation de l'information par le procédé de krigeage du logiciel Surfer et une deuxième créée à partir des mêmes données par la méthode d'interpolation de Thiessen. Les données d'ETP utilisées (fournies par le CRU) sont constituées par quatre séries de grilles mensuelles générées à partir d'observations climatologiques de la région : une première grille de valeurs d'ETP est calculée par la méthode de Penman (1956), une deuxième déterminée par la méthode décrite par Shuttleworth (1994), une troisième par la méthode décrite par Thom et Oliver (1977), alors que la quatrième grille de données est générée par la FAO (Food and Agriculture Organization). Quatre séries de grilles mensuelles de données sur la capacité de rétention en eau du sol ont été testées. Trois d'entre elles ont été construites à

partir de la carte des sols diffusée par la FAO alors que la quatrième est fournie par le CRU. En s'appuyant sur la granulométrie du sol, le couvert végétal, les valeurs de la profondeur racinaire et les valeurs limites de succion, la FAO définit sept classes de capacité en eau classées de A à F, auxquelles elle s'ajoute une dernière classe correspondant aux "Zones Humides" ou *Wetlands*. Chaque classe de sols comprend des valeurs minimales et maximales de capacité en eau. A partir de ces valeurs, trois grilles ont été construites en utilisant respectivement les valeurs minimales, moyennes et maximales de la capacité en eau des sols. Une quatrième grille est obtenue à partir d'un procédé qui utilise la fonction de pédo-transfert décrite par Reynolds *et al.* (1999) pour modifier la capacité en eau des sols fournie par la FAO.

### **Performances des modèles et validation des résultats**

Les modèles ont été calés et validés sur la base des observations de la période sans régulation (1943-1969) des écoulements de la Sanaga. Les valeurs du critère de Nash obtenues avec les meilleures combinaisons de données en phase de validation des modèles sont de 88% (contre 93% en phase de calage) pour le modèle GR2M contre 62% pour le modèle de Yates. Les performances du GR2M sont par conséquent meilleures sur notre bassin. La Fig. 2 en présente une illustration graphique.

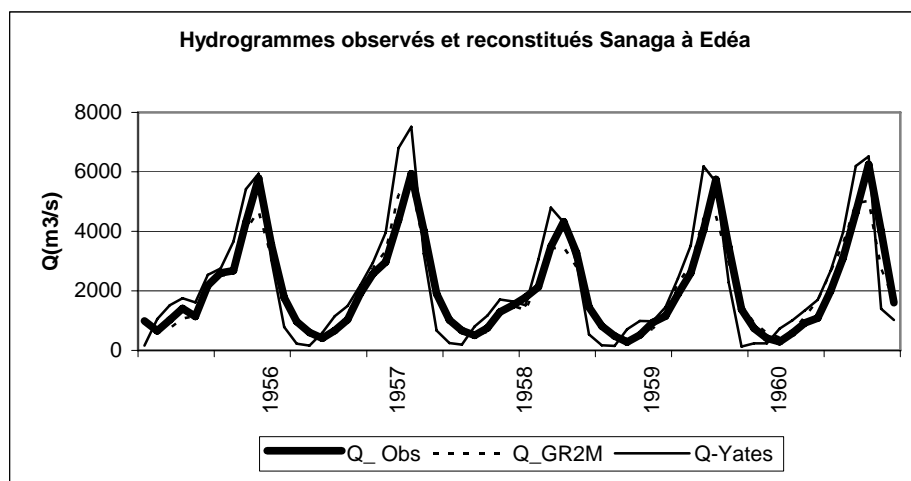


Fig. 2: Comparaison des débits observés et simulés par les deux modèles.

Les grilles de pluies calculées par la méthode du krigeage et celle de Thiessen donnent des résultats comparables pour les deux modèles, avec un léger avantage pour la méthode du krigeage. Pour les données d'ETP par contre, bien que les différences entre les résultats obtenus par les différentes méthodes signalées plus haut soient assez importantes (jusqu'à 60%), la comparaison des résultats obtenus par le modèle GR2M avec les quatre grilles d'ETP montre des différences peu significatives. Le modèle de Yates semble par contre plus sensible aux données d'ETP, mais reconstitue moins bien les écoulements sur le bassin. Pour ce qui concerne les données relatives à la capacité en eau des sols, les grilles construites à partir des valeurs de la capacité de rétention maximale en eau du sol conduisent aux meilleurs résultats sur notre bassin. Des efforts sont cependant encore à réaliser pour une meilleure estimation des paramètres de nos deux modèles dont l'ETP et la capacité en eau des sols en particulier. Toutefois, si de nombreux aspects de la question restent à documenter, les conclusions de nombreux travaux sur le sujet sont globalement encourageantes.

En effet, en dépit de leurs insuffisances, parallèlement aux efforts maintenus en vue de l'amélioration de leurs performances, les modèles hydrologiques sont de plus en plus utilisés de nos jours. En particulier, l'actualité des questions de changement climatique et l'importance de la prévision de leurs effets sur les ressources en eau conduisent à s'intéresser à leurs impacts sur le régime des écoulements de même que sur leurs relations avec les activités socio-économiques. La comparaison entre les débits observés à Edéa et ceux reconstitués au moyen du modèle GR2M, qui permet la meilleure reconstitution des hydrogrammes des écoulements, montre des différences (entre 2 à 10%, soit 6% en moyenne) qui sont voisines de la marge d'erreur sur la mesure. La robustesse de ce modèle est confirmée par des résultats similaires enregistrés sur d'autres bassins versants de la région tropicale africaine. Nous l'utiliserons par conséquent pour estimer les flux hydriques du XXI<sup>ème</sup> siècle sur la Sanaga à Edéa. Cette estimation sera

réalisée sur la base des informations fournies par des modèles climatiques. Avant d'aborder cet aspect de l'étude, nous analyserons brièvement l'impact des fluctuations climatiques récentes sur les écoulements de la Sanaga.

## IMPACT DES FLUCTUATIONS CLIMATIQUES RECENTES SUR LES ECOULEMENTS DE LA SANAGA.

L'étude de la variabilité des écoulements se limitera à l'analyse des modules. Les données analysées sont constituées des observations des débits naturels de la Sanaga de la période 1943-1969 et des débits simulés au moyen du modèle GR2M à partir des données d'observation de précipitations et d'ETP de la période 1970-2000. Ces derniers sont, considérés comme suffisamment représentatifs des écoulements (annuels) naturels de cette période pour permettre de se faire une idée de l'impact du changement climatique sur le régime hydrologique du fleuve. La Fig. 3 montre l'évolution des modules observés et reconstitués de la période 1943-2000.

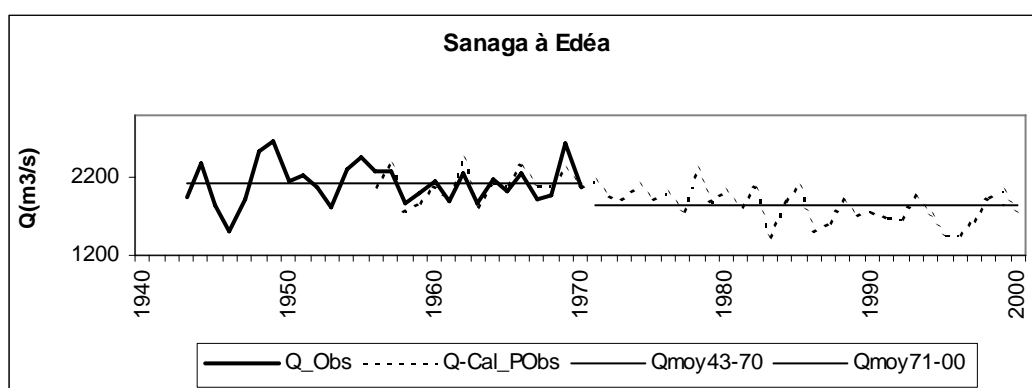


Fig. 3: Variations des écoulements de la Sanaga à Edéa depuis 1943.

Comme la majeure partie des cours d'eau du pays, après deux décennies (1950 et 1960) relativement humides, on note une baisse des modules à partir du début de la décennie 1970. La baisse est de plus en plus marquée à partir de la décennie 1980 et se poursuit jusqu'à la fin du siècle en dépit de quelques années humides. La comparaison des écoulements des périodes d'avant et après 1970 montre une diminution du module de la Sanaga de l'ordre de 15% après cette date. Cette valeur est voisine du déficit moyen (-14%) enregistré sur les cours d'eau de la région Sud du Cameroun (Sighomnou, 2004).

## PROSPECTIVES DES ECOULEMENTS DE LA SANAGA POUR LE XXI<sup>EME</sup> SIECLE

Il est indispensable de disposer des informations sur les prévisions des modèles climatiques relatives aux données d'entrée des modèles hydrologiques pour les analyses prospectives des écoulements de la Sanaga. Si les prévisions des précipitations et d'ETP sont fournies par ces modèles, aucune information n'est disponible sur la capacité en eau des sols. Dans ces conditions, et bien que cela soit assez restrictif, nous avons fait l'hypothèse de la conservation de la capacité de rétention en eau des sols dans une situation voisine de leur état actuel, au cours du XXI<sup>eme</sup> siècle. D'autre part, des différences très importantes existent entre les données de prévision de précipitations et d'ETP fournies par les modèles climatiques. Il conviendrait d'en tenir compte dans l'interprétation des résultats.

### Les modèles de prévision climatique

En se basant sur la compréhension actuelle des processus qui régissent le système solaire, de nombreuses représentations mathématiques simplifiées du système climatique de la terre ont été proposées. Il s'agit de Modèles de la Circulation Générale (MCG) qui permettent de simuler les réactions du système climatique

et prévoient son évolution future. Les meilleurs résultats sont obtenus de nos jours avec les Modèles Couplés Atmosphère-Océans. Ces modèles utilisent des scénarios de l'évolution future des agents de forçage (tels les gaz à effet de serre et les aérosols), pour établir un ensemble de projections décrivant ce qui pourrait se produire à l'avenir en matière de changement climatique. Selon les résultats d'analyses reconnues d'une grande fiabilité, depuis le début de l'ère industrielle, l'effet de serre naturel est renforcé par diverses émissions d'origine humaine, ce qui contribue à accentuer le réchauffement de la surface de la terre. Le troisième rapport (IPCC, 2001) d'évaluation de l'IPCC (*Intergovernmental Panel on Climate Change*), sert de référence de nos jours pour les changements observés et les projections pour l'évolution future du système climatique. On y retrouvera plus de détails sur ces modèles. Bien que leurs performances soient encore peu satisfaisantes, ces derniers sont les seuls moyens utilisés de nos jours pour évaluer l'impact du changement climatique sur le cycle de l'eau et partant, sur les ressources en eau. Les performances de quatre modèles climatiques (HadCM3, CSIRO-Mk2, ECHAM4/OPYC3 et NCAR-PCM) parmi ceux recommandés par l'IPCC, sont classées parmi les meilleures dans notre région d'étude (Arnell *et al.*, 1999 ; Hulme *et al.*, 2000 ; Mkankam Kamga, 2000). En raison de la disponibilité des données simulées sur la période 1950-2099 qui inclue la période observée (1950-2000) sur notre bassin, le modèle HadCM3 a été retenu dans le cas de notre étude. Les données analysées sont celles basées sur le scénario d'émission A2 (variations des températures comprises entre 1,5 et 4,5°C d'ici la fin du siècle), qui considère un XXI<sup>ème</sup> siècle où aucune mesure concertée mondiale n'est prise pour enrayer l'augmentation des gaz à effet de serre. Ce modèle comme tous les autres, ne reproduit cependant pas correctement les observations de la période instrumentée, notamment celles des précipitations : volumes annuels précipités, leur variabilité interannuelle et la dynamique des saisons. En général, les observations sont surestimées ou sous-estimées en fonction des modèles et du scénario d'émission utilisés. Deux procédés de construction de grilles de précipitations et d'ETP proposés par Ardoïn-Bardin (2004) permettent cependant d'obtenir des valeurs réalistes qui respectent la dynamique de répartition mensuelle des deux paramètres. En utilisant les informations disponibles sur les trois dernières décennies (1970-2000) comme données de référence, le premier procédé génère des séries de données qui prennent en compte les prévisions du modèle climatique pour chaque mois donné et les écarts (ou Anomalies) entre ces prévisions par rapport à la valeur moyenne calculée sur la période de référence (Scénario A). Le second procédé prend en compte les variations à trois horizons définis par l'IPCC (2020, 2050 et 2080) et calcule les taux de variation des précipitations et d'ETP mensuelles par rapport aux informations disponibles sur la période 1970-2000 également retenue comme référence (Scénario B). Les deux jeux de données de précipitations et d'ETP ainsi créés sont utilisés pour la simulation des écoulements sur notre bassin. Les détails sur le procédé de construction des grilles de données des différents paramètres sont décrits dans la référence citée ci-dessus. Il convient cependant de rester conscient des limites et des incertitudes qui restent à lever sur les prévisions des modèles climatiques. Pour estimer la fiabilité des prévisions du modèle pour notre région d'étude, nous avons fait une comparaison entre les résultats de simulations du climat passé et actuel avec les observations sur le bassin de la Sanaga. Les prévisions du scénario A, utilisé dans notre étude, sur la période 1956-2099 qui inclut la période d'observation ont été utilisées. La Fig. 4 montre une comparaison entre les hydrogrammes observés et ceux reconstitués à partir des données observées et celles prévues par le modèle climatique pour une même période.

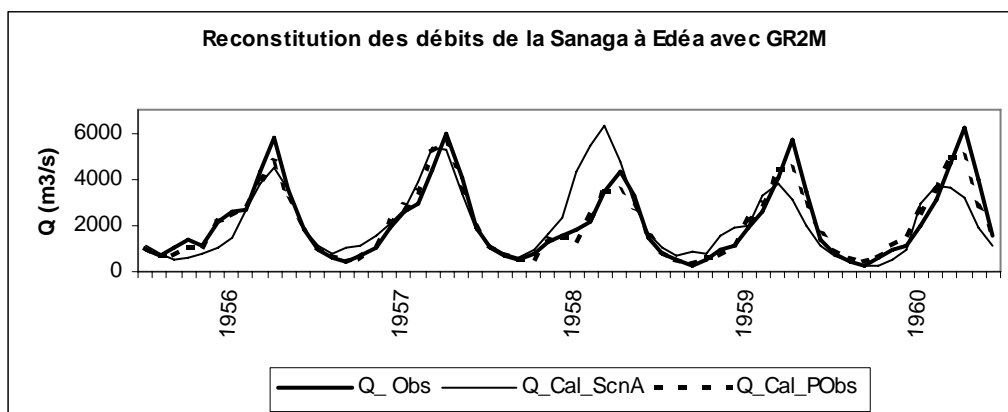


Fig. 4: Comparaison débits observés ( $Q_{\text{Obs}}$ ) et reconstitués à partir des pluies observées ( $Q_{\text{cal\_PObs}}$ ) et celles prévues par le scénario A ( $Q_{\text{cal\_ScnA}}$ ) pour la même période.

La différence entre les hydrogrammes observés et ceux reconstitués à l'aide des grilles d'ETP et de précipitations prévues par le modèle climatique peut être très importante, mais dans l'ensemble, les hydrogrammes simulés conservent l'allure générale des observations (coefficient de corrélation mensuelle de 61%). D'autre part, si des incertitudes très importantes peuvent subsister entre des informations relatives à des faibles pas de temps, les modèles de prévision donnent une idée acceptable des tendances générales de l'évolution des écoulements sur des durées suffisamment grandes pour intégrer les fluctuations naturelles des débits. Ces résultats constituent par conséquent une hypothèse valable de travail qu'il conviendrait d'affiner à mesure que les modèles climatiques vont s'améliorer.

## SYNTHESE DES RESULTATS

Le tableau 1 présente, suivant divers horizons, les taux de variation des précipitations, de l'ETP et des écoulements de la Sanaga à Edéa d'après les prévisions des deux grilles de données testées, alors que la Fig. 5 présente leur évolution dans le temps.

Tab. 1 : Variation (%) des paramètres du bilan hydrologique de la Sanaga à Edéa par rapport à la période 1971-2000 suivant deux scenarii.

	Horizon 2020		Horizon 2050		Horizon 2080		Horizon 2095	
	Scen_A	Scen_B	Scen_A	Scen_B	Scen_A	Scen_B	Scen_A	Scen_B
Précipitations	+3,2	+0,4	+1,5	+1,8	+0,8	+4,8	+3,4	+7,4
ETP	+5,0	+6,3	+11	+10	+21	+21	+33	+26
Écoulements	+3,8	+0,9	-4,3	-0,5	-15	-1,4	-20	+1,1

On note dans l'ensemble que les données issues des deux modes de construction sont différentes entre elles. Après une période 2000-2050 où les précipitations moyennes sur le bassin restent globalement comparables à celles de la période récente (1971-2000), une légère reprise s'amorce pour atteindre un maximum de l'ordre de +7% vers la fin du XXI<sup>ème</sup> siècle pour le scénario B. L'ETP moyenne annuelle croît par contre graduellement, suivant l'ensemble des scenarii, pour atteindre un maximum de +26 à +33% suivant le cas vers la fin du siècle. Par rapport à la même période de référence, les écoulements varient entre +4 et -20% (soit +18 à -93 mm/an en terme de lame écoulée sur le bassin) suivant le scénario.

En raison de la régulation des débits de la Sanaga à partir de 1970, les variations des écoulements ont été également calculées par rapport à la période 1943-1969 connue dans la région pour son caractère humide. Les deux scénarios testés prévoient des écoulements plus faibles (-10 à -32%, soit -52 à -162 mm/an en terme de lame écoulée) que ceux de cette période tout au long du XXI<sup>ème</sup> siècle.

Les observations des différents paramètres ainsi que les prévisions fournies par un des deux scenarii pour la période actuelle sont également présentées dans la figure à titre de comparaison. Il en ressort que des différences importantes peuvent exister entre les prévisions et les observations.

### Impacts sur l'utilisation des ressources en eau.

La planification des usages des ressources en eau de ce bassin au cours du XXI<sup>ème</sup> siècle devrait tenir compte de ces principales conclusions. Les eaux de la Sanaga sont utilisées de nos jours principalement pour l'hydroélectricité. Les autres principaux usages de la ressource vont de la demande *in situ* du milieu naturel, à l'agriculture irriguée et pluviale. Le développement de l'agriculture devrait tenir particulièrement compte d'une pluviosité qui devrait rester globalement proche de celle de la période récente pour une évapotranspiration plus importante.

De ce point de vue et en raison de son impact positif sur le rendement agricole, il est fort envisageable que le potentiel important des terres irrigables disponibles sur le bassin soit mis à profit dans un proche avenir. Des études montrent (Sharma, 2003) qu'un accroissement de la température de 3°C conduit à une augmentation de l'ordre de 26% des besoins en eau d'irrigation, en raison de l'accroissement de

l'évapotranspiration. La demande en eau pour le secteur agricole devrait en conséquence être beaucoup plus importante, de même que celle du milieu naturel.

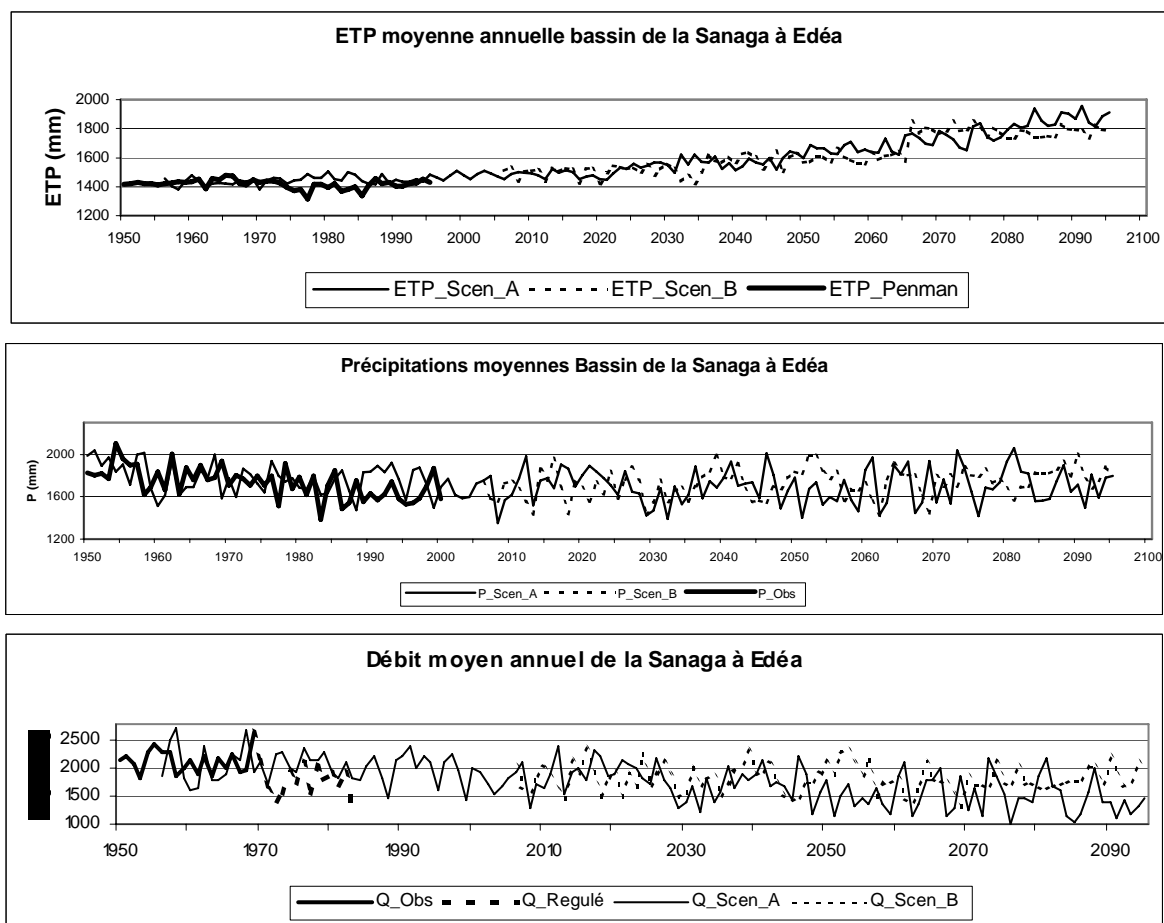


Fig. 5: Evolution des paramètres du bilan hydrologique de la Sanaga suivant les scenarii en regard des valeurs observées, de haut en bas : ETP (mm), Pluie (mm), débit ( $m^3s^{-1}$ ).

Cette situation devrait contribuer à accroître la baisse des écoulements. Il conviendrait d'en tenir compte dans l'exploitation des aménagements en cours et en projet sur la Sanaga. La variété des processus en œuvre dans les modèles climatiques, dans les bassins ainsi que dans leur agrégation temporelle et spatiale est cependant telle que les conclusions peuvent différer profondément d'un modèle à l'autre et d'un bassin à un autre. En particulier, les conclusions dépendent fortement des "images du futur possible" que proposent les scenarii climatiques. Nos analyses permettent cependant de se faire une idée des prévisions en terme de moyenne et de fréquence de distribution des variables climatiques et hydrologiques étudiées sur notre bassin.

## CONCLUSION

Après une analyse des performances de deux modèles hydrologiques (GR2M et Yates) sur le bassin de la Sanaga à Edéa, la meilleure reconstitution des débits est obtenue avec le modèle GR2M. En s'appuyant sur les résultats de simulation de ce modèle, deux jeux de données construits à partir des données brutes du modèle climatique HadCM3 sont utilisés pour évaluer l'impact des changements climatiques futurs sur l'évolution des ressources en eau de la Sanaga. Par rapport à la période 1971-2000 les deux scenarii utilisés prévoient des variations de précipitations moyennes annuelles sur le bassin qui vont de 0 à +7,4 % dans le courant du XXI<sup>ème</sup> siècle. Contrairement aux précipitations, l'évapotranspiration moyenne annuelle augmente graduellement pour atteindre un taux d'accroissement de plus de 30% vers 2100. Par rapport à la même période de référence, les écoulements varient entre +4 et -20% (+18 à -93 mm/an)

suivant le scénario. Si l'on se réfère aux débits non régulés de la période 1943-1969 par ailleurs reconnue pour son caractère humide dans la région, les deux scénarii testés montrent qu'une période comparable ne sera jamais retrouvée durant tout le XXI<sup>ème</sup> siècle. Ils prévoient des débits annuels globalement inférieurs (-10 à -32%) tout au long du XXI<sup>ème</sup> siècle, soit -52 à -162 mm/an en terme de lame écoulée sur le bassin. La planification des usages futurs des ressources en eau du bassin de la Sanaga devrait tenir compte de cette situation.

## REFERENCES

- Ardoin-Bardin, S. (2004) *Variabilité hydroclimatique et impacts sur les ressources en eau de grands bassins hydrographiques en zone soudano-sahélienne*. Thèse de doct. Univ. Montpellier II, France. 440 p.
- Arnell, N.W. (1999) Climate change and global water resources. *Global Environment Change*, 9, S31-S49.
- Arnell, N.W., Reynard, N.S. (1996) The effect of climate change due to global warming on river flows in Great Britain. *J. Hydrol.*, 183, 397-424.
- Dunne, K.A. and Willmott, C.J. (1996) Global distribution of plan-extractable water capacity of soil. *J. Climatol.*, 16, 841-859.
- Hulme, M., Wigley, T.M.L., Barrow, E.M., Raper, S.C.B., Centella, A., Smith, S., Chipansky, A.C. (2000) *Using a Climate Scenario Generator for Vulnerability and Adaptation Assessments: MAGICC and SCENGEN Version 2.4 Workbook*. Climatic Research Unit, Norwich, UK, 52 p.
- IPCC (2001b) *Climate Change 2001 : Impacts, adaptation and Vulnerability*. Contribution of Working Group II to the Third Assessment Report of the IPCC. (Ed. by McCarthy J.J., Canziani O.F., Leary N.A., Dokken D.J., White K.S.) Cambridge University Press, UK, 1032 p.
- Makhlouf, Z. (1994) *Compléments sur le modèle Scen-débit GR4J et essai d'estimation de ses paramètres*. Thèse de doctorat, Université Paris - Sud, France, 413 p.
- Mkankam Kanga, F. (2001) Impact of greenhouse gas induced climate change on the runoff of the upper Benue River (Cameroon). *J. Hydrol.*, 252, 145-156.
- Mkankam Kanga, F. (2000) Validation of general circulation climate models and projections of temperature and rainfall change in Cameroon and some of its neighbouring areas. *Theor. Appl. Climatol.*, 67, 97-107.
- Nash, J.E., Sutcliffe, J.V. (1970) River flow forecasting through conceptual models. Part I : a discussion of principles. *J. Hydrol.*, 10, 282-290.
- Olivry, J.C. (1986) *Fleuves et rivières du Cameroun*. Monographies hydrologiques, MESRES/ORSTOM, n° 9, 733 p.
- Ouedraogo, M. (2001) *Contribution à l'étude de l'impact de la variabilité climatique sur les ressources en eau en Afrique de l'Ouest. Analyse des conséquences d'une sécheresse persistante : normes hydrologiques et modélisation régionale*. Thèse de doctorat, Université de Montpellier II, France, 257 p.
- Penman, H. L. (1956) Evaporation : An introduction survey. *Netherlands J. Agri. Sci.*, 1, 9-29.
- Reynold, C.A., Jackson, T.J., Rawls, W.J. (1999) Estimating available water content by linking the FAO soil map of the World with Global Soil Profile Data bases and pedo-transfer Functions. *Proceedings of the AGU 1999 Spring Conf.*, Boston, MA. May 31 -June 4, 1999.
- Sharma, U.C. (2003) Impact of population growth and climate change on the quantity and quality of water resources in the northeast of India. *IAHS Pub.* 281, 349-357.
- Sighomnou, D. (2004) *Analyse et redéfinition des régimes climatiques et hydrologiques du Cameroun : perspectives d'évolution des ressources en eau*. Thèse de Doctorat d'Etat ès Sciences, Université de Yaoundé I, Cameroun, 290 p.
- Shuttleworth, W.J. (1994) Evaporation. In: *Handbook of Hydrology* (ed. by R. D. Maidment), Chapter 4, McGraw-Hill.
- Thom, A.S., Oliver, H.R. (1977) On Penman's equation for estimating regional evapotranspiration. *Q.J.R. Met. Soc.*, 193, 345-357.
- Yates, D.N. (1997) Approaches to continental scale runoff for integrated assessment models. *J. Hydrol.*, 201, 289-310.



# COMPARISON OF DIFFERENT SOURCES OF UNCERTAINTY IN CLIMATE CHANGE IMPACT STUDIES IN GREAT BRITAIN

Christel PRUDHOMME, Helen DAVIES

Centre for Ecology and Hydrology, Wallingford, OXON, OX10 0QN, UK

C.Prudhomme@ceh.ac.uk

## ABSTRACT

The paper assesses the range of changes from a comprehensive set of scenarios describing uncertainties due to climate modelling and climate projections for the 2080s. The study focuses on the mean annual flow ANN and the low flow regime indicator Q95. The changes are represented by confidence bands including 90% of the future simulations and are compared with estimated variations in ANN and Q95 due to natural climatic variability. The climatic projections include uncertainty in future emissions of greenhouse gases, in modelling global climate and in downscaling methodologies, while the natural variability is assessed through data resampling. Results are analysed to assess which of the considered uncertainties is largest for one British test catchment, and to provide guidance for incorporating uncertainty in future impact studies.

**Keywords:** Water resource; Climate change impact; hydrological modelling; uncertainty

## COMPARAISON DE DIFFERENTES SOURCES D'INCERTITUDE DANS UNE ETUDE D'IMPACT DU CHANGEMENT CLIMATIQUE EN GRANDE BRETAGNE

## RESUME

L'article analyse les changements dus à un ensemble de scénarii décrivant les incertitudes relatives à la modélisation climatique pour la période 2080. L'étude se concentre sur le débit moyen annuel ANN et l'indicateur d'étiage Q95. Ces changements sont représentés par une bande de confiance comprenant 90% des simulations futures et sont comparés aux variations de ANN et Q95 dues à la variabilité climatique. Les incertitudes sur les projections climatiques tiennent compte des incertitudes sur les futures émissions de gaz à effet de serre, sur les modèles climatiques globaux et sur les méthodes de désagrégation, et la variabilité naturelle est estimée par re-échantillonnage. Les résultats sont analysés pour évaluer lesquelles des incertitudes considérées sont les plus importantes pour un bassin versant test en Grande Bretagne, et pour fournir des guides sur la prise en compte de l'incertitude dans des études de changement climatique.

**Mots clefs :** ressource en eau, impacts du changement climatique, modélisation hydrologique, incertitude

## INTRODUCTION

There is increasing concern about the impact of climate change on water resources, and potential implications for water resource management. According to the IPCC, future GCMs projections indicate that temperature and precipitation patterns are likely to change in Britain, with summer runoff, water availability and soil moisture likely to decrease in southern Europe, and both variables (temperature and precipitation) likely to increase everywhere in Europe (Intergovernmental Panel on Climate Change, 2001). Global Climate Models (GCMs) provide us at present with the most reliable and robust methods for assessing the response of the climate system to changes in forcing. These GCMs are based upon the fundamental laws of physics and on assumptions on the content of greenhouse gases (in terms of CO<sub>2</sub> equivalent) in the atmosphere, such as the IPCC-SRES scenarios (based on assumptions on societal development). However, it is recognised that different climate models provide different projections. For example, Prudhomme *et al.* (2003) found that GCMs uncertainty was larger than emission uncertainty in

the impact on the flood regime in Britain, and recommended to consider different GCMs when undertaking any impact study on the hydrological regime.

*GCMs are subject to a number of limitations*, in particular the limited spatial detail of the relatively coarse grid of a GCM and consequently the inadequacy to model appropriately the short-time scale variability. Techniques to downscale the results of the GCM integrations to the appropriate scale for climate change impact assessments in hydrology have been developed to overcome the limitations of coarse scales, such as:

- Complex models, such as dynamical downscaling, use atmospheric general circulation model (AGCMs) outputs as limiting conditions for high-resolution regional climate models (RCMs) and provide daily climate outputs at a 50x50 km grid over Britain;
- Statistical downscaling techniques are simpler and computationally less expensive than dynamical models and can be repeatedly re-run to generate large ensembles of daily precipitation series at the point/catchment scale for uncertainty assessment;
- Simple models, such as the delta method, use monthly factors (average changes for each GCMs grid) to perturb observed series to produce changed series (e.g. Prudhomme *et al.*, 2003).

## METHODOLOGY

### Climate change uncertainty

Two main sources of uncertainty in climate change modelling have been considered.

**GCMs and emission scenarios uncertainty.** Three GCMs were considered: HadCM3 from the Hadley Centre for Climate Prediction and Research (Met.Office, UK); CCGCM2, from the Canadian Centre for Climate Modelling and Analysis (CCCMA; Canada) and CSIRO-Mk2 from the Commonwealth Science and Industrial Research Organisation (CSIRO, Australia). These were chosen because daily outputs of range of climate variables were available through the LINK project IPCC-DDC (<http://ipcc-ddc.cru.uea.ac.uk/>). For the emission uncertainty, two SRES scenarios were considered, A2 and B2, that encompass most of the range of the SRES scenarios. Results from A2 and B2 runs are considered together when assessing uncertainty in GCMs and downscaling techniques, and separately when assessing emission scenarios uncertainty.

**Uncertainty in downscaling methodologies.** Three downscaling techniques have been considered: (1) dynamical downscaling, with daily outputs from the Hadley Centre's regional model, HadRM3H at a 25x25 km grid-scale, driven indirectly from the HadCM3 simulation under the A2 scenario. (2) Statistical downscaling, with the Statistical DownScaling Model (SDSM), described as a hybrid between regression-based and stochastic weather generation techniques (Wilby *et al.*, 2002). It uses empirical regression equations between large-scale atmospheric conditions and the observed daily local weather conditions, combined with a stochastic element to improve the reproduction of daily variability not suitably captured by the large-scale variables. In this study, 20 separate runs were made for each of the GCM and emission scenario combinations (Osborn *et al.*, 2005). The final regression equation models were chosen after various combinations of predictors were tested and the model verified on an independent period. (3) A simple 'delta' (or proportional) approach that creates scenarios in perturbing observed baseline series according to average monthly factors of change (e.g. a +10% factor for January leads to a new series where all observed daily records for January are increased by 10% to produce a new future series; see Prudhomme *et al.*, 2003). This is the most commonly used technique in climate change impact studies. The factors used are the four 'UKCIP02 scenarios' (i.e. monthly factors of change), specifically developed for impact studies in Britain by the UK Climate Impact Project (Hulme *et al.*, 2002) from HadRM3 runs with four SRES emissions scenarios.

A schematic of the different uncertainty sources considered and the corresponding scenarios is provided in Fig. 1 (for the future time horizon 2080s).

**PE scenarios.** These were derived using the delta method, with factors of change calculated using the Penman Monteith equations (Allen *et al.*, 1994) for PE estimates from the relevant climate variables from all the combinations of GCMs, RCMs and emissions scenarios.

Downscaling Methods/ GCM	Dynamical	SDSM						Factor			
	HadRM3	HadCM3	CCGCM2	CSIRO-Mk2	HadRM3						
SRES Emission scenario	A2	A2	B2	A2	B2	A2	B2	A1	A2	B1	B2
No. runs	1	20	20	20	20	20	20	1	1	1	1
No. resampling	100	5 (x20)	5 (x20)	5 (x20)	5 (x20)	5 (x20)	5 (x20)	1	1	1	1
Total no. scenario	100	100	100	100	100	100	100	1	1	1	1

Fig. 1: Schematic diagram of graph of the suite of scenarios considered in the study to define each uncertainty.

### Uncertainty due to natural climate variability

**Natural variability.** Oceanic climate such as observed in the British Isles is extremely variable, and the inter-annual climatic variability is significant. Yet, this natural climate variability (hereafter natural variability) is generally ignored in climate impact studies. A simple methodology of block resampling with replacement has been used to define and incorporate natural climate variability. The resampling procedure randomly selects 3-month blocks from the original series (respecting the annual sequences) to create a new series the same length as the original. A three month resampling was preferred to a 1-month resampling so that the medium-term seasonal structure of the rainfall is maintained, as this is particularly important for the recharge process. For this study, 99 new series were produced using that method, thus providing a set of 100 scenarios including the observed series.

**Climate variability.** Natural variability, as defined with resampling of short records of observed series, does not incorporate any extreme event that is not included in the observations nor any change in the inter-seasonal variability (due to the 3-month resampling procedure, the original 3-months sequences are maintained in all resamples). One way of more extensively capturing the climate variability is via the modelling of the climate. The random element built in SDSM introduces some variability in each of the simulated series and hence has been used to derive 20 daily precipitation series for each GCM representative of the baseline time horizon (1961-1990). A further 5 block-resamplings of each of the 20 series was done to finally produce 100 scenarios (same scenario group size as used to assess the natural variability).

Only precipitation series were derived with SDSM. For current climate, observed PE series were used for simulations of current conditions except for dynamical downscaling (modelled).

### Calculation of changes and uncertainty

**Reference indicator and calculation of changes.** The reference indicators are calculated from the daily flow series simulated with the observed rainfall and PE (and NOT from the flow records). This is to eliminate the bias due to hydrological model errors. For each simulated flow series, an indicator is calculated and the difference with the reference indicator expressed as percentage of that reference value. For example, for a reference value of 20 and a scenario value of 22, the change is 10%.

**Uncertainty.** For one indicator type and a given source of uncertainty, the uncertainty is represented by the range comprising 90% of the simulated indicators (or 90% Confidence Interval CI). Ranking all the 100 indicators in ascending order, CI is defined by the 5<sup>th</sup> and the 95<sup>th</sup> values (corresponding to the 5<sup>th</sup> and 95<sup>th</sup> percentiles). The 25<sup>th</sup> and 75<sup>th</sup> percentiles are also derived, showing the range comprising half of the simulations around the median. These percentiles are graphically shown by a box-plot diagram, with the whiskers representing the 5<sup>th</sup> (lower) and 95<sup>th</sup> (upper) percentiles, and the black boxes the 25<sup>th</sup> (lower limit) and 75<sup>th</sup> (upper limit) percentiles (e.g. Fig. 2). For example, let's consider the results from the SDSM downscaling method with the outputs from the Hadley Centre Model HadCM3 run for the 2080s time horizon with the A2 SRES emission scenario. The 100 precipitation series (the 20 SDSM series, each resampled 5 times) and the same future PE series are used in the hydrological model to produce 100 daily flow series. The indicators are calculated for each of the 100 simulated flow series, and ranked to provide the 5<sup>th</sup>, 25<sup>th</sup>, 75<sup>th</sup> and 95<sup>th</sup> percentiles values of the Confidence Interval.

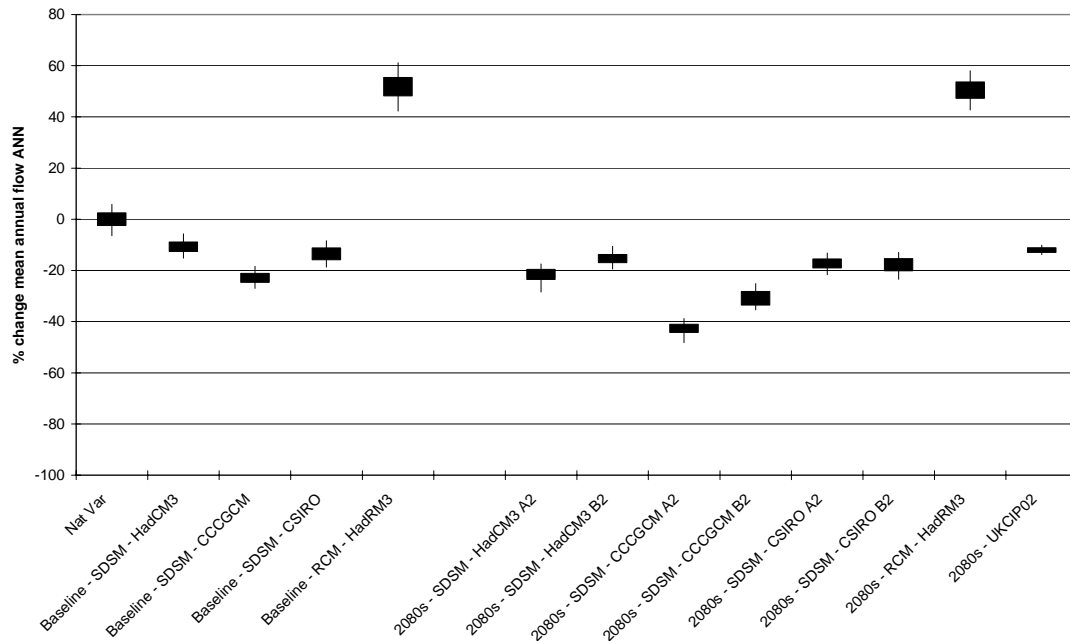


Fig. 2: Uncertainty in mean annual flow ANN for baseline climate due to hydrological modelling (3 boxes in right-hand side), climate variability and downscaling (baseline-marked scenarios), and for future projections 2080s due to GCMs (all 2080s scenarios), downscaling (HadCM3, HadRM3 and UKCIP02 scenarios) and emission scenarios (legend with A2 and B2 scenarios). Box plots show (from bottom to top) the 5<sup>th</sup> (lower whisker), 25<sup>th</sup> (lower limit of black box), 75<sup>th</sup> (higher limit of black box) and 95<sup>th</sup> (higher whiskers) percentiles. The black box contains 50% of the simulations around the median.

## CASE STUDY

### Catchment

The catchment selected is the Thrushel at Tinday, a rural catchment with grazing and low grade agriculture located in South West of Britain in Cornwall (Marsh and Lees, 2003). It has an area of 113 km<sup>2</sup> and an average altitude of 175 m. The mean annual rainfall is 1195 mm; the Base Flow Index, a measure of permeability of the catchment, is 0.42, indicating that around 42% of the river flow is from stored sources. The catchment was selected from a pool of good hydrometric quality, natural, gauged catchments from the National River Flow Archive held at CEH-Wallingford using the classification system of Gustard *et al.* (1992).

### Data used

Daily time series of catchment average precipitation for the study period 1969-97 was derived using the Meteorological Office daily rainfall library and a modified version of the Triangular Planes interpolation methodology of Jones (1983). Time series of potential evaporation (PE) was estimated for each catchment from the Meteorological Office of Rainfall and Evaporation Calculation System (MORECS) II potential evaporation estimates available at a 40 km grid resolution.

### **Hydrological model**

The hydrological model used is based on the Probability Distributed Model theory (Moore, 1985) that represents the soil storage capacity as a probability distribution and has two second-order linear routing reservoirs simulating quick and slow flows. The model includes an interception storage term and a soil-moisture related drainage term and has five free parameters for calibration. The parameters of the equations are calibrated so that the river flow time series simulated by the model provide a good match with the observed river flow records of the same period as the input data (bias and errors minimized). Evaluation is done on a separate period than the calibration. Uncertainties due to hydrological modelling are not discussed in this paper.

## **RESULTS**

Two indicators of river flow are analysed: the annual mean flow (ANN) and the flow exceeded or equalled 95% of the time (Q95). For practicality, the results are named after the GCM and the downscaling technique used to derive the input series. Results are shown as box-plot graphs (Fig. 2 and Fig. 3).

### **Current climate uncertainty**

For the current climate, the variation (in % change compared to the reference value) of ANN is smaller than that of Q95 (Fig. 2 and Fig. 3, baseline scenarios). Because of the small absolute value of Q95 (Q95 in this catchment is about 10% of ANN), large percentage variations in Q95 can be associated to a small absolute change. This larger uncertainty size for Q95 is in no way reflecting a poor modelling performance of the low flows.

Uncertainty due to 'climate variability' (as defined by running a range of scenarios derived by SDSM simulations and resampling techniques under current conditions) is smaller than the natural variability (as defined by running resamples of observed series) for ANN with the CI size varying from 8.7% (CCGCM) to 10.4% (CSIRO). This may be because the stochastic element integrated within SDSM does not produce extreme scenarios. Conversely, the climate variability is larger than natural variability for Q95 (from 36.7% (CSIRO) to 43% CCGCM). For all GCMs ANN is underestimated and Q95 overestimated. Those results highlight the difficulty that GCMs encounter in modelling the climate (and in particular precipitation). The potential bias in reproducing current climate should always be borne in mind when analysing any projected changes in climate change impact studies.

Results from HadRM3 outputs show significant bias, with overestimation of ANN (ranging from 42 to 61%) and large uncertainty for Q95 (62.3%). The difference in the sign of the 'errors' between statistical and dynamical downscaling of the Hadley Centre model is partly explained by the bias correction that is introduced within the SDSM calibration procedure. This bias correction is absent from the HadRM3 precipitation outputs that were directly used as input of the hydrological model.

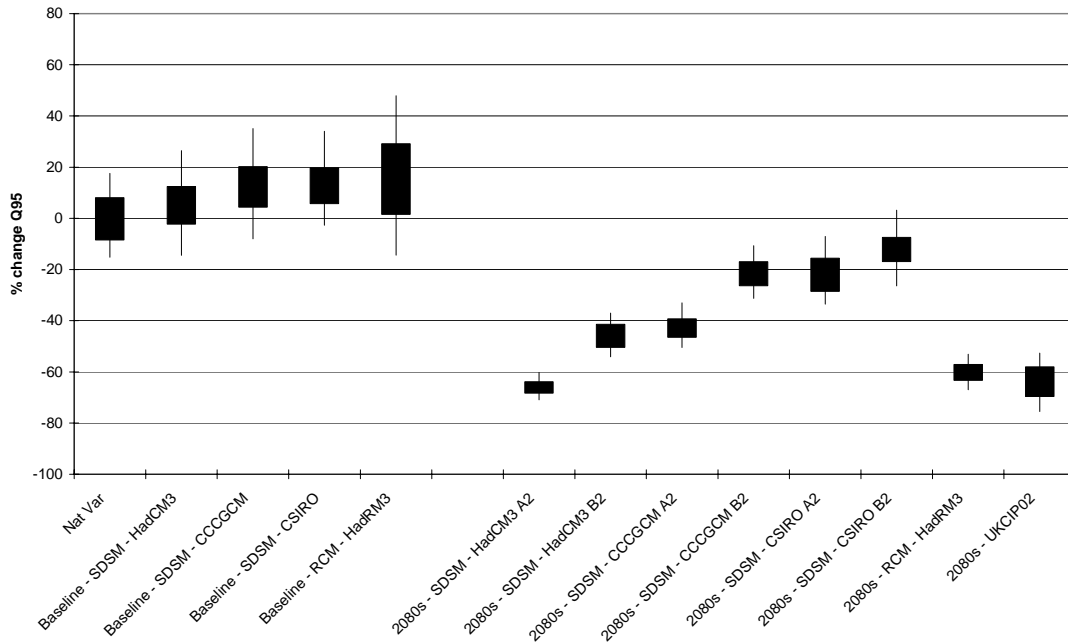


Fig. 3: Uncertainty in Q95 for baseline climate due to hydrological modelling (3 boxes in right-hand side), climate variability and downscaling (baseline-marked scenarios), and for future projections 2080s due to GCMs (all 2080s scenarios), downscaling (HadCM3, HadRM3 and UKCIP02 scenarios) and emission scenarios (legend with A2 and B2 scenarios). Box plots as in Fig. 2.

### Future climate uncertainty

Uncertainty (i.e. size of 90% CI) associated with SDSM-derived scenarios increases for all three GCMs for 2080s future projections compared to current climate projections (ANN) or remains the same (Q95). All scenarios show a decrease in ANN, with changes in the median between current and future projections ranging between 3.9% (CSIRO) to 14.4% (CCGCM) (Fig. 2). Compared to the reference indicators, the decreases in ANN appear much greater, up to a 37.2% median decrease for CCGCM (Fig. 2). This is because all GCMs underestimate ANN during current conditions and that underestimation is propagated to future projections. Uncertainty due to each downscaling methodology (SDSM-HadCM3 or HadRM3) is of similar magnitude for ANN (around 15%), but they are very large discrepancies in terms of the sign of the changes of the projections by the different methods: HadRM3 scenarios show an increase of ANN in 2080s when compared to natural variability (+50.4% for the median of simulations), but these changes are insignificant when comparing current and future projections of HadRM3 (current median simulation has a +52.3% bias compared to the reference value. the annual pattern of HadRM3 projections, however, shows considerable variation (not shown) between the two time horizons); SDSM-HadCM3 projects a decrease between 6.2 and 11.7%. The overall uncertainty in ANN due to downscaling is therefore extremely large for that catchment.

Q95 is also projected to decrease by the 2080s (Fig. 3) by all GCMs and downscaling methods, but the magnitude of that decrease greatly differs from one GCM to another, with HadCM3 projecting the largest reduction (median of changes by both A2 and B2 scenarios of -56.2%) and CSIRO the smallest (-16.5%). Unlike for ANN, the downscaling methods using the Hadley Centre GCM show consistent results in terms of sign of change and magnitudes, with a reduction of Q95 ranging from -39 to -70% (SDSM-HadCM3), -53 to -67% for HadRM3, and -47 to -71 for UKCIP02 (factors).

The uncertainty due to the emission scenarios (range between A2 and B2 for each GCM) is smaller than that of GCMs or downscaling methodology for ANN: uncertainty due to emission is about half of that of GCMs for both ANN and Q95, and smaller than that due to downscaling methods for ANN and about the same size for Q95. This is reflected by the UKCIP02 range not capturing the full range of uncertainty of climate change impact due to other sources than emission.

## CONCLUSION

The results obtained are specific for this catchment: they are only examples of how the uncertainty in hydrological modelling and climate change impact study can be assessed. They are in no way an assessment of the quality of any of the modelling techniques considered. However, they depict features inherent to climate change modelling that should be considered when undertaking a climate change impact study:

- Different flow indicators can show different changes. Assessment studies should specify the indicator analysed and results should not be generalised further;
- Natural variability comprises some uncertainty. It is important to compare potential climate change impact and its uncertainty to uncertainty due to natural variability ;
- GCMs (downscaled with sophisticated or simple techniques) do not always accurately reproduce current climate (see the modelling of the current climate). Their ability to do so should be borne in mind when assessing climate change impact;
- For future projections, GCMs carry the largest uncertainty: it would be misleading to only undertake an impact study solely from outputs from one single GCM ;
- Downscaling uncertainty can be significant: statistical methods compensate for modelling errors in the current climate, but the assumptions they are based upon may not remain true in the future; dynamical models cater for changes in the atmospheric processes producing precipitation, but retaining potential bias in the model;
- Uncertainty in the emission scenarios is the smallest of the GCM-associated uncertainties. Instead of undertaking impact studies with several scenarios from different emission assumptions but the same GCM (e.g. UKCIP02 scenarios), it would be preferable to use different GCM outputs under the same emission assumption, to carry more of the uncertainty surrounding future climate projections.

In this study, the hydrological model parameters were assumed to remain valid under changing climatic conditions, and the same sets used both for current and future simulations. However, there is concern that this assumption may not be true under drier, hotter conditions where the soil moisture deficit may be aggravated and hence hydrological processes modified. This was not tackled by the study, firstly because of the absence of available records long enough to show different periods with significantly different climate characteristics for two parameter sets to be calibrated; secondly because the analysis focused on comparing GCMs uncertainty with natural variability under current conditions, and how GCM uncertainty is projected to vary in the future, all the rest being equal.

## ACKNOWLEDGMENT

The research work is jointly funded by the UK Water Industry Research Ltd and the Environment Agency for England and Wales. Data from the Hadley Centre's HadRM3 were kindly provided by Dr. Richard Jones (Hadley Centre). The SDSM scenarios were produced by Carol McSweeney and Dr Tim Osborn (Climate Research Unit at the UEA).

## REFERENCES

- Allen, R.G., Smith, M., Pereira, L.S. and Perrier, A. (1994) An update for the calculation of reference evapotranspiration. *ICID Bulletin*, 43.
- Gustard, A., Bullock, A. and Dixon, J.M. (1992) Low flow estimation in the United Kingdom, *Institute of Hydrology Report 108*, Wallingford.
- Hulme, M. *et al.* (2002) *Climate Change Scenarios for the United Kingdom: The UKCIP02 Scientific Report*. Tyndall Centre for Climate Change Research, School of Environmental Sciences, Norwich.
- Intergovernmental Panel on Climate Change, I. (2001) *Climate change 2001: Impacts, Adaptation, and Vulnerability. Summary for policymakers and technical summary of the working group II report*. Contribution to the Third Assessment Report of the Intergovernmental Panel on Climate Change. World Meteorological Organization, Geneva, 89 p.

- Jones, S.B. (1983) The estimation of catchment average point rainfall profiles, *Institute of Hydrology Report 87*, Wallingford.
- Marsh, T.J. and Lees, M.L. (Editors) (2003) *Hydrological data UK - Hydrometric register and statistics 1996-2000*. Centre for Ecology and Hydrology, Wallingford, 208 p.
- Moore, R.J. (1985) The probability-distributed principle and runoff production at point and basin scales. *Hydrol. Sci. J.*, 30, 2, 273-297.
- Osborn, T.J., McSweetney, C., Prudhomme, C., Davies, H. and Viner, D. (2005) Climate change scenarios for UK catchments generated by statistical downscaling from multiple greenhouse gas scenarios *UKWIR CL04/B Technical report 1*.
- Prudhomme, C., Jakob, D. and Svensson, C. (2003) Uncertainty and climate change impact on the flood regime of small UK catchments. *J. Hydrol.*, 277, 1-2, 1-23.
- Wilby, R.L., Dawson, C.W. and Barrow, E.M. (2002) SDSM - a decision support tool for the assessment of regional climate change impacts. *Environmental Modelling and Software*, 17, 2, 145-157.
- Young, A.R. (2002) River flow simulation within ungauged catchments using a daily rainfall-runoff model. *BHS Occasional Paper*, 13, 23-30.

## Compte rendu de l'atelier 1

### Activités humaines, climat ressource en eau et environnement Human activities, climate, environnement and water resources

**Session Chairmen** : Natasha Carmi, Eduardo Planos, Téléphore Brou Yao

Le groupe de travail a réuni des membres de 5 groupes FRIEND :

- Afrique Australe ; Amérique Latine ; Asie-Pacifique ; Alpes et Méditerranée ; Afrique Occidentale et Centrale.

La plupart des groupes FRIEND ont mentionné le bon fonctionnement de leur réseau :

- une bonne coopération entre les partenaires de leur groupe,
- une bonne coopération avec le bureau local de l'UNESCO,
- une bonne coopération avec certains groupes FRIEND,
- des études scientifiques importantes ont été menées sur des thèmes spécifiques à leur région, notamment sur :
  - la sécheresse et la vulnérabilité en Afrique Ouest et Centrale, en Afrique Australe et en Amérique latine,
  - la gestion des catastrophes climatiques en Amérique Latine et en Asie-Pacifique,
  - la gestion des inondations en Asie-Pacifique,
  - la modélisation des pluies/débit et l'analyse des séries chronologiques dans le bassin méditerranéen et sur le Danube,
- des activités de formation et des publications ont été effectuées,
- des bases de données ont été établies.

A côté de ces points forts, il existe des difficultés :

- l'étendue des territoires des groupes FRIEND, marquée par une grande diversité qui entraîne des problèmes de communications entre les sous-groupes de travail pour le transfert des connaissances, des problèmes de spécifications des problématiques par région et d'intégration des différents intérêts de recherche ;
- l'un des problèmes le plus important qui ressort de tous les groupes FRIEND, c'est le problème du financement pour le fonctionnement du réseau : les voyages au sein du réseau et participation aux conférences internationales (ex de la 5<sup>ème</sup> conférence Mondiale FRIEND à Cuba), les publications, les projets de recherche ;
- une confusion entre certains projets de l'IHP (HELP, PUB et ECO-hydrologie) et les projets FRIEND à cause du fait qu'on retrouve les mêmes chercheurs au sein de ces différents projets ;
- Dans certains pays comme la Chine, il existe une nécessité de faire converger les services d'hydrologie et les services météorologiques.

Pour faciliter le transfert des compétences, les participants ont proposé la mise à disposition des outils d'analyse des bases données aux instituts nationaux aux services gouvernementaux

Sur la contribution des hydrologues dans le développement socio-économique, les participants on évoqué le fait qu'il existe encore beaucoup d'incertitude scientifiques :

- l'inventaire des problèmes socio-économiques liés à l'eau,
- le renforcement des équipes,
- la mobilisation des ressources en eau pour les populations,
- la gestion des eaux en partage,
- la qualité des eaux,
- les échanges d'expériences dans le cadre de la gestion intégrée,
- les problèmes d'échelles,

- les problèmes de dépopulations liés aux maladies comme le SIDA,
- le renforcement des activités de prévisions saisonnières et journalières.

Sur l'avenir des projets FRIEND :

- Les participants ont proposé la mise en place d'un site global de FRIEND au sein duquel se trouveraient des liens entre les différents groupes régionaux.
- On note la convergence entre les différentes disciplines environnementales, notamment entre la météorologie et l'hydrologie.
- Une meilleure intégration de l'utilisation du sol dans les modèles d'analyse et de prévision est souhaitable.
- Mettre en place des modèles basés sur les processus en lieu et place des modèles statistiques est encouragé.

## Workshop 2 Summary

### Climatic scenarios for the 21<sup>st</sup> century and prediction of water resources Scénarios climatiques et prediction des ressources en eau au 21<sup>ème</sup> siècle

**Session Chairmen:** Roland Schulze, Christel Prudhomme, Declan Conway

What is FRIEND doing and recommendations for future?

#### DATA–Fundamental issues

- **Monitoring** – Lack of long term strategy, no follow-up of programmes, series too short.
- **Sharing** – Essential for understanding water resources and improving management. But political tensions (e.g. India/Pakistan and Bangladesh) and commercial value are main constraints.
- **Access** – Difficult in some countries. Interlocutor not know
- **Updating** – Real problem. But not specific to FRIEND (Exists at national donor level). Monitoring not always a priority at national level (no funds for data acquisition and management). In Western Africa: works well through AGRHYMET, but not all have access

→**FRIEND: Data Holding, collection, dissemination organisation. Establishment of benchmark catchments of various sizes** but FRIEND role, or national problematic? Could FRIEND have a role as lobbying voice for international cooperation on data sharing? But difficulty in getting the message across

#### CAPACITY BUILDING

- **Collaboration** – Problem of groups working on their own, not enough in real collaboration
- **Capacity building** – e.g. HKH funded by UNESCO. But difficult to transfer to engineering/public/decision makers/managers
- **Continental research** – e.g. Aride

→**FRIEND: Provide capacity building facility**

#### Opportunities to contribute to climate impact and change research?

- Research: to become more policy relevant
- Research topics relevant to **local** socio-economic needs (e.g catchment scale analysis)
- Raise global awareness on climate change problem

#### Major scientific questions

- Understanding impact of climate change on society (e.g. agriculture, etc.).
- Share problems/ understanding across regions: e.g. glacier hydrology in HKH and Andes
- How to incorporate climate change uncertainty into water resources management?
- Multi-disciplinary research

#### Future activities for FRIEND

- Communication! To researchers, politicians, public, water managers etc... all specifics
- More application of knowledge

**FRIEND International Seminar  
Montpellier 22-24 November 2005**

**Climatic and Anthropogenic Impacts on the Variability of Water Resources**

**Plenary Session Summary**

**Session Chairmen:** Trevor Daniell and Luc Sigha

The theme developed from the discussions of both workshops for a “raison d’être” of FRIEND to progress and for further collaboration between researchers in various regions into the next phase is:

To examine how systems cope with variability across:

- Different landuse systems;
- Different scales;
- Different regions; and
- Different cultures:

firstly in the present climate and secondly with various climate change scenarios.

To achieve sustainability of resources requires that systems need to be robust and resilient to the demands placed upon them both in terms of quality and quantity and this needs to be examined.

There were various aspects that were considered to be important including the planning and socio-economics of extreme events including both floods and droughts. The implications on planning for the population demographics especially with regards to HIV needs to be considered across many regions.

The establishment and transference of data between FRIEND global researchers needs to be considered in the context variability of hydrology of regions being determined by climate change.

The FRIEND program and goals need to be more advertised among scientific community, data holders and public. There is a need for more collaboration between scientists, national services, who are data holders, and stake holders, to increase the knowledge transfer from research to applications and end-users.

FRIEND program might be associated with other UN institutions like UNDP and UNEP, to help raising funds to ensure a more important funding of basic activities within the FRIEND regional networks.

## PROGRAMME

### Tuesday 22 November

15h00-19h00 Registering and welcoming. Set of posters.

### Wednesday 23 November

Scientific Sessions.

- 8h30-8h45 **Opening of the Seminar**  
Eric SERVAT - Gil MAHE
- 
- 8h45-8h50 **Presentation of Theme 1** *Knowledge of climatic regimes and drainages and their spatio-temporal variability*
- 
- CHAIRMEN** **HASNAIN - SIGHA**
- 8h50-9h10 **Janicot S.** Climat et relations avec océan et atmosphère  
*Présenté par Gil Mahé*
- 9h10-9h30 **Hubert P., Bader J.P., Bendjoudi H.** Un siècle de débits annuels du fleuve Sénégal.  
*Présenté par Raymond Malou (Senegal)*
- 9h30-9h45 **Mkhandi S.H., Valimba P.** Predictability of the Short rains in Northeast Tanzania.
- 9h45-10h00 **Kingston D. G., McGregor G. R., Lawler D. M., Hannah D. M.** Assessing large-scale hydroclimatic linkages in northwest Europe.
- 10h00-10h15 **Sonbol M.A., El-Bihery M.A., Abdel-Motaleb M.** A Suitable Selection of Rainfall-Runoff Forecasting Models for the Nile River Basin
- 10h15-10h45 **Coffee Break**
- 10h45-11h00 **Valimba P., Mkhandi S.H., Servat E., Hughes D.** Changing flow regimes in Southern Africa and its relationship to rainfall variations.
- 11h00-11h15 **Dobhal D.P., Gergan J.T., Thayyen R.J.** Mass balance and snout recession measurements (1991-2000) of Dokriani placier, Garhwal Himalaya, India.
- 11h15-11h30 **Kumar R., Hasnain S.I., Chevallier P., Wagnon P.** Climate change signals detected through mass balance measurements on benchmark placier, Himachal Pradesh, India.  
*Présenté par Syed Hasnain (Inde)*
- 
- 11h30-11h35 **Presentation of Theme 2** *Relationships between human activities, climate, water resources and environment*
- 
- CHAIRMEN** **PLANOS - CARMÍ**
- 11h35-11h55 ( Servat E. Hydrologie tropicale, ressources en eau et développement. )
- 11h55-12h15 **Diello P., Mahé G., Paturel J.E., Karambiri H., Servat E.** Diminution des pluies et augmentation des écoulements au Sahel : relations entre hydrologie, dégradation du sol et dynamique de la population.
- 12h15-12h30 **Carmi N., Bachir B., Rabi A.** Drought analysis and the effect of climate change in the West Bank/Palestine.
- 12h30-12h45 **Laftouhi N., Persoons E.** Influences des variations climatiques sur le régime hydrologique du bassin versant du Qsob (Essaouira Maroc).
- 12h45-14h00 **Lunch**
- 14h00-14h15 **Tallaksen L., Demuth S., van Lanen H.** Low flow and drought studies within the NE-FRIEND group.  
*Présenté par Christel Prudhomme*
- 14h15-14h30 **Gutiérrez-López A., Onibon H.** Comparative hydrological drought-flood risk modelling in northern Mexico and West African Sahel regions.
- 14h30-14h45 **Bereciartua P.** Climate change and opportunities for innovative water management strategies in Argentina: the case of the Pampas System.
- 14h45-15h00 **Daniell T., White I.** Bushfires and their implications for management of future water supplies in the Australian Capital Territory.
- 15h00-15h15 **White I., Falkland T., Metutera T., Metai E., Perez P., Dray A., Overmars M.** Climatic and Human Influences on Water Resources in Low Atolls

---

**15h15-15h20 Presentation of Theme 3** *Climatic scenarios for XXI<sup>st</sup> century and forecasted water resources*

---

**CHAIRMEN**

**SCHULZE - PRUDHOMME**

**15h20-15h40 Conway D.** Climate scenarios and water resources forecasting: the Parana and the Nile case studies.

**15h40-16h00 Planos Gutiérrez E.** Variability and changes in the hydrological variables and perspectives hydrological scenarios in the Caribbean Region.

**16h00-16h30 Coffee Break**

**16h30-16h50 Ardoin S., Mahé G.** Prévision des ressources en eau en Afrique au 21<sup>ème</sup> siècle.

**16h50-17h05 Opoku-Ankomah Y., Minia Z.** Climate change scenarios and impacts on the surface water resources of the volta river basin.

**17h05-17h20 (Sighomnou D., Sigha L., Liéno G., Dezetter A., Mahé G., Servat E., Paturel J.E., Olivry J.C., Tchoua F., Ekodeck G.E.** Impacts des fluctuations climatiques sur le régime des écoulements du fleuve Sanaga au Cameroun, perspectives pour le XXI<sup>ème</sup> siècle.)

**17h20-17h35 Schulze R.E., Lumsden T.G., Horan M.** Findings from, and challenges in, climate change impact studies on water resources in South Africa.

**17h35-17h50 Prudhomme C.** Comparison of different sources of uncertainty in climate change impact studies on a low flow indicator in Great Britain.

**17h50-18h15 Discussions**

**18h15-18h30 End of the first day**

**Gil MAHE**

Presentation of the workshops topics.

**Thursday 24 November**

Workshops in the morning, and plenary session in the afternoon.

Workshop 1 : *Theme* : Human activities, climate, water resources and environment relationships

**PLANOS - CARMi - BROU YAO**

**Conference Room**

Workshop 2 : *Theme* : Climatic scenarios for the XXI<sup>st</sup> century and prediction of water resources

**SCHULZE - PRUDHOMME - CONWAY**

**Room 104**

**9h00-10h20 Workshops 1<sup>st</sup> part**

**10h20-10h50 Coffee Break**

**10h50-11h45 Workshops 2<sup>nd</sup> part**

**11h45-12h45 Workshops reports**

**PLANOS - CARMi - BROU YAO**

**SCHULZE - PRUDHOMME - CONWAY**

**12h45-14h15 Lunch**

**14h15-15h45 Plenary session 1<sup>st</sup> part**

**Trevor DANIELL Luc SIGHA**

**15h45-16h15 Coffee Break**

**16h15-17h30 Plenary session 2<sup>nd</sup> part**

**Trevor DANIELL Luc SIGHA**

**17h30-18h00 End of the Seminar**

## LISTE DES PARTICIPANTS

NOM	INSTITUTION	PAYS	MAIL
ARDOIN Sandra	HydroSciences Montpellier	FRANCE	sandra.ardoin@msem.univ-montp2.fr
ARNAUD Yves	IRD LGGE Grenoble	FRANCE	yves.arnaud@ird.fr
BERECIARTUA Pablo	Universidad de Buenos Aires	ARGENTINE	pberec@fi.uba.ar pbereciartua@gmail.com
BONELL Mike	UNESCO Paris	FRANCE	m.bonell@unesco.org
BOYER Jean François	HydroSciences Montpellier	FRANCE	jean-francois.boyer@msem.univ-montp2.fr
BROU YAO Telesphore	Université Cocody Abidjan	COTE D'IVOIRE	telesphore.brou@msem.univ-montp2.fr
CARMI Natacha	Hydrology Group Jerusalem	PALESTINE	natasha@phg.org
CONWAY Declan	Université East Anglia Norwich	ROYAUME UNI	d.conway@uea.ac.uk
COUDRAIN Anne	IRD Great Ice Montpellier	FRANCE	coudrain@ird.fr
DANIELL Trevor	University of Adelaide	AUSTRALIE	trevord@civeng.adelaide.edu.au
DELCLAUX François	HydroSciences Montpellier	FRANCE	delclaux@msem.univ-montp2.fr
DEZETTER Alain	HydroSciences Bamako	MALI	alain.dezetter@ird.fr
DIELLO Pierre	HydroSciences Montpellier	BURKINA FASO	pierre.diello@msem.univ-montp2.fr
DIEULIN Claudine	HydroSciences Montpellier	FRANCE	claudine.dieulin@msem.univ-montp2.fr
DIOP NGOM Fatou	Université Cheikh Anta Diop Dakar	SENEGAL	raymalou@ucad.sn
DOBHAL Prasad	Wadia Institute of Himalayan Geology Dehradun	INDE	dpdobhal@rediffmail.com
DOUMOUYA Inza	Université Cocody Abidjan	COTE D'IVOIRE	doumouyai@uabobo.ci
EL-BEHIRY Medhat	National Water Research Center Cairo	EGYPTE	wrri@wrri.org.eg
FRITSCH Jean-Marie	Représentant IRD	AFRIQUE DU SUD	irdafsud@iafrica.com
GNANDI Kissao	Université de Lomé	TOGO	kgnandi@yahoo.fr
GOERTZ Herman	Environnement Canada	CANADA	herman.goertz@ec.gc.ca
GUTIERREZ LOPEZ Alfonso	IMTA Morelos	MEXIQUE	agutierrez@tlaloc.imta.mx
HASNAIN Syed Iqbal	Université de Calicut	INDE	iqbalhasnain@hotmail.com
HORAN Mark	Université Pietermaritzburg	AFRIQUE DU SUD	horan@ukzn.ac.za
HUBERT Pierre	Ecole des Mines Paris	FRANCE	hubert@cig.ensmp.fr
JANICOT Serge	LOCEAN Paris	FRANCE	serge.janicot@lodyc.jussieu.fr
KAMAGATE Bamory	HydroSciences Montpellier	COTE D'IVOIRE	kmagate@msem.univ-montp2.fr
KANE Alioune	Université Cheikh Anta Diop Dakar	SENEGAL	akane@ucad.sn
KINGSTON Daniel	University of Birmingham	ROYAUME UNI	dkg366@bham.ac.uk
KONATE Yacouba	EIER-ETSHER Ouagadougou	BURKINA FASO	hamma.yacouba@eieretsher.org
LAFTOUHI Nour Eddine	Université de Marrakech	MAROC	nouredine.laftouhi@ucam.ac.ma
L'HOTE Yann	IRD Great Ice Montpellier	FRANCE	lhote@msem.univ-montp2.fr
LIENOU Gaston	Université Yaoundé 1	CAMEROUN	liengast@yahoo.fr
LIMIA Myriam	Meteorologie Nationale La Havane	CUBA	limia@met.inf.cu
MAHE Gil	HydroSciences Montpellier	FRANCE	gil.mahe@msem.univ-montp2.fr
MALOU Raymond	Université Cheikh Anta Diop Dakar	SENEGAL	raymalou@ucad.sn

<b>MBAYE Moussa</b>	<b>Université Cheickh Anta Diop Dakar</b>	SENEGAL	moussa.mbaye@msem.univ-montp2.fr
<b>MKHANDI Simon</b>	<b>Université Dar Es Salam</b>	TANZANIE	s_mkhandi@yahoo.com
<b>MOUKOLO Noël</b>	<b>CERGECE Brazzaville</b>	CONGO	moukolo2@yahoo.fr
<b>NAAH Emmanuel</b>	<b>UNESCO Nairobi</b>	KENYA	emmanuel.naah@unesco.unon.org
<b>NDAM Jules Rémy</b>	<b>Université Yaoundé 1</b>	CAMEROUN	jrdam@yahoo.fr
<b>NGOUNOU NGATCHA Benjamin</b>	<b>Université Ngaoundéré</b>	CAMEROUN	ngatchangou@yahoo.fr
<b>OPUKU-ANKOMAH Yaw</b>	<b>Water Research Institute Accra</b>	GHANA	y_ankomah@yahoo.com
<b>PATUREL Jean Emmanuel</b>	<b>HydroSciences Montpellier</b>	FRANCE	jean-emmanuel.paturel@msem.univ-montp2.fr
<b>PLANOS Eduardo</b>	<b>Meteorologie Nationale La Havane</b>	CUBA	planos@met.inf.cu
<b>PRUDHOMME Christel</b>	<b>C E H Wallingford</b>	ROYAUME UNI	c.prudhomme@ceh.ac.uk
<b>RENARD Benjamin</b>	<b>CEMAGREF Lyon</b>	FRANCE	renard@lyon.cemagref.fr
<b>SAMBOU Soussou</b>	<b>Université Cheickh Anta Diop Dakar</b>	SENEGAL	sousamb@smtp.refer.sn
<b>SCHULZE Roland</b>	<b>Université Pietermaritzburg</b>	AFRIQUE DU SUD	schulzer@ukzn.ac.za
<b>SERVAT Eric</b>	<b>HydroSciences Montpellier</b>	FRANCE	Eric.Servat@msem.univ-montp2.fr
<b>SEUNA Pertti</b>	<b>Hydrology and Water Management Division Helsinki</b>	FINLANDE	pertti.seuna@saunalahti.fi
<b>SIGHA Luc</b>	<b>CRH Yaoundé</b>	CAMEROUN	lucsigha@yahoo.fr
<b>TALLAKSEN Lena</b>	<b>Department of GeoSciences Oslo</b>	NORVEGE	lena.tallaksen@geo.uio.no
<b>VALIMBA Patrick</b>	<b>Université Dar Es Salam</b>	TANZANIE	pvalimba@hotmail.com
<b>WHITE Ian</b>	<b>Australian National University Canberra</b>	AUSTRALIE	ian.white@anu.edu.au
<b>YACOUBA Hamma</b>	<b>EIER-ETSHER Ouagadougou</b>	BURKINA FASO	hamma.yacouba@eieretsher.org
<b>ZHIJIA Li</b>	<b>Hohai University Nanjing</b>	CHINE	zhijia-li@vip.sina.com zjli@hhu.edu.cn

ר

ע

י